

**GEORGIA DOT RESEARCH PROJECT 18-03**

**FINAL REPORT**

**DEVELOPMENT OF CONCRETE MATERIAL  
PROPERTY DATABASE  
FOR *PAVEMENT ME* INPUT**



**OFFICE OF PERFORMANCE-BASED  
MANAGEMENT AND RESEARCH**

**600 WEST PEACHTREE STREET NW  
ATLANTA, GA 30308**

## TECHNICAL REPORT DOCUMENTATION PAGE

<b>1. Report No.</b> FHWA-GA-21-1803	<b>2. Government Accession No.</b> N/A	<b>3. Recipient's Catalog No.</b> N/A	
<b>4. Title and Subtitle</b> Development of Concrete Material Property Database for <i>Pavement ME</i> Input		<b>5. Report Date</b> February 2021	
		<b>6. Performing Organization Code</b> N/A	
<b>7. Author(s)</b> S. Sonny Kim, Ph.D., P.E., F.ASCE.; Stephan A. Durham, Ph.D., P.E.; Mi G. Chorzepa, Ph.D., P.E.; Davis Wing; Chandler Banks		<b>8. Performing Organization Report No.</b> 18-03	
<b>9. Performing Organization Name and Address</b> University of Georgia, College of Engineering Driftmier Engineering Center, Athens, GA 30602 Phone: (706) 542-9804, Email: kims@uga.edu		<b>10. Work Unit No.</b> N/A	
		<b>11. Contract or Grant No.</b> PI# 0016336	
<b>12. Sponsoring Agency Name and Address</b> Georgia Department of Transportation Office of Performance-based Management and Research 600 West Peachtree Street NW Atlanta, GA 30308		<b>13. Type of Report and Period Covered</b> Final Report (Oct. 2018–Feb. 2021)	
		<b>14. Sponsoring Agency Code</b> N/A	
<b>15. Supplementary Notes</b> Conducted in cooperation with the U.S. Department of Transportation, Federal Highway Administration			
<b>16. Abstract</b> <p>The Georgia Department of Transportation (GDOT) has been moving toward using the <i>Mechanistic–Empirical Pavement Design Guide</i> (MEPDG), which deploys mechanistic and mathematical principles to analyze the material behaviors. For the smooth transition to this updated pavement design approach for rigid pavement design, GDOT has been developing a statewide database of concrete mixture properties to select appropriate input variables and levels for rigid pavement designs, which are consistent with the level of importance required for specific pavement design projects. The key mechanical inputs for rigid pavement design in the MEPDG are compressive strength (<math>f'_c</math>), modulus of elasticity (MOE), and modulus of rupture (MOR). In addition to these mechanical properties, the MEPDG requires thermal properties inputs, such as the coefficient of thermal expansion (CTE), portland cement concrete (PCC) heat capacity, thermal conductivity, % reversible shrinkage, days to develop 50% of ultimate shrinkage, and ultimate shrinkage. This study aims to develop the aforementioned concrete materials database specific to Georgia's rigid pavements. For this study, twelve (12) GDOT-approved concrete mixtures using Georgia-specific concrete materials were batched, tested, and analyzed for these properties. The study investigates which of these properties are most critical in rigid pavement design through sensitivity analysis conducted with AASHTOWare Pavement ME Design at input levels 1, 2, and 3. With the measured mechanical and thermal properties as a part of the GDOT RP 18-03 study, the relationships among the concrete materials properties and the performance of rigid pavement were further investigated to better understand their interrelationship. Ultimately, this study provides design recommendations for critical mechanical and thermal properties, as well as guidance for which input level to use for the design of Georgia rigid pavements.</p>			
<b>17. Key Words</b> Concrete, MEPDG, Pavement ME, Mechanical property, Thermal property		<b>18. Distribution Statement</b> No Restrictions	
<b>19. Security Classification (of this report)</b> Unclassified	<b>20. Security Classification (of this page)</b> Unclassified	<b>21. No. of Pages</b> 197	<b>22. Price</b> Free

GDOT Research Project 18-03

Final Report

DEVELOPMENT OF CONCRETE MATERIAL PROPERTY DATABASE  
FOR *PAVEMENT ME* INPUT

By

S. Sonny Kim, Ph.D., P.E., F.ASCE  
Associate Professor

Stephan A. Durham, Ph.D., P.E.  
Professor

Mi G. Chorzepa, Ph.D., P.E.  
Associate Professor

Davis Wing, M.S.  
Graduate Research Assistant

Chandler Banks, M.S.  
Graduate Research Assistant

Civil Engineering, College of Engineering  
University of Georgia

Contract with  
Georgia Department of Transportation

In cooperation with  
U.S. Department of Transportation  
Federal Highway Administration

February 2021

The contents of this report reflect the views of the authors who are responsible for the facts and the accuracy of the data presented herein. The contents do not necessarily reflect the official views or policies of the Georgia Department of Transportation or the Federal Highway Administration. This report does not constitute a standard, specification, or regulation.

SI* (MODERN METRIC) CONVERSION FACTORS				
APPROXIMATE CONVERSIONS TO SI UNITS				
Symbol	When You Know	Multiply By	To Find	Symbol
<b>LENGTH</b>				
in	inches	25.4	millimeters	mm
ft	feet	0.305	meters	m
yd	yards	0.914	meters	m
mi	miles	1.61	kilometers	km
<b>AREA</b>				
in <sup>2</sup>	square inches	645.2	square millimeters	mm <sup>2</sup>
ft <sup>2</sup>	square feet	0.093	square meters	m <sup>2</sup>
yd <sup>2</sup>	square yard	0.836	square meters	m <sup>2</sup>
ac	acres	0.405	hectares	ha
mi <sup>2</sup>	square miles	2.59	square kilometers	km <sup>2</sup>
<b>VOLUME</b>				
fl oz	fluid ounces	29.57	milliliters	mL
gal	gallons	3.785	liters	L
ft <sup>3</sup>	cubic feet	0.028	cubic meters	m <sup>3</sup>
yd <sup>3</sup>	cubic yards	0.765	cubic meters	m <sup>3</sup>
NOTE: volumes greater than 1000 L shall be shown in m <sup>3</sup>				
<b>MASS</b>				
oz	ounces	28.35	grams	g
lb	pounds	0.454	kilograms	kg
T	short tons (2000 lb)	0.907	megagrams (or "metric ton")	Mg (or "t")
<b>TEMPERATURE (exact degrees)</b>				
°F	Fahrenheit	5 (F-32)/9 or (F-32)/1.8	Celsius	°C
<b>ILLUMINATION</b>				
fc	foot-candles	10.76	lux	lx
fl	foot-Lamberts	3.426	candela/m <sup>2</sup>	cd/m <sup>2</sup>
<b>FORCE and PRESSURE or STRESS</b>				
lbf	poundforce	4.45	newtons	N
lbf/in <sup>2</sup>	poundforce per square inch	6.89	kilopascals	kPa
APPROXIMATE CONVERSIONS FROM SI UNITS				
Symbol	When You Know	Multiply By	To Find	Symbol
<b>LENGTH</b>				
mm	millimeters	0.039	inches	in
m	meters	3.28	feet	ft
m	meters	1.09	yards	yd
km	kilometers	0.621	miles	mi
<b>AREA</b>				
mm <sup>2</sup>	square millimeters	0.0016	square inches	in <sup>2</sup>
m <sup>2</sup>	square meters	10.764	square feet	ft <sup>2</sup>
m <sup>2</sup>	square meters	1.195	square yards	yd <sup>2</sup>
ha	hectares	2.47	acres	ac
km <sup>2</sup>	square kilometers	0.386	square miles	mi <sup>2</sup>
<b>VOLUME</b>				
mL	milliliters	0.034	fluid ounces	fl oz
L	liters	0.264	gallons	gal
m <sup>3</sup>	cubic meters	35.314	cubic feet	ft <sup>3</sup>
m <sup>3</sup>	cubic meters	1.307	cubic yards	yd <sup>3</sup>
<b>MASS</b>				
g	grams	0.035	ounces	oz
kg	kilograms	2.202	pounds	lb
Mg (or "t")	megagrams (or "metric ton")	1.103	short tons (2000 lb)	T
<b>TEMPERATURE (exact degrees)</b>				
°C	Celsius	1.8C+32	Fahrenheit	°F
<b>ILLUMINATION</b>				
lx	lux	0.0929	foot-candles	fc
cd/m <sup>2</sup>	candela/m <sup>2</sup>	0.2919	foot-Lamberts	fl
<b>FORCE and PRESSURE or STRESS</b>				
N	newtons	0.225	poundforce	lbf
kPa	kilopascals	0.145	poundforce per square inch	lbf/in <sup>2</sup>

\*SI is the symbol for the International System of Units. Appropriate rounding should be made to comply with Section 4 of ASTM E380.  
(Revised March 2003)

## TABLE OF CONTENTS

EXECUTIVE SUMMARY .....	1
Mechanical Property Conclusions.....	1
Thermal Property Conclusions .....	2
Pavement Performance Analysis.....	3
CHAPTER 1. INTRODUCTION .....	6
CHAPTER 2. LITERATURE REVIEW .....	8
Types of Rigid Pavement .....	8
History of Pavement Design.....	18
AASHTO Design Guides .....	20
Material Inputs for the Mechanistic–Empirical Pavement Design Guide.....	20
CHAPTER 3. MOVEMENT TOWARD MEPDG.....	45
Georgia DOT .....	46
Florida DOT .....	54
Mississippi DOT.....	58
CHAPTER 4. PROBLEM STATEMENT.....	62
CHAPTER 5. MATERIALS .....	64
Aggregates.....	64
Cement.....	70
Fly Ash .....	71
Chemical Admixtures .....	72
CHAPTER 6. EXPERIMENTAL DESIGN .....	74
Design Plan.....	74
Concrete Mixtures Testing Matrix .....	74
Experimental Procedures.....	76
CHAPTER 7. EXPERIMENTAL RESULTS .....	83
Concrete Mixtures .....	83
Test Results .....	86
CHAPTER 8. SENSITIVITY ANALYSIS .....	130
Sensitivity to Mechanical Properties .....	136
Sensitivity Analyses for Thermal Properties.....	142
CRCP Results .....	151
Sensitivity to Input Levels.....	155
Statistical Analysis .....	159

CHAPTER 9. CONCLUSIONS AND RECOMMENDATIONS .....	161
APPENDICES .....	164
Appendix A – Material Specification Sheets .....	164
Appendix B – Mixture Designs.....	171
Appendix C – Sensitivity Analysis Process .....	183
Appendix D – Proposed Standard Operating Procedures (SOPs).....	184
ACKNOWLEDGMENTS .....	193
REFERENCES .....	194

## LIST OF FIGURES

Figure 1. Photo. Longitudinal bars in CRCP. ....	9
Figure 2. Photo. CRCP in construction.....	9
Figure 3. Diagram. Transverse cracking in CRCP. ....	10
Figure 4. Diagram. Typical CRCP layers. ....	11
Figure 5. Diagram. JPCP typical layout.....	12
Figure 6. Photo. JPCP in construction. ....	13
Figure 7. Photo. Example of punchout. ....	16
Figure 8. Diagram. AASHO Road Test, loop 5.....	18
Figure 9. Bar graphs. Performance of JPCP with different aggregates: (a) percent slab cracked, (b) mean joint faulting, and (c) IRI. ....	22
Figure 10. Line graph. Thermal conductivity's effect on distresses. ....	24
Figure 11. Graph. Shrinkage of concrete as a result of varying moisture content.....	29
Figure 12. Diagram. Cracking due to restrained drying shrinkage.....	30
Figure 13. Diagram. Flexural stress caused by curling.....	33
Figure 14. Graph. CTE's effect on IRI. ....	43
Figure 15. Graph. MOE's effect on IRI.....	44
Figure 16. Map. State status on MEPDG use for concrete pavements. ....	45
Figure 17. Map. Rigid test sections. ....	52
Figure 18. Line graph. Compressive strength of Mix-01, -02, and -03, Florida State.....	57
Figure 19. Line graph. Flexural strength of Mix-01, 02, and 03, Florida State.....	58
Figure 20. Map. Quarry locations. ....	65
Figure 21. Line graph. Coarse aggregate gradation. ....	67
Figure 22. Line graph. Fine aggregate gradation.....	68
Figure 23. Images. Stockbridge granite rock. ....	69
Figure 24. Images. Adairsville dolomite rock. ....	69
Figure 25. Bar graph. Unit weight results.....	88
Figure 26. Bar graph. Air content results.....	88
Figure 27. Bar graph. Slump results. ....	89
Figure 28. Bar graph. Air content comparison for different mixture trials.....	92
Figure 29. Bar graph. Slump comparison for different mixture trials. ....	92
Figure 30. Bar graph. Unit weight comparison for different mixture trials.....	93
Figure 31. Line graph. Compressive strength vs. age, mixtures 1 and 2, w/cm change.....	95
Figure 32. Line graph. Compressive strength vs. age, mixtures 3 and 4, w/cm change.....	96
Figure 33. Line graph. Compressive strength vs. age; mixtures 4, 5, 6, and 7; FA percentage change.....	97
Figure 34. Line graph. Compressive strength vs. age, mixtures 7 and 9, CA volume change. ....	98
Figure 35. Line graph. Compressive strength vs. age, mixtures 8 and 10, CA volume change. ..	98
Figure 36. Line graph. Compressive strength vs. age, mixtures 9 and 10, CA type change. ....	100
Figure 37. Line graph. Compressive strength vs. age, mixtures 11 and 12, air content change.....	100
Figure 38. Line graph. MOE vs. age, mixtures 1 and 2, w/cm change.....	103

Figure 39. Line graph. MOE vs. age, mixtures 3 and 4, w/cm change.....	103
Figure 40. Line graph. MOE vs. age; mixtures 4, 5, 6, and 7; fly ash percentage change. ....	104
Figure 41. Line graph. MOE vs. age, mixtures 7 and 9, CA volume change. ....	104
Figure 42. Line graph. MOE vs. age, mixtures 8 and 10, CA volume change. ....	105
Figure 43. Line graph. MOE vs. age, mixtures 9 and 10, CA type change. ....	105
Figure 44. Line graph. MOE vs. age, mixtures 11 and 12, air content change.....	106
Figure 45. Bar graph. Static MOE vs. dynamic MOE. ....	108
Figure 46. Bar graph. 28-day Poisson's ratio values. ....	110
Figure 47. Graph. MOR linear regression adjustment. ....	111
Figure 48. Line graph. MOR vs. age, mixtures 1 and 2, w/cm change. ....	113
Figure 49. Line graph. MOR vs. age, mixtures 3 and 4, w/cm change. ....	113
Figure 50. Line graph. MOR vs. age; mixtures 4, 5, 6, and 7; fly ash percentage change. ....	114
Figure 51. Line graph. MOR vs. age, mixtures 7 and 9, CA volume change.....	114
Figure 52. Line graph. MOR vs. age, mixtures 8 and 10, CA volume change.....	115
Figure 53. Line graph. MOR vs. age, mixtures 9 and 10, CA type change.....	115
Figure 54. Line graph. MOR vs. age, mixtures 11 and 12, air content change. ....	116
Figure 55. Line graph. AASHTOWare Pavement ME Design estimated MOR, ACI estimated MOR, and measured values. ....	117
Figure 56. Bar graph. MOR test results comparison. ....	118
Figure 57. Line graph. Shrinkage, mixtures 1 and 2, w/cm change. ....	120
Figure 58. Line graph. Shrinkage, mixtures 3 and 4, w/cm change. ....	120
Figure 59. Line graph. Shrinkage, all mixtures (except mixtures 1, 2, and 5).....	121
Figure 60. Line graph. Ultimate shrinkage plot. ....	123
Figure 61. Scatterplot. Effect of density on thermal conductivity.....	128
Figure 62. Scatterplot. CTE and thermal conductivity plot. ....	129
Figure 63. Diagram. JPCP layers used in sensitivity analysis. ....	134
Figure 64. Diagram. CRCP layers used in sensitivity analysis.....	134
Figure 65. Line graph. Compressive strength vs. percent slabs cracked, JPCP. ....	139
Figure 66. Line graph. MOR vs. percent slabs cracked, JPCP. ....	139
Figure 67. Line graph. MOE vs. percent slabs cracked, JPCP. ....	140
Figure 68. Line graph. Poisson's ratio vs. percent slabs cracked, JPCP.....	140
Figure 69. Line graph. Ultimate shrinkage vs. percent slabs cracked, JPCP.....	141
Figure 70. Line graph. Unit weight vs. mean joint faulting, JPCP. ....	142
Figure 71. Line graph. CTE's effect on terminal IRI. ....	144
Figure 72. Line graph. CTE's effect on mean joint faulting.....	145
Figure 73. Line graph. CTE's effect on transverse cracking. ....	146
Figure 74. Line graph. Thermal conductivity's effect on terminal IRI. ....	147
Figure 75. Line graph. Thermal conductivity's effect on mean joint faulting.....	148
Figure 76. Line graph. Thermal conductivity's effect on transverse cracking. ....	148
Figure 77. Line graph. Heat capacity's effect on terminal IRI. ....	150
Figure 78. Line graph. Heat capacity's effect on mean joint faulting. ....	150
Figure 79. Line graph. Heat capacity's effect on transverse cracking.....	151
Figure 80. Line graph. Compressive strength vs. punchout, CRCP. ....	152



Figure 81. Line graph. MOR vs. punchout, CRCP.....	153
Figure 82. Line graph. MOE vs. punchout, CRCP. ....	153
Figure 83. Line graph. Poisson's ratio vs. punchout, CRCP. ....	154
Figure 84. Line graph. Ultimate shrinkage vs. punchout, CRCP. ....	154
Figure 85. Line graph. Unit weight vs. punchout, CRCP. ....	155
Figure 86. Diagram. JPCP structure used in sensitivity analyses. ....	156
Figure 87. Bar graph. Design levels compared for JPCP distresses. ....	158
Figure 88. Bar graph. Design levels compared for JPCP distresses below failure. ....	158
Figure 89. Bar graph. Optimized thicknesses by level for JPCP. ....	159
Figure 90. Diagrams. Concrete compressive strength fracture types .....	190

## LIST OF TABLES

Table 1. Rigid pavement distress types.....	14
Table 2. Initial IRI values. ....	17
Table 3. Terminal IRI values. ....	17
Table 4. JPCP threshold values.....	17
Table 5. CRCP threshold values. ....	17
Table 6. AASHTO Road Test axle configurations.....	19
Table 7. CTE of different aggregates.....	21
Table 8. Heat capacity and thermal conductivity units.....	24
Table 9. Concrete mixture designs for thermal conductivity.....	25
Table 10. Specific heat values of concrete mixture materials. ....	27
Table 11. Input levels in MEPDG.....	36
Table 12. Values needed for each input level in AASHTOWare Pavement ME Design. ....	37
Table 13. JPCP sensitive inputs.....	38
Table 14. CRCP sensitive inputs. ....	40
Table 15. Concrete mixture design for CTE testing. ....	47
Table 16. Aggregate type effect on CTE. ....	50
Table 17. Aggregate proportion effect on CTE. ....	50
Table 18. Fly ash type effect on CTE. ....	50
Table 19. Statistics of CTE at 28 and 120 days. ....	51
Table 20. Transfer function coefficients.....	53
Table 21. Mixture design by Florida State.....	54
Table 22. Tests performed by Florida State.....	55
Table 23. Input values level 1, Florida State. ....	55
Table 24. Input values level 2, Florida State. ....	56
Table 25. Input values level 3, Florida State. ....	56
Table 26. Optimized thicknesses, Florida State.....	56
Table 27. MDOT mixtures.....	59
Table 28. MDOT 28-day test averages. ....	60
Table 29. Flexural model coefficients. ....	61
Table 30. MDOT Model 9 regression coefficients. ....	61
Table 31. Quarries used. ....	65
Table 32. Specific gravity and absorption of aggregates.....	66
Table 33. Coarse Aggregate Gradation Limits #57 <i>ASTM C33</i> .....	66
Table 34. Fine aggregate gradation limits, GDOT Section 801. ....	68
Table 35. Cement chemical properties.....	70
Table 36. Cement physical properties.....	71
Table 37. Fly ash chemical analysis. ....	72
Table 38. Fly ash physical analysis.....	72
Table 39. Concrete mixture matrix. ....	75
Table 40. Fresh concrete properties testing matrix.....	78
Table 41. Hardened concrete properties testing matrix. ....	78

Table 42. Specimen sizes.....	80
Table 43. GDOT-approved mixtures.....	84
Table 44. Mixture identification.....	85
Table 45. Fresh properties.....	87
Table 46. Fresh concrete properties for first round of thermal conductivity.....	90
Table 47. Fresh concrete properties for MOR and $f_c'$ testing.....	90
Table 48. Fresh concrete properties for second round of thermal conductivity.....	90
Table 49. Compressive strength values.....	94
Table 50. Static MOE results.....	101
Table 51. Poisson's ratio results.....	109
Table 52. MOR beam size comparison.....	111
Table 53. MOR results.....	112
Table 54. Shrinkage results.....	119
Table 55. Ultimate shrinkage test results.....	122
Table 56. CTE test results.....	124
Table 57. Thermal conductivity test results.....	126
Table 58. Density measurements.....	127
Table 59. Mechanical inputs by level.....	131
Table 60. Traffic inputs.....	132
Table 61. JPCP and CRCP design properties.....	133
Table 62. Layer properties.....	135
Table 63. Default values and sensitivity ranges for JPCP.....	137
Table 64. Default values and sensitivity ranges for CRCP.....	137
Table 65. Input effect test, JPCP.....	160
Table 66. Input effect test, CRCP.....	160
Table 67. Specimen dimensions.....	185
Table 68. Fresh concrete property standards.....	186
Table 69. Concrete placement guide.....	187
Table 70. Consolidation recommendations.....	188

## **EXECUTIVE SUMMARY**

This study batched, tested, and analyzed 12 GDOT-approved concrete mixtures for compressive strength, modulus of rupture (MOR), modulus of elasticity (MOE), Poisson's ratio, coefficient of thermal expansion (CTE), thermal conductivity, heat capacity, and shrinkage. The 12 mixtures varied in cement content, fly ash percentage, water-to-cement ratio (w/cm), coarse aggregate (CA) type, CA fraction, and air content. The impacts these different mixture variables had on the concrete's material properties are analyzed and discussed in this report. Using AASHTOWare Pavement ME Design, a series of sensitivity analyses was performed to identify which of the mechanical and thermal properties tested in this study were critical to the performance of rigid pavements. Additionally, the laboratory-tested values from the 12 GDOT mixtures were used to complete rigid pavement designs at input levels 1, 2, and 3. The results of these analyses were compared to construct guidelines for which input level to use in future GDOT designs.

## **MECHANICAL PROPERTY CONCLUSIONS**

Major findings from the experimental investigation specific to the mechanical properties of the concrete mixtures investigated in this study include:

- Compressive strength values ranged from 4,140 psi (28.5 MPa) to 6,650 psi (45.9 MPa) at 28 days of age. Factors influencing compressive strength were w/cm, air content, fly ash replacement, CA type, and CA fraction. It was concluded that higher w/cm and higher air contents had similar effects of lowering concrete compressive strength. Fly ash was found to have no effect on the initial strength of concrete, but it led to higher 90-day strengths when compared to mixtures without fly ash. Granite led to higher compressive strengths

than dolomite mixtures, despite being less angular. Finally, lower CA fractions led to lower compressive strengths.

- Modulus of elasticity 28-day measured values ranged from 3,150 to 6,400 ksi (21.7 to 44.1 GPa). Factors influencing MOE were w/cm, fly ash replacement, and CA type. Higher w/cm led to lower MOE values, similar to the compressive strength results. Fly ash was found to lower the MOE in the resulting mixtures by around 1,000 ksi (6.9 GPa). The use of dolomite instead of granite was determined to have the largest effect on MOE. Mixtures using dolomite achieved MOE values around 2,000 ksi (13.8 GPa) higher than mixtures using granite.
- Poisson's ratio did not vary much across mixtures. Mixtures using dolomite, however, resulted in higher values for Poisson's ratio.
- A linear relationship between 3×4×16-inch (76.2×101.6×406.4-mm) and 6×6×22-inch (152.4×152.4×558.8-mm) modulus of rupture beams was established with an  $R^2$  of 0.79. The equation relating large beams and small beams is  $6 \times 6 \times 22\text{-inch } MOR(psi) = 0.5439(3 \times 4 \times 16\text{-inch } MOR) + 246.9$ .
- MOR values at 28 days ranged from 620 to 805 psi (4.3 to 5.6 MPa). Air content was determined to have the largest effect on the resulting MOR values. Higher air contents resulted in lower MOR values.

## THERMAL PROPERTY CONCLUSIONS

Major findings from the experimental investigation specific to the thermal properties of the concrete mixtures investigated in this study include:

- Aggregate type was identified as the leading factor contributing to the CTE values. Concrete mixtures containing the dolomite aggregate type resulted in relatively higher CTE values than similar mixtures containing granite aggregate type.
- Shrinkage specimens were observed to experience an initial growth during the first 28 days of age, followed by shrinkage at later days of age. Water-to-cement ratio exhibited the largest effect on shrinkage results. A higher w/cm led to increased shrinkage values.
- The density of the concrete mixture impacts the thermal property significantly. A higher density results in a higher thermal conductivity value. Moisture also plays an important role in thermal conductivity test values; specimens with a higher moisture content resulted in a higher thermal conductivity value. Similar to CTE, mixtures containing the dolomite aggregate type exhibited higher thermal conductivity values than similar mixtures containing granite.
- A relationship between CTE and thermal conductivity was established. It is attributed to concrete mixtures with lower thermal conductivity values serving as a better thermal buffer than mixtures with high thermal conductivity test results. This relationship can be utilized to estimate a thermal conductivity value from CTE value when a lab-tested thermal conductivity value is not readily available for the *Mechanistic–Empirical Pavement Design Guide* (MEPDG).
- During the sensitivity analyses, CTE demonstrated itself to be the most critical thermal property for all pavement predictions in regard to the Pavement ME Design.

## PAVEMENT PERFORMANCE ANALYSIS

Major findings from the pavement performance and sensitivity analysis conducted within this study include:

- Jointed plain concrete pavement (JPCP) displayed sensitivity to MOR, compressive strength, unit weight, and Poisson's ratio. MOR and compressive strength were found to be critical inputs for percent slabs cracked and international roughness index (IRI). Unit weight and Poisson's ratio were found to be critical for predicting mean joint faulting.
- JPCP displayed sensitivity to MOE at levels 1 and 3. MOE values over 5,500 ksi (39.7 GPa) predicted a drastic increase of distresses.
- Continuous reinforced concrete pavement (CRCP) displayed sensitivity to MOR and compressive strength only. These two inputs were found to be critical in predicting punchout and IRI.
- CTE and thermal conductivity were discovered to be controlling properties in mean joint faulting prediction. An increase in CTE resulted in an increase in mean joint faulting, while a decrease in thermal conductivity resulted in an increase in mean joint faulting. This is attributed to concrete mixtures with a lower thermal conductivity acting as a better insulator. Unit weight is also an important factor affecting mean joint faulting. This is most likely attributed to lower unit weight mixtures allowing an increase in curling deflection.
- CTE and MOR were identified as the key factors affecting terminal IRI. An increase in CTE resulted in an increase in terminal IRI, while an increase in MOR resulted in a lower terminal IRI.
- CTE and MOR played a major role in the performance prediction of transverse cracking. An increase in CTE resulted in more transverse cracking, while a higher MOR resulted in less transverse cracking. The PCC layer thickness was also identified as an important factor in JPCP structures in terms of cracking.

- It should be noted that the design thickness of JPCP does not always increase as the input level goes from 1 to 3. Instead, material properties such as  $f'_c$ , MOR, MOE, and CTE significantly affect the thickness design. While level 1 and 3 analyses require the measured MOE as an input value, level 2 estimates the MOE from measured  $f'_c$ .
- Initially, the decrease of slab cracking was expected as MOE increases. However, an MOE greater than 5,500 ksi (39.7 GPa) was prone to predict significant percent slab cracking. Thus, caution should be taken when a level 2 input with over 5,500 ksi MOE value is utilized.



## CHAPTER 1. INTRODUCTION

Traditionally, pavement structures have been designed using equations and design guides formulated from empirical testing. Empirical testing is a method of gaining knowledge from observed failure. The American Association of State and Highway Transportation Officials (AASHTO) first developed these empirical design methods by observing a section of roadway constructed in Illinois in the late 1950s. Historically, the Georgia Department of Transportation (GDOT) has used these guides, specifically the *AASHTO 1972* and *1981 Pavement Design Guide*, to design its roadways. As material science has progressed, significant research has led to a more mechanistic understanding of the material utilized in pavement design, construction, and rehabilitation. Mechanistic approach differs from empirical approach by using the understanding of material properties and mathematical principles to predict performance, rather than using observations from existing structures' failures to predict future performance. This approach has led to improved modeling of the pavement structure and its behavior. This new method, presented in AASHTO's *Mechanistic-Empirical Pavement Design Guide* (MEPDG), combines new mechanistic understandings of how materials behave with existing empirical observations.

GDOT plans to implement the MEPDG for future critical pavement designs in Georgia. In order to fully incorporate the MEPDG, the development of a material database is necessary. This study aims to develop a concrete materials database for reliable rigid pavement design for GDOT. This includes producing, testing, and analyzing concrete mixtures for compressive strength ( $f'_c$ ), modulus of elasticity (MOE), modulus of rupture (MOR), coefficient of thermal expansion (CTE), thermal conductivity, and ultimate shrinkage. These properties are required to complete a rigid pavement design in the MEPDG. Since the mechanical properties of concrete will vary from mixture to mixture, a matrix was established to vary mixture characteristics. The following

properties were varied for this study: water-to-cement ratio (w/cm), cementitious content, fly ash content, coarse aggregate (CA) type, coarse aggregate volume fraction, and air content. The variation of these mixture variables creates a wide variety of mixtures that will be included in the database. To ensure these mixtures satisfy GDOT requirements, GDOT-approved mixtures are selected for batching and testing.

Additionally, this study investigates which material properties have the most significant impact on rigid pavements. Sensitivity analysis is performed for input levels 1, 2, and 3 for both jointed plain concrete pavement (JPCP) and continuous reinforced concrete pavement (CRCP). Level 3 designs require the least amount of input and, therefore, provide preliminary insight into how sensitive predicted distresses are to each mechanical and thermal property. The results from the input levels are compared and used to help make recommendations on which level should be utilized in new rigid pavement designs in Georgia. The development of this database and the resulting sensitivity analysis is critical for the implementation of the MEPDG in Georgia. With the correct input values and a complete understanding of their impacts on predicted performance, GDOT will be able to fully implement the MEPDG for rigid pavement design.

## CHAPTER 2. LITERATURE REVIEW

### TYPES OF RIGID PAVEMENT

Pavement structures are typically classified as either *flexible pavements*, which are road structures constructed using asphaltic materials, or *rigid pavements*, which are constructed from concrete. Rigid pavements are classified as being either: (1) continuous reinforced concrete pavement, (2) jointed plain concrete pavement, or (3) jointed reinforced concrete pavement (JRCP). This section provides an overview of the design methodology for CRCP and JPCP as it relates to the development of a material input library for Georgia. JRCP is not included since it is not commonly used in Georgia. JRCP combines design elements from CRCP and JPCP.

#### CRCP Overview

CRCP is a type of rigid pavement that is typically used for interstate applications where high traffic loads are expected. Reinforcing steel is placed throughout the slab width and length, providing continuous reinforcement. These steel bars are spaced relatively close together to help provide support for transverse cracks, as well as to effectively limit the width of cracks as they form. Images of CRCP construction are shown in figure 1 and figure 2.

CRCP is expected to develop cracks very early in its life. These cracks are caused by the stresses associated with restricting concrete expansion. The concrete's tensile strength is often not high enough to resist these strains, thus transverse cracking occurs (Advanced Concrete Pavement Technology 2012). Figure 3 illustrates narrowly spaced transverse cracking, which is the common cracking associated with CRCPs.



**Figure 1. Photo. Longitudinal bars in CRCP.  
(Advanced Concrete Pavement Technology 2012)**



**Figure 2. Photo. CRCP in construction. (Federal Highway Administration 2016)**

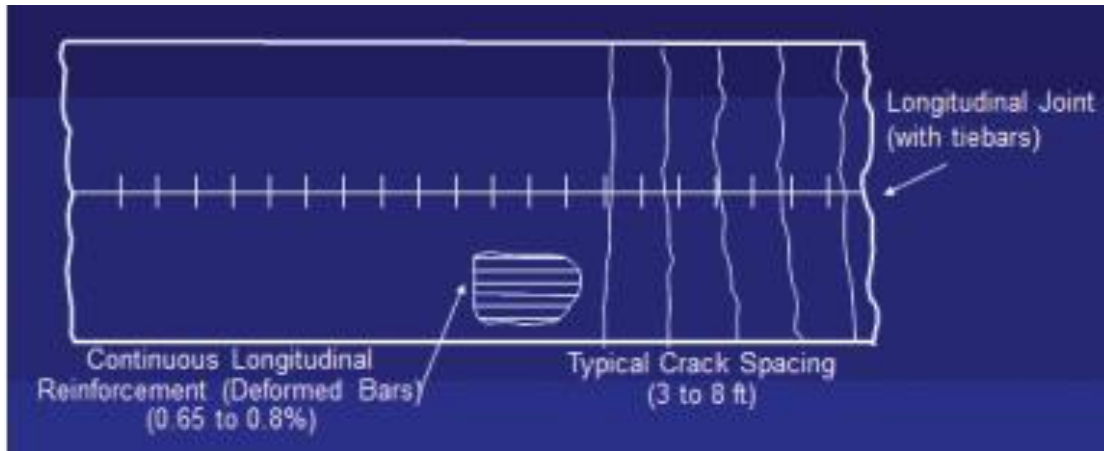


**Figure 3. Diagram. Transverse cracking in CRCP.  
(Advanced Concrete Pavement Technology 2012)**

Due to the expected cracking in CRCP, it is important to place longitudinal steel reinforcement high enough in the cross section to provide adequate load transfer across the cracks. The Federal Highway Administration (FHWA) recommends the bars be placed between  $\frac{1}{3}$  and  $\frac{1}{2}$  the pavement depth with a minimum depth of 3.5 inch (88.9 mm) (FHWA 2016).

In Georgia, typical CRCP layers include an 11.0–12.0-inch (279.4–304.8-mm) slab placed over a 3-inch (76.2-mm) asphalt concrete (AC) bond breaker layer, and a minimum 8.0-inch (203.2-mm) thick graded aggregate base (GAB) layer. Figure 4 illustrates this design configuration. Typical steel reinforcement includes a #6 reinforcing bar in the longitudinal direction with a #4 reinforcing bar in the transverse direction to support the longitudinal steel. Steel is placed between 3.50 and 4.25 inch (88.90 to 107.95 mm) below the slab surface to ensure adequate cover while preventing cracks from widening (Tsai and Wang 2014).

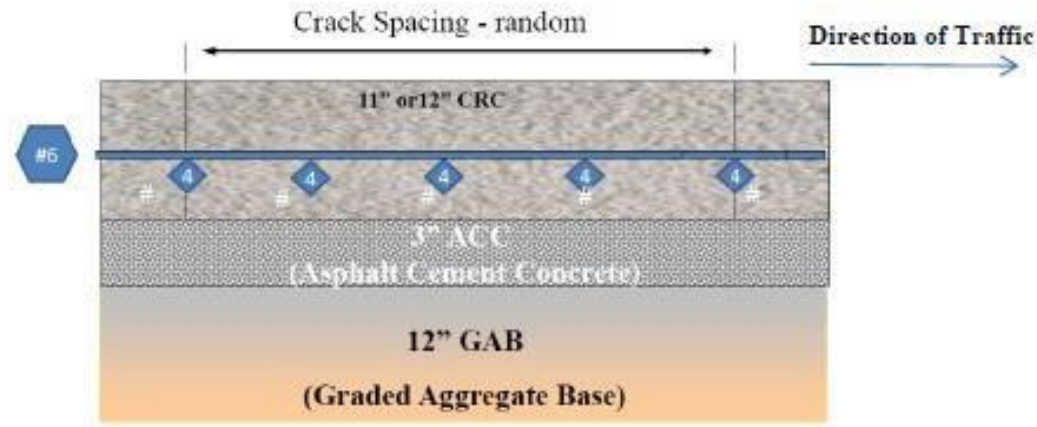


**Figure 4. Diagram. Typical CRCP layers. (Tsai and Wang 2014)**

There are advantages and disadvantages to using CRCPs. CRCPs, if installed correctly, are virtually maintenance free and have a service life that well exceeds its design life. CRCP sections in California have performed for over 60 years (Advanced Concrete Pavement Technology 2012). Typically, “CRCP sections can be expected to provide over 40 years of exceptional performance with minimal maintenance when properly designed and constructed” (FHWA 2016). This pavement type maintains its initial smoothness over its design life. Willis et al. (2015) outline how rolling resistance increases when pavements are rougher. Rolling resistance is defined as “the mechanical energy converted into heat by a tire moving a unit distance of roadway” (Schuring 1977). Rolling resistance contributes to fuel efficiency in cars, and the road smoothness may lower gas consumption by as much as 4.5 percent (Willis et al. 2015). Concrete surfaces have the smoothest surfaces with the least amount of rolling resistance. Further, concrete surfaces are maintained longer due to the durability of CRCP. Lastly, CRCP has the lowest life-cycle costs, providing for the most cost-effective pavement when subjected to large loads over its service life. The disadvantages of CRCP include high initial costs, complex construction, and potential threats of punchout distress.

## JPCP Overview

JPCP is a type of rigid pavement without steel reinforcement that is jointed at relatively short intervals, i.e., 10–20 ft (3–6 m), with the option of placing a dowel bar between transverse joints to allow for improved load transfer. In addition, tie bars are used between longitudinal joints (Caltrans 2015). A schematic of a typical JPCP design is shown in figure 5.

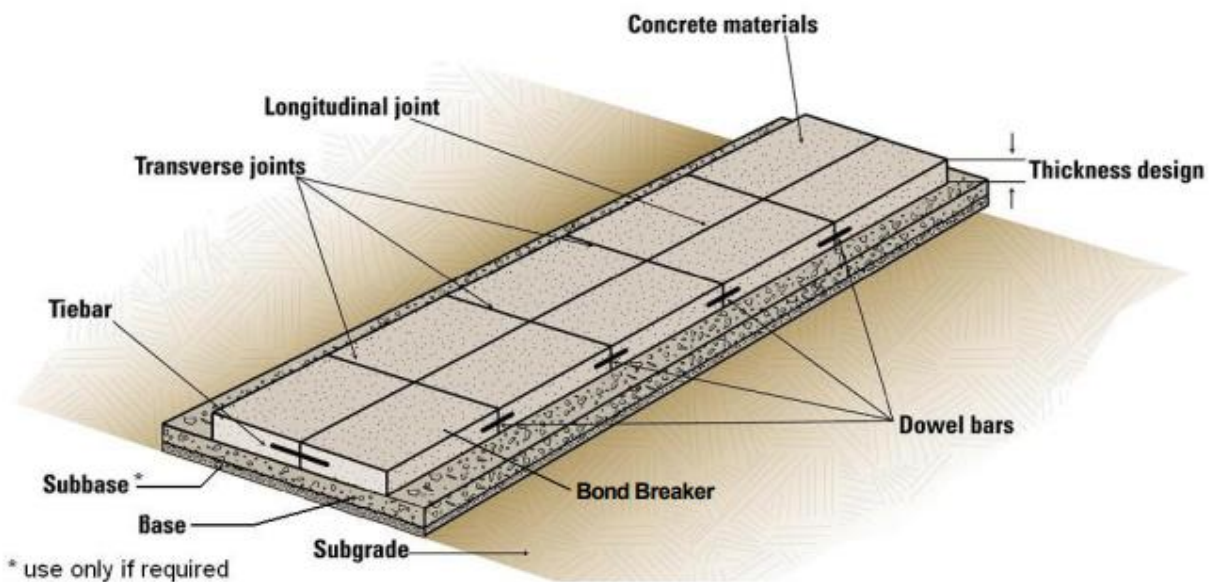


**Figure 5. Diagram. JPCP typical layout. (Caltrans 2015)**

The advantages of JPCP include appearance, lower initial cost, and a simpler construction compared to its counterpart. One concern of CRCP is that citizens could interpret the closely spaced transverse cracks as a premature concrete failure (Chen and Texas Department of Transportation 2013). With JPCP, the transverse cracks are replaced by predetermined joints so the pavement can appear better to the public. JPCP has a lower initial cost than CRCP since it does not utilize steel reinforcement throughout its cross section, with the exception of tie reinforcing bars between slabs. Further, JPCP provides for a more simplistic design than CRCP, allowing for easier and lower-cost construction. JPCP is often utilized in areas where the pavement approaches



structures or railways and where traffic loading is not as significant as that expected for CRCs (Chen and Texas Department of Transportation 2013). An image of JPCP during construction is shown in figure 6.



**Figure 6. Photo. JPCP in construction.**  
(Chen and Texas Department of Transportation 2013)

### **Failure Mechanisms and Performance Criteria**

FHWA published a report discussing the distresses experienced by different pavement types (Miller and Bellinger 2014). The distress types that affect pavements and a brief description of each are summarized in table 1.



**Table 1. Rigid pavement distress types. (Miller and Bellinger 2014)**

<b>Distress Type</b>	<b>Unit of Measure</b>	<b>J P C P</b>	<b>C R C P</b>	<b>Description</b>
Corner Breaks	Number	✓		A portion of the slab is separated by a crack, which intersects the adjacent transverse and longitudinal joints, describing approximately a 45-degree angle with the direction of traffic. The length of the sides is from 0.3 m to half the width of the slab on each side of the corner.
Durability (“D” Cracking)	Number of slabs, Area affected	✓	✓	Closely spaced crescent-shaped hairline cracking pattern. Occurs adjacent to joints, cracks, or free edges. Initiates at the intersection (e.g., cracks and a free edge). Dark coloring of the cracking pattern and surrounding area.
Longitudinal Cracking	Number, Width	✓	✓	Cracks that are predominantly parallel to the pavement centerline.
Transverse Cracking	Number, Width	✓	✓	Cracks that are predominantly perpendicular to the pavement centerline. This cracking is expected in a properly functioning CRCP. All transverse cracks that intersect an imaginary longitudinal line at mid-lane and propagate from the pavement edges (centerline joint or the edge joint) shall be counted as individual cracks. Cracks that do not cross the mid-lane are not counted.
Transverse Joint Seal Damage	Percent of joint	✓		Joint seal damage is any condition that enables incompressible materials or a significant amount of water to infiltrate into the joint from the surface. Typical types of joint seal damage include extrusion, hardening, adhesive failure (bonding), cohesive failure (splitting), or complete loss of sealant.
Longitudinal Joint Seal Damage	Number, Length	✓	✓	Joint seal damage is any condition that enables incompressible materials or a significant amount of water to infiltrate into the joint from the surface. Typical types of joint seal damage include extrusion, hardening, adhesive failure (bonding), cohesive failure (splitting), or complete loss of sealant.
Spalling of Longitudinal Joints	Number, Width	✓	✓	Cracking, breaking, chipping, or fraying of slab edges within 0.3 m of the longitudinal joint.
Transverse Construction Joint Deterioration	Number		✓	A series of closely spaced transverse cracks or a large number of interconnecting cracks occurring near the construction joint.
Spalling of Transverse Joints	Number, Width	✓		Cracking, breaking, chipping, or fraying of slab edges within 0.3 m from the face of the transverse joint.

<b>Distress Type</b>	<b>Unit of Measure</b>	<b>J P C P</b>	<b>C R C P</b>	<b>Description</b>
Map Cracking	Number, Area affected	✓	✓	A series of cracks that extend only into the upper surface of the slab. Larger cracks frequently are oriented in the longitudinal direction of the pavement and are interconnected by finer transverse or random cracks
Scaling	Number, Area affected	✓	✓	Scaling is the deterioration of the upper concrete slab surface, normally 3 to 13 mm, and may occur anywhere over the pavement.
Polished Aggregate	Area affected	✓	✓	Surface mortar and texturing worn away to expose coarse aggregate.
Popouts	Not measured	✓	✓	Small pieces of pavement broken loose from the surface, normally ranging in diameter from 25 to 100 mm and in depth from 13 to 50 mm.
Blowups	Number	✓	✓	Localized upward movement of the pavement surface at transverse joints or cracks; often accompanied by shattering of the concrete in that area.
Faulting of Transverse Joints and Cracks	Depth	✓	✓	Difference in elevation across a joint or crack.
Lane-to-Shoulder Dropoff	Depth	✓	✓	Difference in elevation between the edge of slab and outside shoulder; typically occurs when the outside shoulder settles.
Lane-to-Shoulder Separation	Width	✓	✓	Widening of the joint between the edge of the slab and the shoulder.
Patch Deterioration	Number, Area affected	✓	✓	A portion greater than or equal to 0.1 m <sup>2</sup> or all of an original concrete panel that has been removed and replaced or additional material applied to the pavement after original construction.
Water Bleeding and Pumping	Number, Length affected	✓	✓	Seeping or ejection of water from beneath the pavement through cracks or joints. In some cases, it is detectable by deposits of fine material left on the pavement surface, which were eroded (pumped) from the support layers and have stained the surface.
Punchout	Number		✓	The area enclosed by two closely spaced (usually <0.6 m) transverse cracks, a short longitudinal crack, and the edge of the pavement or a longitudinal joint. Also includes “Y” cracks that exhibit spalling, breakup, or faulting. An area that is enclosed by two distressed transverse cracks that are spaced between 0.6 m and 1 m, a short longitudinal crack, and the edge of the pavement or a longitudinal joint is also considered a punchout.

The two primary performance criteria addressed in the AASHTOWare Pavement ME Design for CRCP are punchout and international roughness index (IRI). Punchout and IRI are used as the main design criteria because they represent conditions that would incite a major rehabilitation or reconstruction of the pavement (ARA 2015). While punchout and IRI are the main design criteria for CRCP, the other distresses listed in table 1 will still incite needed maintenance over the pavement's life. Punchout is a localized failure where a slab portion is broken into several pieces (Pavement Interactive n.d.), which occurs when a longitudinal crack connects two transverse cracks, as shown in figure 7.



**Figure 7. Photo. Example of punchout. (Pavement Interactive n.d.)**

IRI is a standard measure of pavement roughness, which is interpreted as the smoothness of the pavement bearing surface (Pavement Interactive 2001). For JPCP designs, the amount of faulting and percent slabs cracked are important failure criteria. The *GDOT Pavement ME Design User Input Guide* has specified threshold values for these failure criteria, which are specifically

checked by Pavement ME Design. The threshold values are shown in table 2, table 3, table 4, and table 5.

**Table 2. Initial IRI values. (ARA 2015)**

Type of Pavement	Type of Wearing Surface	Initial IRI Rating, in./mi
Rigid	JPCP	64
	CRCP	50

**Table 3. Terminal IRI values. (ARA 2015)**

Roadway Type <sup>a</sup>		Pavement Type	
		JPCP	CRCP
		IRI Rating, in./mi	IRI Rating, in./mi
Non-Interstate Route	2-Lane, State	220	175
	4-Lane Roadway	175	175
Interstate Route	Rural & Urban	175	175

<sup>a</sup> Number of lanes are in both directions.

**Table 4. JPCP threshold values. (ARA 2015)**

Roadway Type <sup>a</sup>		Performance Indicator	
		Faulting, in.	Slabs Cracked, %
Non-Interstate	2-Lane, State Route	0.20	10.0
	4-Lane Roadway	0.20	10.0
Interstate	Rural and Urban	0.125	10.0

<sup>a</sup> Number of lanes are in both directions.

**Table 5. CRCP threshold values. (ARA 2015)**

Roadway Type <sup>a</sup>		Performance Indicator
		Number of Punchouts per Mile
Non-Interstate	2-Lane, State Route	10
	4-Lane Roadway	10
Interstate	Rural and Urban	5

<sup>a</sup> Number of lanes are in both directions.

## HISTORY OF PAVEMENT DESIGN

The American Association of State Highway Officials (AASHO) was established on December 12, 1914, with the purpose to “study the various materials, methods of construction and maintenance, and other highway problems of the United States for the purpose of conserving the capital invested in highway construction and maintenance by producing the highest possible efficiency” (Weingroff 2014). After its formation, AASHO discovered a growing need for factual data for resolving the problem of increasing traffic loadings’ impact on pavements (Highway Research Board 1962). In order to meet this demand, a large-scale pavement test was conducted and later became known as the AASHO Road Test.

The AASHO Road Test took place near Ottawa, Illinois, from 1958 through 1960. Tests consisted of constructing six test loops, where each segment consisted of a four-lane divided highway. A test section containing both flexible and rigid pavements was specified in each of these loops. Each test section had different pavement layers to help analyze the influence of different structural variables on pavement performance. Variables included surface thickness, base layer thickness, and subgrade thickness. A typical loop layout is shown in figure 8.

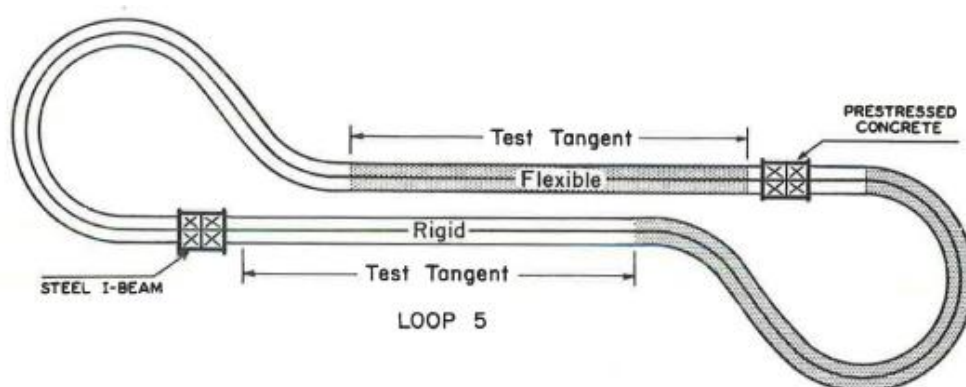


**Figure 8. Diagram. AASHO Road Test, loop 5. (Highway Research Board 1962)**

Tests were conducted for 2 years with varying vehicle types consisting of different axle configurations and weights. These vehicles were routinely driven on the loop during the 25-month test period. A total accumulation of 1,114,000 axle-load applications was obtained by driving either four, six, or eight vehicles in each lane of the test loops. Typical test vehicles and axle configuration for each loop are listed in table 6.

**Table 6. AASHO Road Test axle configurations.  
(Highway Research Board 1962)**

<b>Loop</b>	<b>Lane</b>	<b>Total Number of Axles</b>	<b>Front Axle (lb)</b>	<b>Load Axle Type</b>	<b>Load Axle (lb)</b>	<b>Gross Weight (lb)</b>
2	1	2-axle	2,000	Single	2,000	4,000
	2	2-axle	2,000	Single	6,000	8,000
3	1	3-axle	4,000	Single	12,000	28,000
	2	5-axle	6,000	Tandem	24,000	54,000
4	1	3-axle	6,000	Single	18,000	42,000
	2	5-axle	9,000	Tandem	32,000	73,000
5	1	3-axle	6,000	Single	22,400	50,800
	2	5-axle	9,000	Tandem	40,000	89,000
6	1	3-axle	9,000	Single	30,000	69,000
	2	5-axle	12,000	Tandem	48,000	108,000

Structural sections were continually tested for serviceability and performance as deterioration occurred over the 25-month test period. These data became the basis for future design guides produced by AASHO. AASHO was officially renamed to the American Association of State Highway and Transportation Officials, or AASHTO, on November 13, 1973 (Weingroff 2014).

## **AASHTO DESIGN GUIDES**

Immediately following the AASHTO Road Test, the *AASHTO Interim Guide for the Design of Rigid Pavement Structures* (1962) was released. Versions following this initial release included: the *AASHTO Interim Guide for the Design of Pavements* (1972); *AASHTO Rigid Pavement Design Revisions* (1981); *AASHTO Guide for Design of Pavement Structures* (1986); *AASHTO Guide for Design of Pavement Structures* (1993); *AASHTO Guide for Design of Pavement Structures, Supplement* (1998); *NCHRP 1-37A Development of the 2002 Guide for the Design of New and Rehabilitated Pavement Structures* (1998–2004); *AASHTO Mechanistic–Empirical Pavement Design Guide—A Manual of Practice* (2008); and *AASHTOWare Pavement ME Design* (2011).

## **MATERIAL INPUTS FOR THE MECHANISTIC–EMPIRICAL PAVEMENT DESIGN GUIDE**

The following inputs are required when completing a new rigid pavement design for the concrete layer:  $f'_c$ , MOE, MOR, CTE, ultimate shrinkage, and PCC thermal conductivity.

### **Thermal Properties Inputs**

Portland cement concrete (PCC) mixtures have unique thermal properties, such as CTE, PCC thermal conductivity, and heat capacity, which provide a basic understanding of heat flow inside the material (Shin and Kodide 2012).

#### ***Coefficient of Thermal Expansion***

CTE has traditionally not been included as a design parameter for pavement design. However, this value is important as it directly relates to crack spacing, crack width, and crack load transfer efficiency, which in turn directly affects cracking, punchout, and smoothness (Mallela et al. 2005).

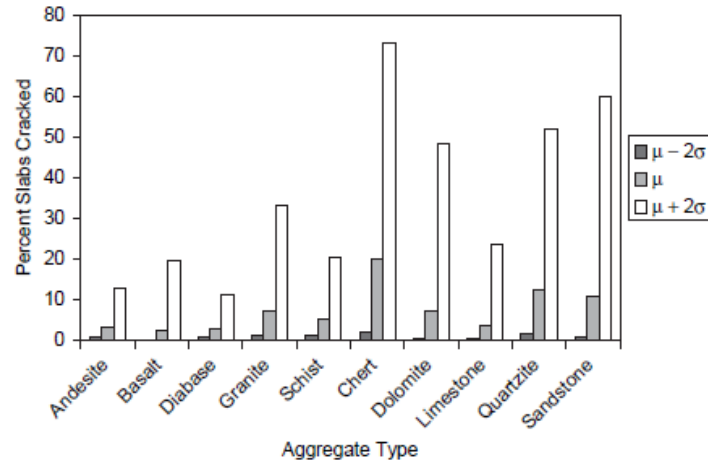
CTE is a property that is governed by the aggregate type, cement content, water-to-cement ratio, relative humidity, porosity, and degree of paste hydration (Kosmatka et al. 2002). Since the aggregate constitutes a majority of the concrete volume, up to 80 percent, it has shown to have the greatest effect on the CTE value (Mallela et al. 2005). In Georgia, two different coarse aggregate types, granite and dolomite, are commonly used in concrete mixtures (Kim 2012). Mallela et al. (2005) performed a sensitivity analysis in the MEPDG for CTE to see how varying values affected the performance of JPCP. A trend was observed from their study that showed the higher CTE values led to accelerated pavement deterioration. Their study only varied the aggregate type in order to change CTE values since aggregate was most influential. Further study is required to determine how cement content, w/cm, relative humidity, porosity, and degree of paste hydration would vary the CTE. Table 7 shows the different CTE values found for different aggregates. Figure 9a, b, and c show aggregate types' effect on pavement performance.

**Table 7. CTE of different aggregates. (Mallela et al. 2005)**

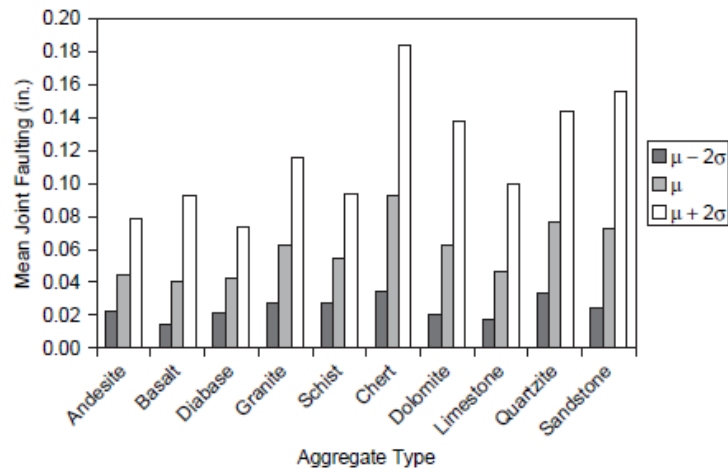
Primary Origin	Primary Aggregate Class	Average CTE	Standard Deviation	Sample Count ( <i>n</i> )
Igneous (extrusive)	Andesite	5.3	0.5	23
Igneous (extrusive)	Basalt	5.2	0.7	47
Igneous (extrusive)*	Diabase	4.6	0.5	4
Igneous (plutonic)	Diabase	5.2	0.5	17
Igneous (plutonic)*	Gabbro	5.3	0.6	4
Igneous (plutonic)	Granite	5.8	0.6	83
Metamorphic	Schist	5.6	0.5	17
Sedimentary	Chert	6.6	0.8	28
Sedimentary	Dolomite	5.8	0.8	124
Sedimentary	Limestone	5.4	0.7	236
Sedimentary	Quartzite	6.2	0.7	69
Sedimentary	Sandstone	6.1	0.8	18
Lightweight <sup>1</sup>	Expanded shale	5.7	0.5	3

NOTE: Long-Term Pavement Performance (LTPP) test section results: testing conducted by FHWA at the Turner-Fairbank Highway Research Center. Units are in in./in. per °F × 10<sup>-6</sup>.

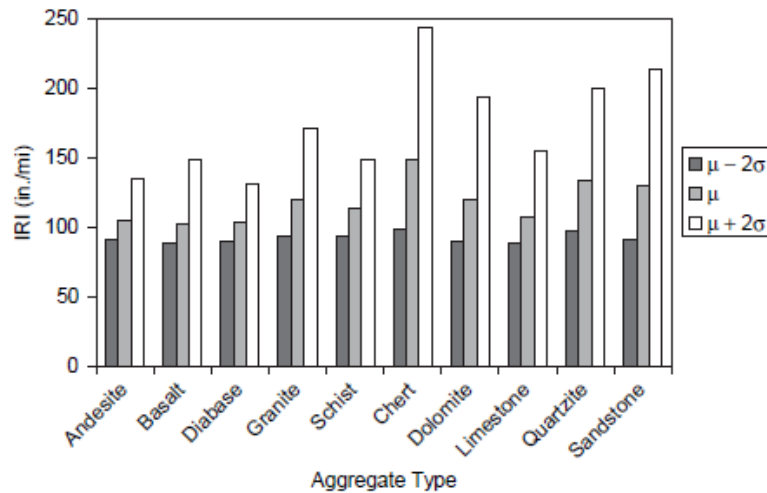




(a) Percent slabs cracked



(b) Mean joint faulting



(c) IRI

**Figure 9. Bar graphs. Performance of JPCP with different aggregates: (a) percent slab cracked, (b) mean joint faulting, and (c) IRI. (Mallela et al. 2005)**

### ***PCC Thermal Conductivity***

Thermal conductivity is the ratio of heat flux to the temperature gradient. This ratio, in a designated sample thickness, indicates the uniform flow of heat from one side of the sample to the other. Heat transfer in concrete is similar to that of metals due to its porous and heterogeneous nature as a solid material. Multiple factors, including aggregate type, temperature and moisture of local environment, cement paste content, coarse and fine aggregate, along with porosity and admixtures, affect the thermal conductivity of concrete (Kodide 2010). Thermal conductivity can be calculated using equation 1.

$$k = \frac{\Delta Q * x}{\Delta t * A * \Delta T} \quad (1)$$

where,

$k$  = Thermal conductivity

$\Delta Q$  = Change in heat energy between two points

$x$  = Distance between two points

$\Delta t$  = Change in time

$A$  = Area of object being measured

$\Delta T$  = Change in temperature that produced the heat flow

The primary influencing factors of PCC thermal conductivity are aggregate type, proportion of coarse aggregate, moisture content, and the use of supplementary cementitious materials (SCMs) (Shin and Kodide 2012). Notably, the size and shape of the mold has no effect on PCC thermal conductivity (Shin and Kodide 2012). It has been found that as thermal conductivity increases, the associated distresses decrease, as shown in figure 10.

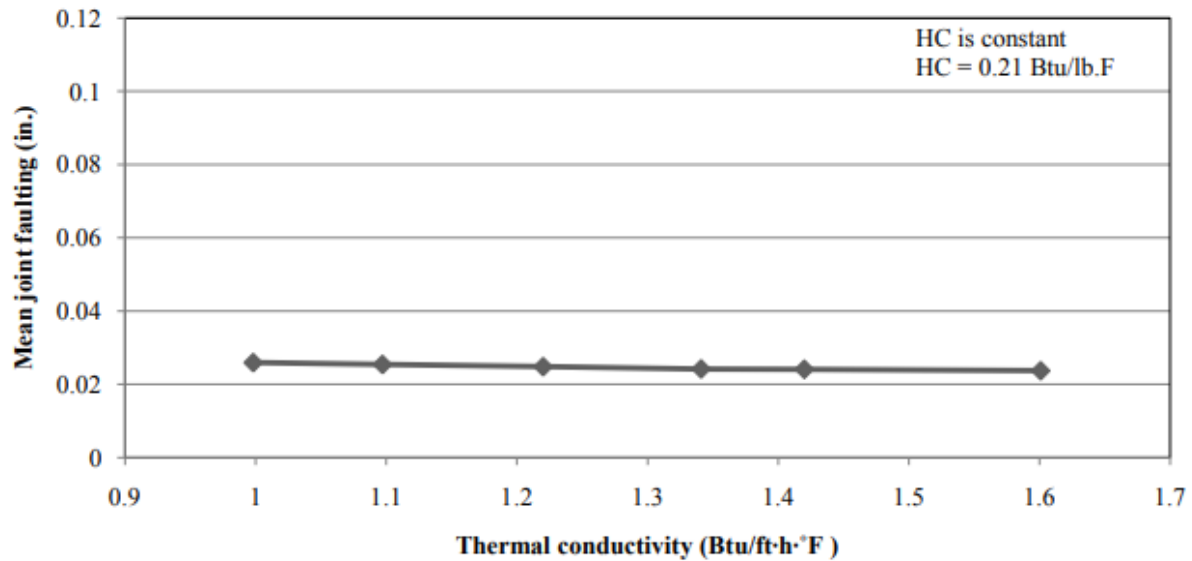


**Figure 10. Line graph. Thermal conductivity's effect on distresses. (Kodide 2010)**

The study performed by Kodide (2010) used a variety of concrete mixtures that contained different aggregates to identify the relevance that aggregate has on the thermal conductivity of concrete (see table 8). The mixtures used are shown in table 9.

**Table 8. Heat capacity and thermal conductivity units. (Kodide 2010)**

Parameters	SI <sup>a</sup> Unit	Conversion Factor	English Unit
Thermal Conductivity	1 W/m-K	0.5779	Btu/ft-h-°F
Heat Capacity	1 J/m <sup>3</sup> -K	1.49×10 <sup>-5</sup>	Btu/ft <sup>3</sup> -°F

<sup>a</sup> International System of Units

**Table 9. Concrete mixture designs for thermal conductivity. (Kodide 2010)**

Mixtures	Unit	K65 (0.451)	K20 (0.547)	K80 (0.451)	G65 (0.451)	M65 (0.451)
Holcim Type II (GP) Portland Cement	lbs/yd <sup>3</sup>	475	475	475	475	475
Sand, A133 TXI Dennis Mills	lbs/yd <sup>3</sup>	1,171	2,551	637	1,131	1,149
Kentucky Limestone, AB29 Martin Marietta	lbs/yd <sup>3</sup>	2,104	654	2,612	-	-
Gravel, A133 TXI Dennis Mills	lbs/yd <sup>3</sup>	-	-	-	2,027	-
Mexican Limestone, AA36	lbs/yd <sup>3</sup>	-	-	-	-	2,071
% by volume Fine Aggregate	%	36.2	80	20	35.0	35.7
% by volume Coarse Aggregate	%	63.8	20	80	65.0	64.3
Water	lbs/yd <sup>3</sup>	214	260	214	214	214
Water Cement Ratio		0.451	0.547	0.451	0.451	0.451
Admixture (Daravair 1400)	Dosage (oz/100ct)	0.50	0.50	0.50	0.50	0.50
Admixture (WRDA 35)	Dosage (oz/100ct)	3.50	10.0	2.0	6.40	20.00
ASTM C 1064 Air Temperature	°F	68.5	75.3	70.0	69.0	71.2
ASTM C 1064 Concrete Temperature	°F	72.0	78.0	70.9	73.5	74.6
ASTM C 143 Slump	inches	0.25	0.0	0.25	1.50	1.25
ASTM C 231 Pressure Air Content	%	7.00	3.50	3.60	6.30	4.00
ASTM C 138 Unit Weight	lbs/ft <sup>3</sup>	144.4	143.2	148.8	140.0	149.2
Specific gravity	-	2.69	2.69	2.69	2.53	2.62
Water absorption	%	1.0	1.0	1.0	2.2	3.5

(K: Kentucky limestone; G: Gravel; M: Mexican limestone)

Thermal conductivity can be measured through a number of means, but this research is primarily focused on the transient heat line approach utilized in the American Society for Testing and Materials (ASTM) *D5334-14* test method, *Standard Test Method for Determination of Thermal Conductivity of Soil and Soft Rock by Thermal Needle Probe Procedure*. A line source of heat is applied by an electrical probe inserted into the concrete specimen. Then, the thermal conductivity is determined by measuring the rate at which the concrete specimen's temperature changes in response to the applied heat.

In Kodide's study, the aggregates were determined to play a major role in the thermal conductivity of the concrete mixtures. The mixtures containing the gravel aggregate had a much higher thermal conductivity than the mixtures containing limestone. That study also demonstrated

a linear relationship between the increase in thermal conductivity and moisture content. Moisture has proven to be a crucial factor affecting thermal conductivity in concrete specimens. Kodide (2010) also investigated the relevance of thermal conductivity on a pavement section using an MEPDG analysis. The study found that while there was little interaction between thermal conductivity and mean joint faulting, thermal conductivity did have an effect on transverse cracking. A higher thermal conductivity value reduced the temperature difference from the top to the bottom of the pavement structure, which caused a reduction in predicted distresses.

Another study concluded that the porosity of a concrete specimen had a dramatic influence on the thermal conductivity (Dos Santos 2003). The material porosity levels allow for the water to have a large impact due to moisture storage in the specimen itself. Concrete specimens with high porosities allow for a larger absorption of water, which directly relates to a higher thermal conductivity value (Dos Santos 2003).

Bentz et al. (2011) from the National Institute of Standards and Technology conducted a study exploring the relationship between density and thermal conductivity in concrete mixtures. Varying amounts of fly ash were substituted for the cement to produce a lower density concrete mixture. The study demonstrated a positive correlation between density and thermal conductivity in the tested specimens. Bentz et al. (2011) concluded that a larger fly ash replacement percentage resulted in a lower density, which produced a lower thermal conductivity. The study went on to discover that lower thermal conductivity values result in lower thermal diffusivity. A lower thermal diffusivity allows concrete to serve as a thermal buffer and be less affected by changes in environmental temperature.

### ***Heat Capacity***

Heat capacity ( $C_p$ ) is also a thermal property required for an MEPDG approach. It is simply the ability of a mixture to store its internal energy while being subjected to temperature change and remaining in the same physical state. Therefore, it is the actual amount of heat energy required to change the temperature of a unit mass by a single degree (Chintakunta 2007). The heat capacity of a substance is mainly dependent on a mixture's mass and the size of its constituents. Heat capacity differs from thermal conductivity in this manner. The thermal conductivity values for coarse and fine aggregates are the same; however, the heat capacity of fine aggregate would be much lower than that of coarse aggregate due to its reliance on mass and size. For concrete mixtures, the water content, along with porosity, will also play a role in heat capacity (Kodide 2010). Heat capacity demonstrated an inverse relationship with a linear decrease in heat capacity as the moisture increased.

Fly ash has been proven to have little impact on specific heat capacity test results in concrete mixtures. Bentz et al. (2011) concluded that water content was the key factor affecting the specific heat capacity of concrete. Table 10 illustrates the varying specific heat capacity values for materials in a concrete mixture. These data illustrate that water's specific heat value of 4.18 J/(g K) is significantly higher than that of other materials and provides an explanation for water playing the largest role in specific heat capacity values for concrete mixtures.

**Table 10. Specific heat values of concrete mixture materials. (Bentz et al. 2011)**

<b>Material</b>	<b>Specific Heat Capacity (J/(g K))</b>
Water	4.18
Cement (Type IP)	0.76
Fly Ash (Class F)	0.72
Limestone Sand	0.76

The study performed by Chintakunta (2007) explored the sensitivity of thermal properties of pavement materials using the MEPDG. That study performed sensitivity analyses to help identify the general behavior of the thermal properties in the MEPDG models. The research outcomes are as follows:

- The transverse cracking in JPCP was proven to be sensitive to both thermal conductivity and CTE, and the faulting model was similarly sensitive to thermal conductivity and CTE, as well as dowels and surface shortwave absorptivity (SSA). International roughness index exhibited sensitivity with respect to CTE, SSA, and thermal conductivity. These analyses proved the obvious correlations between thermal properties and common pavement distresses.
- CTE proved to be the most critical input for IRI and punchouts, while crack spacing, ultimate shrinkage strain, SSA, thermal conductivity, and climate also played a role in punchouts for CRCP structures.
- Cracking in JPCP structures is most affected by thermal conductivity, heat capacity, SSA, and CTE.
- Punchouts in CRCP structures are most affected by thermal conductivity, ultimate shrinkage, heat capacity, SSA, and CTE.

### ***Volume Stability Inputs***

Drying shrinkage is a mixture input of particular interest to this thesis. Due to varying moisture throughout the concrete slab, differential shrinkage may occur, causing warping, high cracking potential, and faulting. Drying shrinkage is caused by moisture changes within the concrete after it has hardened (Kosmatka and Wilson 2016). The moisture changes that occur are usually a result

of humidity changes in the air surrounding the concrete or from the evaporation of water trapped within the concrete during the mixing operation. This cycle of concrete swelling and shrinking with changes in moisture content is shown in figure 11.

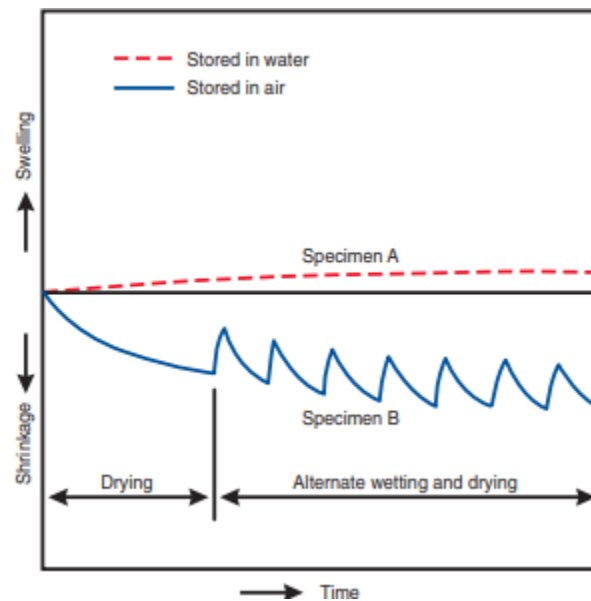


**Figure 11. Graph. Shrinkage of concrete as a result of varying moisture content. (Kosmatka and Wilson 2016)**

Within pavement structures, stresses that are developed because of drying shrinkage lead to tensile cracks within the pavement. The tensile stresses are due to the pavement being restrained. Unable to freely move, tensile stresses will exceed the capacity of the concrete and crack. This restraint and cracking of the slab is shown in figure 12.



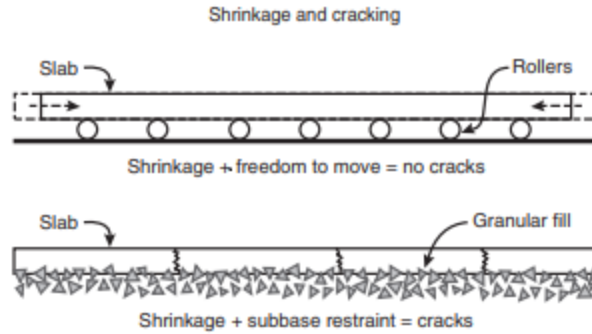


**Figure 12. Diagram. Cracking due to restrained drying shrinkage.  
(Kosmatka and Wilson 2016)**

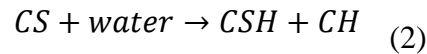
Reinforced concrete structures, such as CRCP, will have less drying shrinkage than plain, unreinforced structures due to the reinforcing steel restricting the shrinkage (Kosmatka and Wilson 2016). Since JPCP has no reinforcement, shrinkage is viewed as a more critical input for JPCP than for CRCP.

The best method to limit drying shrinkage is to control the amount of water per unit concrete (Kosmatka and Wilson 2016). Mixtures with less water have less potential for volume change due to drying shrinkage, as a result of a smaller water volume that must be evaporated. Since drying shrinkage is a paste property, it is possible to reduce the shrinkage by the appropriate selection of aggregate type and quantity, causing an increase in the hardened concrete density (Kosmatka and Wilson 2016). A higher volume of aggregate instead of paste reduces the amount of shrinkage potential. In addition, curing methods provide a way to reduce the shrinkage of mixtures. When moisture is trapped inside hardened concrete for a long period of time, the shrinkage after curing is much less (Kosmatka and Wilson 2016). Therefore, methods—such as spraying compounds, wet burlap wrapping, and fogging—that trap water in the mixture for a longer period during the cement hydration process may help reduce long-term shrinkage.

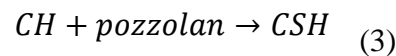
## Mechanical Properties Inputs

Mechanical properties of concrete pavement have a significant influence on the pavement performance. Properties considered influential are compressive strength, Young's modulus, and MOR.

Compressive strength, denoted by  $f'_c$ , is usually considered to reach its peak value at 28 days. However, cement inside the concrete will continue to hydrate and gain strength as long as heat and moisture are present (Kosmatka and Wilson 2016). Additionally, with the use of SCMs, such as fly ash, concrete will continue to gain strength at a similar rate for a longer period. Fly ash has a delayed effect on concrete strength as a result of the pozzolanic reaction. The primary chemical reaction for concrete strength is shown in equation 2, using the abbreviated cement chemistry notation.



Calcium silicate hydrate (CSH) is the main contributor to concrete strength (Kosmatka and Wilson 2016). When pozzolans, such as fly ash, are present in a concrete mixture, a secondary reaction occurs, as presented in equation 3.



The calcium hydroxide (CH) produced from the primary reaction of water and the calcium silicates within the cement from equation 2 will react with the silica derived from the pozzolan to create more CSH (Kosmatka and Wilson 2016). This is the reason for the delayed strength gain associated with fly ash. The reaction cannot occur until the hydration of cement has produced enough CH to

react with the pozzolan. It is for this reason that the MEPDG requires strength inputs measured at 7, 14, 28, and 90 days of age.

Many factors affect the compressive strength of a concrete mixture, including cement content, water content, air content, aggregate gradation, aggregate shape, and curing methods. Lower w/cm, lower air content, and high cement content typically lead to higher concrete strength. The aggregate gradation has been found to influence concrete performance (Taylor et al. 2014). A dense aggregate gradation that creates less voids will result in higher compressive strength. Further, aggregates with a rougher angular shape will result in higher compressive strength. This is due to better bonding between aggregates and paste, as well as the shape, leading to improved aggregate stability within the matrix, increasing the compressive strength (Taylor et al. 2014).

Young's modulus or the modulus of elasticity, denoted by  $E_c$ , is a measure of the hardened concrete stiffness. Values for Young's modulus are estimated from the concrete compressive strength because of the linear relationship that exists in the early portion of concrete's stress-strain curve. The modulus is estimated for normal weight concrete using equation 4 (Kosmatka and Wilson 2016).

$$E_c = 57,000\sqrt{f'_c}(psi) \quad (4)$$

Alternatively, a laboratory test can be performed to measure the value of Young's modulus. An increase in the stiffness of concrete pavements leads to a proportional decrease in the distresses experienced (Sabih and Tarefder 2016). Since the stiffness is related to the concrete strength, techniques used to increase the compressive strength will increase the MOE. There are two main tests for MOE: static and dynamic. Dynamic tests will yield higher results, which have exhibited

a linear relationship in previous studies (Salman and Al-Amawee 2006). This relationship is shown in equation 5.

$$E_{Static} = 0.83 * E_{Dynamic} \quad (5)$$

MOR is a measure of the flexural strength of concrete. MOR is an important design value because of the different flexural stresses that pavements experience over their service life. For example, when a pavement section is subjected to curling, a cantilevered section is formed, resulting in flexural stress within the pavement as the wheel load passes over the slab. This flexural stress is shown in figure 13. Since concrete is known to be weak in tension, this is the limiting factor in flexural strength. This is because when a load is applied to a beam or slab, both compressive and tensile stresses are created. To illustrate, imagine a simply-supported beam. The beam is subject to a point load, which produces bending stresses. The top half of the beam's cross section will experience compressive stresses, while the bottom half will experience tensile stresses. The area of concrete subject to tensile stresses will fail much quicker than the top half in compression. For this reason, concrete often has steel reinforcement.

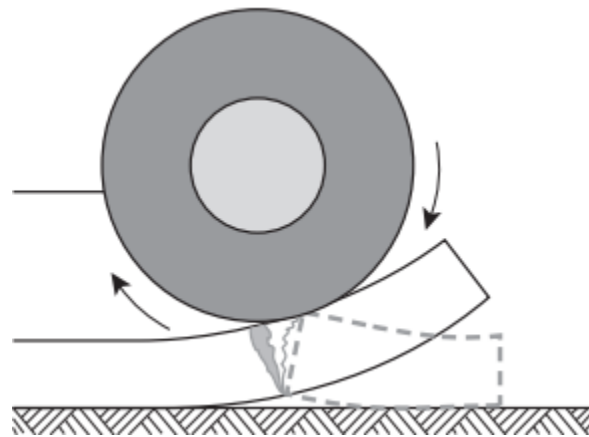


**Figure 13. Diagram. Flexural stress caused by curling.**  
(Kosmatka and Wilson 2016)

MOR is a value that can be estimated from compressive strength or found through beam testing. MOR is usually estimated to be 8–12 percent of the concrete compressive strength (Kosmatka and Wilson 2016). If MOR cannot be measured in the laboratory, it is often estimated using the American Concrete Institute (ACI) empirical equation 6.

$$MOR = 7.5 * \sqrt{f'_c} (psi) \quad (6)$$

Values for MOR found from laboratory testing may vary depending on specimen size. It has been documented that larger MOR specimens will typically have lower MOR values than the same mixture tested using smaller beams (Tanesi et al. 2013). Research has been performed to develop a linear regression equation to relate different sizes of beams (Tanesi et al. 2013).

### **Aggregate Type**

AASHTOWare Pavement ME Design allows for the input of different types of coarse aggregate. In Georgia, the two most common coarse aggregates used in concrete mixtures are granite and dolomite. Granite and dolomite will display different physical properties; thus, it is important to understand the key differences between these two types of coarse aggregates. Specifically, the differences between compressive strength and MOE values between the two rock types are discussed.

One particular study analyzed the impact that aggregate type had on MOE and concrete compressive strength. That study found that dolomite was a denser material than granite, with a relative density of 2.81, as opposed to the density of granite at 2.65 (Alexander and Milne 1995). When comparing similar mixtures, the mixtures using dolomite exhibited MOE values approximately 2200–2900 ksi (15–20 GPa) higher, on average, than the same granite mixtures

(Alexander and Milne 1995). However, no significant difference was found between the compressive strengths of these mixtures. Another study obtained very similar results, concluding that concrete mixtures with dolomite are stiffer than those with granite (Rashid et al. 2002).

The aggregate amount used in mixtures will impact MOE and compressive strength. When lower coarse aggregate fractions are used, the resulting compressive strength is lower than mixtures with higher CA fractions (Kim 2012). The MOE values are proportional to the compressive strength; lower coarse aggregate fractions will produce lower MOE values, while higher coarse aggregate fractions produce higher MOE values (Meddah et al. 2010). The shape and surface texture of the aggregate will affect the compressive strength, as well. Generally, more angular aggregates will produce higher compressive strengths due to the improved interlocking between the aggregate and paste (Taylor et al. 2014).

### **Input Levels**

AASHTOWare Pavement ME software has varying design levels that are constructed based on site-specific knowledge. These levels are described simply as level 1, level 2, and level 3. Level 3 designs are based on the designer having access to the least amount of information. In this design level, many national default values are used to fill information gaps. Designs using a level 3 analysis are considered the least reliable, although they have the potential to produce results similar to the higher levels. Level 2 refers to values that have been calibrated to a state instead of to national default values. Regression values are used within this input level to obtain the best fit for a specific project (ARA 2015). Level 1 input values are those that are site-specific. For a level 1 design, a comprehensive laboratory investigation is performed where the design inputs are measured, thereby providing the highest level of accuracy for the pavement design. In addition, level 1 designs are the costliest since they involve significantly more data collection and laboratory

testing. In general, level 2 designs are recommended for routine pavement designs, as they are more accurate than level 3 and more cost-effective than level 1. Table 11 provides a summary of the AASHTOWare Pavement ME Design input levels and a general outline of when to use each.

**Table 11. Input levels in MEPDG. (ARA 2015)**

<b>Input Level</b>	<b>Definition of the Level</b>
1	Input parameter based on site-specific data and information. Level 1 represents the case when the user has the greatest knowledge about the input parameter for the specific project. This input level has the highest level of testing (data collection costs) for determining the input value. Input level 1 is recommended for projects having unusual site features and/or considering the use of new materials.
2	Regression equations are used to determine the input value. The data collection and testing for this input level is simpler and less costly. Input level 2 is recommended for use for routine pavement designs and standard materials.
3	Level 3 inputs are based on “best-guessed” (default) values. The level 3 inputs are based on global or regional default values. This input level requires the minimum amount of testing, and as such, results in the least knowledge about the input parameter for the specific project. Input level 3 is recommended for use when the other input levels are unavailable.

In many cases, designs will not have every input value available for the target design level. For example, if the target design level is level 2 but there are missing values, the designer may be forced to use the national default values. This is allowed and is to be expected. AASHTOWare Pavement ME Design will use the same equations and distress models for each input level, such that a combination of input value levels may be used. For this reason, it is recommended to use the highest level of input accuracy available for each design value. Table 12 lists the concrete materials properties expected at each input level. The strength inputs are the most critical in reaching a level 1 design. The other inputs stay consistent for all design levels.

**Table 12. Values needed for each input level in AASHTOWare Pavement ME Design.**

Category	Level 1	Level 2	Level 3
PCC	<ul style="list-style-type: none"> <li>Poisson's Ratio</li> <li>Unit Weight (UW)</li> </ul>		
Thermal	<ul style="list-style-type: none"> <li>PCC CTE</li> <li>PCC Heat Capacity</li> <li>PCC Thermal Conductivity</li> </ul>		
Mixture	<ul style="list-style-type: none"> <li>Aggregate Type</li> <li>Cementitious Material Content</li> <li>Cement Type (I/II)</li> <li>Water-to-cement Ratio (w/cm)</li> <li>Reversible Shrinkage (%)</li> <li>PCC Zero-stress Temperature</li> <li>Time to Develop 50% of Ultimate Shrinkage</li> <li>Ultimate Shrinkage</li> </ul>		
Strength	<ul style="list-style-type: none"> <li>MOR and MOE at 7, 14, 28, and 90 days</li> </ul>	<ul style="list-style-type: none"> <li><math>f'_c</math> at 7, 14, 28, and 90 days</li> </ul>	<ul style="list-style-type: none"> <li>28-day MOR or <math>f'_c</math></li> </ul>
	<ul style="list-style-type: none"> <li>Estimated MOR and MOE Ratio of 20-year to 28-day</li> </ul>	<ul style="list-style-type: none"> <li>Estimated <math>f'_c</math> Ratio of 20-year to 28-day</li> </ul>	<ul style="list-style-type: none"> <li>28-day MOE</li> </ul>

### ***Sensitivity to Inputs***

Extensive research has been conducted on the sensitivity of design inputs in the MEPDG. One particular study published by Iowa State University investigates the impact design parameters of JPCP and CRCP and ranks their sensitivity levels as *hypersensitive*, *very sensitive*, or *sensitive* (Schwartz et al. 2011). Their study looked at all design parameters, but the discussion that follows focuses on the material properties inputs they used.

The study concluded that the two most sensitive material properties for JPCP are unit weight and CTE. These two inputs were classified as very sensitive for all predicted distresses: faulting, transverse cracking, and IRI. MOR was the most sensitive value for transverse cracking. The sensitivity results for JPCP are presented in table 13.



**Table 13. JPCP sensitive inputs. (Schwartz et al. 2011)**

<b>Distress</b>	<b>Input Category</b>	<b>Hypersensitive</b>	<b>Very Sensitive</b>	<b>Sensitive</b>
Faulting	PCC Properties		<ul style="list-style-type: none"> <li>• UW</li> <li>• CTE</li> </ul>	<ul style="list-style-type: none"> <li>• 28-day MOR</li> <li>• Surface Shortwave Absorptivity</li> <li>• W/cm</li> <li>• Thickness</li> <li>• 20-year to 28-day MOR</li> <li>• Cement Content</li> <li>• Poisson's Ratio</li> </ul>
	Aggregate Base Properties			<ul style="list-style-type: none"> <li>• Resilient Modulus</li> <li>• Erodibility Index</li> <li>• Thickness</li> <li>• Edge Support LTE</li> </ul>
	Subgrade Properties			<ul style="list-style-type: none"> <li>• Resilient Modulus</li> </ul>
	Other Properties	<ul style="list-style-type: none"> <li>• Slab Width</li> </ul>	<ul style="list-style-type: none"> <li>• Design Lane Width</li> </ul>	<ul style="list-style-type: none"> <li>• Joint Spacing</li> <li>• Dowel Diameter</li> <li>• Traffic Volume</li> <li>• Construction Month (+0.1)</li> </ul>
Transverse Cracking	PCC Properties		<ul style="list-style-type: none"> <li>• 28-day MOR</li> <li>• Thickness</li> <li>• UW</li> <li>• CTE</li> <li>• 20-year to 28-day MOR</li> <li>• 28-day MOE</li> <li>• Surface Shortwave Absorptivity</li> <li>• W/cm</li> <li>• Thermal Conductivity</li> </ul>	<ul style="list-style-type: none"> <li>• Poisson's Ratio</li> <li>• Cement Content</li> </ul>
	Base Properties			<ul style="list-style-type: none"> <li>• Thickness</li> <li>• Resilient Modulus</li> <li>• Erodibility Index</li> <li>• Loss of Friction</li> </ul>
	Subgrade Properties			<ul style="list-style-type: none"> <li>• Groundwater Depth</li> <li>• Resilient Modulus</li> </ul>

<b>Distress</b>	<b>Input Category</b>	<b>Hypersensitive</b>	<b>Very Sensitive</b>	<b>Sensitive</b>
	Other Properties	<ul style="list-style-type: none"> <li>Slab Width</li> </ul>	<ul style="list-style-type: none"> <li>Design Lane Width</li> <li>Joint Spacing</li> </ul>	<ul style="list-style-type: none"> <li>Dowel Diameter</li> <li>Traffic Volume</li> <li>Edge Support LTE</li> <li>Construction Month</li> </ul>
IRI	PCC Properties		<ul style="list-style-type: none"> <li>CTE</li> <li>UW</li> </ul>	<ul style="list-style-type: none"> <li>W/cm</li> <li>PCC 28-day MOR</li> <li>Surface Shortwave Absorptivity</li> <li>Thickness</li> <li>28-day MOE</li> <li>20-year to 28-day MOR</li> <li>Thermal Conductivity</li> <li>Poisson's Ratio</li> <li>Cement Content</li> </ul>
	Base Properties			<ul style="list-style-type: none"> <li>Resilient Modulus</li> <li>Erodibility Index</li> </ul>
	Subgrade Properties			<ul style="list-style-type: none"> <li>Resilient Modulus</li> </ul>
	Other Properties	<ul style="list-style-type: none"> <li>Slab Width</li> </ul>		<ul style="list-style-type: none"> <li>Design Lane Width</li> <li>Joint Spacing</li> <li>Dowel Diameter</li> <li>Traffic Volume</li> </ul>

CRCP designs were found to be hypersensitive to a variety of inputs. PCC strength and stiffness properties were consistently in this hypersensitive category. As a general note, CRCP designs seem to be much more sensitive to inputs when compared to JPCP designs. The CRCP sensitivity results are listed in table 14.

**Table 14. CRCP sensitive inputs. (Schwartz et al. 2011)**

<b>Distress</b>	<b>Input</b>	<b>Hypersensitive</b>	<b>Very Sensitive</b>	<b>Sensitive</b>
Punchout	PCC/Steel Properties	<ul style="list-style-type: none"> <li>• Thickness</li> <li>• 28-day MOR</li> <li>• 20-year to 28-day MOR</li> <li>• UW</li> <li>• Percent Steel</li> <li>• 28-day Indirect Tensile Strength</li> <li>• 28-day MOE</li> <li>• W/cm</li> <li>• Cement Content</li> <li>• CTE</li> </ul>	<ul style="list-style-type: none"> <li>• Surface Shortwave Absorptivity</li> <li>• Poisson's Ratio</li> <li>• 20-year to 28-day Indirect Tensile Strength</li> </ul>	
	Base Properties	<ul style="list-style-type: none"> <li>• Resilient Modulus</li> </ul>	<ul style="list-style-type: none"> <li>• Base Slab Friction</li> <li>• Thickness</li> </ul>	
	Subgrade Properties		<ul style="list-style-type: none"> <li>• Resilient Modulus</li> </ul>	<ul style="list-style-type: none"> <li>• Groundwater Depth</li> </ul>
	Other Properties	<ul style="list-style-type: none"> <li>• Bar Diameter</li> <li>• Traffic Volume</li> <li>• Steel Depth</li> </ul>	<ul style="list-style-type: none"> <li>• Edge Support LTE</li> <li>• Construction Month</li> </ul>	

<b>Distress</b>	<b>Input</b>	<b>Hypersensitive</b>	<b>Very Sensitive</b>	<b>Sensitive</b>
Crack Width	PCC/Steel Properties	<ul style="list-style-type: none"> <li>• 28-day Indirect Tensile Strength</li> <li>• 28-day MOR</li> <li>• UW</li> <li>• W/cm</li> <li>• Cement Content</li> <li>• Percent Steel</li> <li>• 28-day MOE</li> <li>• Thickness</li> <li>• 20-year to 28-day MOR</li> <li>• 20-year to 28-day Indirect Tensile Strength</li> <li>• CTE</li> <li>• Surface Shortwave Absorptivity</li> </ul>	<ul style="list-style-type: none"> <li>• Poisson's Ratio</li> </ul>	
	Base Properties	<ul style="list-style-type: none"> <li>• Base Slab Friction</li> </ul>	<ul style="list-style-type: none"> <li>• Resilient Modulus</li> <li>• Thickness</li> </ul>	
	Subgrade Properties		<ul style="list-style-type: none"> <li>• Resilient Modulus</li> <li>• Groundwater Depth</li> </ul>	
	Other Properties	<ul style="list-style-type: none"> <li>• Bar Diameter</li> <li>• Steel Depth</li> </ul>	<ul style="list-style-type: none"> <li>• Construction Month</li> <li>• Edge Support LTE</li> <li>• Traffic Volume</li> </ul>	
Crack LTE	PCC/Steel Properties		<ul style="list-style-type: none"> <li>• 28-day MOR</li> <li>• Thickness</li> <li>• 28-day Indirect Tensile Strength</li> <li>• Percent Steel</li> </ul>	<ul style="list-style-type: none"> <li>• W/cm</li> <li>• Cement Content</li> <li>• 28-day MOE</li> <li>• UW</li> <li>• 20-year to 28-day MOR</li> <li>• Surface Shortwave Absorptivity</li> <li>• 20-year to 28-day Indirect Tensile Strength</li> </ul>

<b>Distress</b>	<b>Input</b>	<b>Hypersensitive</b>	<b>Very Sensitive</b>	<b>Sensitive</b>
	Base Properties			<ul style="list-style-type: none"> <li>• Base Slab Friction</li> <li>• Resilient Modulus</li> <li>• Thickness</li> </ul>
	Subgrade Properties			
	Other Properties		<ul style="list-style-type: none"> <li>• Bar Diameter</li> </ul>	<ul style="list-style-type: none"> <li>• Steel Depth</li> <li>• Traffic Volume</li> <li>• Edge Support LTE</li> </ul>
IRI	PCC/Steel Properties	<ul style="list-style-type: none"> <li>• Thickness</li> <li>• 28-day MOR</li> </ul>	<ul style="list-style-type: none"> <li>• 20-year to 28-day MOR</li> <li>• UW</li> <li>• Percent Steel</li> <li>• 28-day Indirect Tensile Strength</li> <li>• 28-day MOE</li> <li>• W/cm</li> <li>• Cement Content</li> <li>• CTE</li> </ul>	<ul style="list-style-type: none"> <li>• Surface Shortwave Absorptivity</li> <li>• Poisson's Ratio</li> <li>• 20-year to 28-day Indirect Tensile Strength</li> </ul>
	Base Properties		<ul style="list-style-type: none"> <li>• Resilient Modulus</li> </ul>	<ul style="list-style-type: none"> <li>• Base Slab Friction</li> <li>• Thickness</li> </ul>
	Subgrade Properties		<ul style="list-style-type: none"> <li>• Resilient Modulus</li> </ul>	
	Other Properties		<ul style="list-style-type: none"> <li>• Bar Diameter</li> <li>• Traffic Volume</li> <li>• Steel Depth</li> </ul>	<ul style="list-style-type: none"> <li>• Edge Support LTE</li> <li>• Construction Month</li> </ul>

Based on that research, it was recommended that for high-value projects, level 1 inputs would need to be found through laboratory testing (Schwartz et al. 2011). This is especially true for CRCP pavements because of the hypersensitive nature of the material properties.

Similarly, a study was performed looking at the impact of CTE, MOE, MOR, and compressive strength on predicted performance of JPCP using AASHTOWare Pavement ME Design. It was concluded that for an increase in CTE, the associated distresses will increase (Sabih and Tarefder 2016). This adverse effect of CTE on predicted performance is illustrated in figure 14. In the same study, the predicted distresses decreased as the MOE, MOR, and compressive strength increased in value. One would expect a stiffer and stronger pavement structure to deteriorate at a slower rate than a weaker pavement. The impact of increased MOE on predicted distress is presented in figure 15; the graphs for MOR and compressive strength show a similar trend.

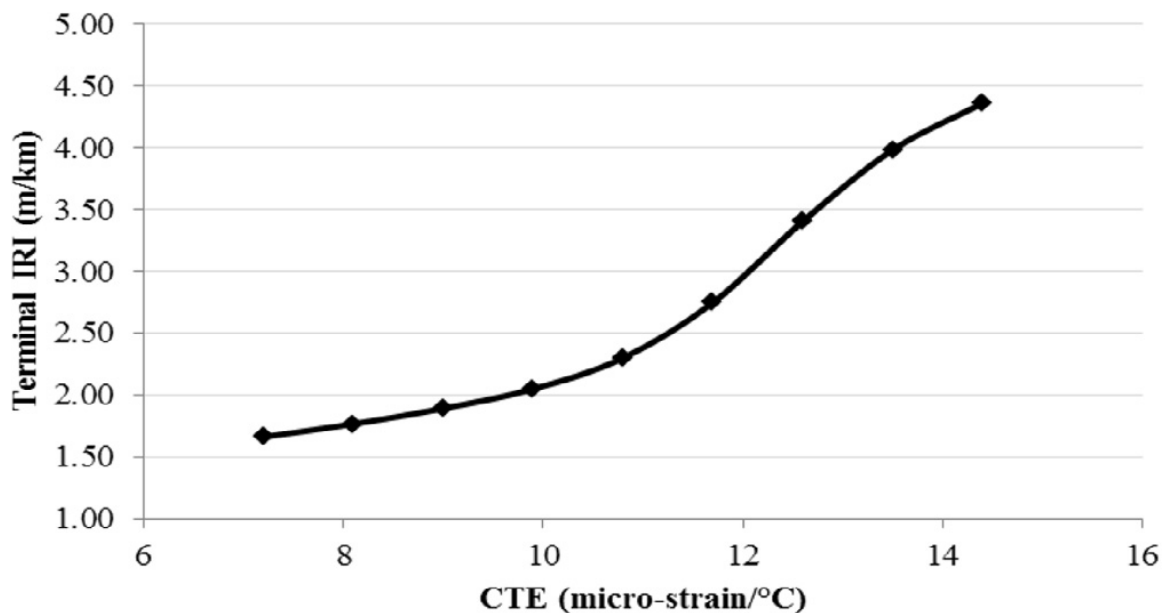


**Figure 14. Graph. CTE's effect on IRI. (Sabih and Tarefder 2016)**

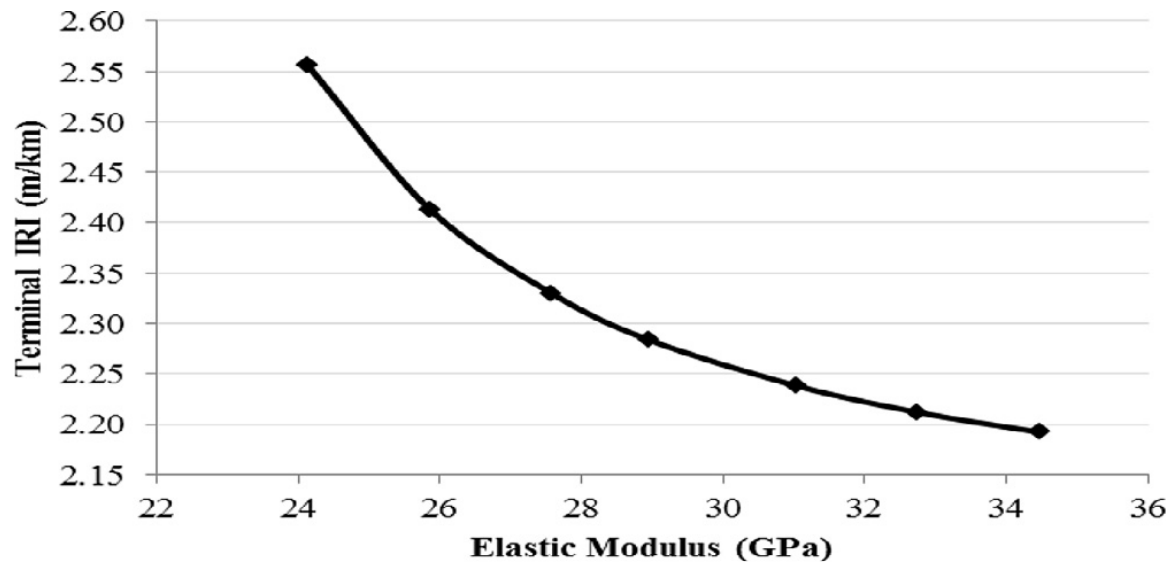


**Figure 15. Graph. MOE's effect on IRI. (Sabih and Tarefder 2016)**

## CHAPTER 3. MOVEMENT TOWARD MEPDG

According to an MEPDG national user group meeting that took place in December 2016, 13 states have implemented the MEDPG for concrete pavements and 32 states have plans to implement the MEPDG for concrete pavements. These states are shown in figure 16. States such as Tennessee, North Carolina, South Carolina, and Alabama with similar geographic location as Georgia are planning to implement MEPDG. These states are in a preliminary stage of this process, completing projects related to traffic, climate, and local calibration of the transfer functions. Because of the preliminary nature of their studies, they are not included in this chapter. Studies from Florida and Mississippi are discussed in further detail, along with Georgia.

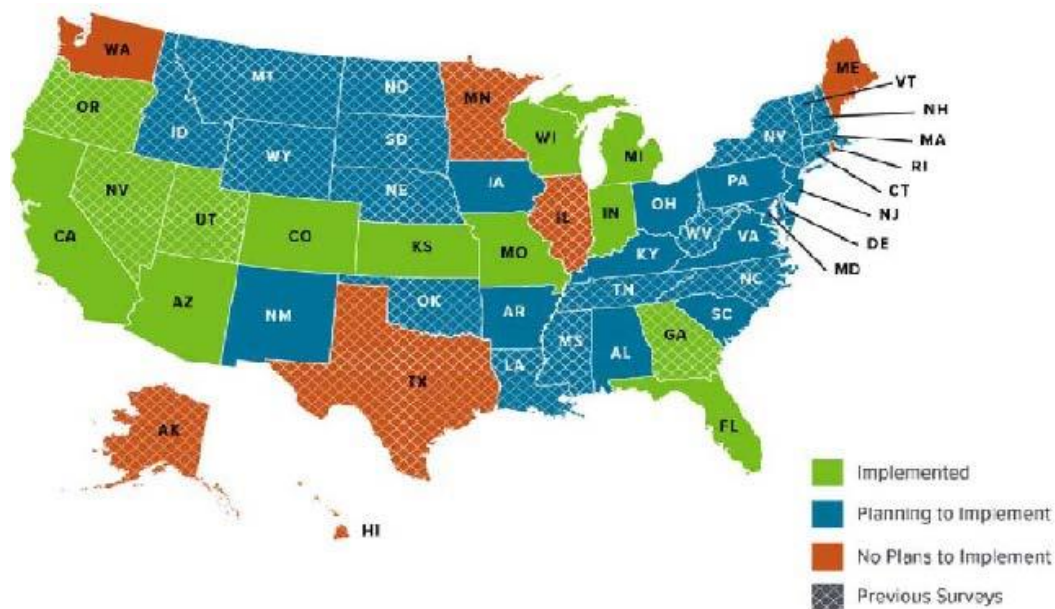


**Figure 16. Map. State status on MEPDG use for concrete pavements. (Merine 2018)**



## **GEORGIA DOT**

Since 2010, GDOT has started moving toward using the MEPDG for rigid pavement design. As a first step, GDOT has begun to establish a concrete material library to utilize the AASHTOWare Pavement ME Design, which uses mechanistic–empirical design principles.

Significant work has been conducted to develop an initial material input library for concrete pavement design in Georgia. Kim (2012) developed a coefficient of thermal expansion database for granite, dolomite, and limestone materials. That study examined seven different material variables that affect CTE values and ultimately determined the significance of each. The material variables included: coarse aggregate type, coarse aggregate content, fine aggregate type, fly ash type, fly ash percent content, w/cm, and air content. A total of 68 batches with 5 replicates were produced, varying the concrete mixture attributes, and tested for CTE and compressive strength. These mixtures are listed in table 15.

**Table 15. Concrete mixture design for CTE testing. (Kim 2012)**

<b>CTE No.</b>	<b>Batch No.</b>	<b>Granite CA (lb/yd<sup>3</sup>)</b>	<b>Dolomite CA (lb/yd<sup>3</sup>)</b>	<b>Limestone CA (lb/yd<sup>3</sup>)</b>	<b>MS (lb/yd<sup>3</sup>)</b>	<b>NS (lb/yd<sup>3</sup>)</b>	<b>C-Ash (lb/yd<sup>3</sup>)</b>	<b>F-Ash (lb/yd<sup>3</sup>)</b>	<b>Cement (lb/yd<sup>3</sup>)</b>	<b>Air Content (%)</b>	<b>Slump (in.)</b>
1	1	2100	0	0	950	0	20	0	530	3	2
2	2	2100	0	0	950	0	20	0	530	6	2
3	17	2100	0	0	950	0	160	0	460	3	2
4	18	2100	0	0	950	0	160	0	460	6	2
5	33	2100	0	0	950	0	0	20	530	3	2
6	34	2100	0	0	950	0	0	20	530	6	2
7	49	2100	0	0	950	0	0	160	460	3	2
8	50	2100	0	0	950	0	0	160	460	6	2
9	5	2100	0	0	0	950	20	0	530	3	2
10	6	2100	0	0	0	950	20	0	530	6	2
11	21	2100	0	0	0	950	160	0	460	3	2
12	22	2100	0	0	0	950	160	0	460	6	2
13	37	2100	0	0	0	950	0	20	530	3	2
14	38	2100	0	0	0	950	0	20	530	6	2
15	53	2100	0	0	0	950	0	160	460	3	2
16	54	2100	0	0	0	950	0	160	460	6	2
17	3	1150	0	0	1900	0	20	0	530	3	2
18	4	1150	0	0	1900	0	20	0	530	6	2
19	19	1150	0	0	1900	0	160	0	460	3	2
20	20	1150	0	0	1900	0	160	0	460	6	2
21	35	1150	0	0	1900	0	0	20	530	3	2
22	36	1150	0	0	1900	0	0	20	530	6	2
23	51	1150	0	0	1900	0	0	160	460	3	2
24	52	1150	0	0	1900	0	0	160	460	6	2
25	7	1150	0	0	0	1900	20	0	530	3	2
26	8	1150	0	0	0	1900	20	0	530	6	2
27	23	1150	0	0	0	1900	160	0	460	3	2
28	24	1150	0	0	0	1900	160	0	460	6	2
29	39	1150	0	0	0	1900	0	20	530	3	2
30	40	1150	0	0	0	1900	0	20	530	6	2
31	55	1150	0	0	0	1900	0	160	460	3	2
32	56	1150	0	0	0	1900	0	160	460	6	2
33	9	0	2100	0	950	0	20	0	530	3	2
34	10	0	2100	0	950	0	20	0	530	6	2
35	25	0	2100	0	950	0	160	0	460	3	2
36	26	0	2100	0	950	0	160	0	460	6	2
37	41	0	2100	0	950	0	0	20	530	3	2

<b>CTE No.</b>	<b>Batch No.</b>	<b>Granite CA (lb/yd<sup>3</sup>)</b>	<b>Dolomite CA (lb/yd<sup>3</sup>)</b>	<b>Limestone CA (lb/yd<sup>3</sup>)</b>	<b>MS (lb/yd<sup>3</sup>)</b>	<b>NS (lb/yd<sup>3</sup>)</b>	<b>C-Ash (lb/yd<sup>3</sup>)</b>	<b>F-Ash (lb/yd<sup>3</sup>)</b>	<b>Cement (lb/yd<sup>3</sup>)</b>	<b>Air Content (%)</b>	<b>Slump (in.)</b>
38	42	0	2100	0	950	0	0	20	530	6	2
39	57	0	2100	0	950	0	0	160	460	3	2
40	58	0	2100	0	950	0	0	160	460	6	2
41	13	0	2100	0	0	950	20	0	530	3	2
42	14	0	2100	0	0	950	20	0	530	6	2
43	29	0	2100	0	0	950	160	0	430	3	2
44	30	0	2100	0	0	950	160	0	430	6	2
45	45	0	2100	0	0	950	0	20	530	3	2
46	46	0	2100	0	0	950	0	20	530	6	2
47	61	0	2100	0	0	950	0	160	460	3	2
48	62	0	2100	0	0	950	0	160	460	6	2
49	11	0	1150	0	1900	0	20	0	530	3	2
50	12	0	1150	0	1900	0	20	0	530	6	2
51	27	0	1150	0	1900	0	160	0	460	3	2
52	28	0	1150	0	1900	0	160	0	460	6	2
53	43	0	1150	0	1900	0	0	20	530	3	2
54	44	0	1150	0	1900	0	0	20	530	6	2
55	59	0	1150	0	1900	0	0	160	460	3	2
56	60	0	1150	0	1900	0	0	160	460	6	2
57	15	0	1150	0	0	1900	20	0	530	3	2
58	16	0	1150	0	0	1900	20	0	530	6	2
59	31	0	1150	0	0	1900	160	0	460	3	2
60	32	0	1150	0	0	1900	160	0	460	6	2
61	47	0	1150	0	0	1900	0	20	530	3	2
62	48	0	1150	0	0	1900	0	20	530	6	2
63	63	0	1150	0	0	1900	0	160	460	3	2
64	64	0	1150	0	0	1900	0	160	460	6	2
65	65	0	0	2100	950	0	160	0	460	3	2
66	66	0	0	1150	1900	0	160	0	460	3	2
67	67	0	0	2100	0	950	160	0	460	3	2
68	68	0	0	1150	0	1900	160	0	460	3	2

Several conclusions were made after analyzing the test results from the 68 mixtures:

- The most significant factors affecting CTE in order of magnitude are: aggregate type, stone volume, and sand type. The aggregate content of concrete mixtures can be as high as 80 percent by volume. Due to this higher volume, it has more impact on the thermal properties of the mixture.
- The impact of each variable is different due to the varying volume of each in concrete mixtures.
- Limestone was discovered during this study to have considerably lower CTE values than granite and dolomite mixtures, with dolomite and granite mixtures having similar CTE values, as shown in table 16.
- Relatively higher CTE values were also observed when natural sand (NS) was used in mixtures compared to the mixtures with manufactured sand (MS). The effects of aggregate proportion on CTE are shown in table 17.
- When high fly ash contents were used in mixtures, class C-fly ash mixtures were observed to have significantly higher CTE values than mixtures containing class F-fly ash. The results of fly ash type are shown in table 18.

It was recommended by that study that more quarries be tested in order to develop a complete database for CTE values in the state of Georgia (Kim 2012). In addition, it was recommended that the laboratory-tested values be compared and validated with in situ pavement conditions.

**Table 16. Aggregate type effect on CTE. (Kim 2012)**

Coarse Aggregate	Average CTE	Standard Deviation
Limestone	3.836 $\mu\epsilon / ^\circ\text{F}$ (6.905 $\mu\epsilon / ^\circ\text{C}$ )	0.44 $\mu\epsilon / ^\circ\text{F}$ (0.792 $\mu\epsilon / ^\circ\text{C}$ )
Granite	4.751 $\mu\epsilon / ^\circ\text{F}$ (8.552 $\mu\epsilon / ^\circ\text{C}$ )	0.4 $\mu\epsilon / ^\circ\text{F}$ (0.72 $\mu\epsilon / ^\circ\text{C}$ )
Dolomite	4.847 $\mu\epsilon / ^\circ\text{F}$ (8.725 $\mu\epsilon / ^\circ\text{C}$ )	0.35 $\mu\epsilon / ^\circ\text{F}$ (0.63 $\mu\epsilon / ^\circ\text{C}$ )

**Table 17. Aggregate proportion effect on CTE. (Kim 2012)**

Coarse Aggregate	Stone Volume	Sand Type	Average CTE		Standard Deviation	
			( $\mu\epsilon / ^\circ\text{F}$ )	( $\mu\epsilon / ^\circ\text{C}$ )	( $\mu\epsilon / ^\circ\text{F}$ )	( $\mu\epsilon / ^\circ\text{C}$ )
Granite	High	MS	4.384	7.891	0.115	0.208
		NS	4.906	8.831	0.168	0.303
	Low	MS	4.442	7.996	0.119	0.214
		NS	5.272	9.490	0.184	0.332
Dolomite	High	MS	4.623	8.322	0.126	0.228
		NS	4.982	8.967	0.152	0.273
	Low	MS	4.534	8.162	0.120	0.216
		NS	5.318	9.573	0.131	0.235
Limestone	High	MS	3.367	6.06	0.13	0.233
		NS	3.795	6.831	0.193	0.348
	Low	MS	3.701	6.661	0.137	0.247
		NS	4.481	8.067	0.106	0.19

**Table 18. Fly ash type effect on CTE. (Kim 2012)**

Coarse Aggregate	Volume	Sand Type	Average CTE ( $\mu\epsilon / ^\circ\text{F}$ )				Average CTE ( $\mu\epsilon / ^\circ\text{C}$ )			
			C-Fly Ash		F-Fly Ash		C-Fly Ash		F-Fly Ash	
			Low	High	Low	High	Low	High	Low	High
Granite	High	MS	4.384	4.481	4.454	4.216	7.892	8.065	8.017	7.590
		NS	5.046	4.990	4.895	4.694	9.082	8.982	8.811	8.448
	Low	MS	4.439	4.593	4.454	4.284	7.990	8.268	8.017	7.710
		NS	5.426	5.429	5.218	5.017	9.766	9.772	9.392	9.030
Dolomite	High	MS	4.735	4.681	4.636	4.440	8.523	8.426	8.345	7.993
		NS	5.128	5.085	4.938	4.776	9.231	9.153	8.889	8.596
	Low	MS	4.640	4.598	4.549	4.351	8.351	8.277	8.189	7.831
		NS	5.456	5.393	5.277	5.147	9.821	9.707	9.499	9.264

Kim et al. (2015) investigated the effect of age and materials on CTE of concrete paving mixtures at 28 and 120 days (Kim et al. 2015). Multiple mixtures that were examined for this study contained different types of aggregate and underwent scanning electron microscopy, allowing for the observation of the microstructures of these varying mixtures. The understanding of these microstructures would offer insight regarding the relationship between volume change in concrete and the formation of microcracks. Kim et al. (2015) used statistical analyses, as shown in table 19, to illustrate the CTE values of the specimens measured at 120 days were significantly lower than the values measured at 28 days. Their study observed that age does affect the coefficient of thermal expansion values in concrete specimens.

**Table 19. Statistics of CTE at 28 and 120 days. (Kim et al. 2015)**

Descriptive statistics	CTE ( $\mu\epsilon/^\circ\text{C}$ ) measured at	
	28 days	120 days
Min.	8.05	7.48
Max.	9.87	9.79
Median	8.83	8.39
Mean	8.88	8.50
Stdev	0.66	0.70

GDOT's efforts involve calibrating the distress transfer functions inside the AASHTOWare Pavement ME Design. In a report submitted by Applied Research Associates (ARA), the efforts taken to calibrate the software are detailed (Quintus et al. 2015). Using the *AASHTO Guide for the Local Calibration of the Mechanistic–Empirical Pavement Design Guide*, GDOT looked at the Long Term Pavement Performance Program (LTPP) to accurately represent the performance of Georgia roadways (Quintus et al. 2015). The study examined the calibration of the software for both flexible and rigid pavements. Focusing on rigid pavements, there were 11 LTPP sections for JPCP and 2 for CRCP. Due to changes in GDOT's standard design for JPCP

pavements, non-LTPP test sections were included as samples to encompass newer design features, such as an AC interlayer between the GAB layer and the PCC layer. The locations of these test sections are shown in figure 17.

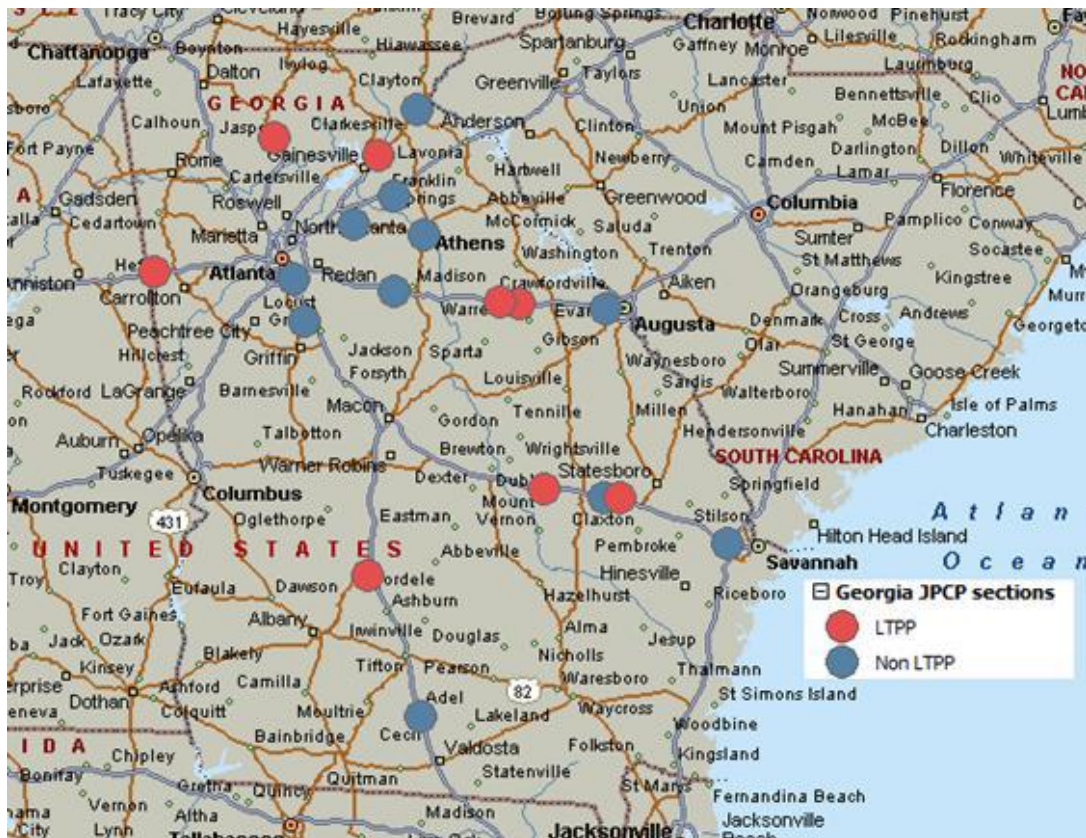


**Figure 17. Map. Rigid test sections. (Quintus et al. 2015)**

When using global transfer functions, significant differences were found between LTPP and non-LTPP data when comparing their distresses with predicted distresses from AASHTOWare Pavement ME Design. Transfer functions predict distresses such as faulting and fatigue cracking, which directly relate to pavement smoothness (Quintus et al. 2015). After data comparison, the transfer function coefficients were modified from the global values, as shown in table 20. After calibrating the transfer functions for Georgia, ARA developed an input guide for GDOT engineers to use when designing pavement structures, *The GDOT Pavement ME Design User Input Guide*

(Quintus et al. 2015). This guide outlines the procedure, using a checklist to guide engineers to select input values for each variable of pavement design. *The GDOT Pavement ME Design User Input Guide* has been updated in 2020 (Kim et al. 2020).

**Table 20. Transfer function coefficients. (Quintus et al. 2015)**

<b>JPCP Faulting</b>		
<b>Transfer Function Coefficient</b>	<b>Global Value</b>	<b>GDOT Value</b>
C1	1.0184	0.595
C2	0.91656	1.636
C3	0.0021848	0.00217
C4	0.000883739	0.00444
C5	250	250
C6	0.4	0.47
C7	1.83312	7.3
C8	400	400
Standard Deviation	$\text{Pow}(0.0097 \cdot \text{FAULT}, 0.5178) + 0.014$	$0.07162 \cdot \text{Pow}(\text{FAULT}, 0.368) + 0.00806$
<b>JPCP Mid-Slab Cracking</b>		
<b>Transfer Function Coefficient</b>	<b>Global Value</b>	<b>GDOT Value</b>
C1	2.0	2.0
C2	1.22	1.22
C4	1.00	0.52
C5	-1.98	-2.17
Standard Deviation	$\text{Pow}(5.3116 \cdot \text{CRACK}, 0.3903) + 2.99$	$3.5522 \cdot \text{Pow}(\text{CRACK}, 0.3415) + 0.75$
<b>CRCP Punchout</b>		
<b>Transfer Function Coefficient</b>	<b>Global Value</b>	<b>GDOT Value</b>
C1	2	2
C2	1.22	1.22
C3	216.8421	107.73
C4	33.15789	2.475
C5	-0.58947	-0.785
Standard Deviation	$2 + 2.2593 \cdot \text{Pow}(\text{PO}, 0.4882)$	$2.208 \cdot \text{Pow}(\text{PO}, 0.5316)$



## FLORIDA DOT

A project similar to this study of material properties and their impact on AASHTOWare Pavement ME Design's predicted performance was completed by the Florida Department of Transportation (FDOT) in 2008. This project tested three different concrete mixtures for MEPDG design input level mechanical and thermal properties for rigid pavement designs. The mixture specifics and tests performed are provided in table 21 and table 22, respectively.

This project specifically investigated how different MEPDG input levels would affect the pavement design thickness. The material properties for each design input are listed in table 23, table 24, and table 25. These material properties for the three mixtures were used as inputs to determine the optimized concrete layer thickness. The resulting optimized slab thicknesses are presented in table 26.

**Table 21. Mixture design by Florida State. (Ping 2008)**

	<b>Mixture 1</b>	<b>Mixture 2</b>	<b>Mixture 3</b>
<b>Cement</b>	511 lb	415 lb	470 lb
<b>Fly Ash</b>	132 lb	105 lb	—
<b>Coarse Aggregate</b>	1,750 lb	1,900 lb	1,921 lb
<b>Fine Aggregate</b>	1,191 lb	1,278 lb	1,235 lb
<b>Water</b>	279.1 lb	258 lb	267 lb
<b>Target Strength</b>	4,500 psi	3,000 psi	3,000 psi
<b>Target Slump</b>	1.5–4.5 in.	2.0–4.0 in.	3.0–5.0 in
<b>Target Air</b>	1.0–6.0%	3.0–6.0%	3.0–6.0%
<b>Target Unit Weight</b>	143.1 pcf	146.6 pcf	144.2 pcf
<b>W/C Ratio</b>	0.43	0.50	0.57

— No data

**Table 22. Tests performed by Florida State. (Ping 2008)**

Property Tested	Test Interval
Slump	Batching day
Temperature	Batching day
Air Content	Batching day
Compressive Strength	7, 14, 28, 90 days of age
Splitting Tensile Strength	28, 90 days of age
Modulus of Elasticity	7, 14, 28, 49, 70, 90 days of age
Poisson's Ratio	7, 14, 28, 49, 70, 90 days of age
Coefficient of Thermal Expansion	7, 28, 90 days of age

**Table 23. Input values level 1, Florida State. (Ping 2008)**

	Unit	MIX-01	MIX-02	MIX-03
CTE	$\mu\text{in/in./}^{\circ}\text{F}$	6.79	6.84	5.99
Poisson's Ratio	—	0.23	0.27	0.21
MOE (7-day)	psi	4,370,000	4,530,000	3,290,000
MOE (14-day)	psi	4,590,000	4,590,000	3,470,000
MOE (28-day)	psi	4,420,000	4,360,000	3,680,000
MOE (90-day)	psi	4,180,000	4,905,000	4,020,000
20-year/28-day Ratio	—	1.2		
MOR (7-day)	psi	714	777	545
MOR (14-day)	psi	745♦	825♦	604♦
MOR (28-day)	psi	776	873	662
MOR (90-day)	psi	844	831	707
20-year/28-day Ratio	—	1.2		

♦ Denotes where tested values are different from expected ranges. Averages of all tests are used instead in these cases.

— No data

**Table 24. Input values level 2, Florida State. (Ping 2008)**

	<b>Unit</b>	<b>MIX-01</b>	<b>MIX-02</b>	<b>MIX-03</b>
CTE	$\mu\text{in/in.}/^{\circ}\text{F}$	6.44	6.67	6.92
Poisson's Ratio	–	0.23	0.27	0.21
Compressive Strength (7-day)	psi	4,832	6,183	3,489
Compressive Strength (14-day)	psi	6,067	7,442	4,225
Compressive Strength (28-day)	psi	6,908	8,256	4,883
Compressive Strength (90-day)	psi	7,856	9,188	5,794
20-year/28-day Ratio	–	1.2		

– No data

**Table 25. Input values level 3, Florida State. (Ping 2008)**

	<b>Unit</b>	<b>MIX-01</b>	<b>MIX-02</b>	<b>MIX-03</b>
CTE	$\mu\text{in/in.}/^{\circ}\text{F}$	7		
Poisson's Ratio	–	0.25		
MOR (28-day)	psi	776	873	662
MOE (28-day)	psi	4,420,000	4,360,000	3,680,000

– No data

**Table 26. Optimized thicknesses, Florida State. (Ping 2008)**

	<b>Unit</b>	<b>Mix-01</b>	<b>Mix-02</b>	<b>Mix-03</b>
<b>Level-1 thickness (h)</b>	in.	8.75	8.25	9.00
<b>Level-2 thickness (h)</b>	in.	10.25	10.75	13.50
<b>Level-3 thickness (h)</b>	in.	10.50	7.50	12.00

One would expect the optimized thickness to increase as the input level goes from 1 to 3. This is because level 3 is the most conservative input level, which should yield the largest slab

thicknesses. Only Mix-01 displays the expected increase in optimized layer thickness. The unexpected results of the other two mixtures are explained when comparing flexural and compressive strength data. For level 2 designs, compressive strength values are used for 7, 14, 28, and 90 days of age, which AASHTOWare Pavement ME Design then uses to estimate the MOR. For Mix-02, the 28-day MOR value is unexpectedly high, and the value predicted in the level 2 analysis is much lower, resulting in a larger slab thickness. Similarly, the reduction in slab thickness for level 3 is explained due to only the 28-day compressive strength being used, rather than the full 90-day test data. The compressive and flexural values for each of the three mixtures are presented in figure 18 and figure 19, respectively. This Florida DOT study highlights the sensitive nature of AASHTOWare Pavement ME Design to MOR inputs. The equation used to estimate MOR from compressive strength was proven to be inaccurate in two out of the three mixtures, resulting in inconsistent design thicknesses.

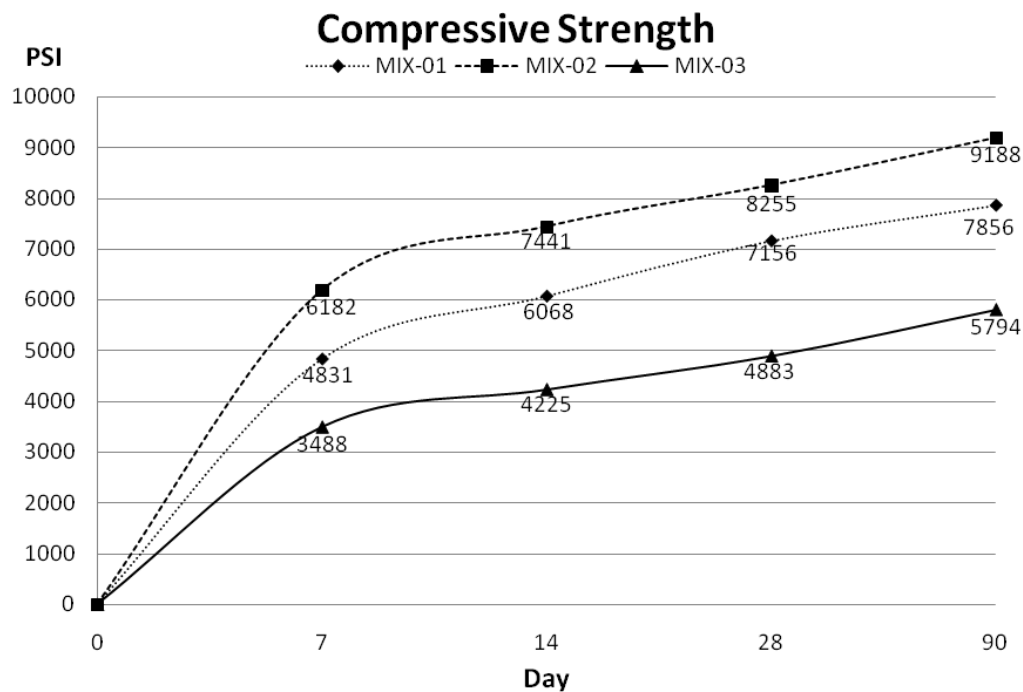


**Figure 18. Line graph. Compressive strength of Mix-01, -02, and -03, Florida State. (Ping 2008)**

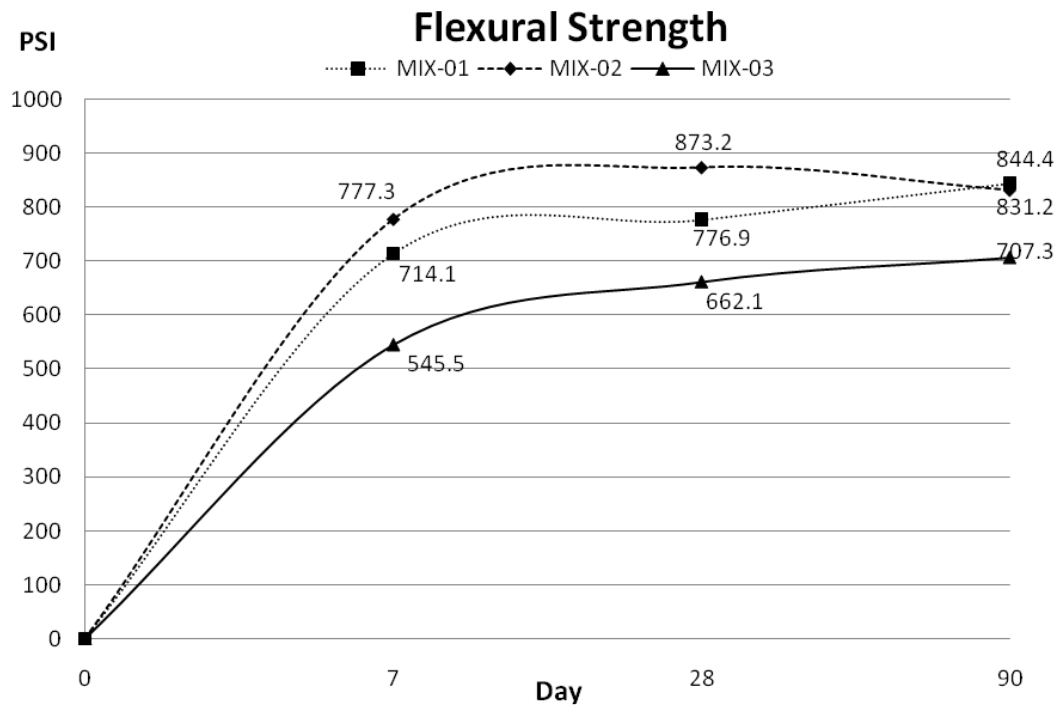


**Figure 19. Line graph. Flexural strength of Mix-01, 02, and 03, Florida State. (Ping 2008)**

## MISSISSIPPI DOT

A study was performed for the Mississippi Department of Transportation (MDOT) that analyzed 20 different concrete mixtures and tested for PCC material properties required by AASHTOWare Pavement ME Design. Properties that were examined included: MOR, compressive strength, MOE, Poisson's ratio, CTE, and shrinkage (Rao 2014). Additionally, the study created statistical models to estimate 90-day data from 28-day values to be used for level 2 designs. In addition, this study included concrete mixtures with five different coarse aggregates and four different cementitious material blends. The mixtures tested are listed in table 27. Averages from the 28-day test results are presented in table 28. Values were all above MDOT-required minimums for rigid pavements.

**Table 27. MDOT mixtures. (Rao 2014)**

MIX_ID	Cast date in 2014	Cementitious_ID <sup>1</sup>	CA_ID <sup>2</sup>	Aggregate type	Total cementitious (lb/yd <sup>3</sup> )	Coarse aggregate (lb/yd <sup>3</sup> )	Fine aggregate (lb/yd <sup>3</sup> )	Water (lb/yd <sup>3</sup> )	AEA (fl Oz)	Type A-WR (fl Oz)	w/c
1	4/16	1	1	Chert	548	1929	1129.6	229.2	3.4	27.4	0.42
2	4/18	2	1	Chert	548	1929	1089.6	222.9	8.2	27.4	0.41
3	5/2	3	1	Chert	548	1929	1149.4	210.4	2.7	27.4	0.38
4	5/5	4	1	Chert	548	1929	1103.5	229.2	3.1	30.3	0.42
5	5/7	1	2	Limestone	548	1993	1180.1	231.3	2.7	27.4	0.42
6	5/9	2	2	Limestone	548	1993	1134.6	233.3	6.5	27.4	0.43
7	5/13	3	2	Limestone	548	1993	1183.3	225.0	3.0	29.6	0.41
8	5/15	4	2	Limestone	548	1993	1151.3	237.5	5.4	29.2	0.43
9	5/19	1	3	Limestone	548	2029	1228.2	231.3	2.1	27.4	0.42
10	5/21	2	3	Limestone	548	2029	1171.7	233.3	4.4	27.4	0.43
11	5/27	3	3	Limestone	548	2029	1231.5	220.8	3.7	27.4	0.40
12	6/2	4	3	Limestone	548	2029	1191.1	237.5	3.5	27.4	0.43
13	6/9	1	4	Chert	548	2031	1152.0	208.3	2.7	27.4	0.38
14	6/12	2	4	Chert	548	2031	1109.2	208.3	4.7	27.4	0.38
15	6/16	3	4	Chert	548	2031	1160.7	195.8	2.7	27.4	0.36
16	6/18	4	4	Chert	548	2031	1120.4	216.7	3.1	27.4	0.40
17	6/24	1	5	Chert	548	2012	1079.1	229.2	2.7	27.4	0.42
18	6/26	2	5	Chert	548	2012	1017.1	233.3	5.5	27.4	0.43
19	6/30	3	5	Chert	548	2012	1076.8	216.7	2.7	27.4	0.40
20	7/2	4	5	Chert	548	2012	1047.5	229.2	3.2	27.4	0.42

**Table 28. MDOT 28-day test averages. (Rao 2014)**

<b>MIX ID</b>	<b>Age (days)</b>	<b>Compressive Strength (psi)</b>	<b>MOR (psi)</b>	<b>MOE (psi)</b>	<b>Poisson's Ratio</b>	<b>Unit Weight (lb/ft<sup>3</sup>)</b>
1	28	6,648	786	5,883,333	0.17	142.2
2	28	5,756	752	5,233,333	0.16	141.2
3	28	7,133	783	6,333,333	0.14	143.8
4	28	7,020	843	5,933,333	0.15	143.4
5	28	6,365	736	5,483,333	0.19	144.4
6	28	5,968	721	5,400,000	0.20	144.5
7	28	7,973	816	6,366,667	0.23	145.7
8	28	8,041	913	5,416,667	0.19	146.1
9	28	7,316	928	6,683,333	0.21	149.3
10	28	6,812	933	6,583,333	0.22	148.6
11	28	7,296	973	6,650,000	0.21	147.7
12	28	7,268	1,047	6,550,000	0.23	147.04
13	28	6,878	858	6,583,333	0.17	146.4
14	28	6,715	850	6,566,667	0.14	144.3
15	28	7,617	901	6,666,667	0.18	145.6
16	28	7,270	1,004	7,533,333	0.15	145.66
17	28	7,217	811	5,833,333	0.14	143.0
18	28	6,631	764	5,700,000	0.15	141.0
19	28	8,237	844	6,250,000	0.15	144.5
20	28	7,908	928	5,816,667	0.15	144.4

Using material properties from the 20 mixtures, models were developed in order to predict 90-day values using 28-day data. These models have different regression coefficients depending upon the type of coarse aggregate. For flexural strength, it was recommended to use either MDOT Model 3 or 4; the regression coefficients are presented in table 29. For MOE, it was recommended to use MDOT Model 9. The regression coefficients for MDOT Model 9 are listed in table 30.

$$MR = a * f_c'^{0.5} (psi) \quad (\text{MDOT Model 3})$$

$$MR = a * f_c'^b (psi) \quad (\text{MDOT Model 4})$$

$$E = a * f_c'^b (psi) \quad (\text{MDOT Model 9})$$

**Table 29. Flexural model coefficients. (Rao 2014)**

Model	CA_ID	a	b
3	1	9.7816	—
	2	9.4012	—
	3	11.028	—
	4	10.805	—
	5	9.6891	—
4	1	7.5366	0.5297
	2	7.6295	0.5235
	3	2.2333	0.6801
	4	1.7049	0.709
	5	6.9302	0.5376

**Table 30. MDOT Model 9 regression coefficients. (Rao 2014)**

Model	CA_ID	a	b
9	1	229467	0.3652
	2	523594	0.2693
	3	2000000	0.1585
	4	654322	0.2627
	5	203805	0.3768



## CHAPTER 4. PROBLEM STATEMENT

Traditionally, pavements in the United States were designed using manuals derived from empirical relationships based on the observed failure of pavements. In 2002, the National Cooperative Highway Research Program (NCHRP) produced the *NCHRP Project 1-37A: Development of the 2002 Guide for the Design of New and Rehabilitated Pavement Structures (1998–2004)*, which proposed implementing the use of a mechanistic understanding of materials to aid in pavement design. Since then, design manuals have been produced incorporating this principle. The most current manual is the *AASHTOWare Pavement ME Design (2011)*, which is commonly referred to as the *Mechanistic–Empirical Pavement Design Guide*. These manuals have been slow to be implemented throughout the United States for a number of reasons, but it is primarily due to the large volume of inputs that must be calibrated for individual states in order to make the software viable.

GDOT is in the process of implementing the use of the MEPDG. In 2015, with the aid of the ARA, GDOT produced an input guide to aid designers in using the MEPDG for Georgia pavements. In addition, GDOT has funded numerous research projects to calibrate the software to Georgia pavement mixtures. In one study, the CTEs for certain mixtures in Georgia were tested for future use in the MEPDG. However, a need remains for additional design inputs to be studied in greater detail and expanded to include additional mixtures.

The overall goal of this research is to establish a database of values for pavement designers to use when designing with the MEPDG. This database will allow engineers to complete level 1, 2, and 3 designs using AASHTOWare Pavement ME Design for a variety of mixtures used in rigid pavements. This database will include laboratory-tested values for compressive strength, Young's modulus, MOR, CTE, thermal conductivity, ultimate shrinkage, and heat capacity. Additionally,

this report aims to look at which of these values are the most critical for input into AASHTOWare Pavement ME Design. Sensitivity tests are conducted for each of the variables mentioned, using the materials tested and reported for the MEPDG database. Recommendations are provided for each of the design levels and their inputs.

With the completion of this concrete materials database, GDOT engineers will be able to confidently complete level 1, 2, and 3 designs for rigid pavements. Along with the completion of the concrete materials database, this study aims to use a statistical analysis and a machine-learning approach to provide an in-depth understanding of a concrete mixture's inputs and characteristics and the role that they play in the mechanical and thermal properties of the concrete.

## **CHAPTER 5. MATERIALS**

This study was designed to test how different mixture design variables affect concrete material properties and to analyze their effect on pavement performance. To understand the various impacts of the mixture variables, the properties of the materials used in this study are documented here.

### **AGGREGATES**

To obtain a representative sample of the aggregates used in Georgia's pavements, the research team selected four different quarries for coarse aggregate and one quarry for fine aggregate. Only one quarry was selected for fine aggregate since material properties are fairly consistent for natural sands. Additionally, NS are more commonly used in Georgia due to their availability and superior finishing qualities when compared to manufactured sands. It was deemed that a representative sample of coarse aggregate would consist of one quarry from North Georgia, one from Middle/South Georgia, and two from Metro Atlanta. Only one quarry was selected for both Middle and South Georgia since there are no quarries south of Macon or Augusta (located in Middle Georgia). Any project south of Macon or Augusta should use one of these quarries for their coarse aggregate. The five quarries that were selected are listed in table 31, followed by a map in figure 20.

**Table 31. Quarries used.**

Location	Company	Quarry Number	Rock Type	Mixtures Using Quarry	Times Used in Study
Metro	Vulcan	Kennesaw 46C	Meta-quartz Diorite, Group II	3,4	2
	Vulcan	Stockbridge 50C	Granite Gneiss, Group II	5,6,7,9	4
North	Vulcan	Adairsville 120C	Dolomite, Group I	8,10	2
Mid State	Martin Marietta	Ruby 054C	Gneiss/Amphibolite, Group II	1,2,11,12	4
Mid State	Atlanta Sand	Roberta 002F	Alluvial/Marine Sand	1–12	12

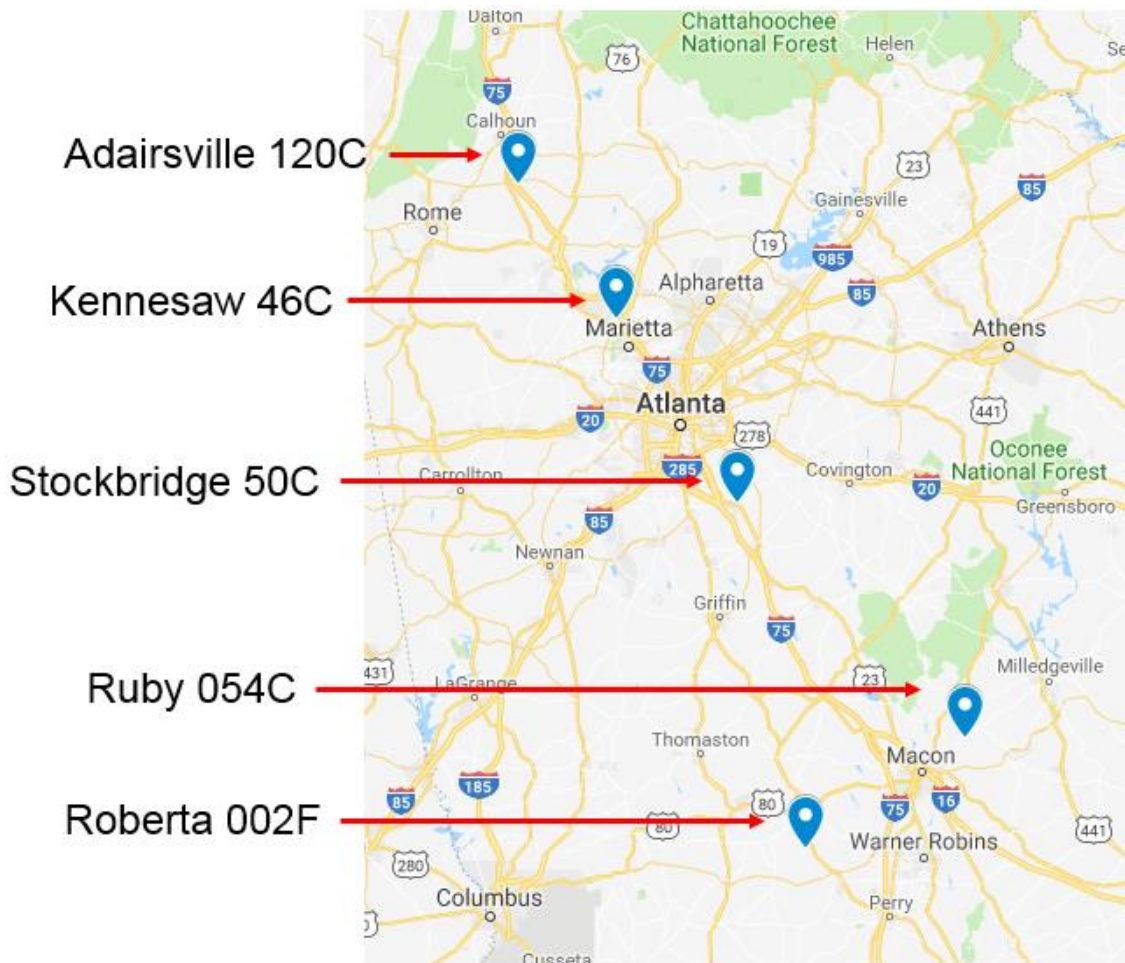


**Figure 20. Map. Quarry locations. (Google 2019)**

A #57 stone gradation was used for all coarse aggregates, as specified in GDOT Section 800. The specific gravity (SG) and absorption capacity for the coarse aggregates are provided in table 32. Further, the *ASTM C33* limits for #57 stone are shown in table 33. The gradation of the coarse aggregates was almost identical, as shown in figure 21. The material data sheets for each quarry are found in appendix A.

**Table 32. Specific gravity and absorption of aggregates.**

Quarry	Specific Gravity (SSD <sup>a</sup> )	Absorption Capacity (%)
Adairsville 120C	2.847	0.08
Kennesaw 46C	2.763	0.65
Stockbridge 50C	2.625	0.60
Ruby 054C	2.732	0.50

<sup>a</sup> Saturated surface dry

**Table 33. Coarse Aggregate Gradation Limits  
#57 ASTM C33**

Sieve Size		Percent Passing
US (in.)	Metric (mm)	(%)
1.5	37.5	100
1	25	95–100
0.5	12.5	25–60
4	4.74	0–10
8	2.36	0–5

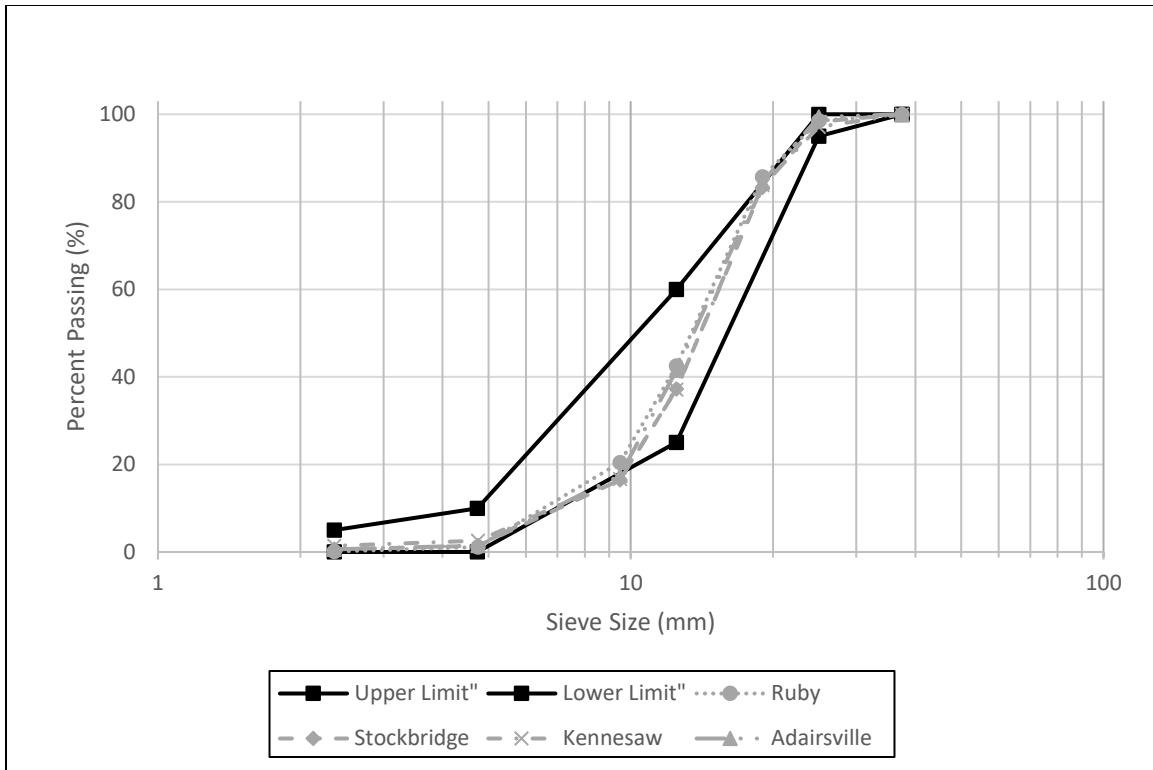


**Figure 21. Line graph. Coarse aggregate gradation.**

The fine aggregate gradation follows the requirements outlined in GDOT Section 801 instead of *ASTM C33*. The percent passing requirements for this gradation are listed in table 34 and the fine aggregate gradation, along with the upper and lower limit requirements, are shown in figure 22. The sand had a fineness modulus of 2.297. The material data sheet for the fine aggregate is located in appendix A.

**Table 34. Fine aggregate gradation limits,  
GDOT Section 801.**

Sieve Size		Percent Passing
US (in.)	Metric (mm)	(%)
0.375	9.5	100
4	4.75	95–100
16	1.18	45–95
30	0.3	8–30
100	0.15	1–10
200	0.075	0–3

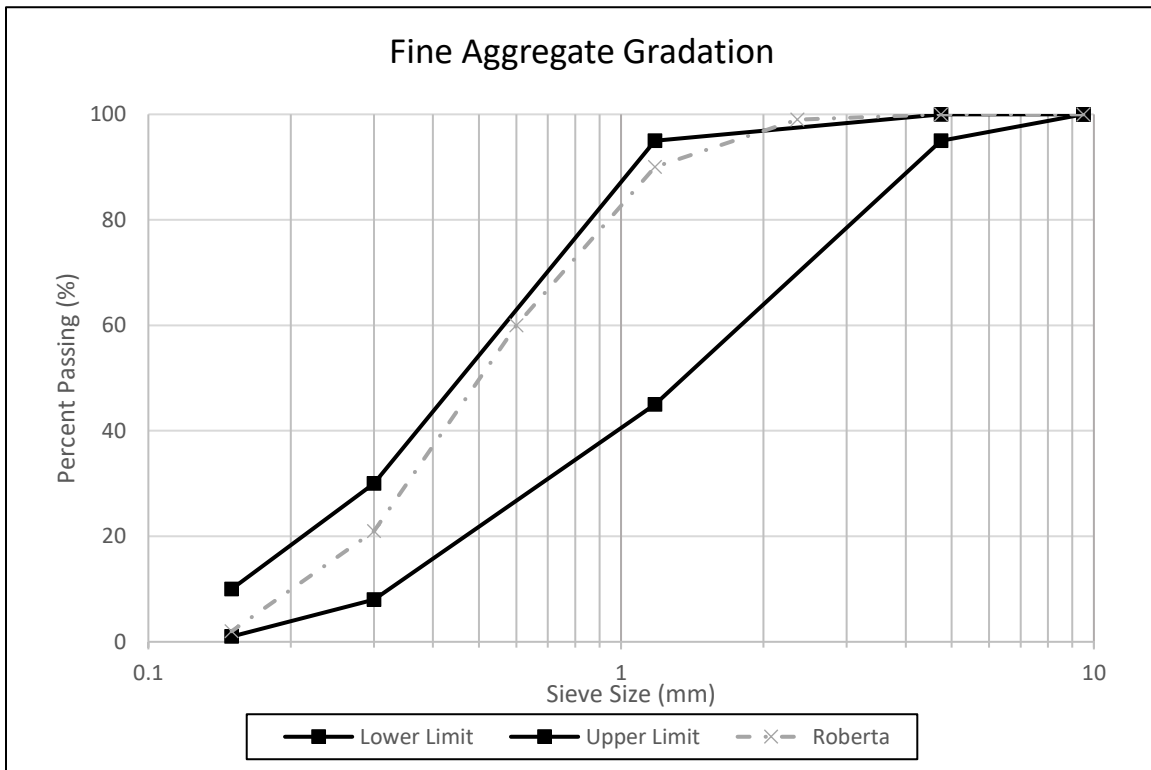


**Figure 22. Line graph. Fine aggregate gradation.**

The texture and angularity of two of the coarse aggregates were compared: Stockbridge and Adairsville. This analysis was performed in order to compare mixtures using granite and dolomite. Angularity is a major factor affecting concrete compressive and flexural strength;

therefore, it was important to be able to quantify differences in the aggregate's shapes. The angularities of the two aggregates were measured using an image analyzer from the University of Illinois. It was determined that the dolomite from the Adairsville quarry was more angular than the granite from the Stockbridge quarry. The mean angularity of Adairsville dolomite was 427.41, while the mean angularity of Stockbridge was 346.13. One would expect the dolomite to exhibit higher compressive strength values due to its increased angularity. Examples of the images collected are shown in figure 23 and figure 24.



**Figure 23. Images. Stockbridge granite rock.**



**Figure 24. Images. Adairsville dolomite rock.**



## CEMENT

Type I/II cement was used for this study and provided by Argos from their Calera, Alabama, cement plant. The specific gravity of the cement was 3.13. The chemical and physical properties are listed in table 35 and table 36, respectfully. The material certification report is in appendix A.

**Table 35. Cement chemical properties.**

<b>Chemical Analysis</b>		
<b>Item</b>	<b>Spec Limit</b>	<b>Test Result</b>
<b>Rapid Method, X-Ray (C114)</b>		
SiO <sub>2</sub> (%)	—	19.8
Al <sub>2</sub> O <sub>3</sub> (%)	—	4.7
Fe <sub>2</sub> O <sub>3</sub> (%)	—	3.2
CaO (%)	—	62.8
MgO (%)	6.0 max	3.0
SO <sub>3</sub> (%)	3.0 max	3.0
Loss on Ignition (%)	3.5 max	2.7
Insoluble Residue (%)	1.5 max	0.51
CO <sub>2</sub> (%)	—	1.7
Limestone (%)	5.0 max	2.3
CaCO <sub>3</sub> in Limestone (%)	70 min	99
Inorganic Process addition (Baghouse Dust)	5.0 max	2.0
<b>Adjusted Potential Phase Composition (C150)</b>		
C <sub>3</sub> S (%)	—	54
C <sub>2</sub> S (%)	—	15
C <sub>3</sub> A (%)	—	7
C <sub>4</sub> AF (%)	—	10
NaEq	0.6 max	0.36

— No data

**Table 36. Cement physical properties.**

<b>Physical Analysis</b>		
<b>Item</b>	<b>Spec Limit</b>	<b>Test Result</b>
Air Content of Mortar (%) (C185)	12 max	7
Blaine Fineness (m <sup>2</sup> /kg) (C204)	260	396
0.325 (%) (C430)	—	97.2
Autoclave expansion (%) (C151)	0.80 max	0.08
<b>Compressive Strength (psi,[Mpa]) (C109)</b>		
1 day	—	2090 [14.4]
3 days	1740 [12.0] min	3910 [27.0]
7 days	2760 [19.0] min	4892 [33.7]
28 days	—	6420 [44.3]
<b>Time of Setting (minutes)</b>		
Vicat Initial (C191)	45–375	101
Heat of Hydration (kj/kg) (C1702)		
3 days	—	298
Mortar Bar Expansion (%) (C1038)	0.020 max	0.003
Specific Gravity (C188)	—	3.13

— No data

## FLY ASH

Fly ash for this study was provided by Boral MC from Plant Bowen in Cartersville, Georgia. The fly ash was class F with a specific gravity of 2.47. Chemical properties are listed in table 37, and the physical properties are provided in table 38. The complete material testing datasheet is included in appendix A.

**Table 37. Fly ash chemical analysis.**

<b>Chemical Analysis</b>		
<b>Item</b>	<b>Result (%)</b>	<b>AASHTO Limit</b>
SiO <sub>2</sub>	47.49	—
Al <sub>2</sub> O <sub>3</sub>	21.3	—
Fe <sub>2</sub> O <sub>3</sub>	18.08	—
Sum(SiO <sub>2</sub> +Al <sub>2</sub> O <sub>3</sub> +Fe <sub>2</sub> O <sub>3</sub> )	86.87	70 min
SO <sub>3</sub>	2.07	5.0 max
CaO	4.26	—
MgO	1.19	—
Na <sub>2</sub> O	0.99	—
K <sub>2</sub> O	2.32	—
Na <sub>2</sub> O+0.658K <sub>2</sub> O	2.52	—
Moisture	0.14	3.0 max
Loss on Ignition	1.23	5.0 max
Available Alkalies, as Na <sub>2</sub> Oe	1.03	1.5 max

— No data

**Table 38. Fly ash physical analysis.**

<b>Physical Analysis</b>		
<b>Item</b>	<b>Result</b>	<b>AASHTO Limit</b>
Fineness, % retained on a 45-μm sieve	14.48%	34 max
<b>Strength Activity Index</b>		
7 day, % of control	82%	75 min
28 day, % of control	82%	75 min
Water Requirement, % control	98%	105 max
Autoclave Soundness	0.01%	0.8 max
Specific Gravity	2.47	—

— No data

## CHEMICAL ADMIXTURES

This study utilized only air entraining admixture as a chemical admixture. The AEA dosage varied for targeted air levels, as well as fly ash percentage. Mixtures with fly ash required higher amounts

of AEA to achieve the same air content as mixtures without fly ash. Darex II AEA was used in this study. The manufacturer's recommended dosage is 0.5 to 5 fl oz per 100 lb of cement. Dosage rates used for this study ranged from 0.3 to 1.1 fl oz per 100 lb of cement.

Air entraining admixture is the only chemical admixture selected in this study. This admixture helps contractors better control the concrete's air levels and is commonly known for its ability to improve concrete's workability. The AEA dosage varied from mixture to mixture, primarily because of its interaction with the mineral admixture fly ash. Mixtures that embody fly ash require a higher AEA dosage to attain the typical 3.0–6.0 percent GDOT target air content, as compared to a mixture without the use of fly ash. This study used Darex II AEA for its concrete mixtures; this admixture complies with *ASTM C260* admixture specifications. Darex recommends this admixture be added to the concrete mixture at approximately  $\frac{1}{2}$ –5 fl oz / 100 lb (30–320 mL / 100 kg) of cement.

## **CHAPTER 6. EXPERIMENTAL DESIGN**

### **DESIGN PLAN**

This study looks to effectively develop a database of input values needed to implement the MEPDG for critical rigid pavement designs in Georgia. In order to accomplish this task, various tests must be performed on GDOT-approved concrete mixtures. The values to be determined from these tests include: compressive strength, Young's modulus, MOR, CTE, shrinkage, thermal capacity, and heat capacity. In addition to these values, fresh concrete properties are recorded for each mixture, including slump, air content, unit weight, and temperature. Additionally, a sensitivity analysis is performed to determine which of these inputs are the most critical to rigid pavement design. Analysis is then performed at input levels 1, 2, and 3 in order to establish thresholds and ensure adequate pavement performance. This chapter outlines the selection of mixtures, as well as the test procedures, to ensure high levels of accuracy and consistency throughout the testing program.

### **CONCRETE MIXTURES TESTING MATRIX**

A concrete testing matrix was established that was composed of 12 different concrete mixtures. These mixtures varied cementitious content, fly ash content, coarse aggregate type, coarse aggregate volume fraction, and air content. The goal of altering these properties throughout the 12 mixtures was to isolate certain variables of pavement design in order to observe effects on concrete's properties and performance. This concrete mixture matrix is presented in table 39. Mixtures were assigned different quarries based on the different material properties to be isolated. For example, if the variable to be isolated was w/cm, then two mixtures would use the same quarry and one would have a high w/cm and one would have a low w/cm. This process was followed for

each of the 12 mixtures to better compare desired values by removing the variable of differing aggregates. The mixtures paired for the same quarry, as well as the variable changing between them, are presented in table 39.

**Table 39. Concrete mixture matrix.**

Mixture Number	Cement Content	Fly Ash	w/cm	CA Type	CA Fraction	Air Content (%)	
1	541	0	0.42	Granite	12.75	5.00	Low cement w/c ratio change
2	541	0	0.51	Granite	12.75	5.00	
3	580	0	0.42	Granite	12.75	5.00	High Cement w/c ratio change
4	580	0	0.51	Granite	12.75	5.00	
5	580	15%	0.42	Granite	12.75	5.00	Fly Ash Content
6	580	20%	0.42	Granite	12.75	5.00	
7	580	25%	0.42	Granite	12.75	5.00	
8	580	20%	0.42	Dolomite	12.75	5.00	Granite Content
9	580	20%	0.42	Granite	10.00	5.00	
10	580	20%	0.42	Dolomite	10.00	5.00	Dolomite Content
11	580	20%	0.42	Granite	12.75	3.00	
12	580	20%	0.42	Granite	12.75	6.50	Air Content

## **EXPERIMENTAL PROCEDURES**

### **Batching**

The batching procedures used in this study were driven by *ASTM C192: Standard Practice for Making and Curing Concrete Test Specimens in the Laboratory*. Before mixing, materials were weighed in specified amounts, placed inside 5-gallon buckets, and set aside in the same climate-controlled mixing room. The cementitious materials were weighed into buckets that contained lids to ensure a moisture-free environment before mixing. Water and admixture amounts were weighed just before mixing. As mentioned previously, only AEA was used in this study and the dosage varied among mixtures due to target air contents and fly ash content. It was observed during this study that mixtures with fly ash required a higher dosage of AEA compared to the mixtures with only cement. On the day of mixing, the moisture contents of the coarse and fine aggregates were measured using a ventilated microwave oven, as specified in *ASTM C566: Standard Test Method for Total Evaporable Moisture Content of Aggregate by Drying*. The water amount to be included in the batch was then adjusted based on the moisture content of the aggregates. Concrete property test specimens were assembled and greased prior to mixing.

### **Mixing Process**

The mixing procedure followed the requirements specified in *ASTM C192: Standard Practice for Making and Curing Concrete Test Specimens in the Laboratory*. Before mixing, the concrete mixer was sprayed with water and then excess water was removed. After the mixer was dampened, all coarse and fine aggregates were added to the mixer and allowed to mix thoroughly for approximately 5 minutes. Then, a portion of the cementitious material was added to the mixer and allowed to blend with the aggregates for a few rotations. Water mixed with chemical admixtures

was then added to the mixture slowly in small amounts. The remaining cementitious material and water was added in an alternating fashion between cementitious material and water to ensure even distribution of materials throughout the mixer and prevent clumped material. If, during the process, concrete became stuck on the mixer side, the rotation was stopped and the concrete was scraped from the sides to ensure all materials were thoroughly integrated into the mixture. When mixing was complete, the concrete was then emptied into a dampened wheelbarrow, tested for its fresh concrete properties, and cast into its appropriate testing molds.

### **Curing Process**

The specimens were removed from the molds approximately 24 hours after placement. All specimens were then cured in water tanks that conformed to *ASTM C511-13: Standard Specification for Mixing Rooms, Moist Cabinets, Moist Rooms, and Water Storage Tanks Used in the Testing of Hydraulic Cements and Concretes*. The water temperature was closely monitored and kept within  $23\pm 2^{\circ}\text{C}$  or  $73.4\pm 3.5^{\circ}\text{F}$ . Per the standards, CaOH powder was added to prevent the leaching of calcium from the specimens. Finally, a circulatory pump was kept in the tank to ensure even temperature and prevent the settling of the excess lime powder.

### **Testing Procedures**

Fresh and hardened concrete properties were tested for each of the 12 mixtures. ASTM standards and AASHTO standards were followed during the testing procedures of this study. The fresh concrete properties tests took place immediately following the batching of the mixture, while the hardened properties were tested at AASHTO-recommended intervals.



### ***Fresh Concrete Properties Tests***

Fresh concrete properties tests describe the behavior of the mixture during construction, as well as provide important insight into the final composition of the mixture. Table 40 indicates the fresh properties tests performed, the standard associated with each test, and the testing interval.

**Table 40. Fresh concrete properties testing matrix.**

<b>Fresh Concrete Property Test</b>	<b>Standard Identification</b>	<b>Test Interval</b>
Slump	<i>ASTM C143/AASHTO T119</i>	Batching Day
Temperature	<i>ASTM C1064/AASHTO T309</i>	Batching Day
Pressure Meter Air Content	<i>ASTM C231/AASHTO T152</i>	Batching Day
Unit Weight	<i>ASTM C138/AASHTO T121</i>	Batching Day

### ***Hardened Concrete Properties Tests***

The hardened concrete properties give indications for the long-term performance of the concrete. These are of special interest to this study as they are direct inputs into the MEPDG. These properties follow a testing schedule as outlined in table 41.

**Table 41. Hardened concrete properties testing matrix.**

<b>Hardened Concrete Property Test</b>	<b>Standard Identification</b>	<b>Test Interval</b>
Ultimate Shrinkage	<i>ASTM C157/AASHTO T160</i>	0, 3, 7, 14, 28, 35, 42, 56, 84, 140, 252 days
Compressive Strength	<i>ASTM C39/AASHTO T22</i>	7, 14, 28, 90 days
Static Modulus of Elasticity	<i>ASTM C49</i>	7, 14, 28, 90 days
Dynamic Modulus of Elasticity	<i>ASTM C215</i>	7, 14, 28, 90 days
Modulus of Rupture	<i>ASTM C78/AASHTO T23</i>	7, 14, 28, 90 days
Density and Void Content	<i>ASTM C1754</i>	28 days
Coefficient of Thermal Expansion	<i>AASHTO T336</i>	28 days
Thermal Conductivity	<i>ASTM D5334-14</i>	28 days

For each day of testing—7, 14, 28, and 90 days of age—three rounds of tests were performed for each of the hardened properties. This was to ensure that a reliable average was determined from each test. If there was a clear outlier from one of the three tests, then the average was taken from only two specimens. An outlier, as defined by *ASTM E178*, is extreme in either direction that appears to deviate markedly from the other members in the sample. For example, the 90-day tests for MOE of mixture 8 resulted in 7,438 ksi (51.3 GPa), 6,584 ksi (45.1 GPa), and 6,628 ksi (45.7 GPa). Since two of the values were within 50 ksi (0.35 GPa) of each other, the 7,438 ksi (51.3 GPa) value was deemed an outlier and not included in the average. This procedure helped to limit the influence of erroneous data due to human or machine error and ensure the data were collected from homogeneous specimens. For compressive strength, Young’s modulus, and Poisson’s ratio, three 4×8-inch (101.6×203.2-mm) cylinders were made for each test interval. The three cylinders were used for each of the tests, since MOE and Poisson’s ratio are nondestructive tests. Thus, the latter two were performed first. MOR testing was conducted on three 3×4×16-inch (76.2×101.6×406.4-mm) beams. Shrinkage was measured from three 4×4×10-inch (101.6×101.6×254-mm) specimens. A summary of the number of specimens, their associated tests, and sizes is shown in table 42.

**Table 42. Specimen sizes.**

<b>Hardened Concrete Property Test</b>	<b>Specimen Size (in.) and Shape</b>	<b>Number Per Batch</b>
Compressive Strength	4×8 Cylinder	12
Young's Modulus (Static and Dynamic)		
Poisson's Ratio		
Coefficient of Thermal Expansion		
Modulus of Rupture	3×4×16 Beam	12
	6×6×22 Beam	12
Shrinkage	4×4×10 Beam	3

The size of beams used for MOR testing has the potential to influence the overall measured values. Specifically, smaller beams typically yield higher values. Because of this expected difference in values, additional mixtures were made for comparing different beam sizes. Three 6×6×22-inch (152.4×152.4×558.8-mm) beams were also cast, along with three 3×4×16-inch (76.2×101.6×406.4-mm) beams, and tested at 28 days. The data from these tests were compared and used to develop a regression model to adjust the skewed values. Establishing a reliable correlation between the two sizes of beams will benefit GDOT toward adopting a practical size of a beam for MOR tests.

Two different tests were performed for MOE: static and dynamic. Static testing requires more specialized equipment and is more complex than the dynamic test. Both tests were performed in order to see if the values found from dynamic MOE can be used to find static MOE values using equation 6. A statistical hypothesis test was performed to determine if the use of this equation is valid for these 12 mixtures. This was conducted to determine whether the dynamic testing may be used in the future because of the simplistic nature of the test. Specifically, one mean hypothesis test was used to determine whether or not the static testing value could be determined using equation 5,  $E_{Static} = E_{Dynamic} * 0.83$ . The ratios between static MOE values and dynamic MOE

values were compared to 0.83. Two conditions needed to be satisfied in order to perform this test: independence and normality.

Two rounds of thermal conductivity testing were conducted using a needle probe through a line source test method. A known current and voltage are issued by the probe, and the temperature increase of the specimen with respect to time was measured. After the probe ceased providing heat to the specimen, the temperature decay of the specimen was measured. The thermal conductivity was then obtained by analyzing the time and temperature relationship between these heat and cooling cycles. The first round of testing was an average of the measurements from three 4×8-inch (101.6×203.2-mm) concrete cylinders for all 12 individual mixtures after a 28-day curing period. The specimens were tested in a room roughly maintaining a temperature of  $73\pm3^{\circ}\text{F}$  ( $23\pm2^{\circ}\text{C}$ ) and a relative humidity of  $50\pm4$  percent. Each specimen underwent 10 individual tests, and any outliers, defined by *ASTM E178*, were removed before averaging the test results.

The second round of thermal conductivity testing was performed on six concrete cylinders for all 12 mixtures, after a 28-day curing period. This round of testing was conducted to determine the impact that density, moisture, and air content have on thermal conductivity in concrete. Each concrete mixture had an extra cylinder that was tested for density following the *ASTM C1754* test method after the 28-day curing period. The six cylinders were tested in three different conditions (i.e., dry, normal, and saturated) with two replicates per condition. The first condition was *oven dry*. This condition was obtained by placing the concrete specimens in an oven at a temperature of  $100\pm5^{\circ}\text{F}$  ( $38\pm3^{\circ}\text{C}$ ) for  $24\pm1$  hour. After this 24-hour time period, the specimen was removed and the mass was determined; this process continued in 24-hour increments until the two subsequent mass determinations had a difference of less than 0.5 percent. The second condition is referred to as a *normal* condition. This condition was obtained by placing two cylinders per GDOT-approved

mixture into a controlled environmental chamber, maintaining a temperature of  $73\pm3^{\circ}\text{F}$  ( $23\pm2^{\circ}\text{C}$ ) and a relative humidity of  $50\pm4$  percent. The specimens remained in this chamber for a 24-hour period to ensure homogeneous temperature and moisture throughout the specimen. After this 24-hour period, the specimens were tested. The final condition was a saturated condition. After 28 days, the concrete specimens were moved from the moisture curing tank to a water tank inside the environmental chamber for a 24-hour period. At the end of this 24-hour period, the saturated specimens were then tested. All specimens in the second round of thermal conductivity testing underwent 10 individual tests.

## **CHAPTER 7. EXPERIMENTAL RESULTS**

### **CONCRETE MIXTURES**

Using the concrete mixture matrix presented in table 39, GDOT-approved mixtures were selected from previous projects that had similar design characteristics. These GDOT mixtures and their GDOT project numbers are listed in table 43. These mixtures have been used in past GDOT pavement projects, and thus would allow the potential to compare the in-situ material properties and performance compared to laboratory results from this research. Batch weights and the moisture content before mixing are found in appendix B.

Mixture IDs were created for easy reference of mixture attributes and ingredients. These IDs describe the cementitious content, fly ash replacement, w/cm, CA type, CA fraction, and resulting air content of the 12 mixtures. The identification for mixture 1 is (541/0FA/0.431/11.91G/4.9). The first number, 541, represents the cementitious content of the concrete mixture. The second number, 0FA, represents the percent of cement replaced by fly ash. The third number, 0.431, represents the w/cm of the concrete mixture. The fourth number, 11.91G, represents the CA fraction followed by either a G or D, meaning granite (G) or dolomite (D). The fifth number, 4.9, represents the air content of the mixture as determined by the fresh concrete property test. These mixture IDs are shown in table 44.

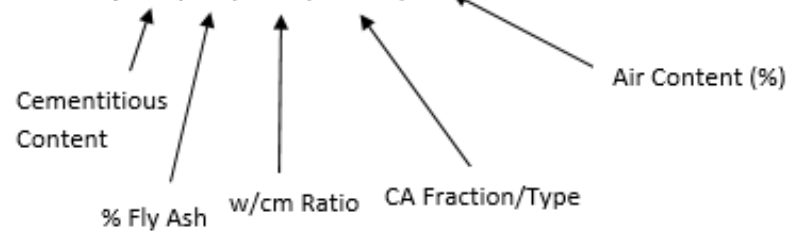
**Table 43. GDOT-approved mixtures.**

<b>Mixture Number</b>	<b>Cementitious Content</b>	<b>Fly Ash (%)</b>	<b>W/cm</b>	<b>CA Type</b>	<b>CA Fraction</b>	<b>Air Content (%)</b>	<b>GDOT Project Number</b>
1	541	0	0.431	Granite	11.91	3.0–6.5	IM-185-1(326)01
2	541	0	0.524	Granite	12.75	3.0–6.5	NH-IM-20-2(145)01
3	595	0	0.43	Granite	11.40	3.0–6.5	EDS00-0072-00(039)
4	600	0	0.47	Granite	11.62	3.0–6.5	NHS00-0005-00(320)
5	580	12.20	0.493	Granite	12.54	3.0–6.5	NH-IM-20-2(145)01
6	579	19.69	0.446	Granite	11.67	3.0–6.5	CSNHS-M002-00(965)01
7	622	26.00	0.422	Granite	12.14	3.0–6.5	NHS-M002-00(434)01
8	605	20.66	0.43	Dolomite	12.09	3.0–6.5	NHSTP-0075-03(203)
9	590	18.64	0.438	Granite	10.87	3.0–6.5	CSSTP-0007-00(239)01
10	590	18.64	0.43	Dolomite	10.87	3.0–6.5	CSSTP-0007-00(239)01
11	600	20.16	0.47	Granite	11.42	3.0	IMNH0-0075-01(227)
12	600	20.16	0.47	Granite	11.42	6.5	IMNH0-0075-01(227)

**Table 44. Mixture identification.**

Mixture Number	Mixture ID	Cementitious Content	Fly Ash (%)	w/cm	CA Type	CA Fraction	Air Content (%)
1	541/0FA/0.431/11.91G/4.9	541	0	0.431	Granite	11.91	4.9
2	541/0FA/0.524/12.75G/4.0	541	0	0.524	Granite	12.75	4.0
3	595/0FA/0.43/11.4G/6.2	595	0	0.43	Granite	11.4	6.2
4	600/0FA/0.47/11.62G/6.1	600	0	0.47	Granite	11.62	6.1
5	580/12.2FA/0.493/12.54G/4.5	580	12.2	0.493	Granite	12.54	4.5
6	579/19.69FA/0.446/11.67G/5.5	579	19.69	0.446	Granite	11.67	5.5
7	622/26FA/0.422/12.14G/3.1	622	26	0.422	Granite	12.14	3.1
8	605/20.66FA/0.43/12.09D/5.0	605	20.66	0.43	Dolomite	12.09	5.0
9	590/18.64FA/0.438/10.87G/4.9	590	18.64	0.438	Granite	10.87	4.9
10	590/18.64FA/0.439/10.87D/5.9	590	18.64	0.439	Dolomite	10.87	5.9
11	600/20.16FA/0.47/11.42G/3.6	600	20.16	0.47	Granite	11.42	3.6
12	600/20.16FA/0.47/11.42G/4.7	600	20.16	0.47	Granite	11.42	4.7

Key: 541/0FA/0.431/11.91G/4.9





## TEST RESULTS

After carefully adhering to the testing procedures outlined in chapter 6, the concrete material properties were measured. In this section, the data are reported and analyzed as they pertain to their use in rigid pavements. Currently, GDOT has certain design acceptance requirements (DAR) for concrete mixtures used in rigid pavements. Before a mixture's approval, trial batches must meet certain threshold values for compressive and flexural strength, outlined in *GDOT Section 430–Portland Cement Concrete Pavement* (GDOT 2013). For class 1 mixtures, compressive and flexural strength should reach minimum values of 3,000 psi (20.7 MPa) and 600 psi (4.1 MPa), respectively. For class 2 mixtures, compressive and flexural strength should reach minimum values of 3,500 psi (24.1 MPa) and 700 psi (4.8 MPa), respectively.

### Fresh Properties

The mixtures had fresh properties consistent with expectations. The fresh properties for each of the mixtures are shown in table 45.

The temperature of the mixtures varied mainly due to the dates batched, which occurred over a 2-month period between March and April. Unit weights are within a reasonable range with values measured between 143.0 to 149.0 pcf (2,290.6 to 2,386.8 kg/m<sup>3</sup>), as shown in figure 25. The air contents of each of the mixtures fits within the allowed tolerance of 3.00–6.50 percent, as specified by GDOT-approved mixtures. Some variability of the air content occurred due to the variation in each of the mixture's constituents, as shown in figure 26. The greatest variability of the mixtures' fresh concrete properties occurred with slump, which has a maximum value of 3.50 inch (88.9 mm) for pavements. Most of this variability is explained by the different w/cm used for the mixtures. Additionally, mixtures using fly ash are typically expected to be more workable than mixtures without (Kosmatka and Wilson 2016). As seen in figure 27, five of the

mixtures were above the acceptable limit on slump. These mixtures are, however, GDOT-approved mixtures with no modifications except for AEA dosage (dosage amounts not provided in specifications). Since slump is only a measure of workability and does not provide insight into strength or the rigidity of the concrete, it is acceptable for these five mixtures to have a higher slump for the purposes of this study, so long as the required mechanical properties are met.

**Table 45. Fresh properties.**

<b>Mixture</b>	<b>Temperature (°F)</b>	<b>Slump (in.)</b>	<b>Air (%)</b>	<b>Unit Weight (lb/ft<sup>3</sup>)</b>
<b>1</b>	82.4	0.50	4.9	147.2
<b>2</b>	83.4	2.25	4	147.4
<b>3</b>	73.7	3.00	6.2	144.4
<b>4</b>	79.3	8.50	6.1	143
<b>5</b>	62.1	7.00	4.5	143.4
<b>6</b>	74.1	6.50	5.5	141.6
<b>7</b>	58.6	4.25	3.1	145.2
<b>8</b>	64.4	5.00	5	148.8
<b>9</b>	66.2	0.50	4.9	145.8
<b>10</b>	75.4	2.50	5.9	147.2
<b>11</b>	70.5	2.75	3.6	146.6
<b>12</b>	85.8	2.75	4.7	146.4

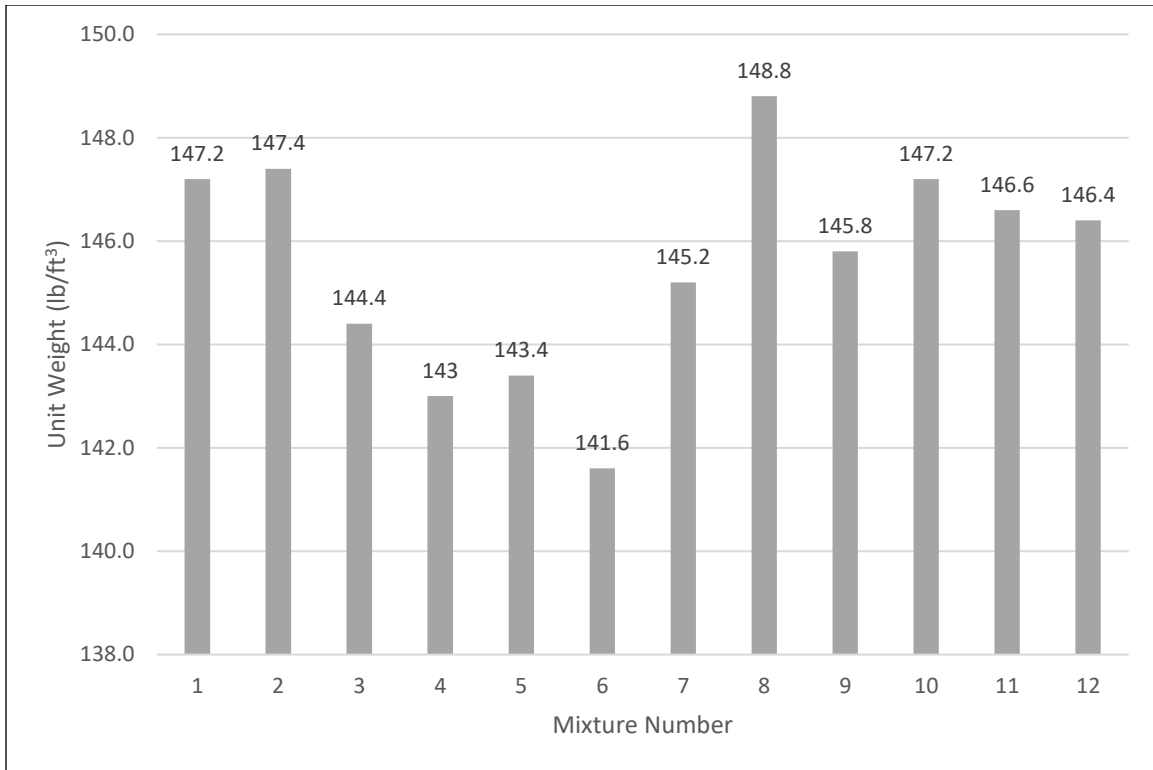


**Figure 25. Bar graph. Unit weight results.**



**Figure 26. Bar graph. Air content results.**

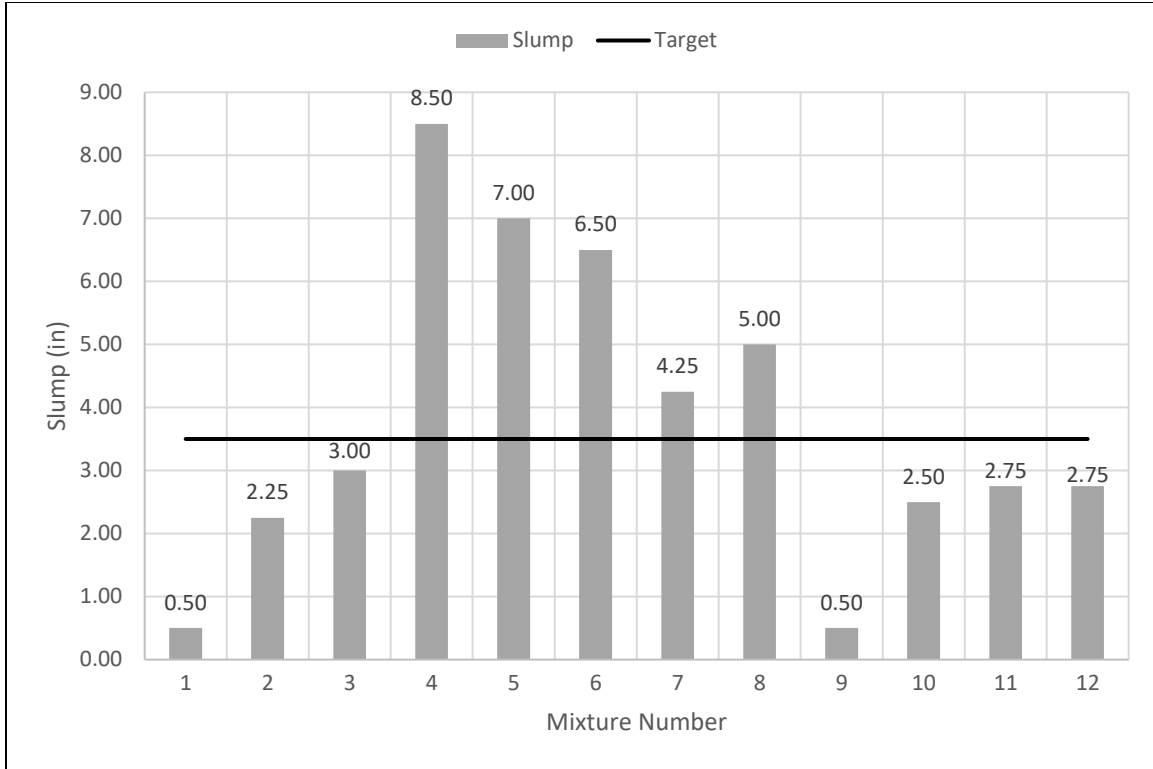


**Figure 27. Bar graph. Slump results.**

To ensure the consistent results of the fresh properties, two additional 4×8-inch cylinders were batched for every mixture that would later be tested for their CTE. Table 46 provides the fresh properties for the first round of thermal conductivity testing. Table 47 and table 48 are the fresh properties measured from the mechanical property mixtures for MOR and  $f'_c$ , and the second round of thermal conductivity batches, respectively.

**Table 46. Fresh concrete properties for first round of thermal conductivity.**

Mixture	Temperature (°F)	Slump (in)	Air (%)	Unit Weight (lb/ft <sup>3</sup> )	Date Batched
1	83.0	0.5	5.0	146.7	3/20/2020
2	83.4	2.0	3.0	151.5	3/20/2020
3	72.4	0.5	3.1	149.6	2/12/2020
4	72.7	2.5	11.5	149.0	2/12/2020
5	71.2	0.5	3.2	141.0	6/18/2020
6	74.1	1.3	2.8	148.6	6/18/2020
7	70.0	2.0	2.0	150.2	6/18/2020
8	68.4	1.5	2.4	148.8	2/25/2020
9	74.0	1.5	3.0	146.6	6/18/2020
10	69.7	1.5	2.8	149.2	2/25/2020
11	70.5	2.0	4.0	151.2	3/20/2020
12	77.0	2.5	5.5	150.6	3/20/2020

**Table 47. Fresh concrete properties for MOR and  $f'_c$  testing.**

Mixture	Temperature (°F)	Slump (in)	Air (%)	Unit Weight (lb/ft <sup>3</sup> )	Date Batched
1	80.0	1.0	4.0	150.0	8/26/2020
2	82.0	2.0	3.1	147.6	8/26/2020
3	78.0	1.0	5.1	17.8	8/27/2020
4	80.0	2.5	4.9	145.4	8/27/2020
5	78.6	0.5	4.1	144.8	8/19/2020
6	80.9	1.5	4.0	143.8	8/19/2020
7	79.0	2.0	3.2	146.4	8/20/2020
8	79.0	1.5	3.3	149.4	8/21/2020
9	82.0	1.5	5.1	143.6	8/20/2020
10	80.0	2.0	5.2	146.8	8/21/2020
11	80.0	2.0	3.5	147.4	8/25/2020
12	81.0	3.0	5.1	144.0	8/25/2020

**Table 48. Fresh concrete properties for second round of thermal conductivity.**

Mixture	Temperature (°F)	Slump (in)	Air (%)	Unit Weight (lb/ft <sup>3</sup> )	Date Batched
1	64.0	0.5	4.1	149.4	9/21/2020
2	64.0	1.5	3.5	150.4	9/21/2020
3	67.0	0.5	3.6	150.4	9/23/2020
4	73.0	2.5	4.7	148.2	9/23/2020
5	81.0	0.5	4.2	145.0	9/2/2020
6	80.0	1.3	3.8	144.8	9/4/2020
7	76.0	2.5	2.4	147.8	9/9/2020
8	76.0	1.5	3.3	151.0	9/15/2020
9	78.8	1.0	4.5	143.0	9/10/2020
10	72.0	1.5	5.4	149.4	9/16/2020
11	75.0	2.0	3.1	148.8	9/17/2020
12	76.0	2.5	4.4	147.8	9/18/2020

During all three trials, the concrete batches displayed good slump values. GDOT recommends for pavements to remain below 3.50 inch (88.9 mm). None of the mixtures batched during this study exceeded this maximum value. A slight variation exists between the temperatures of the mixtures, ranging from 64.0°F to 83.4°F. This variation can be best explained by examining the “Date Batched” column. Georgia is known for its quick transition in seasons, and the mixtures batched in February and September had much lower temperatures than those mixed in March due to this temperature change, as well as the two batches on September 21, 2020, being batched early in the morning. A number of mixtures displayed slightly higher air contents in the initial study conducted (table 46). This may be attributed to a malfunction of the air meter. With a newly purchased air meter, accurate air contents were measured for the more recent mixtures. The unit weights of these mixtures displayed higher values than expected. For concrete mixtures, a typical unit weight range includes 143.0 to 149.0 pcf (2,290.6 to 2,386.8 kg/m<sup>3</sup>). Some of the unit weight tests exceeded this 149.0 pcf (2,386.8 kg/m<sup>3</sup>), however the difference was negligible, and the typical value used in GDOT’s pavement design is 150.0 pcf (2,402.8 kg/m<sup>3</sup>).

Figure 28, figure 29, and figure 30 illustrate the concrete fresh property test results of the three different trials used in this study. Trial 1 refers to the properties shown in table 46; CTE specimens were batched during this trial. The second trial of concrete mixtures (table 47) was used for the ultimate shrinkage and MOR testing. The third trial of concrete mixtures (table 48) was batched for thermal conductivity testing. The three trials are plotted to demonstrate homogeneity across the various concrete mixing trials used in this study.

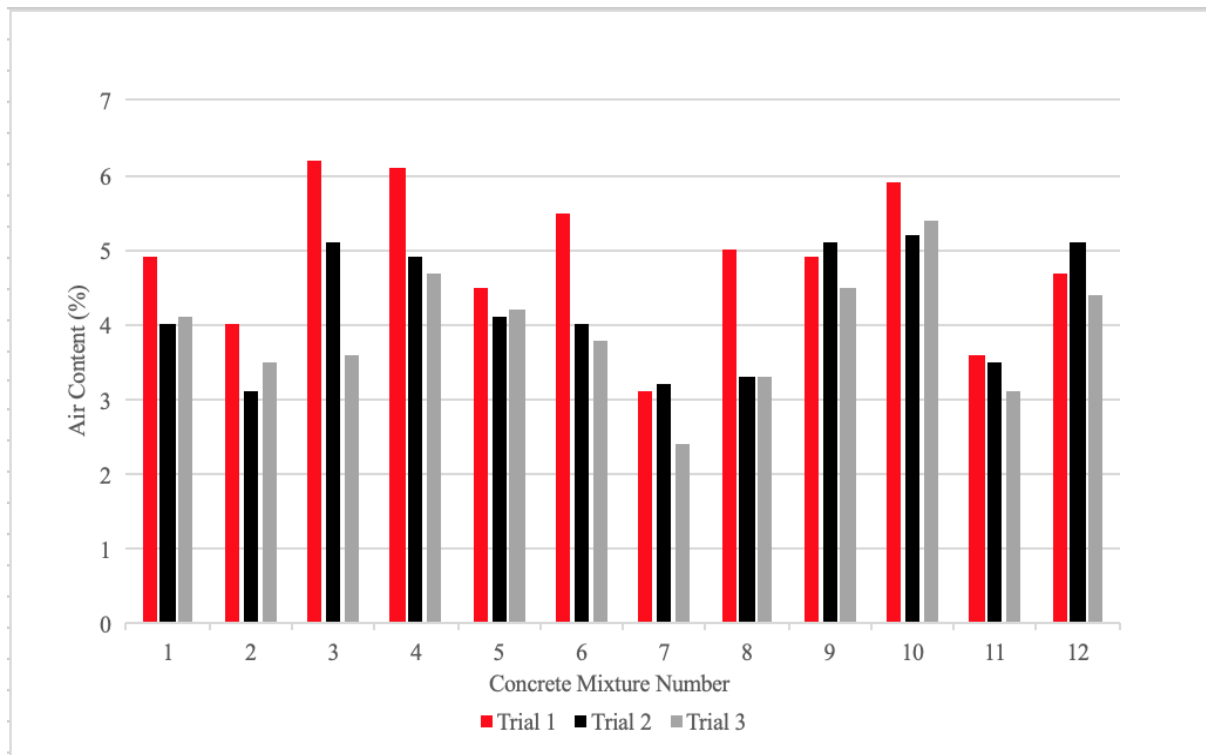


**Figure 28. Bar graph. Air content comparison for different mixture trials.**

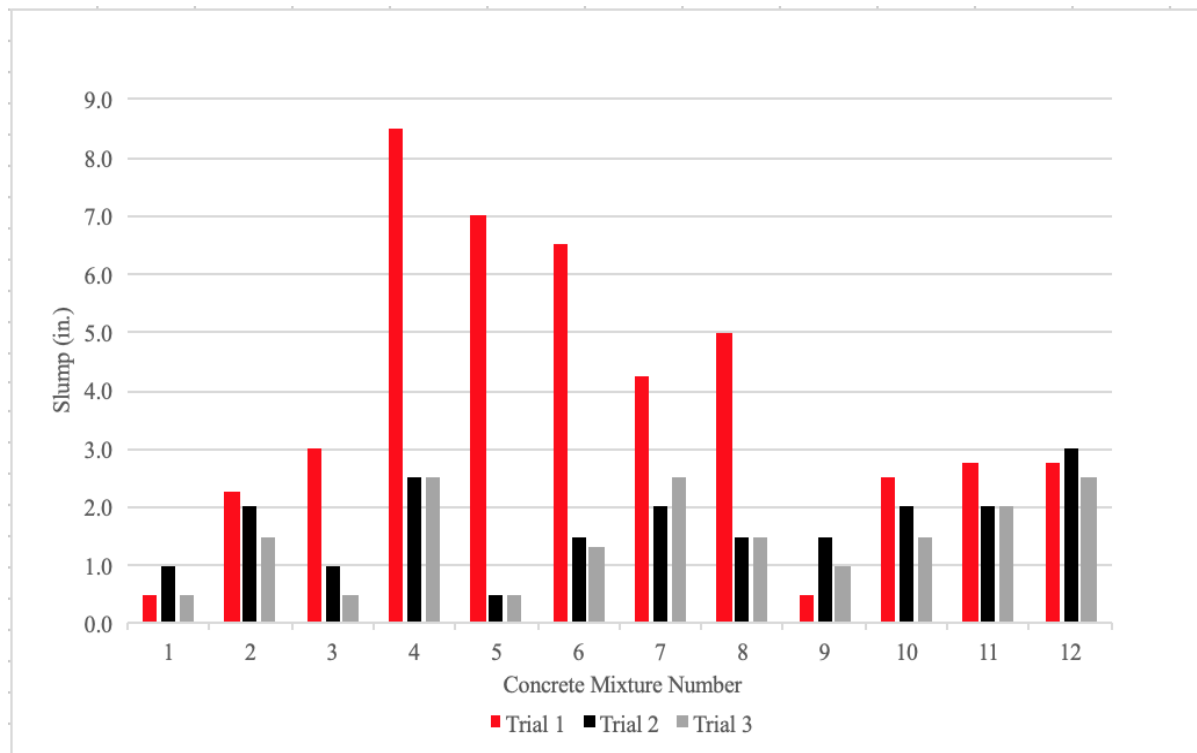


**Figure 29. Bar graph. Slump comparison for different mixture trials.**

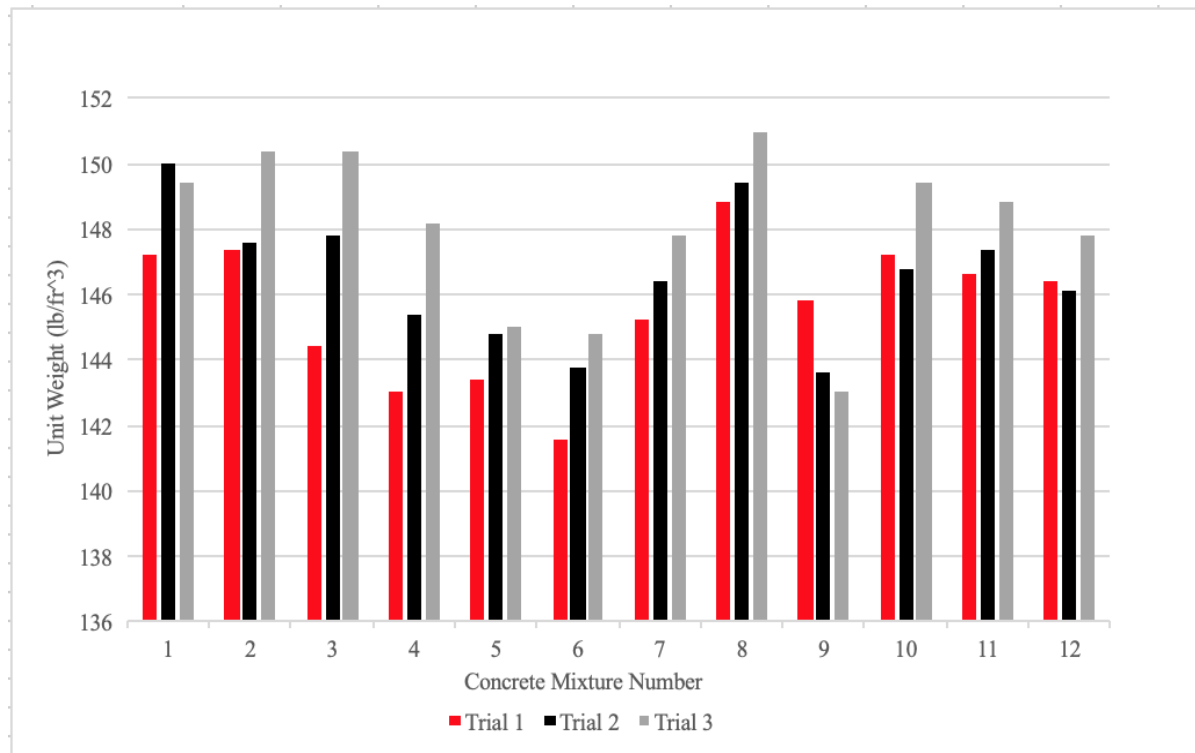


**Figure 30. Bar graph. Unit weight comparison for different mixture trials.**

The three different trials displayed fairly similar fresh concrete property results that provided quality assurance for the research team. Figure 28 proved that most of the concrete air content measurements were in the desired range of 3.0–6.0 percent. The concrete mixtures were desired to maintain slump values below 3.50 inch (88.9 mm). None of the mixtures in the second and third trials exceeded this maximum value. In some cases, trial 1 demonstrated a slight variation from the other two trials. During this initial batching process, fresh air content measurements were lower than expected. Higher dosages of air-entraining admixture were used to combat this issue. This increased admixture usage related directly to the increased air content and slump measurements displayed in figure 28 and figure 29.



## Compressive Strength

Examining the compressive strength values of the mixtures, all 12 satisfied the DAR for class 2 mixtures of 3,500 psi (24.1 MPa). Mixture 6 (579/19.69FA/0.446/11.67G/5.5) had the lowest 28-day compressive strength value at 4,140 psi (28.5 MPa), while mixture 9 (590/18.64FA/0.438/10.87G/4.9) achieved the highest 28-day strength at 6,650 psi (45.9 MPa). The average 28-day strength across all mixtures is 5,400 psi (37.2 MPa). Compressive strengths for all mixtures for each testing age are shown in table 49. As shown in table 39, mixtures have “companion mixtures,” where only one property changed from mixture to mixture. These companion mixtures were plotted to show differences in strength gain as well as final strengths and are presented in figure 31, figure 32, figure 33, figure 34, and figure 35.

**Table 49. Compressive strength values.**

		Age of Specimen (days)			
		7	14	28	90
Mix Number	Mixture ID	Compressive Strength (psi)			
1	541/0FA/0.431/11.91G/4.9	4,680	5,420	6,370	6,240
2	541/0FA/0.524/12.75G/4.0	4,810	5,440	6,300	6,680
3	595/0FA/0.43/11.4G/6.2	4,410	4,870	5,350	5,780
4	600/0FA/0.47/11.62G/6.1	3,130	3,820	4,280	4,490
5	580/12.2FA/0.493/12.54G/4.5	3,190	3,700	4,390	5,340
6	579/19.69FA/0.446/11.67G/5.5	3,090	3,580	4,140	5,420
7	622/26FA/0.422/12.14G/3.1	4,080	4,610	5,420	6,650
8	605/20.66FA/0.43/12.09D/5.0	4,240	4,920	5,700	7,450
9	590/18.64FA/0.438/10.87G/4.9	4,980	5,980	6,650	7,940
10	590/18.64FA/0.439/10.87D/5.9	4,150	4,450	5,220	6,570
11	600/20.16FA/0.47/11.42G/3.6	4,930	5,640	6,020	8,130
12	600/20.16FA/0.47/11.42G/4.7	3,820	4,520	5,190	6,950

Comparing mixtures 1 (541/0FA/0.431/11.91G/4.9) and 2 (541/0FA/0.524/12.75G/4.0), there is almost no difference in strength, as shown in figure 31. Since mixture 1 had a lower w/cm,

it is expected to have higher compressive strength values, similar to what is shown in figure 32 between mixtures 3 (595/0FA/0.43/11.4G/6.2) and 4 (600/0FA/0.47/11.62G/6.1). As part of the MOR testing, new 28-day strengths were obtained for mixtures 1 and 2. Mixture 1 had a 28-day strength of 6,540 psi (45.1 MPa) and mixture 2 had a 28-day strength of 4,930 psi (40.0 MPa) when rebatched. This difference is much more in line with expectations.

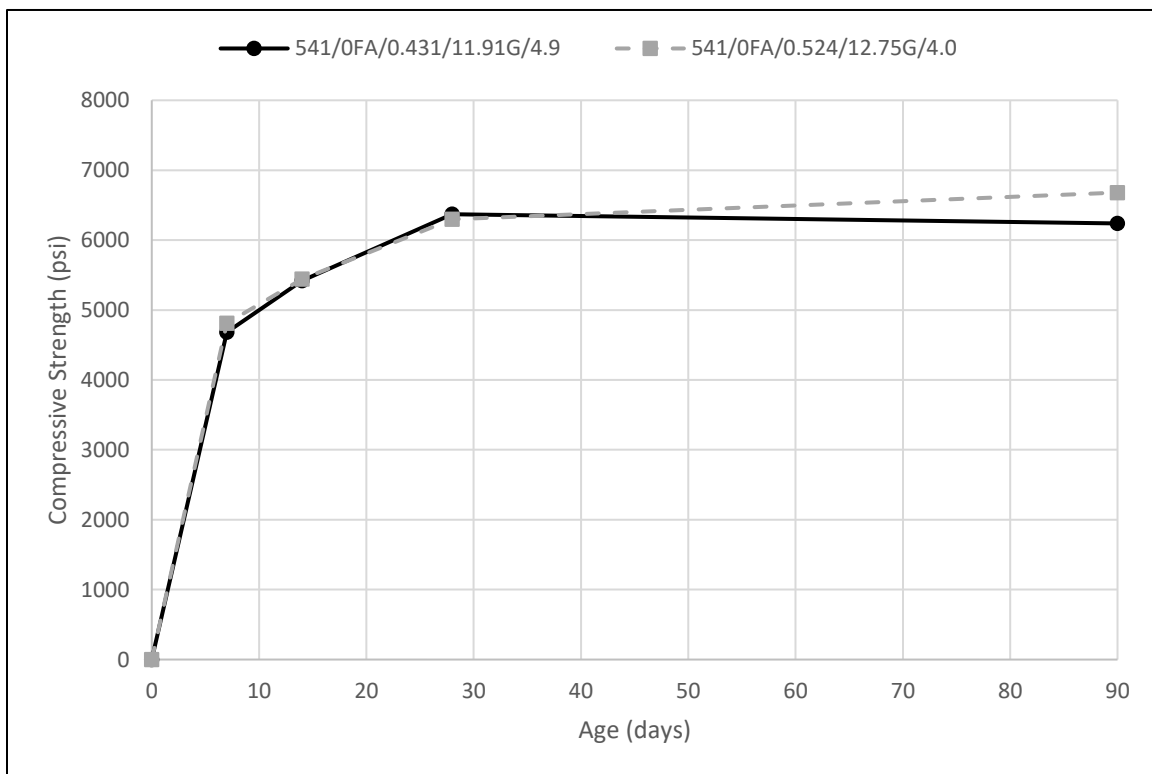


**Figure 31. Line graph. Compressive strength vs. age, mixtures 1 and 2, w/cm change.**

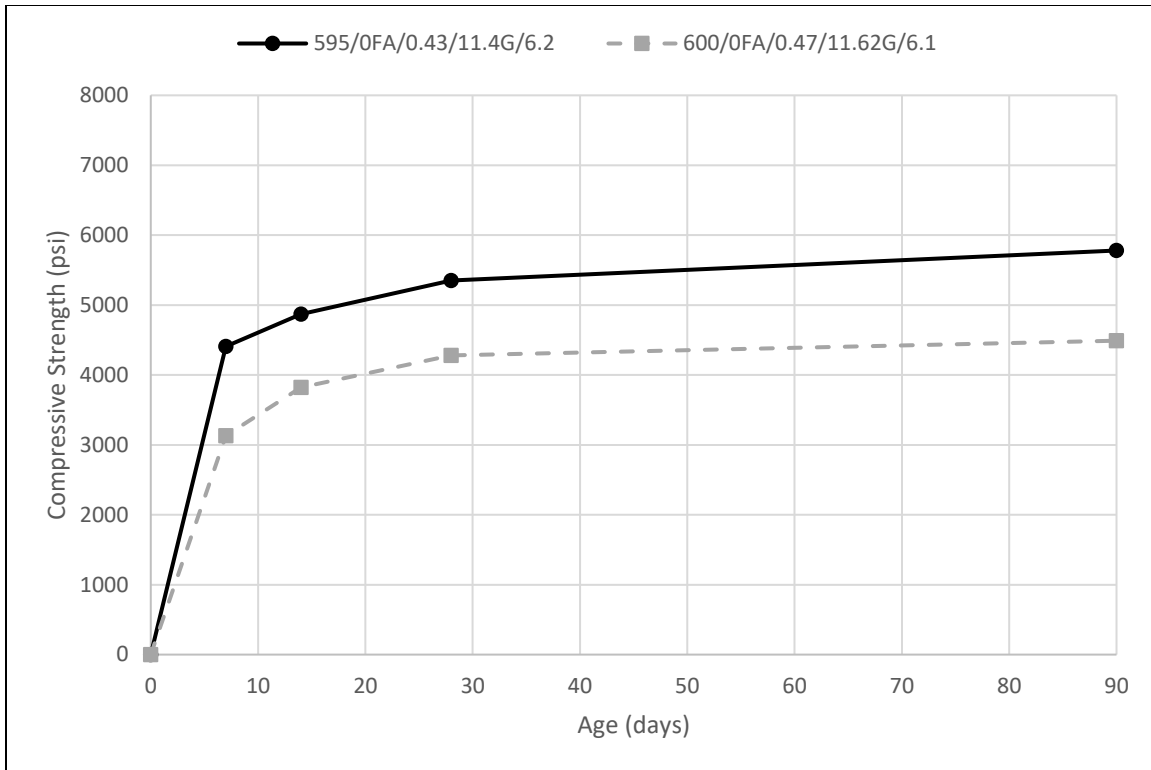


**Figure 32. Line graph. Compressive strength vs. age, mixtures 3 and 4, w/cm change.**

Comparing mixtures 4 (600/0FA/0.47/11.62G/6.1), 5 (580/12.2FA/0.493/12.54G/4.5), 6 (579/19.69FA/0.446/11.67G/5.5), and 7 (622/26FA/0.422/12.14G/3.1) in figure 33, mixtures 4, 5, and 6 performed very similarly while mixture 7 achieved the highest strength. Mixture 4 strengths were almost identical despite having 0.00 percent fly ash replacement. This is probably a result of increased air and w/cm lowering its strength, as well as similar cement contents producing calcium silicate hydrate at similar rates. After 28 days, the mixtures with fly ash continued producing CSH at high rates, while mixture 4's production declined, allowing the mixtures with fly ash to achieve higher strengths. Although mixture 6 has more fly ash than mixture 5, its lower w/cm counteracted the effects, achieving similar strengths to mixture 5, which had less fly ash but a higher w/cm. Mixture 7 likely achieved the highest strengths despite having

the highest fly ash replacement due to its high cement content, as well as having the lowest w/cm of the three mixtures.

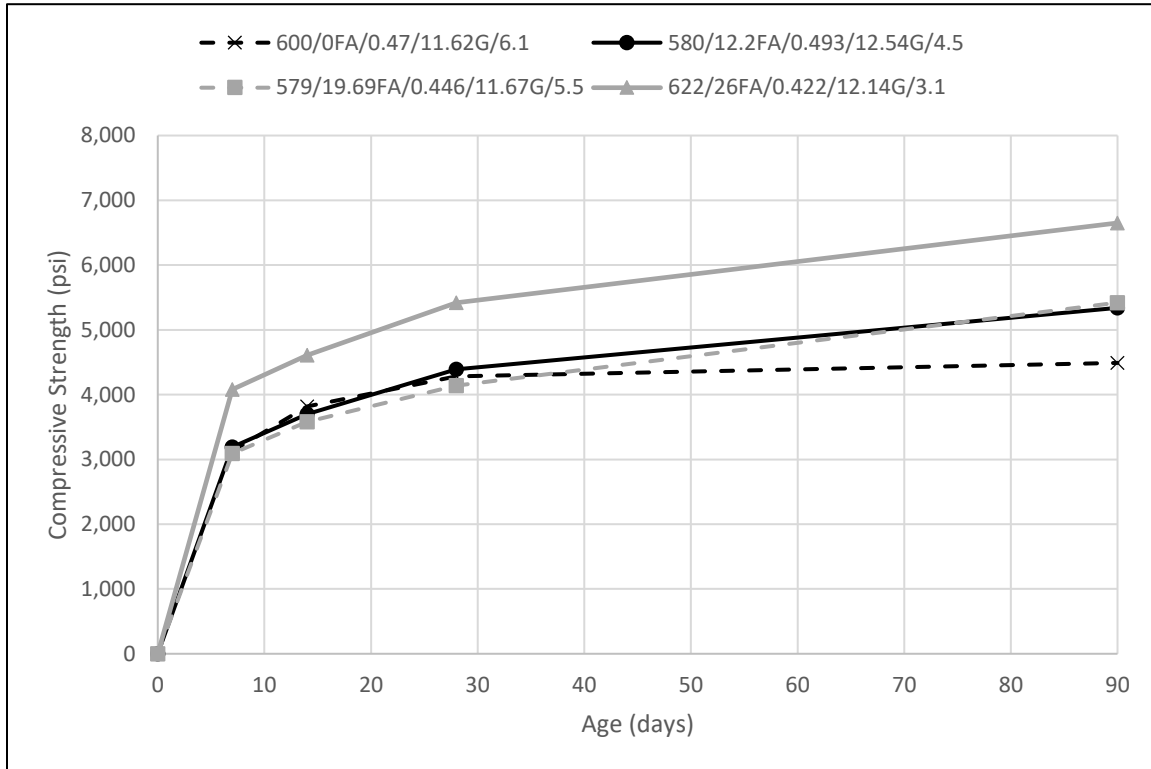


**Figure 33. Line graph. Compressive strength vs. age; mixtures 4, 5, 6, and 7; FA percentage change.**

Figure 34 displays mixtures 7 (622/26FA/0.422/12.14G/3.1) and 9 (590/18.64FA/0.438/10.87G/4.9), whose main difference is coarse aggregate content. Previous studies have found that lower coarse aggregate content leads to lower compressive strength values (Kim 2012). The opposite was observed in figure 34, likely due to fly ash percent replacement differences between the mixtures. Mixtures 8 (605/20.66FA/0.43/12.09D/5.0) and 10 (590/18.64FA/0.439/10.87D/5.9) display the expected trend of lower CA content, leading to the lower strengths presented in figure 35.

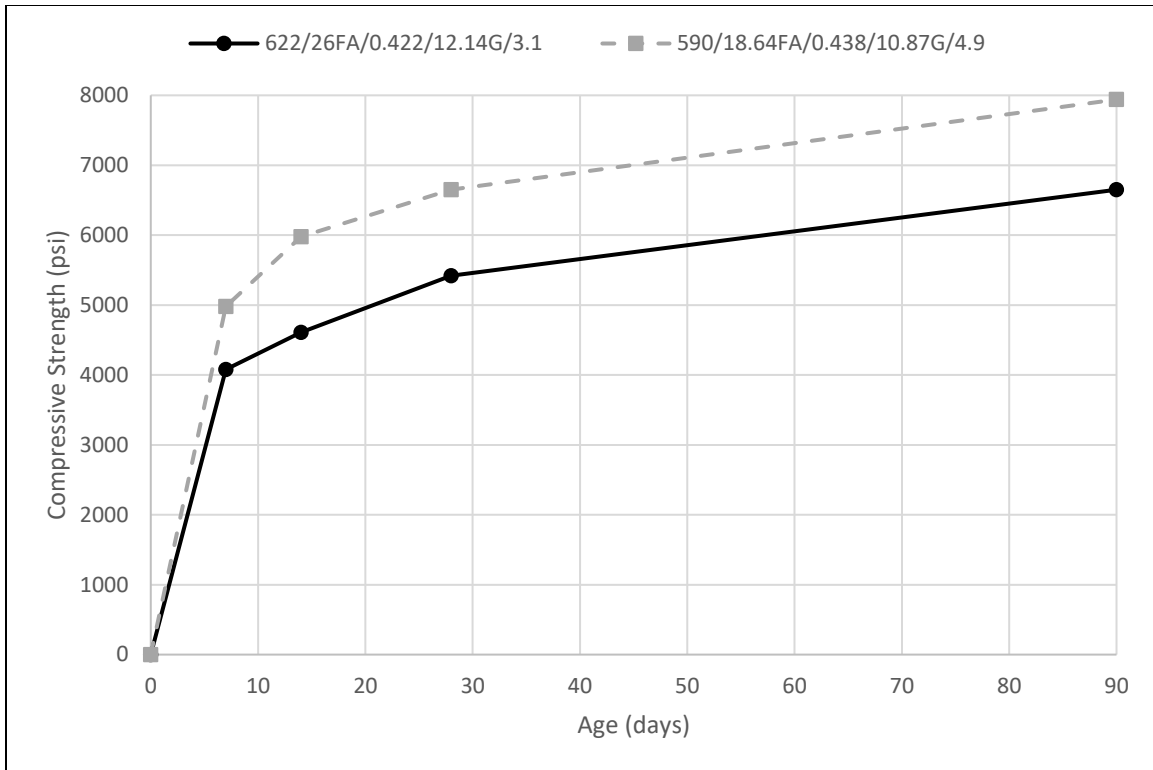


**Figure 34. Line graph. Compressive strength vs. age, mixtures 7 and 9, CA volume change.**

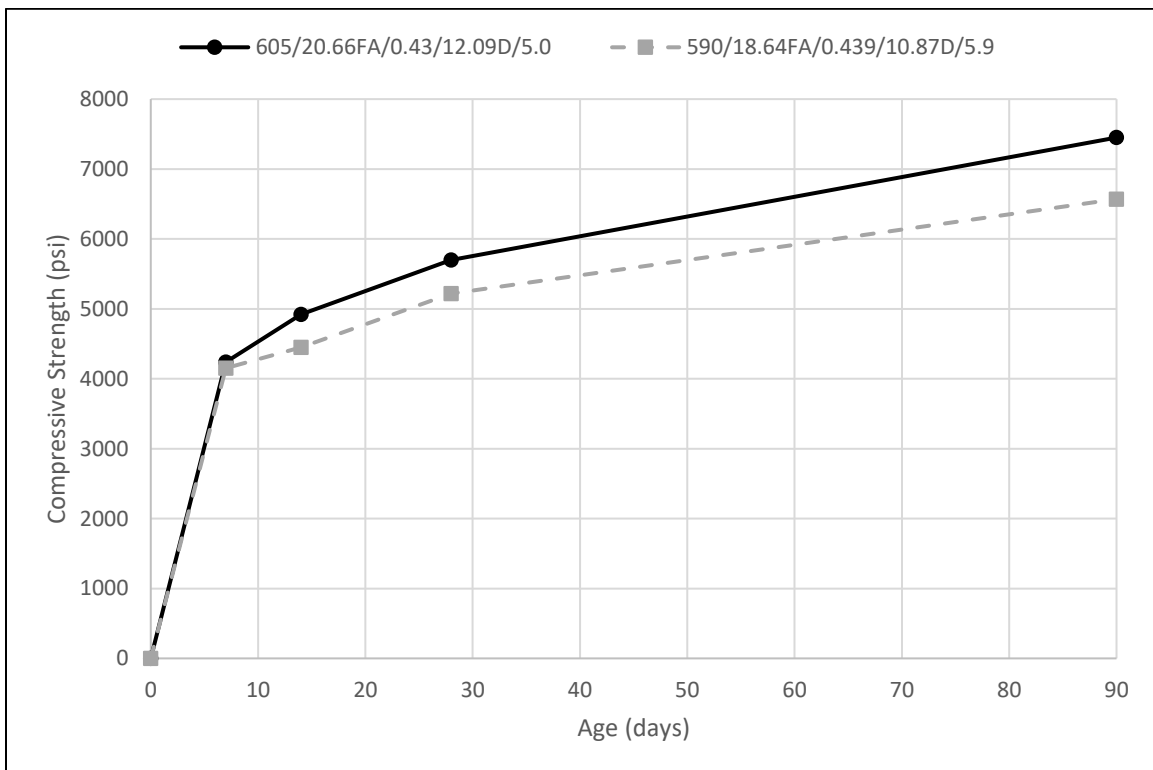


**Figure 35. Line graph. Compressive strength vs. age, mixtures 8 and 10, CA volume change.**

Figure 36 displays mixtures 9 (590/18.64FA/0.438/10.87G/4.9) and 10 (590/18.64FA/0.439/10.87D/5.9), which are the same, except one was made with granite and the other with dolomite. Mixture 9, produced with granite, exhibited higher strengths by providing a better bond between the paste and aggregate and subsequently higher strengths. Since this is a limited sample size, additional mixtures should be analyzed in order to support this trend as it may not support the actual difference between granite and dolomite mixtures. One theory for the differences in tested strengths and expectations is the internal curing provided by the different aggregates. The granite has an air content of 0.60 percent, while the dolomite has an air content of 0.08 percent. This difference in pore structure could have led to an increased hydration in the mixtures using granite, since the aggregate absorbed more of the mixture water and released it slowly as hydration occurred. Mixture 11 (600/20.16FA/0.47/11.42G/3.6) and mixture 12 (600/20.16FA/0.47/11.42G/4.7), shown in figure 37, display a variation in air content. As expected, mixture 11 achieved higher strengths due to a lower air content.

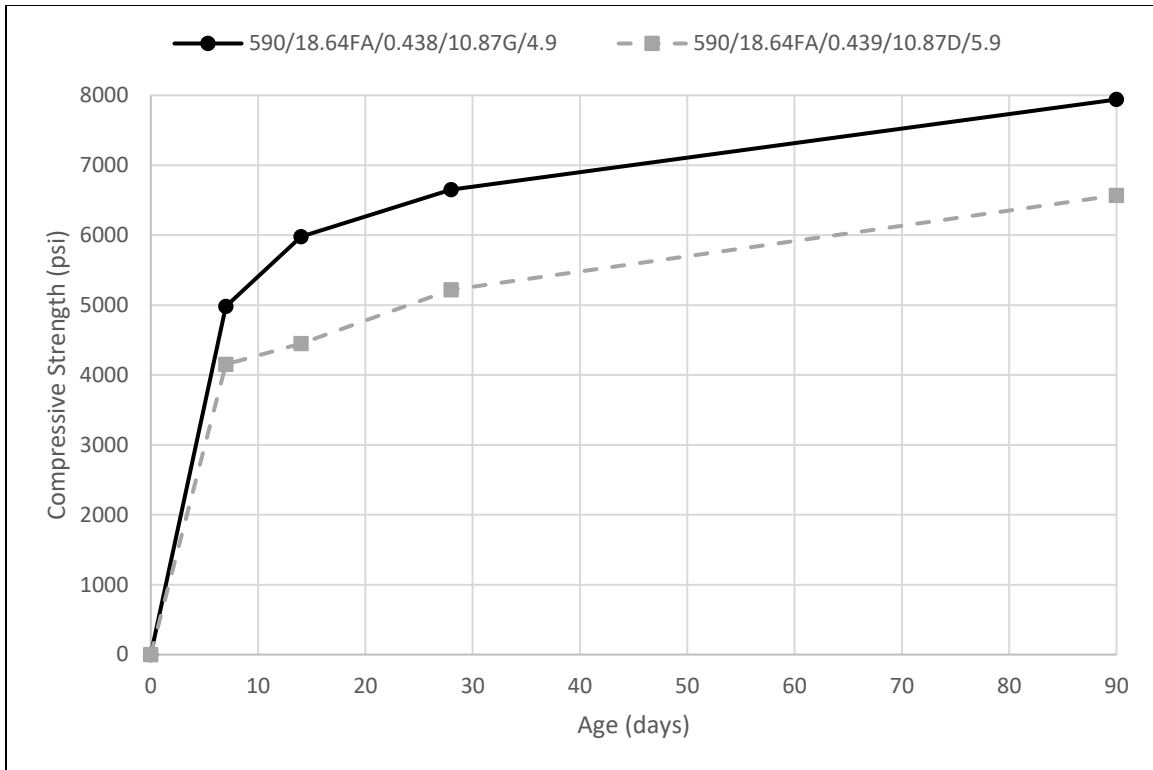


**Figure 36. Line graph. Compressive strength vs. age, mixtures 9 and 10, CA type change.**

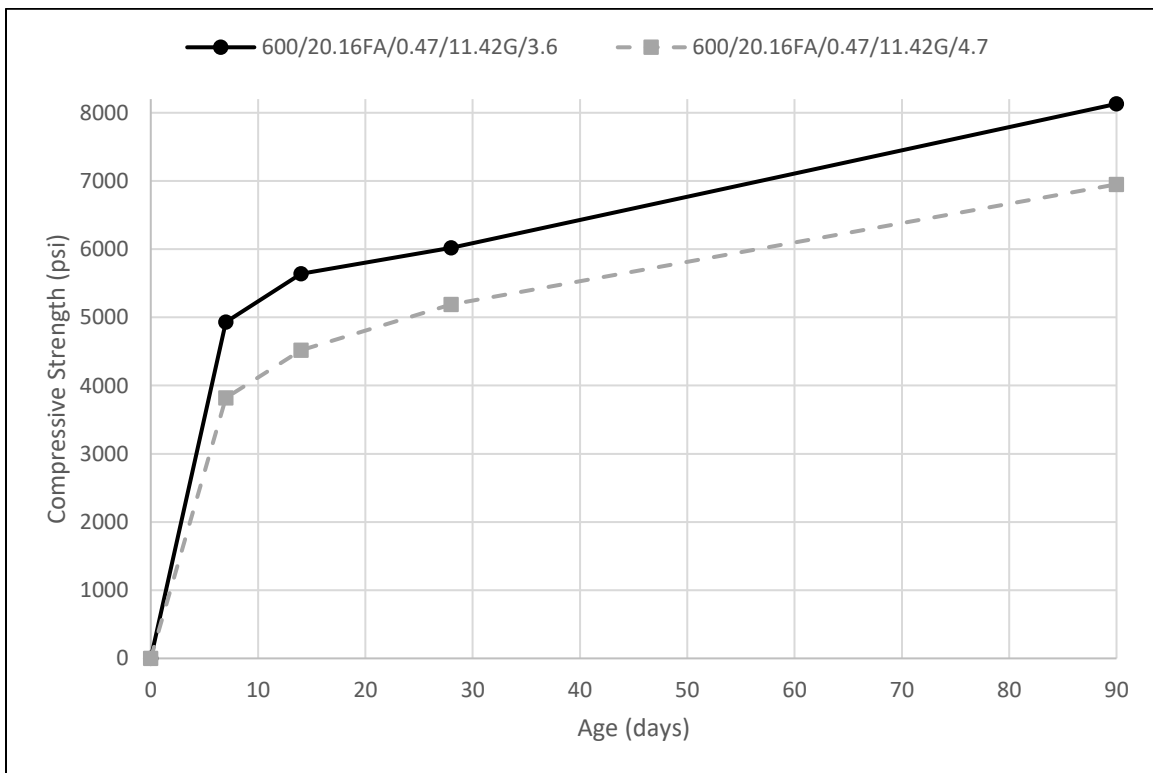


**Figure 37. Line graph. Compressive strength vs. age, mixtures 11 and 12, air content change.**

## Modulus of Elasticity

When examining the MOE test results, the 28-day measured values ranged from 3,150 to 6,400 ksi (21.7 to 44.1 GPa). The average 28-day MOE was 4,700 ksi (32.4 GPa) across all mixtures. The test results for static MOE are shown in table 50. Companion mixtures plotted against time are shown in figure 38 (mixtures 1 and 2), figure 39 (mixtures 3 and 4), figure 40 (mixtures 4, 5, 6, and 7), figure 41 (mixtures 7 and 9), figure 42 (mixtures 8 and 10), figure 43 (mixtures 9 and 10), and figure 44 (mixtures 11 and 12).

**Table 50. Static MOE results.**

Mixtures		Age of Specimen (days)			
		7	14	28	90
Mixture Number	Mixture ID	Static MOE (ksi)			
1	541/0FA/0.431/11.91G/4.9	5,100	5,150	5,350	5,650
2	541/0FA/0.524/12.75G/4.0	4,750	5,100	5,600	5,850
3	595/0FA/0.43/11.4G/6.2	4,350	4,450	4,600	5,100
4	600/0FA/0.47/11.62G/6.1	3,650	3,850	4,100	4,400
5	580/12.2FA/0.493/12.54G/4.5	2,650	2,950	3,150	3,700
6	579/19.69FA/0.446/11.67G/5.5	2,900	2,950	3,200	3,650
7	622/26FA/0.422/12.14G/3.1	3,150	3,350	3,550	4,250
8	605/20.66FA/0.43/12.09D/5.0	5,500	5,950	6,400	6,600
9	590/18.64FA/0.438/10.87G/4.9	3,550	3,900	4,150	4,600
10	590/18.64FA/0.439/10.87D/5.9	5,400	5,550	6,050	7,150
11	600/20.16FA/0.47/11.42G/3.6	4,950	5,050	5,350	5,950
12	600/20.16FA/0.47/11.42G/4.7	4,350	4,850	5,250	5,650



Factors that appear to affect the MOE of mixtures are w/cm, fly ash content, and rock type. Mixtures with higher w/cm have a lower MOE than the similar mixtures with a lower w/cm, as displayed in figure 38 and figure 39. Similarly, fly ash content results in lower MOE values than mixtures without fly ash. Figure 40 shows three mixtures using fly ash that have much lower MOE values when compared to mixture 4 (600/0FA/0.47/11.62G/6.1), which has a similar composition without fly ash. Mixtures with fly ash achieved MOE values of approximately 1,000 ksi (6.9 GPa) less than mixture 4. The type of coarse aggregate was observed to have the largest impact on the MOE of the mixtures. Mixtures using dolomite exhibited MOE values much higher than similar mixtures using granite. Figure 41 shows the same mixture made once with granite and once with dolomite. The resulting dolomite mixture had MOE values almost 2,000 ksi (13.8 MPa) greater than the granite mixture. Similarly, figure 42 shows granite mixtures and figure 43 shows dolomite mixtures with similar constituents. The same trend is observed when comparing these figures, dolomite mixtures result in higher MOE values. This trend is opposite of expectations since dolomite mixtures resulted in lower compressive strength values as previously shown in figure 36. The SG of the dolomite can provide insight to why MOE is higher for dolomite mixtures. The SG of dolomite is 2.847 and the SG of granite is 2.625. This difference in SG shows dolomite is a stiffer material than granite, even though it resulted in lower compressive strengths. The effect of air content on MOE is shown in figure 44.

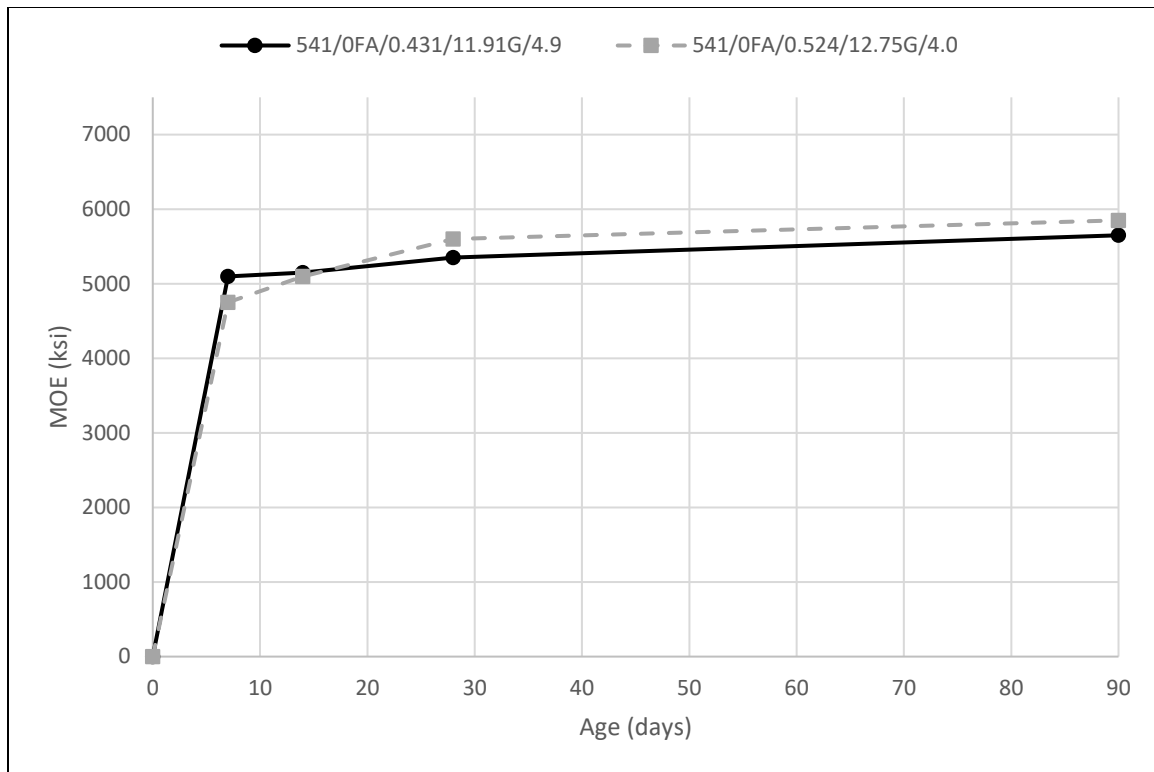


Figure 38. Line graph. MOE vs. age, mixtures 1 and 2, w/cm change.

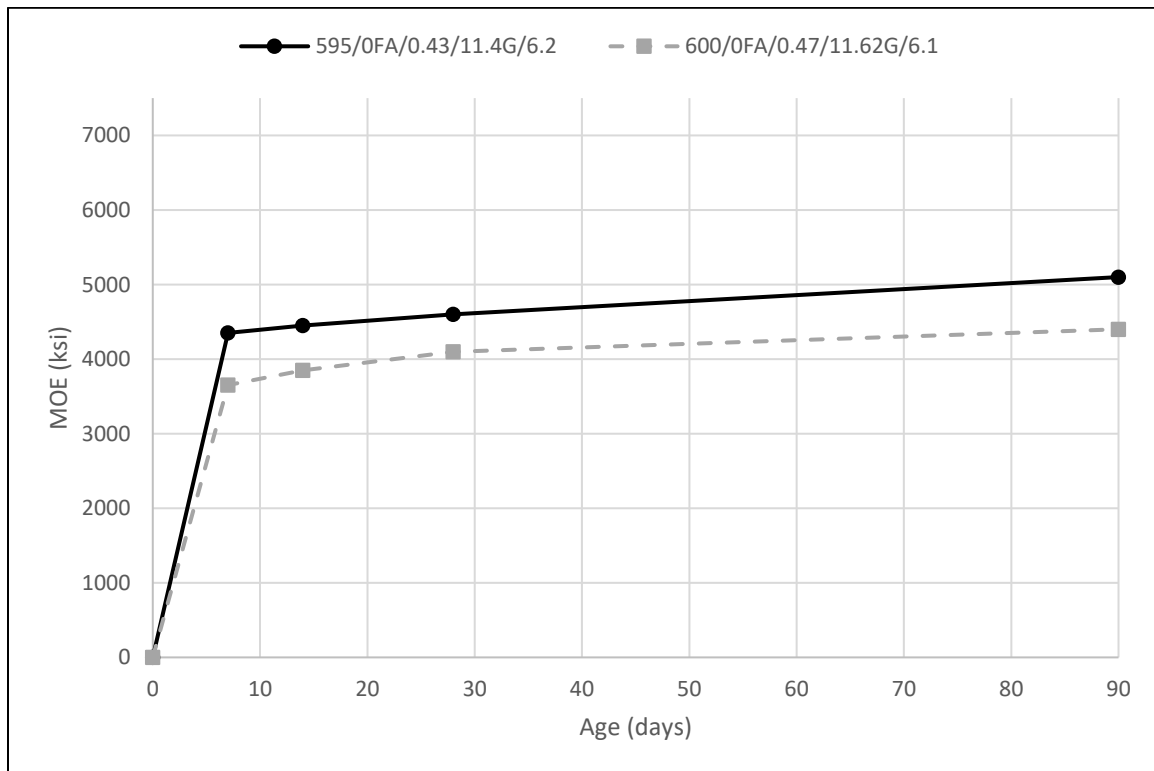
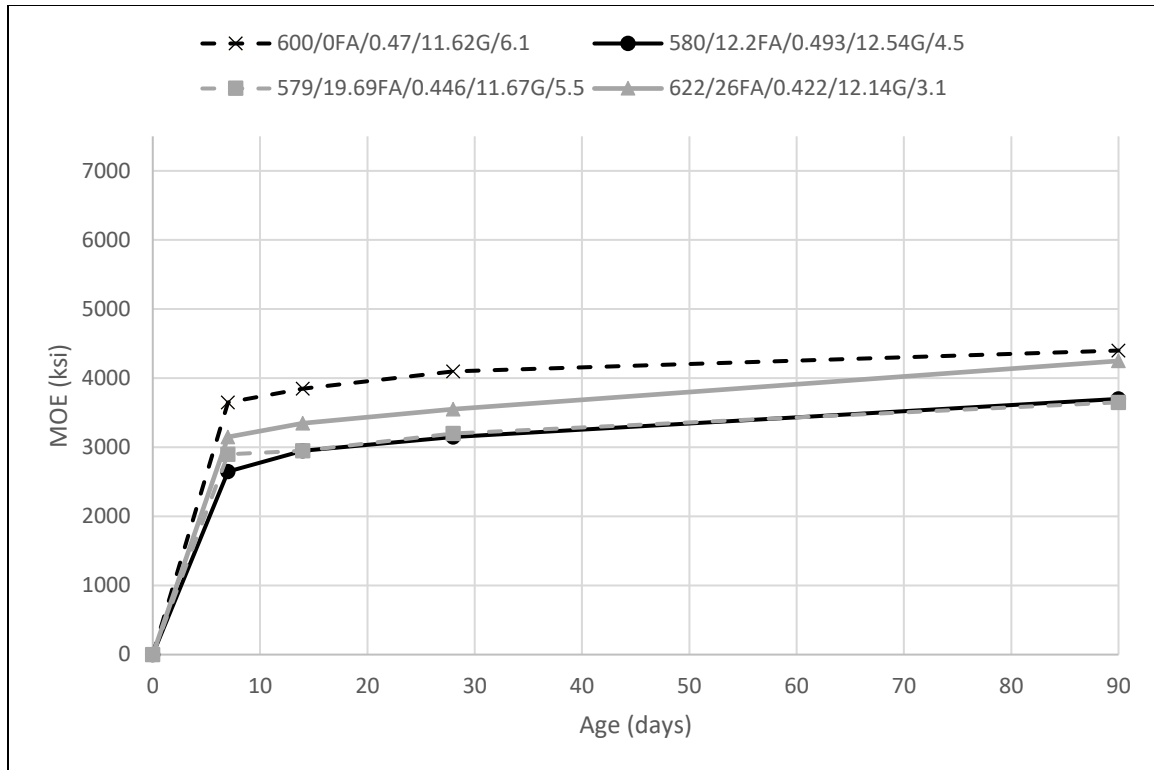
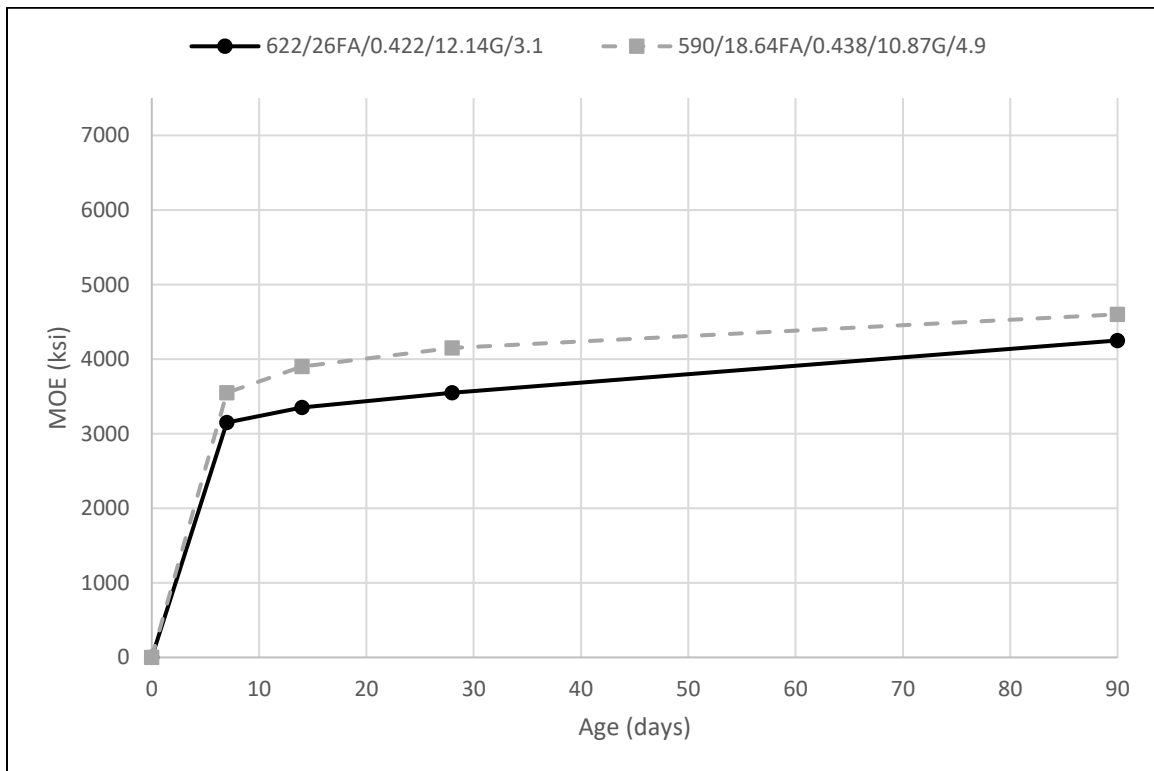


Figure 39. Line graph. MOE vs. age, mixtures 3 and 4, w/cm change.



**Figure 40. Line graph. MOE vs. age; mixtures 4, 5, 6, and 7; fly ash percentage change.**



**Figure 41. Line graph. MOE vs. age, mixtures 7 and 9, CA volume change.**

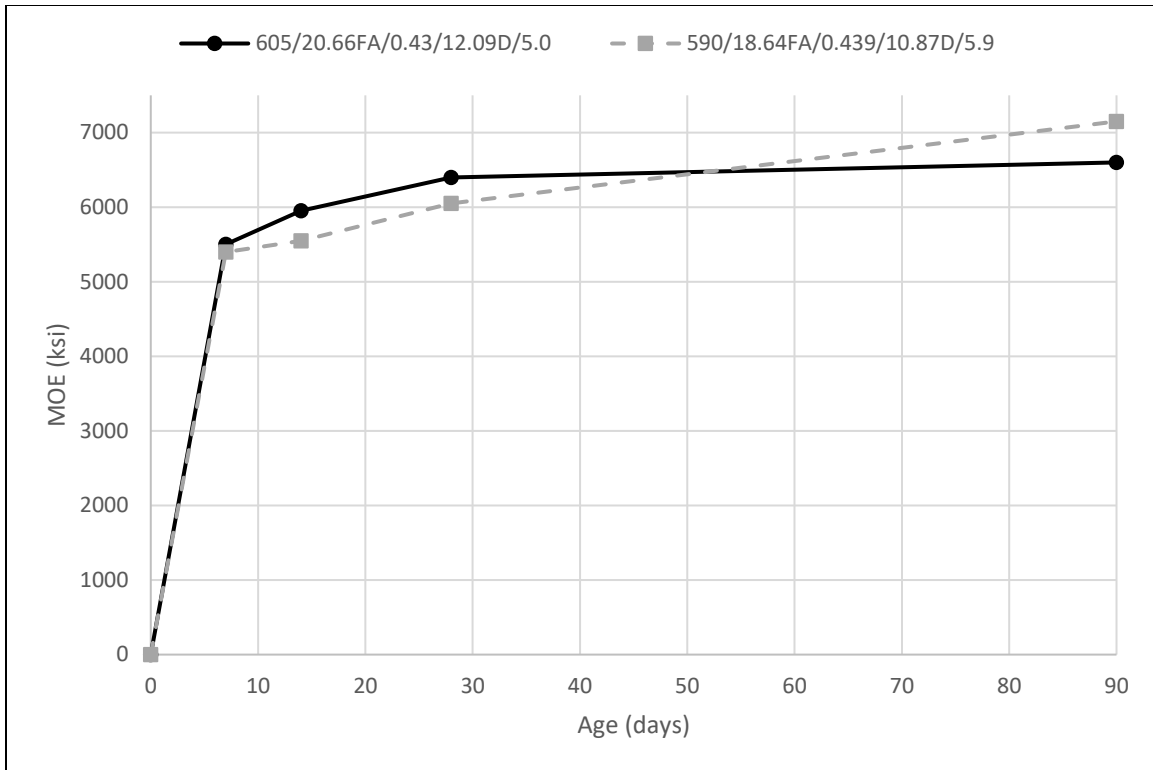


**Figure 42. Line graph. MOE vs. age, mixtures 8 and 10, CA volume change.**

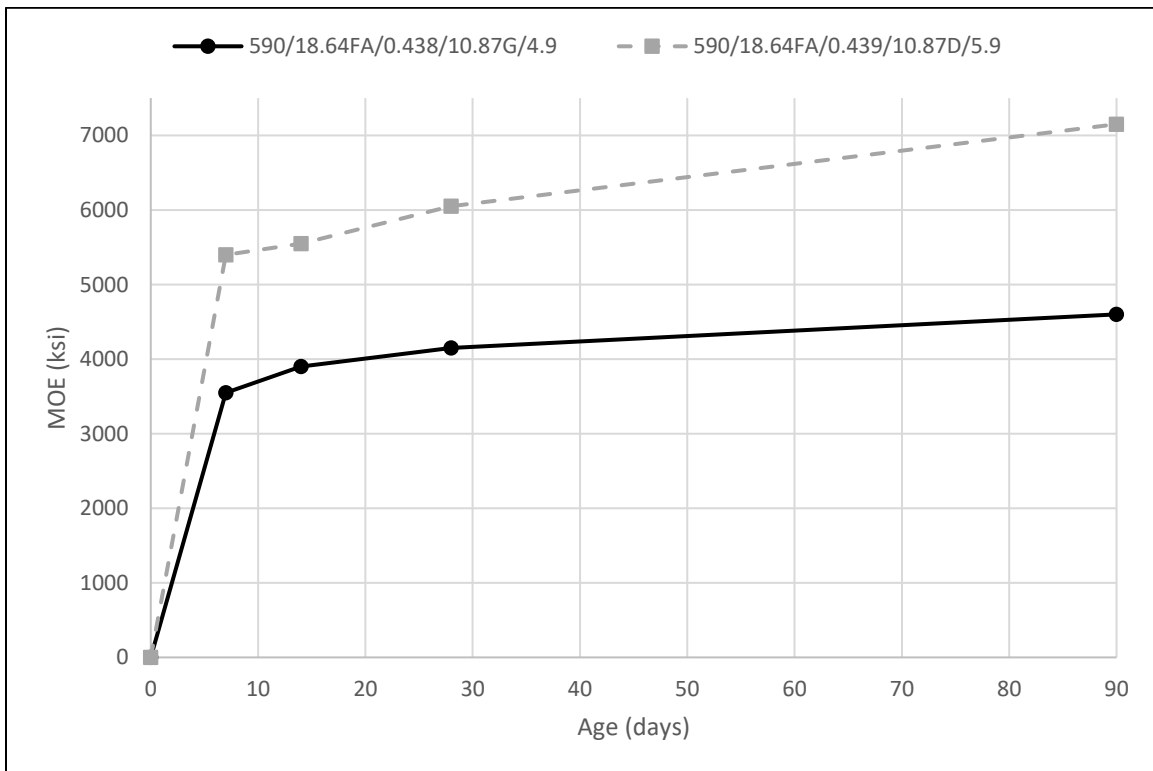


**Figure 43. Line graph. MOE vs. age, mixtures 9 and 10, CA type change.**

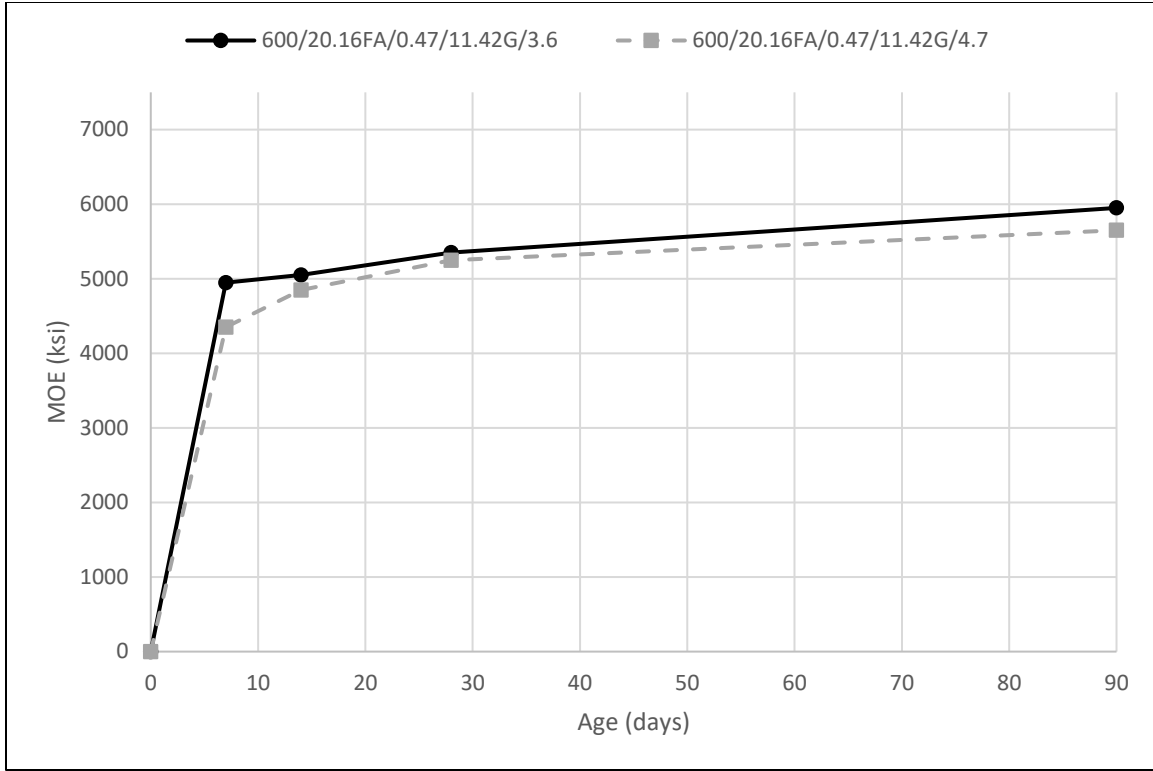


**Figure 44. Line graph. MOE vs. age, mixtures 11 and 12, air content change.**

As part of MOE testing, the static test method was compared with the dynamic test method. A one-mean hypothesis test was used to determine whether or not the static testing value could be determined using equation 5,  $E_{Static} = E_{Dynamic} * 0.83$ . The cylinders from 7, 14, and 28 days of age were compared, creating a sample size of 108 readings. The ratio of static MOE to dynamic MOE was analyzed for normality and had to be transformed by taking the square root in order to obtain a normal distribution. The null and alternative hypotheses are presented as equations 7 and 8. An alpha value of 0.05 was specified for this test.

$$H_0: \sqrt{\frac{MOE_{Static}}{MOE_{Dynamic}}} = \sqrt{0.83} \quad (7)$$

$$H_a: \sqrt{\frac{MOE_{Static}}{MOE_{Dyanamic}}} \neq \sqrt{0.83} \quad (8)$$

After conducting the hypothesis test, a test statistic of 1.983 and a p-value of 0.0035 were obtained. Since the p-value was smaller than alpha of 0.05, the null hypothesis should be rejected. In the context of this study, this means that using the proposed transformation in equation 5 is not acceptable. This is shown in figure 45, when the static and dynamic values are plotted together. It is clear that a pattern is not established; rather, the ratio is inconsistent between tests. When examining figure 45, the dynamic MOE value stays almost constant across the 12 mixtures. This is another sign that the static MOE is more accurate, since it changes as the concrete constituents and subsequent mechanical properties change. The static MOE should be the value used in AASHTOWare Pavement ME Design since a clear transformation has not been found for the dynamic value. This conclusion is consistent with NCHRP's recommendation to use static testing methods instead of dynamic tests (NCHRP 2004).

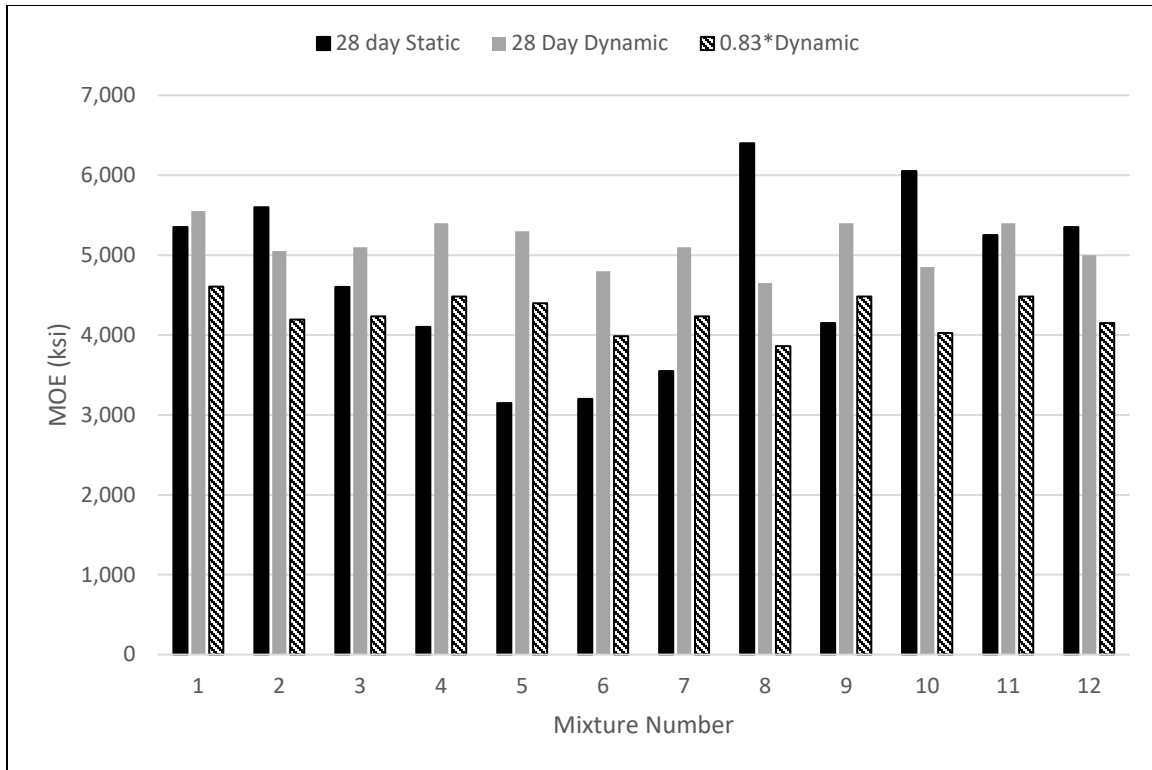


**Figure 45. Bar graph. Static MOE vs. dynamic MOE.**

### Poisson's Ratio

Each mixture was either equal to or higher than the default value of 0.20 for Poisson's ratio, with nine mixtures exhibiting Poisson's ratio values above that. For these mixtures, the predicted lateral strain is lower than what is experienced by the pavement. As a result, AASHTOWare Pavement ME Design will underpredict distresses for these mixtures if the default Poisson's ratio is used. The mixtures with the highest Poisson's ratio include the two using dolomite as the coarse aggregate, while other mixtures stayed fairly consistent between 0.20 and 0.23. Values for Poisson's ratio do not seem to be affected by concrete age. In most cases, the 7-day values are usually identical to the 28-day values. Differences in Poisson's ratio due to age, as shown in table 51, are likely a result of human or machine error. Similar studies did not see a variation in

Poisson's ratio with age (Rao 2014). A plot of the 28-day values is shown in figure 46; 28-day values are used for AASHTOWare Pavement ME Design input at all levels.

**Table 51. Poisson's ratio results.**

<b>Mixtures</b>		<b>Age of Specimen (days)</b>			
		<b>7</b>	<b>14</b>	<b>28</b>	<b>90</b>
<b>Mixture Number</b>	<b>Mix ID</b>	<b>Poisson's Ratio</b>			
1	541/0FA/0.431/11.91G/4.9	0.21	0.22	0.22	0.23
2	541/0FA/0.524/12.75G/4.0	0.22	0.22	0.22	0.23
3	595/0FA/0.43/11.4G/6.2	0.21	0.21	0.23	0.24
4	600/0FA/0.47/11.62G/6.1	0.22	0.21	0.22	0.23
5	580/12.2FA/0.493/12.54G/4.5	0.17	0.21	0.21	0.26
6	579/19.69FA/0.446/11.67G/5.5	0.18	0.21	0.20	0.24
7	622/26FA/0.422/12.14G/3.1	0.19	0.18	0.20	0.25
8	605/20.66FA/0.43/12.09D/5.0	0.25	0.25	0.26	0.27
9	590/18.64FA/0.438/10.87G/4.9	0.17	0.20	0.20	0.20
10	590/18.64FA/0.439/10.87D/5.9	0.20	0.24	0.25	0.27
11	600/20.16FA/0.47/11.42G/3.6	0.20	0.22	0.21	0.23
12	600/20.16FA/0.47/11.42G/4.7	0.22	0.21	0.22	0.23



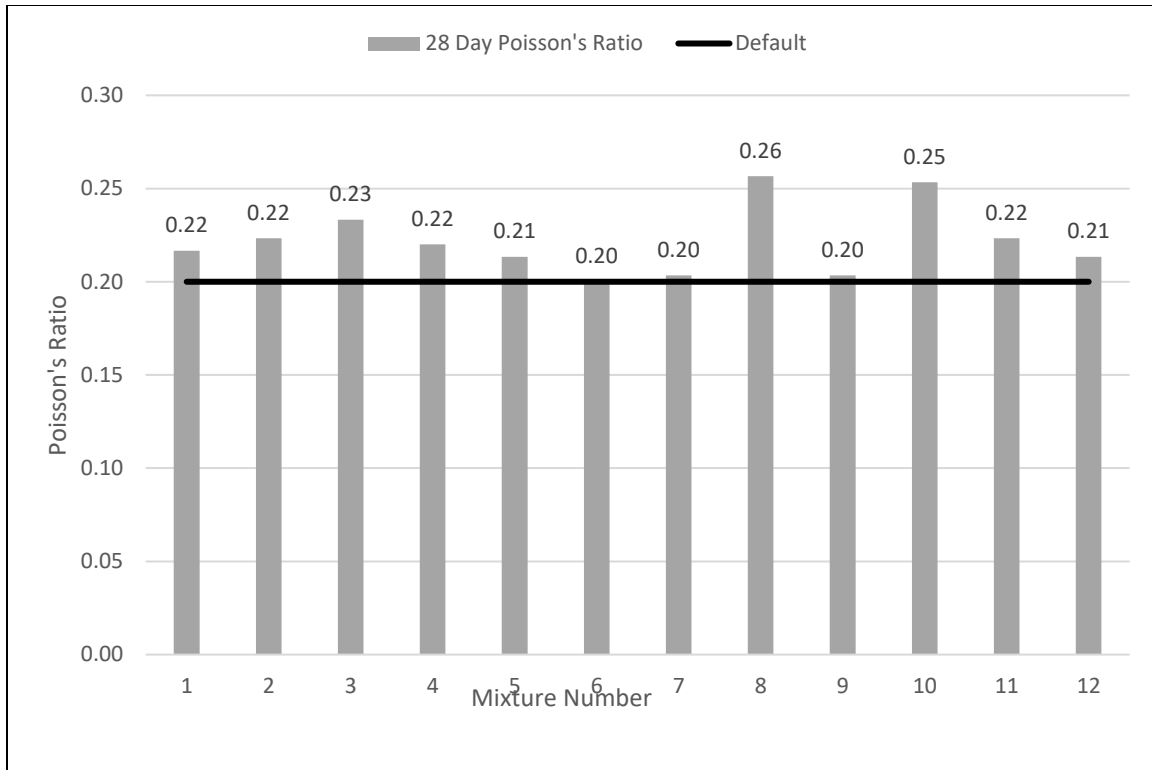


**Figure 46. Bar graph. 28-day Poisson's ratio values.**

### **Modulus of Rupture**

Since the beams used to test MOR were 3×4×16-inch (76.2×101.6×406.4 mm), larger 6×6×22-inch (152.4×152.4×558.8-mm) beams were cast along with the smaller beams for comparison. This was necessary since smaller beams are known to produce larger MOR values when compared with the standard larger beams. In total, six of the study mixtures were rebatched, producing three small beams, three large beams, and three cylinders for each. At 28 days of age, the specimens were tested for MOR and compressive strength. Using the average measured results from the six beams, a linear regression equation was determined to relate the MOR for larger beams with that of smaller beams. The averages of the MOR tests are shown in table 52. The results from mixture 1 were determined to be an outlier to the data and removed from the linear regression model. A plot of the remaining points is shown in figure 47, as well as the resulting

linear regression equation. The  $R^2$  value of the resulting equation is 0.79, which is considered to be a strong relationship (Peck and Devore 1986). All MOR values were then adjusted using this equation, lowering them to more expected values. The values presented in this study are altered using the equation displayed in figure 47. These altered values are input to AASHTOWare Pavement ME Design in the subsequent sensitivity analyses and are presented in table 53.

**Table 52. MOR beam size comparison.**

Mixture	Small Beam MOR (psi)	Large Beam MOR (psi)	Compressive Strength (psi)
1	914	815	6,540
2	850	718	4,930
8	955	776	5,520
10	947	753	5,310
11	849	722	5,170
12	856	690	5,150

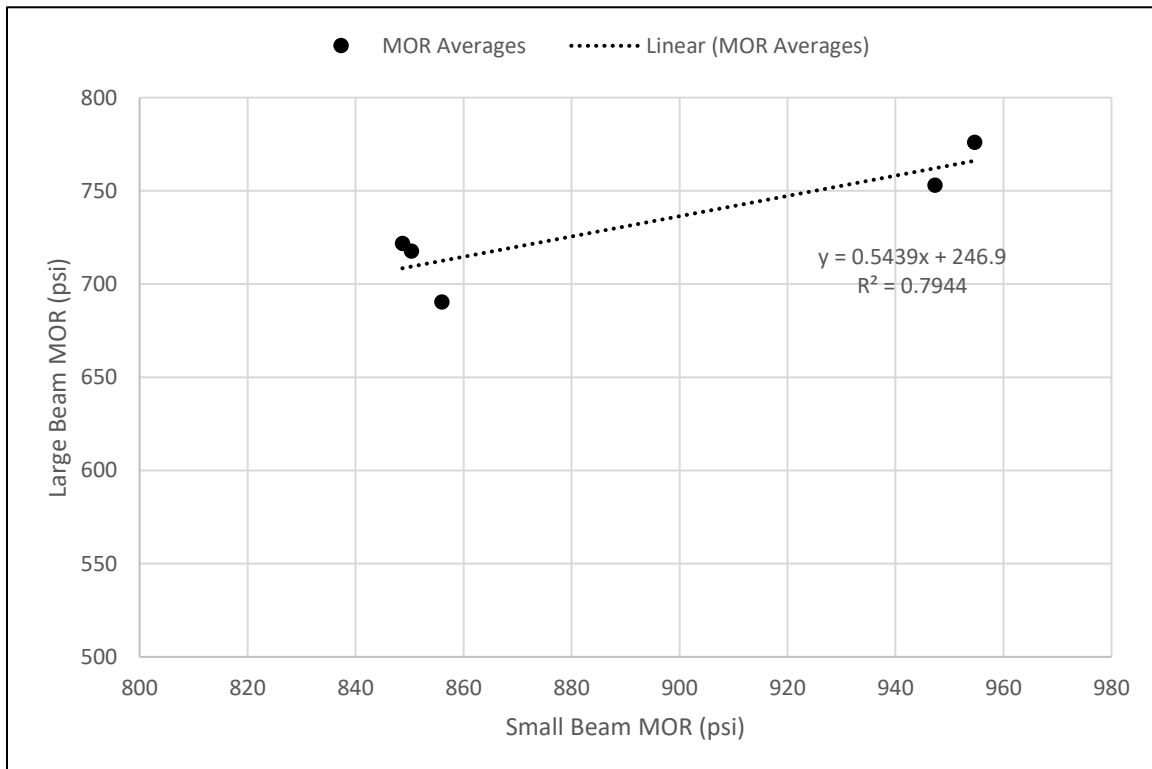


**Figure 47. Graph. MOR linear regression adjustment.**

By 28 days of age, half of the mixtures met the GDOT design acceptance requirement for class 1 mixtures with minimum values of 600 psi (4.1 MPa) and half met the DAR for class 2 mixtures with minimum values of 700 psi (4.8 MPa). An observed trend from the MOR results is the specimens developed most of their flexural strength within the first 7 days of age. There was a 3.84 percent difference between the 7-day MOR and the 14-day MOR, on average. Between 7 and 28 days, the MOR value increased by 9.30 percent, on average. Graphs showing companion mixtures plotted against one another are shown in figure 48 (mixtures 1 and 2), figure 49 (mixtures 3 and 4), figure 50 (mixtures 4, 5, 6, and 7), figure 51 (mixtures 7 and 9), figure 52 (mixtures 8 and 10), figure 53 (mixtures 9 and 10), and figure 54 (mixtures 11 and 12).

**Table 53. MOR results.**

<b>Mixtures</b>		<b>Age of Specimen (days)</b>			
		<b>7</b>	<b>14</b>	<b>28</b>	<b>90</b>
<b>Mixture Number</b>	<b>Mixture ID</b>	<b>MOR (psi)</b>			
1	541/0FA/0.431/11.91G/4.9	685	705	710	730
2	541/0FA/0.524/12.75G/4.0	640	695	725	730
3	595/0FA/0.43/11.4G/6.2	670	665	805	690
4	600/0FA/0.47/11.62G/6.1	630	630	665	665
5	580/12.2FA/0.493/12.54G/4.5	595	640	650	720
6	579/19.69FA/0.446/11.67G/5.5	615	600	620	730
7	622/26FA/0.422/12.14G/3.1	600	640	670	720
8	605/20.66FA/0.43/12.09D/5.0	615	630	660	765
9	590/18.64FA/0.438/10.87G/4.9	700	700	700	755
10	590/18.64FA/0.439/10.87D/5.9	615	645	635	765
11	600/20.16FA/0.47/11.42G/3.6	620	730	785	755
12	600/20.16FA/0.47/11.42G/4.7	650	640	715	740

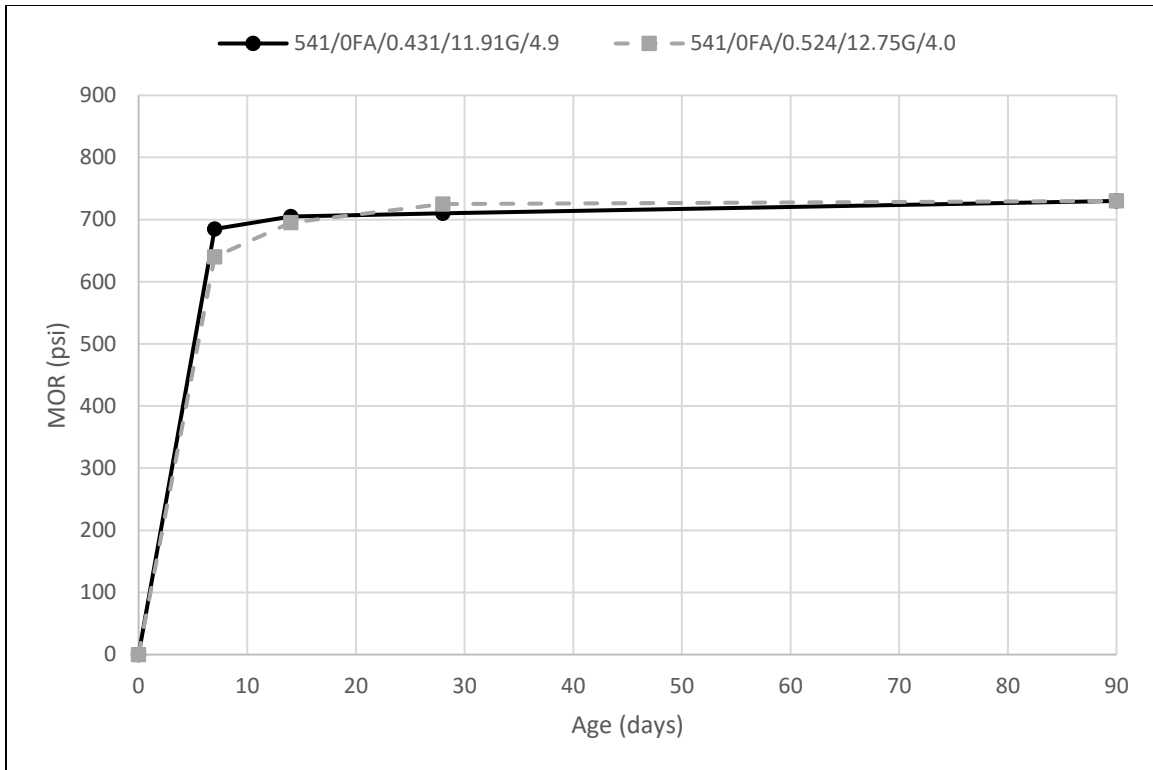


**Figure 48. Line graph. MOR vs. age, mixtures 1 and 2, w/cm change.**

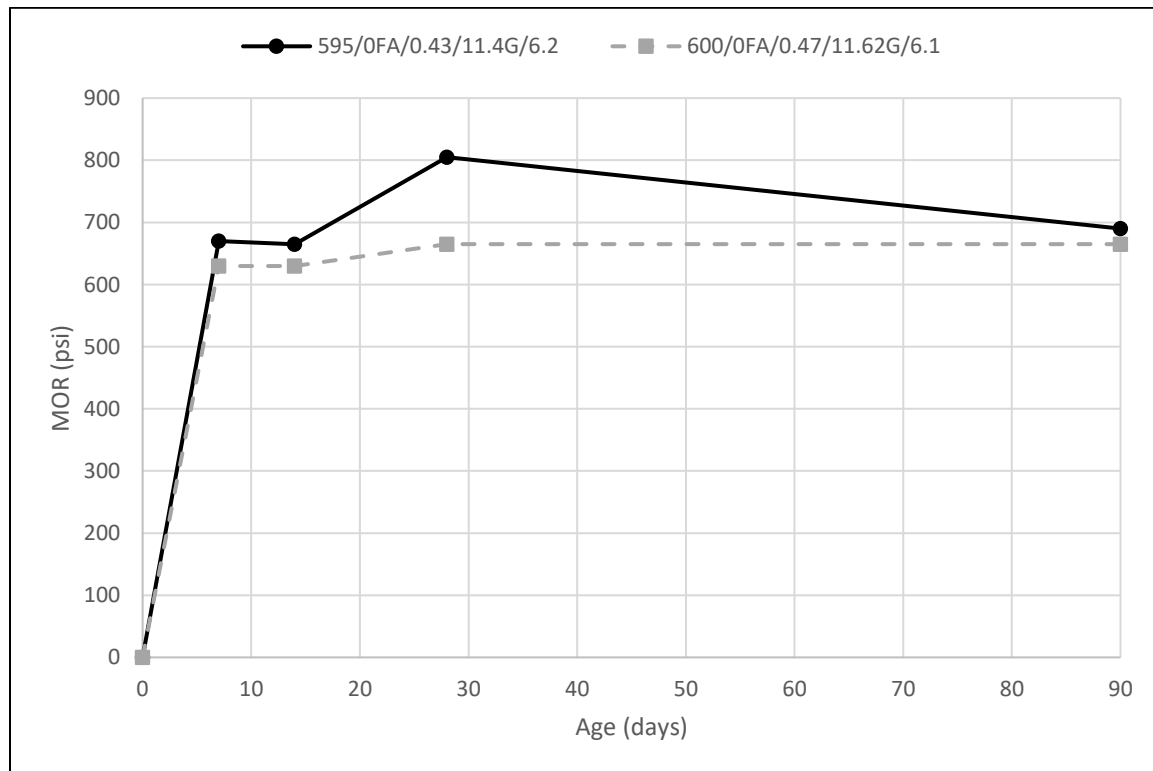


**Figure 49. Line graph. MOR vs. age, mixtures 3 and 4, w/cm change.**

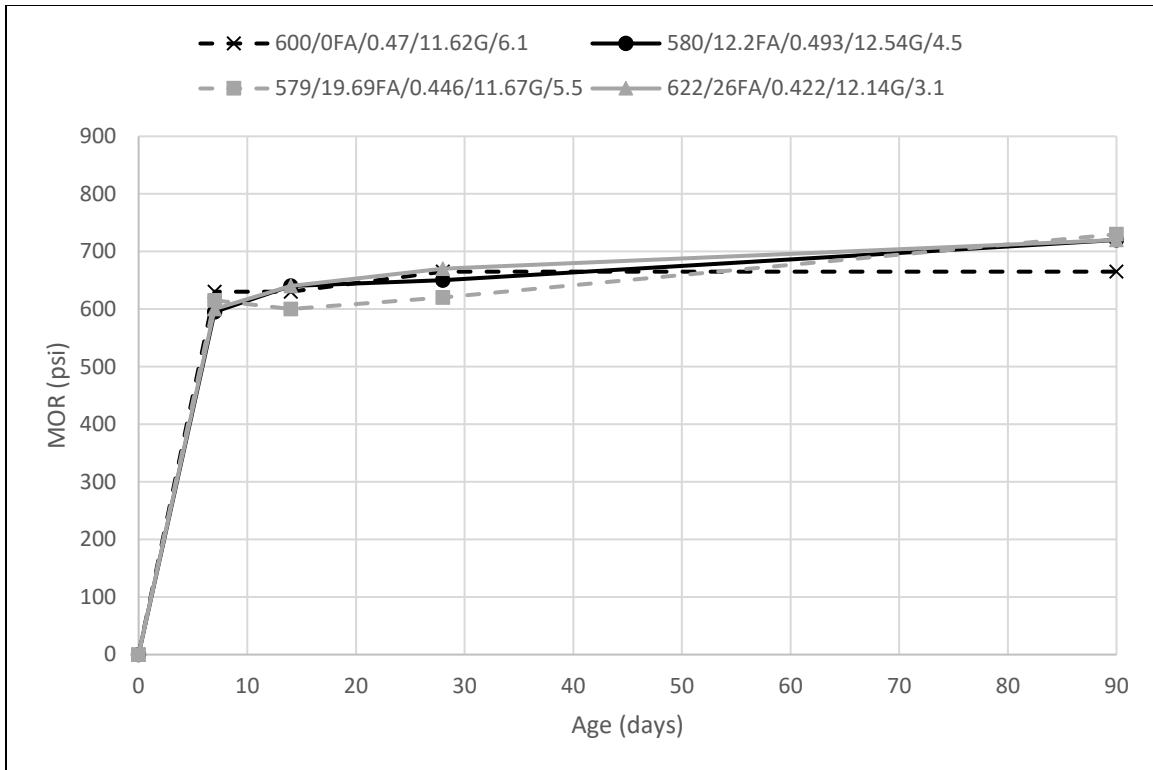


Figure 50. Line graph. MOR vs. age; mixtures 4, 5, 6, and 7; fly ash percentage change.

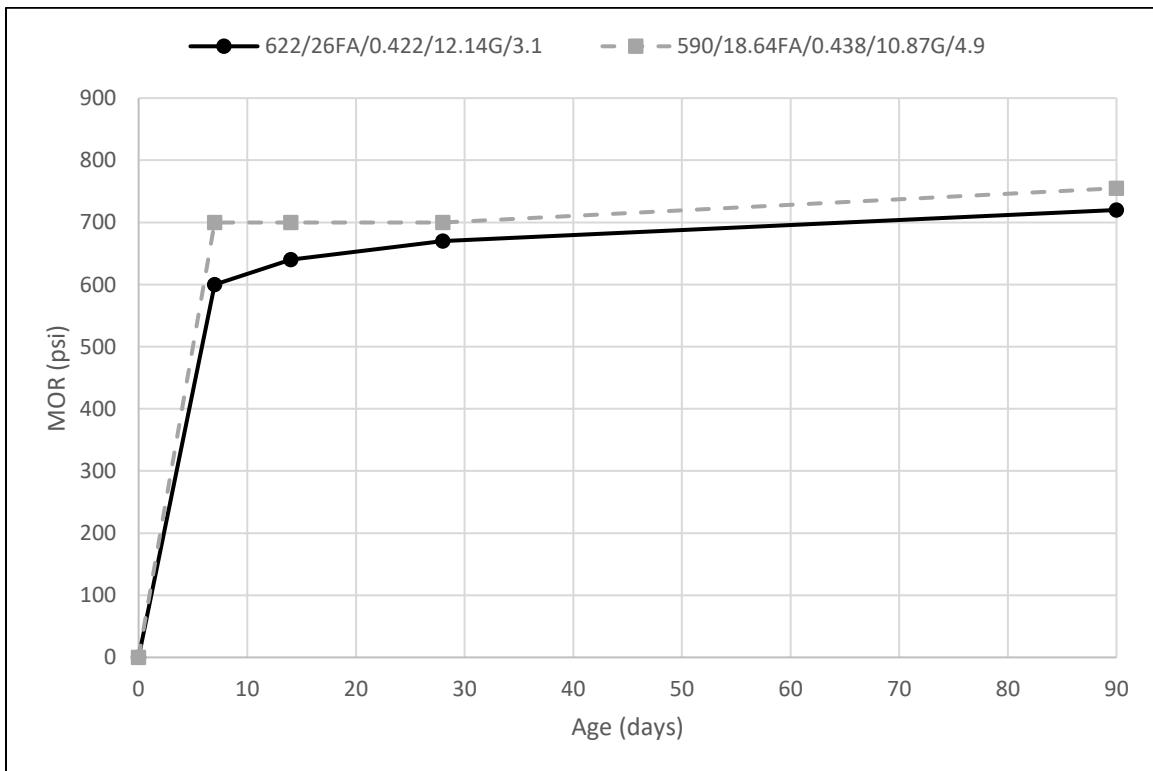
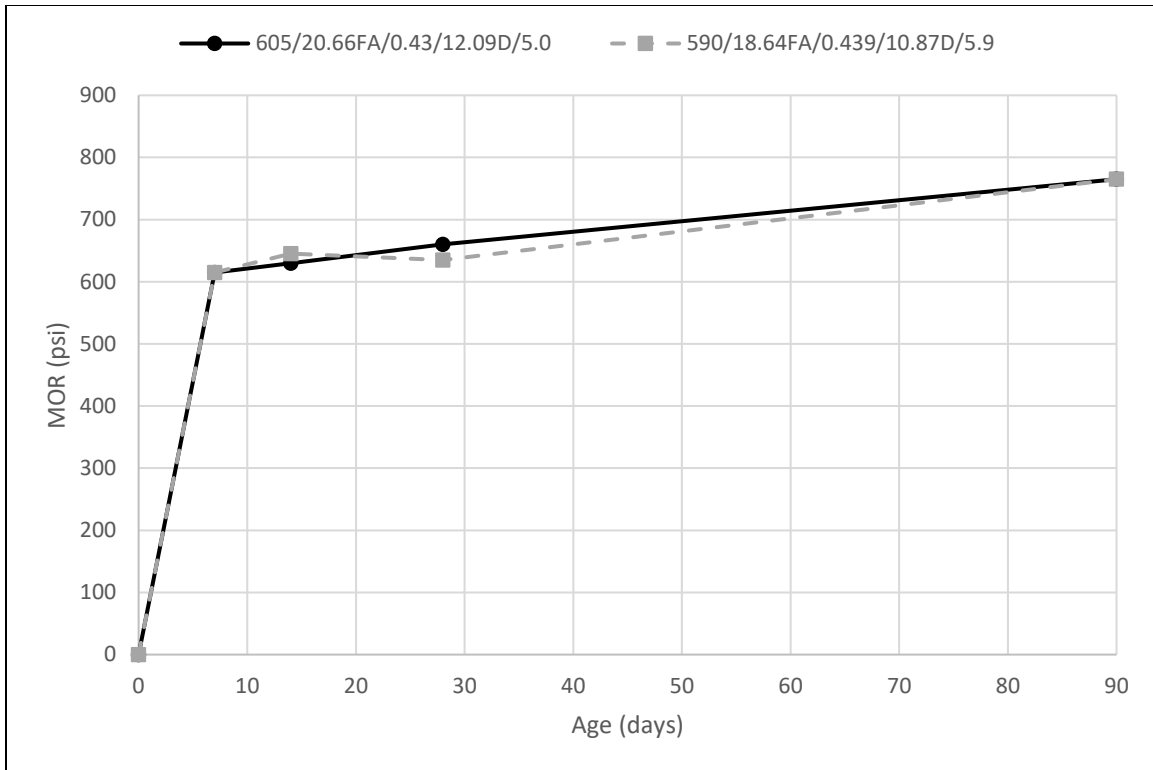
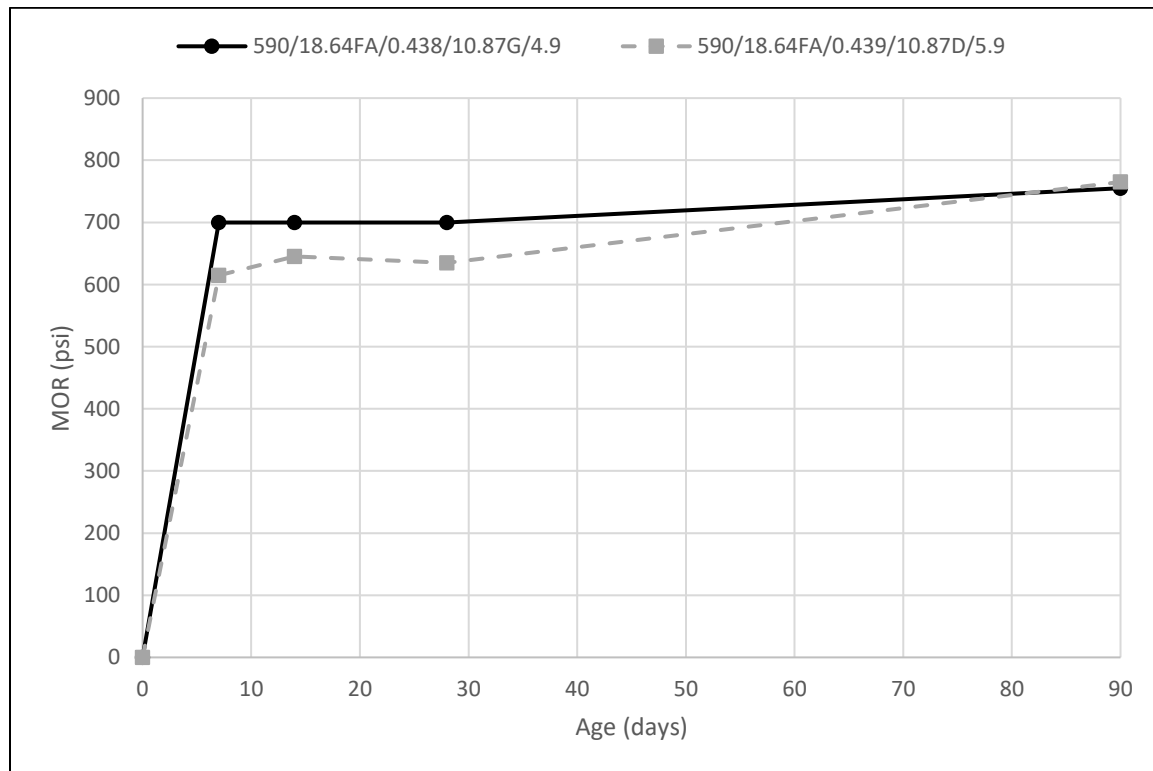


Figure 51. Line graph. MOR vs. age, mixtures 7 and 9, CA volume change.



**Figure 52. Line graph. MOR vs. age, mixtures 8 and 10, CA volume change.**



**Figure 53. Line graph. MOR vs. age, mixtures 9 and 10, CA type change.**

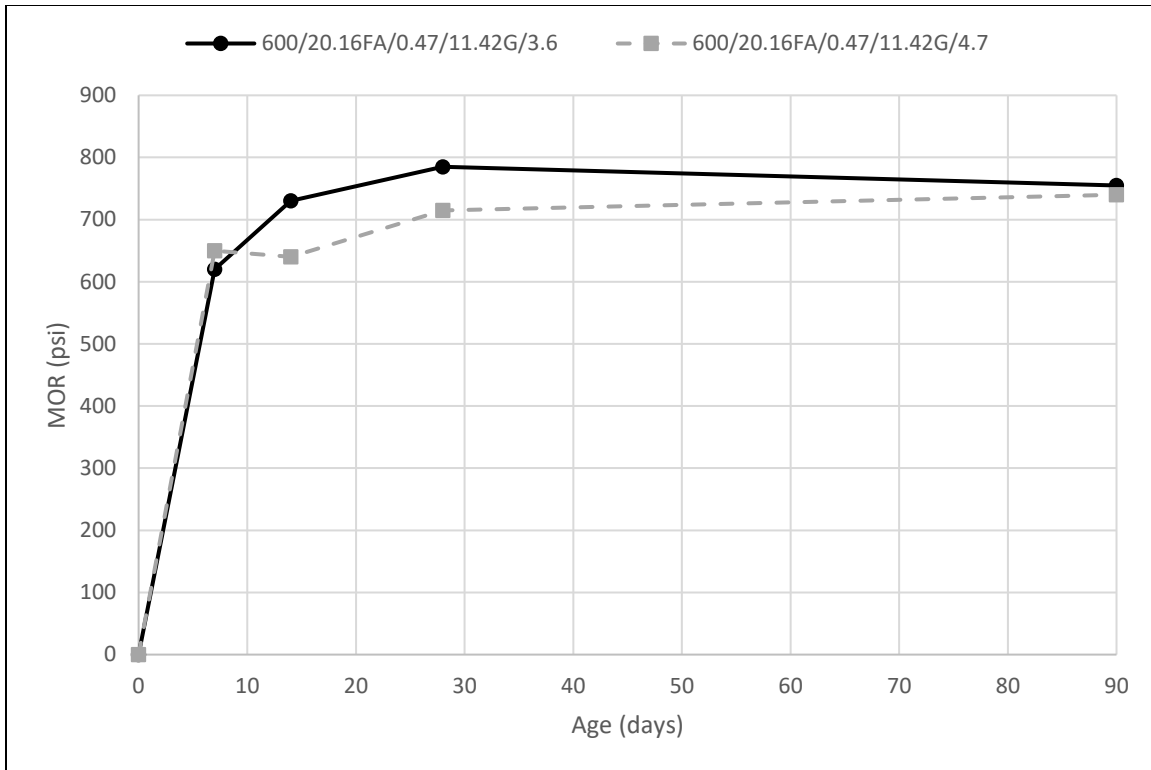


**Figure 54. Line graph. MOR vs. age, mixtures 11 and 12, air content change.**

The measured MOR results are observed to remain fairly consistent for most companion mixtures. Figure 53 and figure 54 show more noticeable differences between the mixtures being compared. In both cases, the lower MOR values correspond to mixtures with a higher air content. Because of the higher air content, there is a decreased distance between voids within the concrete. When tension cracks form, less energy is required for cracks to travel between voids due to this decreased distance, resulting in lower flexural strengths. From these data, air seems to be the most determining factor in the MOR values of mixtures used in rigid pavement design.

It is important to note that AASHTOWare Pavement ME Design does not use equation 6 from ACI to estimate MOR values; rather, it uses  $9.5 * \sqrt{f'_c}$  as the prediction equation. As shown in figure 55, AASHTOWare Pavement ME Design's estimations of MOR values are higher than values predicted by the ACI equation. Laboratory-tested values from 28 days of age were plotted

for comparison; the values fit very closely with the equation used in Pavement ME Design. This graph helps validate the equation used in Pavement ME Design, as tested values are similar to predictions from compressive strength. Statistical analysis was performed to see if there was a significant difference in predicted distresses using MOR or compressive strength. As a result of the test, it was determined that there was not a significant difference in using MOR versus compressive strength at level 3.

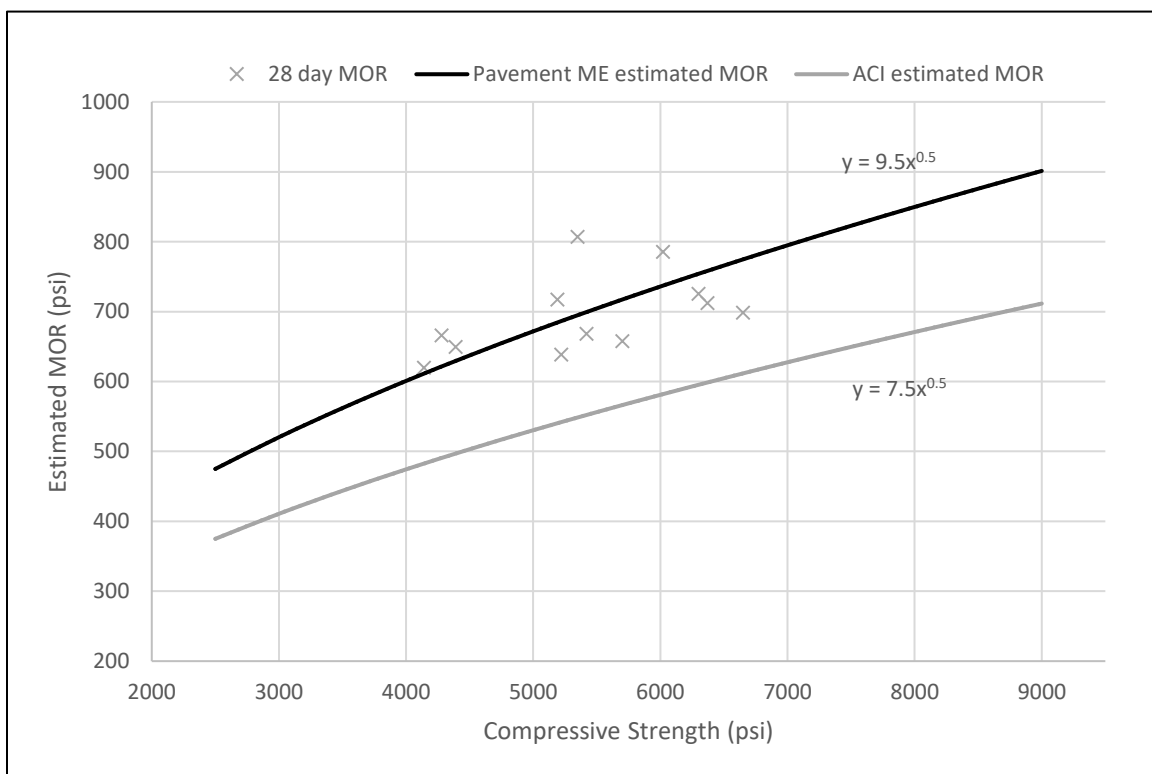


**Figure 55. Line graph. AASHTOWare Pavement ME Design estimated MOR, ACI estimated MOR, and measured values.**

Effect of size of beam on MOR was also investigated. Small beams and a few large beams were tested for MOR values and then a linear regression model was used to validate the MOR test results. The 12 GDOT-approved mixtures were batched to produce cylinders and large beams to relate the mixtures to a previous study using the same mixtures. Each mixture had two large beams



to compare to the previous data at the 28- and 90-day testing periods. The 28- and 90-day MOR test results with different sizes of the beam are shown in figure 56.

While the results are fairly similar, the MOR test values only contain the test value of one large beam specimen. Any variance between the specimens is likely due to only one large beam specimen being tested during the recent comparison results.

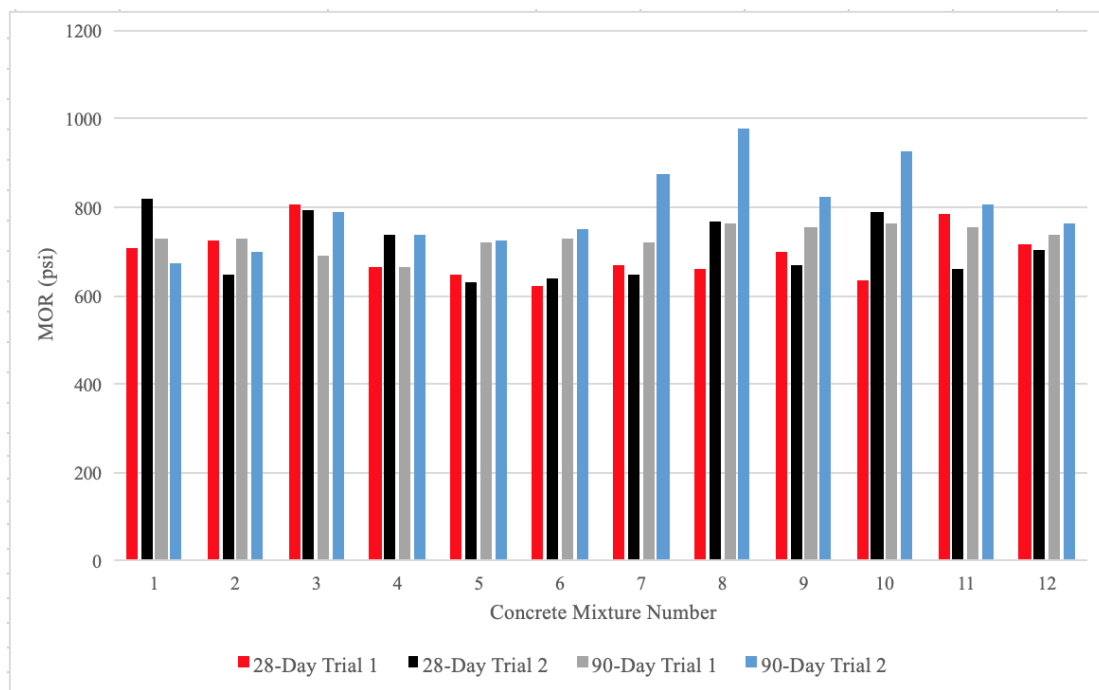


**Figure 56. Bar graph. MOR test results comparison.**

## Shrinkage

The length change-up to 90 days of age was measured. The specimens prepared in this study were continually measured at the appropriate ages. Generally, shrinkage specimens from this study experienced growth in the first 28 days, denoted by a positive percentage difference from the original length. Sometime between 28 and 90 days of age, the specimens began to shrink, denoted by a decrease in the percent difference from the original length. This initial growth is due to the

cement hydration reaction producing the hydration products, which have a larger volume than the original reactants. The percent difference in length of the 12 mixtures is displayed in table 54.

**Table 54. Shrinkage results.**

Mixtures		Age of Specimen (days)				
		1	7	14	28	90
Mixture	Mix ID	Difference from original length (%)				
1	541/0FA/0.431/11.91G/4.9	0.00	−1.82	−3.92	−0.89	−0.62
2	541/0FA/0.524/12.75G/4.0	0.00	−6.01	−7.17	−6.52	−4.60
3	595/0FA/0.43/11.4G/6.2	0.00	0.51	0.42	0.26	0.90
4	600/0FA/0.47/11.62G/6.1	0.00	0.73	1.17	0.76	1.52
5	580/12.2FA/0.493/12.54G/4.5	0.00	3.71	7.32	9.68	7.20
6	579/19.69FA/0.446/11.67G/5.5	0.00	2.37	2.66	2.87	2.86
7	622/26FA/0.422/12.14G/3.1	0.00	−0.38	1.28	−0.06	0.70
8	605/20.66FA/0.43/12.09D/5.0	–	0.00	0.78	0.49	0.33
9	590/18.64FA/0.438/10.87G/4.9	0.00	−1.32	0.16	0.97	0.24
10	590/18.64FA/0.439/10.87D/5.9	0.00	−0.66	−0.66	−0.51	−0.57
11	600/20.16FA/0.47/11.42G/3.6	0.00	−0.20	1.10	3.26	8.92
12	600/20.16FA/0.47/11.42G/4.7	0.00	0.55	0.74	1.24	3.49

\*Mixture 8 length is referenced from day 7 instead of day 1.

– No data

The only factor observed to have a noticeable impact on shrinkage values was w/cm. High w/cm resulted in the largest percentage differences in a specimen's length. In some cases, this length change was positive and, in some cases, negative, as shown by figure 57 and figure 58. Figure 59 shows all the mixtures plotted together for shrinkage, except for mixtures 1, 2, and 5, which were removed since their percent change was much larger than the other mixtures. As shown in figure 59, mixtures 6 (579/19.69FA/0.446/11.67G/5.5) and 11 (600/20.16FA/0.47/11.42G/3.6) experienced the largest growth of approximately 3.0 percent. The remaining mixtures displayed in figure 57 experienced around a 1.0 percent growth or less. No clear trends are established from the shrinkage results of these mixtures, as shown in figure 59.

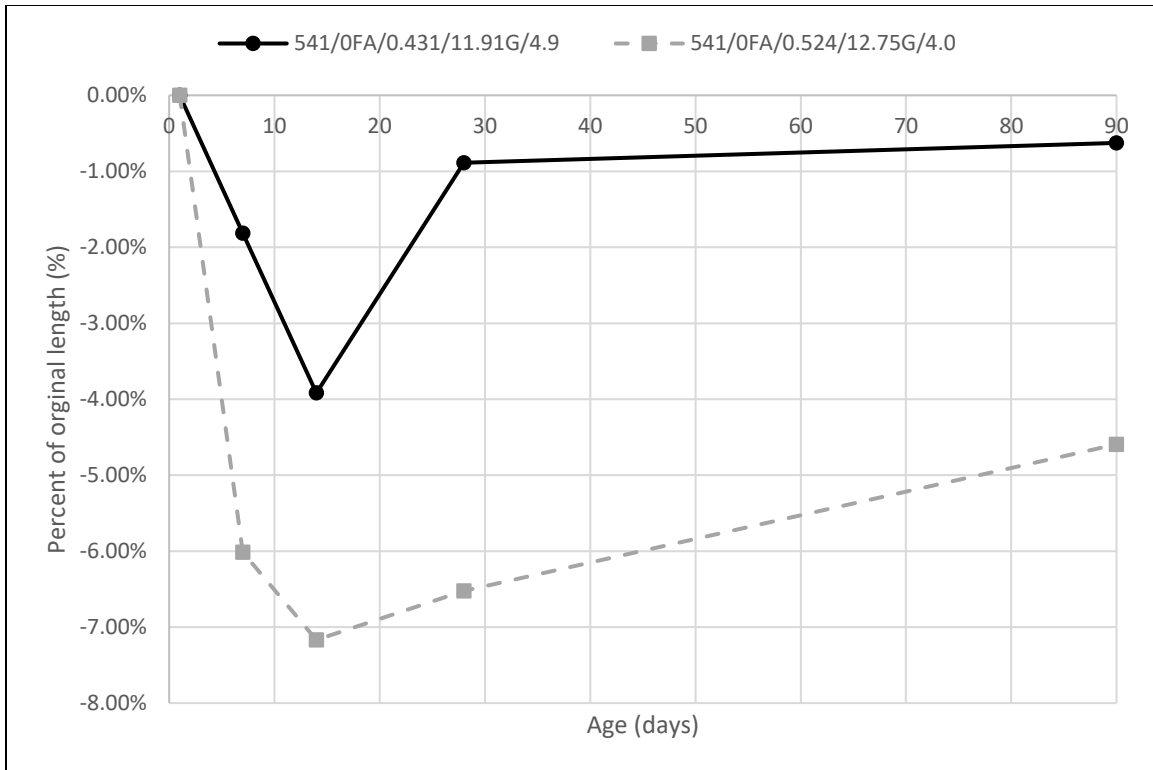


**Figure 57. Line graph. Shrinkage, mixtures 1 and 2, w/cm change.**

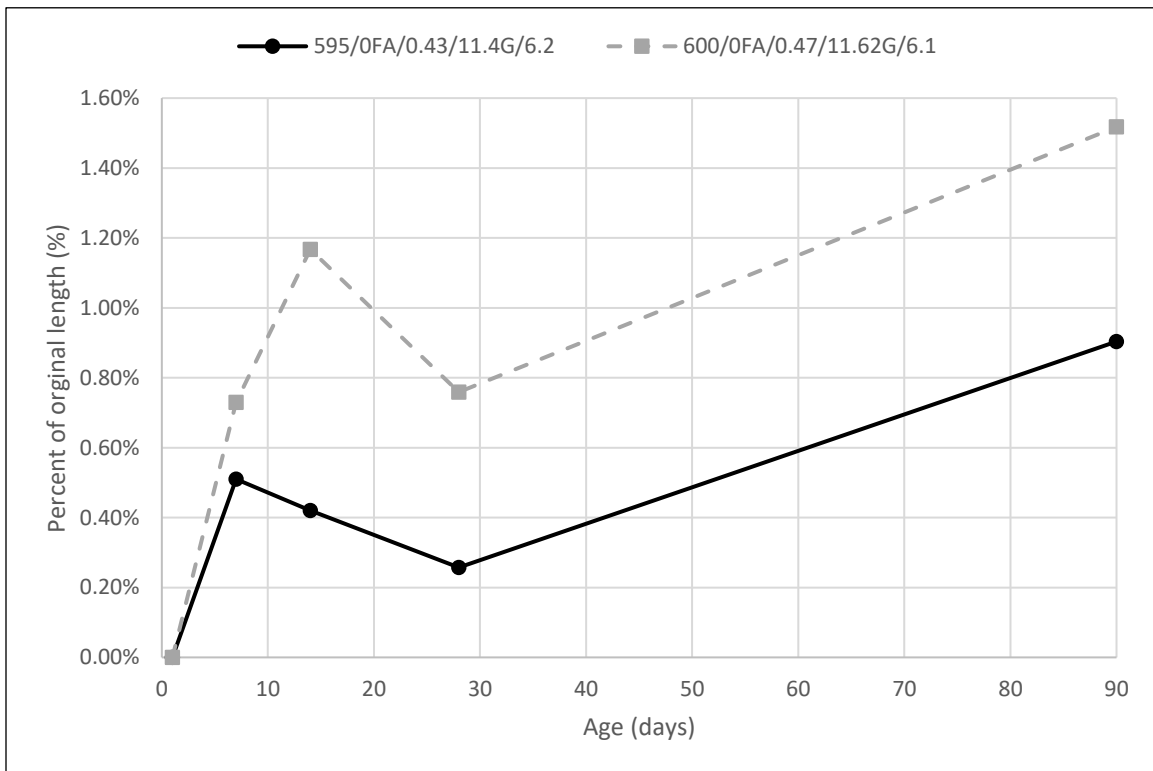


**Figure 58. Line graph. Shrinkage, mixtures 3 and 4, w/cm change.**

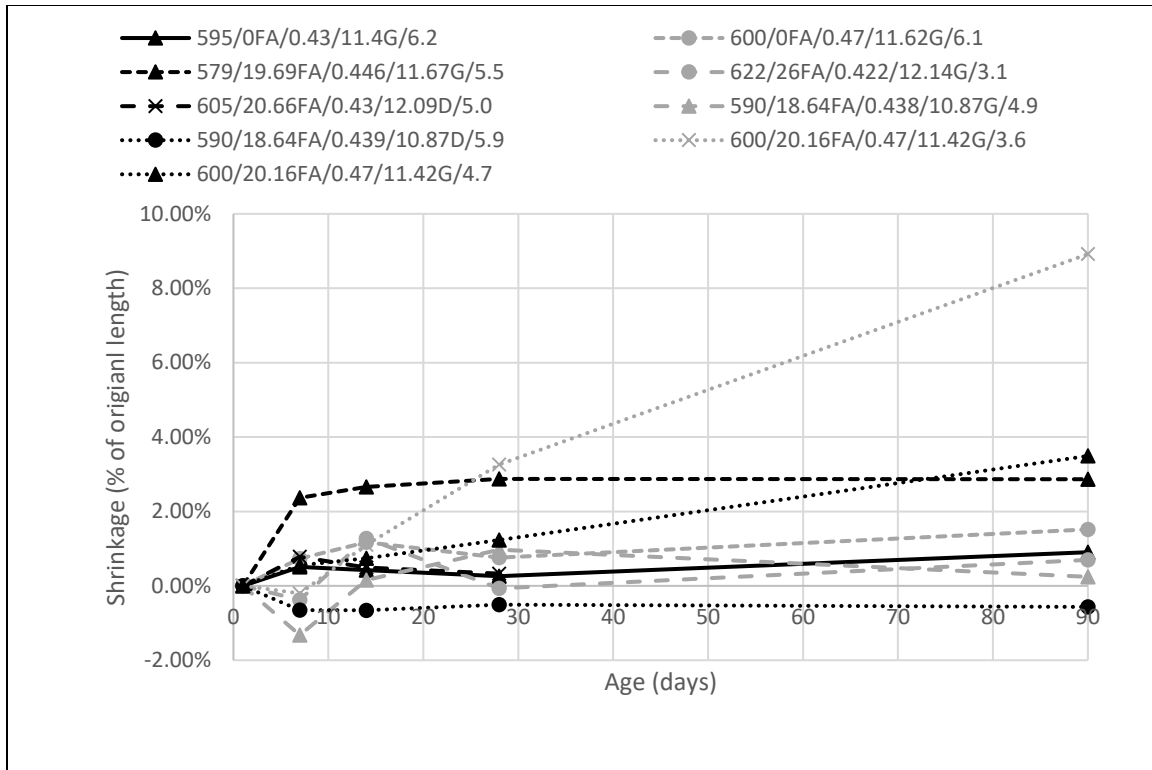


**Figure 59. Line graph. Shrinkage, all mixtures (except mixtures 1, 2, and 5).**

To investigate the meaningful outcomes, additional shrinkage tests were conducted. The additional ultimate shrinkage test results are listed in table 55. Ultimate shrinkage is either calculated or user-defined in level 2 and 3 designs in AASHTOWare Pavement ME Design, and a user-defined input for a level 1 design is required. Due to specimen sensitivity, the specimens were stored in an environmental chamber that maintained a temperature of  $73\pm3^{\circ}\text{F}$  ( $23\pm2^{\circ}\text{C}$ ) and relative humidity of  $50\pm4$  percent. The shrinkage specimens were wet cured for the first 28-day period in this controlled environment and then removed from the curing tanks, where they continued to age in the controlled conditions provided by the environmental chamber.

**Table 55. Ultimate shrinkage test results.**

Mixture Number	Age of Specimens (days)										
	3	7	14	28	35	42	49	56	63	70	77
	Average Percent Difference in Specimen Length (%)										
1	0.0003%	0.0007%	0.0040%	0.0013%	0.0023%	0.0030%	-0.0010%	-0.0037%	-0.0073%		
2	0.0010%	0.0000%	-0.0007%	-0.0007%	-0.0010%	-0.0007%	-0.0053%	-0.0083%	-0.0113%		
3	0.0030%	0.0057%	0.0060%	0.0013%	-0.0023%	-0.0043%	-0.0067%	-0.0090%			
4	0.0057%	0.0077%	0.0107%	0.0077%	-0.0007%	-0.0020%	-0.0120%	-0.0187%			
5	-0.0057%	-0.0007%	0.0020%	-0.0017%	-0.0037%	0.0013%	-0.0023%	-0.0007%	-0.0027%	-0.0107%	-0.0167%
6	-0.0057%	0.0010%	0.0030%	0.0007%	-0.0003%	-0.0020%	-0.0040%	-0.0047%	-0.0070%	-0.0150%	-0.0207%
7	-0.0007%	0.0037%	0.0050%	0.0047%	0.0033%	0.0037%	0.0043%	0.0027%	0.0027%	-0.0063%	-0.0120%
8	0.0093%	0.0140%	0.0160%	0.0077%	0.0057%	0.0043%	0.0030%	-0.0053%			
9	0.0083%	0.0103%	0.0107%	0.0080%	0.0097%	0.0147%	0.0137%	0.0133%	0.0077%	-0.0067%	
10	0.0040%	0.0030%	0.0040%	-0.0010%	-0.0010%	-0.0010%	-0.0015%	-0.0050%	0.0133%		
11	0.0040%	0.0080%	0.0100%	0.0097%	0.0073%	0.0107%	0.0083%	0.0020%	0.0118%		
12	0.0014%	0.0041%	0.0038%	0.0028%	0.0040%	0.0056%	0.0042%	0.0024%	0.0026%		

The results contained the average of three shrinkage specimens tested following *ASTM C157*. The test results successfully passed the precision and bias criteria of water-stored shrinkage requirements. None of the specimens exceeded a maximum range of 0.0266 percent, while the means between the same mixtures' specimens did not exceed 0.0074 percent in 95 percent of the results. A visualization of the shrinkage results up to the 77-day mark is provided in figure 60.

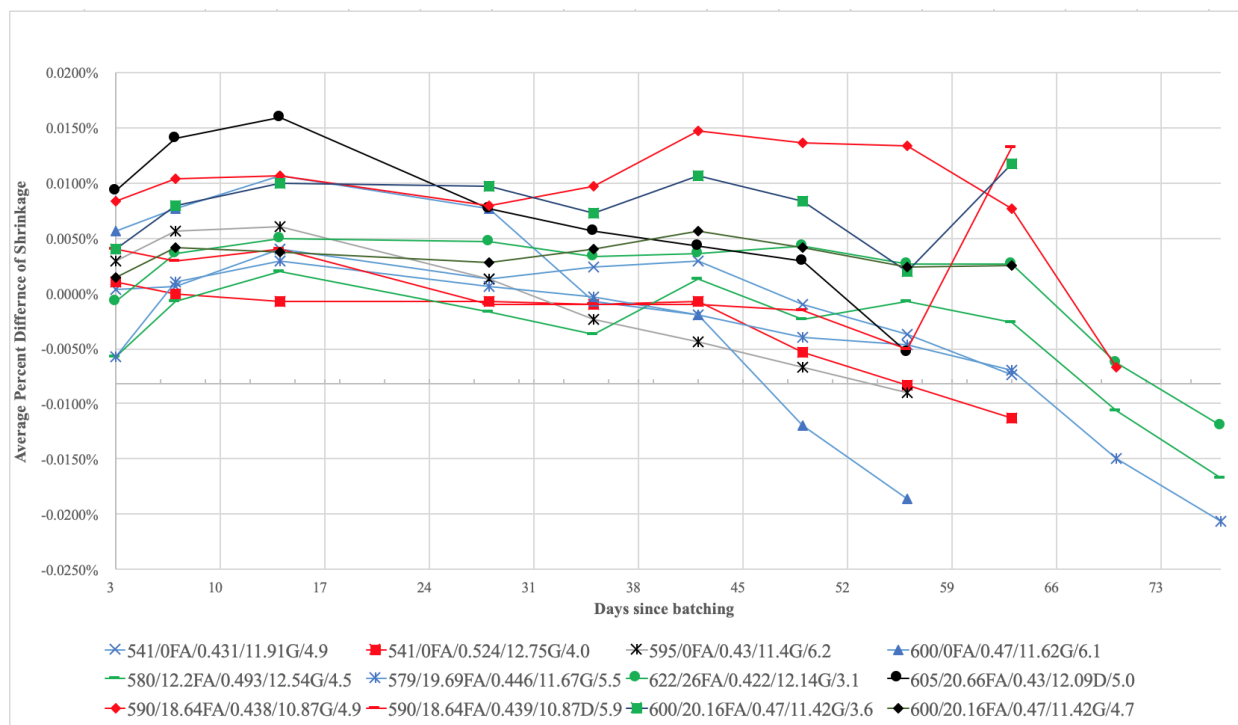


**Figure 60. Line graph. Ultimate shrinkage plot.**

A majority of the shrinkage specimens demonstrated an expected initial expansion during the first 14 days of the moisture-curing process. At the 28-day mark, specimens illustrated a shrinking trend. Mixtures containing fly ash had not fully cured at the 28-day mark and have slightly different shrinkage rates than the mixtures without fly ash.

## Thermal Properties Test Results

The thermal properties test results are the primary focus of this study. The 12 GDOT-approved mixtures were batched multiple times to achieve accurate lab-tested values that can be used for an MEPDG approach. The thermal properties of concern in this section are the coefficient of thermal expansion and thermal conductivity. These properties were tested following the procedures mentioned in chapter 6. CTE test results are listed in table 56.

**Table 56. CTE test results.**

Mixture Number	Mixture ID	CTE (in/in/Fdeg)		
		Specimen 1	Specimen 2	Average
1	541/0FA/0.431/11.91G/4.9	4.81E-06	5.01E-06	4.91E-06
2	541/0FA/0.524/12.75G/4.0	4.62E-06	4.69E-06	4.66E-06
3	595/0FA/0.43/11.4G/6.2	5.18E-06	5.32E-06	5.25E-06
4	600/0FA/0.47/11.62G/6.1	5.03E-06	5.14E-06	5.09E-06
5	580/12.2FA/0.493/12.54G/4.5	5.07E-06	5.19E-06	5.13E-06
6	579/19.69FA/0.446/11.67G/5.5	5.22E-06	5.11E-06	5.16E-06
7	622/26FA/0.422/12.14G/3.1	5.39E-06	5.23E-06	5.31E-06
8	605/20.66FA/0.43/12.09D/5.0	5.33E-06	5.37E-06	5.35E-06
9	590/18.64FA/0.438/10.87G/4.9	5.39E-06	5.23E-06	5.31E-06
10	590/18.64FA/0.439/10.87D/5.9	5.43E-06	5.46E-06	5.45E-06
11	600/20.16FA/0.47/11.42G/3.6	5.02E-06	4.92E-06	4.97E-06
12	600/20.16FA/0.47/11.42G/4.7	4.99E-06	4.99E-06	4.99E-06

These results demonstrate expected trends between the concrete mixtures and typical characteristics of the thermal property. Previous research (Kim 2012) concluded that the main factors affecting CTE were based on aggregates, mainly because of the amount of volume the mixture composed of the aggregate. Concrete mixtures containing dolomite, in particular, were proven to exhibit a higher CTE value than mixtures containing granite. Aggregate type displayed an obvious role in the test results, as shown in table 56. The two mixtures that contained dolomite, mixtures 8 (605/20.66FA/0.43/12.09D/5.0) and 10 (590/18.64FA/0.439/10.87D/5.9), resulted in the two highest CTE values, emphasizing the impact of the aggregate type on a concrete mixture's thermal properties. CTE immediately provided accurate test results because the concrete cylinders

for this property are tested in water in a saturated condition. During the initial thermal conductivity testing, variation in the test results occurred due to the test specimens' varying moisture levels. As mentioned in chapter 6, the 12 mixtures were batched again and tested in three different moisture conditions. The thermal conductivity test results are located in table 57.

These results demonstrate an expected trend between moisture and thermal conductivity. The two have a direct relationship with each other; as the moisture increases, so does the thermal conductivity test value. The oven-dry specimens provided the lowest test results because of the complete lack of moisture in the concrete cylinder undergoing the test. Similarly, the saturated specimens had the highest thermal conductivity results due to the specimens' high moisture content during testing. To provide the most uniform test results for the normal condition specimens, after they were removed from the curing tank, where they were stored for 28 days, the specimens were placed in the environmental chamber for 24 hours. Density has proven to be another key factor affecting thermal conductivity. An extra cylinder was made for each concrete mixture to test for the density after the 28-day curing period. Table 58 contains the lab-tested density values for each mixture.



**Table 57. Thermal conductivity test results.**

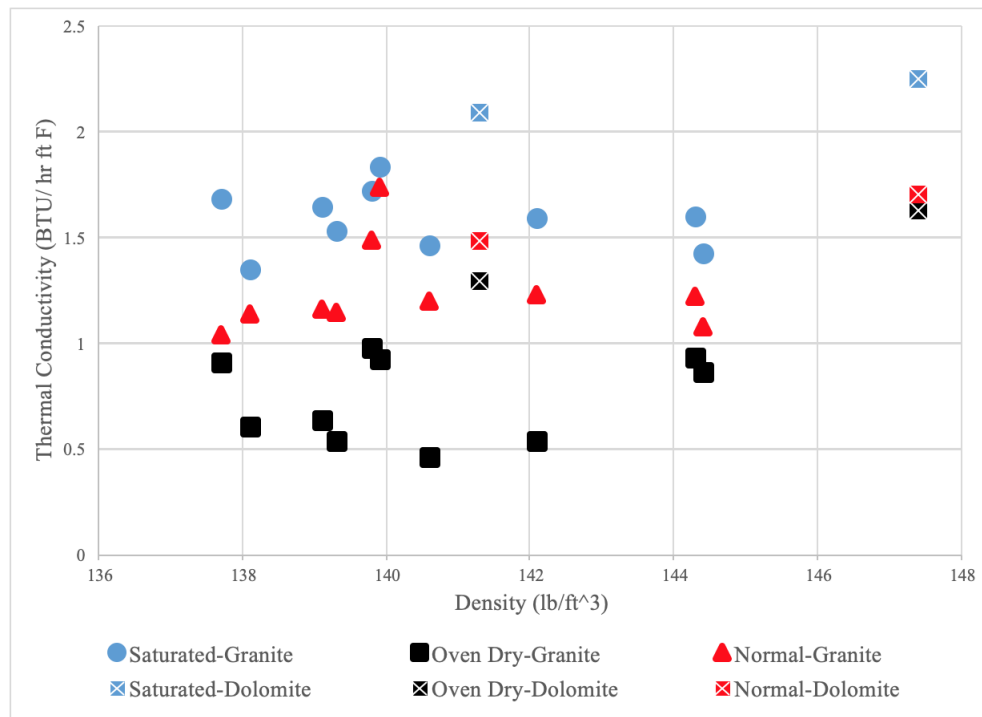
Mixture Number	Thermal Conductivity (BTU/ hr ft F)								
	Normal Condition			Oven Dry Condition			Saturated Condition		
	Specimen 1	Specimen 2	Average	Specimen 1	Specimen 2	Average	Specimen 1	Specimen 2	Average
<b>1</b>	1.054	1.104	1.079	0.789	0.936	0.863	1.428	1.426	1.427
<b>2</b>	1.191	1.269	1.230	0.507	0.573	0.540	1.634	1.559	1.597
<b>3</b>	1.143	1.152	1.148	0.606	0.540	0.537	1.539	1.522	1.531
<b>4</b>	1.213	1.190	1.202	0.463	0.464	0.464	1.507	1.427	1.467
<b>5</b>	1.160	1.164	1.162	0.469	0.806	0.638	1.688	1.609	1.649
<b>6</b>	1.059	1.023	1.041	0.934	0.887	0.911	1.686	1.690	1.688
<b>7</b>	1.354	1.628	1.491	1.048	0.915	0.982	1.535	1.904	1.720
<b>8</b>	1.481	1.929	1.705	1.615	1.640	1.628	2.225	2.273	2.249
<b>9</b>	1.734	1.745	1.740	0.922	0.934	0.928	1.890	1.783	1.837
<b>10</b>	1.407	1.557	1.482	1.399	1.195	1.297	2.104	2.082	2.093
<b>11</b>	1.160	1.282	1.221	0.972	0.900	0.936	1.517	1.693	1.605
<b>12</b>	1.054	1.217	1.136	0.720	0.488	0.604	1.346	1.362	1.354

**Table 58. Density measurements.**

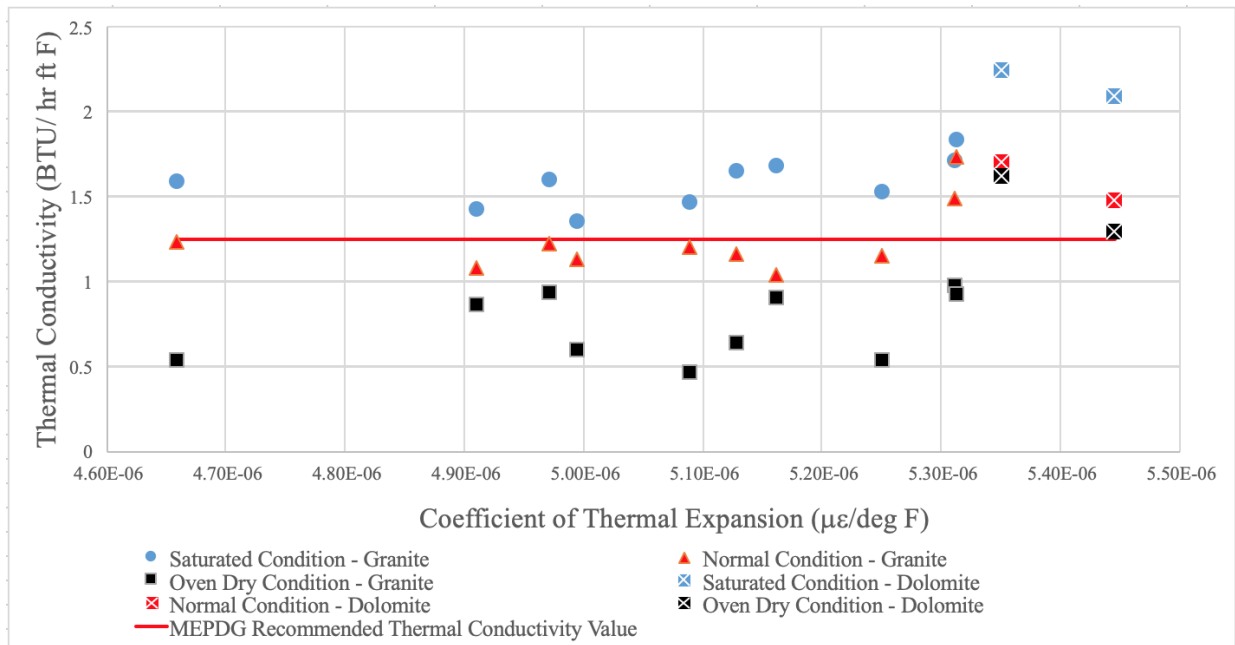
<b>Mixture Number</b>	<b>Mixture ID</b>	<b>Density (kg/m<sup>3</sup>)</b>	<b>Density (lb/ft<sup>3</sup>)</b>
<b>1</b>	541/0FA/0.431/11.91G/4.9	2313.5	144.4
<b>2</b>	541/0FA/0.524/12.75G/4.0	2276.6	142.1
<b>3</b>	595/0FA/0.43/11.4G/6.2	2231.4	139.3
<b>4</b>	600/0FA/0.47/11.62G/6.1	2252.3	140.6
<b>5</b>	580/12.2FA/0.493/12.54G/4.5	2228.7	139.1
<b>6</b>	579/19.69FA/0.446/11.67G/5.5	2205.9	137.7
<b>7</b>	622/26FA/0.422/12.14G/3.1	2239.7	139.8
<b>8</b>	605/20.66FA/0.43/12.09D/5.0	2361.4	147.4
<b>9</b>	590/18.64FA/0.438/10.87G/4.9	2240.9	139.9
<b>10</b>	590/18.64FA/0.439/10.87D/5.9	2263.9	141.3
<b>11</b>	600/20.16FA/0.47/11.42G/3.6	2311.6	144.3
<b>12</b>	600/20.16FA/0.47/11.42G/4.7	2212.5	138.1

Figure 61 illustrates the role that density has on thermal conductivity in concrete. Concrete mixtures are expected to demonstrate an increase in thermal conductivity test results as the mixture's density increases. Density exemplified an obvious effect on the thermal conductivity test results. Density has been proven to have a direct impact on thermal conductivity. Figure 61 generally supported this expected trend by displaying that a higher density generally resulted in a higher thermal conductivity test value. Importantly, dolomite continues to show an effect on the thermal property test results. Concrete mixtures containing the dolomite aggregate reflected a higher thermal conductivity similar to its higher CTE values. Since a higher thermal conductivity value correlates with a better insulating material, it is important to highlight that dolomite's impact on thermal conductivity could minimize the negative impact of providing a higher coefficient of thermal expansion value. Figure 62 illustrates the relationship between thermal conductivity and CTE. As shown in figure 62, an increase in CTE increased thermal conductivity, with the two

dolomite mixtures on the figure's far right side portraying the extreme thermal values. Since thermal conductivity is not yet a commonly performed test, GDOT engineers could refer to this plot when looking for the best estimate option for a thermal conductivity test value based on CTE when using the MEPDG approach.



**Figure 61. Scatterplot. Effect of density on thermal conductivity.**



**Figure 62. Scatterplot. CTE and thermal conductivity plot.**

## CHAPTER 8. SENSITIVITY ANALYSIS

A summary of mechanical inputs required for each input level is listed in table 59. For mechanical properties, level 3 designs require either the 28-day compressive strength or the 28-day MOR value. The 28-day MOE value can be input or left blank and AASHTOWare Pavement ME Design will calculate a value using compressive strength or MOR values. Poisson's ratio can either be set at a default value of 0.2 or specified if the value has been tested. Level 2 requires compressive strength values at 7, 14, 28, and 90 days of age. MOR and MOE values are not required at level 2. Level 1 designs require MOR and MOE values at 7, 14, 28, and 90 days of age. Compressive strength values are not required at level 1.

A number of other inputs are required in order to complete the sensitivity analyses. In this chapter, inputs such as traffic and climate were kept the same for all three levels. Traffic inputs were kept as the default values with a truck traffic classification (TTC) 4, as shown in table 60. Climate data were set to a climate station located in Athens, Georgia (ATHENS\_NARR\_GRIDPOINT,GA[13873]).

**Table 59. Mechanical inputs by level.**

<b>Design Level</b>	<b>Mechanical Property</b>	<b>Required inputs</b>
<b>3</b>	Compressive Strength	28-day value or MOR 28-day
	Modulus of Rupture	28-day value or Compressive 28-day
	Modulus of Elasticity	28-day value or Calculated estimate
	Ultimate Shrinkage	Calculated or User defined
	Poisson's Ratio	0.2 or User defined
<b>2</b>	Compressive Strength	7, 14, 28, 90-day value
	Modulus of Rupture	None
	Modulus of Elasticity	None
	Ultimate Shrinkage	Calculated or User defined
	Poisson's Ratio	0.2 or User defined
<b>1</b>	Compressive Strength	None
	Modulus of Rupture	7, 14, 28, 90-day value
	Split Tensile Strength	28-day value for required for CRCP
	Modulus of Elasticity	7, 14, 28, 90-day value
	Ultimate Shrinkage	User defined
	Poisson's Ratio	User defined

The different design-specific properties for rigid pavement are listed in table 61. Material layers vary between JPCP and CRCP designs. Standard GDOT JPCP and CRCP design layers were used in this project. The layers used in the JPCP and CRCP design are displayed in figure 63 and figure 64. The GAB layer was set as crushed gravel, while the subgrade was set to A-7-6. The properties for the layers used in the design are shown in table 62.

**Table 60. Traffic inputs.**

<b>Item</b>	<b>Input</b>
Design life	20 years
Construction month	June 2021
Vehicle class distribution and growth	TTC 4
Two-way AADTT	4000
Number of lanes	2
Percent trucks in design direction	50
Percent trucks in design lane	95
Operational speed (mph)	60
Traffic capacity cap	Not enforced
Average axle width (ft)	8.5
Tandem axle spacing (inch)	51.6
Dual tire spacing (inch)	12
Quad axle spacing (inch)	49.2
Tire pressure (psi)	120
Tridem axle spacing (inch)	49.2
Design lane width (ft)	12
Mean wheel location (inch)	18
Traffic wander standard deviation	10
Average spacing of long axles	18
Average spacing of medium axles	15
Percent trucks with long axles	61
Percent trucks with medium axles	22
Percent trucks with short axles	17
Average spacing of short axles	12

**Table 61. JPCP and CRCP design properties.**

		<b>Value</b>
<b>JPCP</b>	Surface shortwave absorptivity	0.85
	Doweled joints	Spacing 12, Diameter 1.25
	Erodibility index	Very erodible
	Base contact friction	Full friction with friction loss at 240 months
	Joint spacing (ft)	15
	Permanent curl/warp effective temperature difference (°F)	−10
	Sealant type	Preformed
	Tied shoulders	Not tied
	Widened slab	Widened (12)
<b>CRCP</b>	Surface shortwave absorptivity	0.85
	Bar diameter	0.75
	Base/slab friction coefficient	8.3
	Crack spacing	Generate using prediction model
	Steel (%)	0.725
	Permanent curl/warp effective temperature difference (°F)	−10
	Shoulder type	Asphalt
	Steel depth (inch)	4



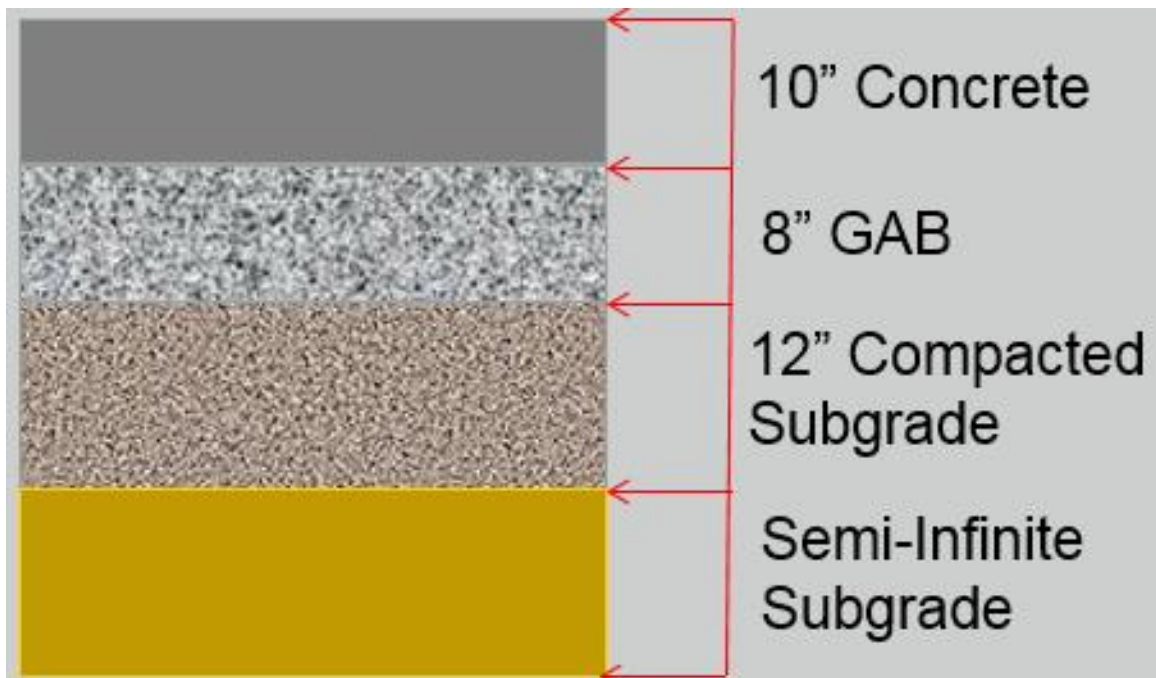


**Figure 63. Diagram. JPCP layers used in sensitivity analysis.**

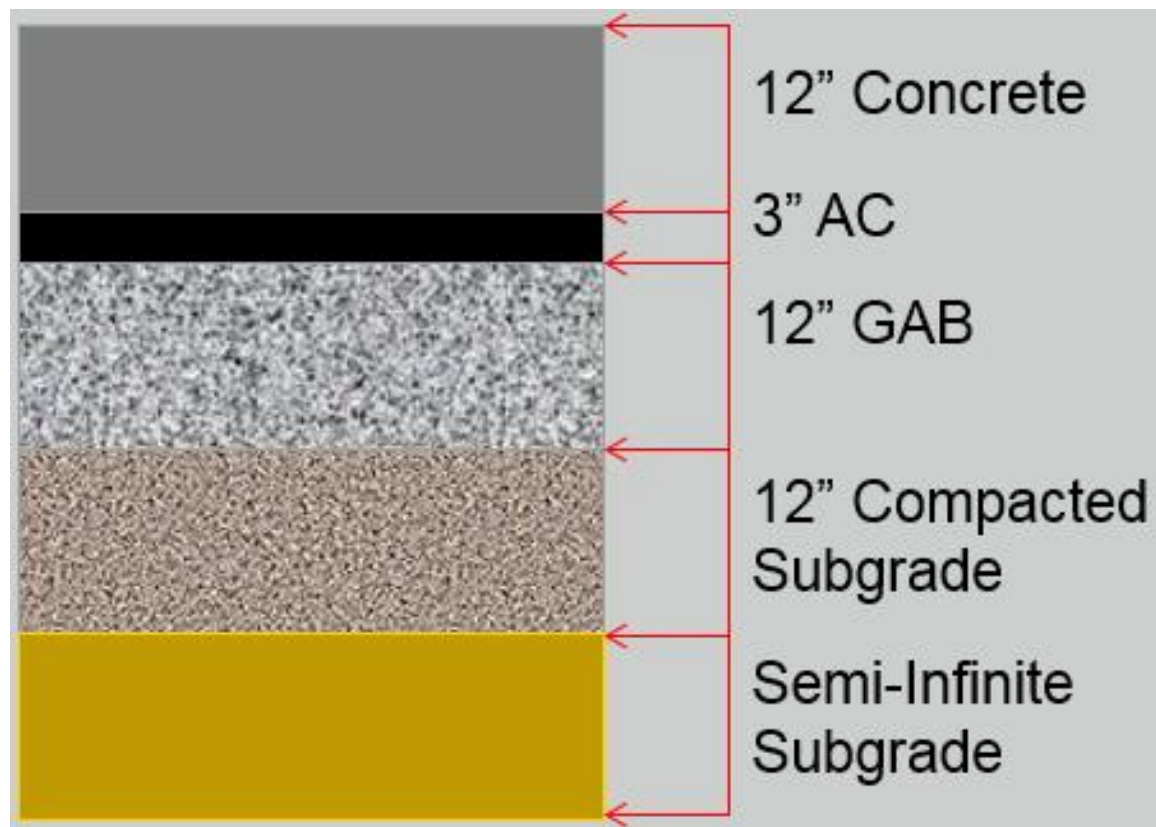


**Figure 64. Diagram. CRCP layers used in sensitivity analysis.**

**Table 62. Layer properties.**

		<b>Value</b>
<b>Concrete Properties</b>	Poisson's ratio	0.2
	Thickness (inch)	10
	Unit weight (pcf)	150
	CTE (in/in/°F×10 <sup>-6</sup> )	5.1
	Heat capacity (BTU/lb-°F)	0.28
	Thermal conductivity (BTU/hr-ft-°F)	1.25
	Aggregate type	Granite (3)
	Cementitious content (lb/yd <sup>3</sup> )	600
	Cement type	Type I
	W/C ratio	0.42
	Curing method	Curing Compound
	Reversable shrinkage (%)	50
	Zero-stress temperature (°F)	Calculated
	Time to develop 50% of ultimate shrinkage (days)	35
	Ultimate shrinkage	Calculated
<b>Asphalt Properties</b>	Air voids (%)	7
	Effective binder content (%)	11.6
	Poisson's ratio	0.35
	Unit weight (pcf)	150
	Asphalt binder	SuperPave:64-22
	Creep compliance (1/psi)	Input level:3
	Dynamic modulus	Input level:3
	HMA Estar predictive model	Viscosity based model
	Reference temperature (°F)	70
	Indirect tensile strength at 14°F (psi)	Input level:3
	Heat capacity (BTU/lb-°F)	0.23
	Thermal conductivity (BTU/hr-ft-°F)	0.67
	Thermal contraction	Calculated
<b>Crushed Gravel Properties</b>	Coefficient of lateral earth pressure (k0)	0.5
	Poisson's ratio	0.35
	Resilient modulus (psi)	25,000
	Gradation	A-1-a
<b>Subgrade A-7-6 Properties</b>	Coefficient of lateral earth pressure (k0)	0.5
	Poisson's ratio	0.35
	Resilient modulus (psi)	13000
	Gradation	A-7-6

## **SENSITIVITY TO MECHANICAL PROPERTIES**

An analysis was performed at a level 3 using Georgia calibration factors, as listed in table 20, in order to determine the sensitivity of the inputs to the predicted distresses. AASHTOWare Pavement ME Design assigns default values for these design parameters if values are not specified. For each input, a range was created that included typical values of the material property. For each input, a predicted IRI, mean joint faulting, and percent slabs cracked after a 20-year design life was generated for the specified range. The default values and the ranges used in this sensitivity analysis are listed in table 63. A flow chart of this process is found in appendix C.

A similar analysis was performed for CRCP pavements using the layers shown in figure 64. Additional default inputs are required to be specified for the CRCP sensitivity. A steel reinforcement ratio of 0.73 was used, which is based on typical values ranging from 0.65 to 0.80 (ARA 2015). The bar diameter was set at 0.75, corresponding to the use of a #6 reinforcing bar. Finally, the steel depth was set to 4-inch (101.6 mm). The depth was chosen based on recommendations that the steel be placed at one third of the slab thickness (Durham et al. 2018). The default values and ranges used in the sensitivity for CRCP are presented in table 64.

**Table 63. Default values and sensitivity ranges for JPCP.**

	<b>Compressive Strength (psi)</b>	<b>MOE (ksi)</b>	<b>MOR (psi)</b>	<b>Poisson's Ratio</b>	<b>IRI (in./mi)</b>	<b>Mean Joint Faulting</b>	<b>Percent Slabs Cracked (%)</b>
<b>Default Values</b>	5,275	4,200	690	0.2	151.56	0.12	2.37
<b>Range</b>	2,000–7,000	3,000–6,500	250–750	0.1–0.26	–	–	–
<b>Increment</b>	500	500	12.5	0.02	–	–	–

– No data

**Table 64. Default values and sensitivity ranges for CRCP.**

	<b>Compressive Strength (psi)</b>	<b>MOE (ksi)</b>	<b>MOR (psi)</b>	<b>Poisson's Ratio</b>	<b>IRI (in./mi)</b>	<b>Punchout (#/Mile)</b>
<b>Default Values</b>	5,275	4,200	690	0.2	73.69	0.1
<b>Range</b>	2,000–7,000	2,500–6,500	250–750	0.1–0.26	–	–
<b>Increment</b>	500	500	12.5	0.02	–	–

The general trend observed was that the stronger the concrete layer, the less distress the pavement experienced. As the concrete compressive strength and MOR increased, the predicted distresses decreased (see figure 65 and figure 66). In contrast to this trend, as MOE increased, the predicted distresses increased. Thus, the pavement was predicted to crack more as the concrete stiffness increased. As seen in figure 67, the increased stiffness did not result in pavement failure until it reached approximately 5,500 ksi (37.9 GPa). Three of the mixtures tested in this study reached MOE values of over 5,500 ksi (37.9 GPa). It is important to note that cracking is a function of many properties, such as climate data and thermal inputs. Therefore, this analysis likely produced these results due to a stiffer material cracking from thermal expansion. In addition, pavement design is often governed by the relative stiffness of the structure, which is a combination of concrete MOE and thickness of the layer. Since the relative stiffness will be different for slabs of different thicknesses with the same MOE, an upper limit for MOE should not be set. IRI, mean joint faulting, and percent slabs cracked were all analyzed for each property; however, only percent slabs cracked was plotted since this value was the first to reach its failure threshold in almost every case. As shown in figure 68 and figure 69, the exception to this was for Poisson's ratios above 0.24 and shrinkage of 1,000 microstrains. For these cases, the mean joint faulting value was 0.13, exceeding the limit of 0.125.

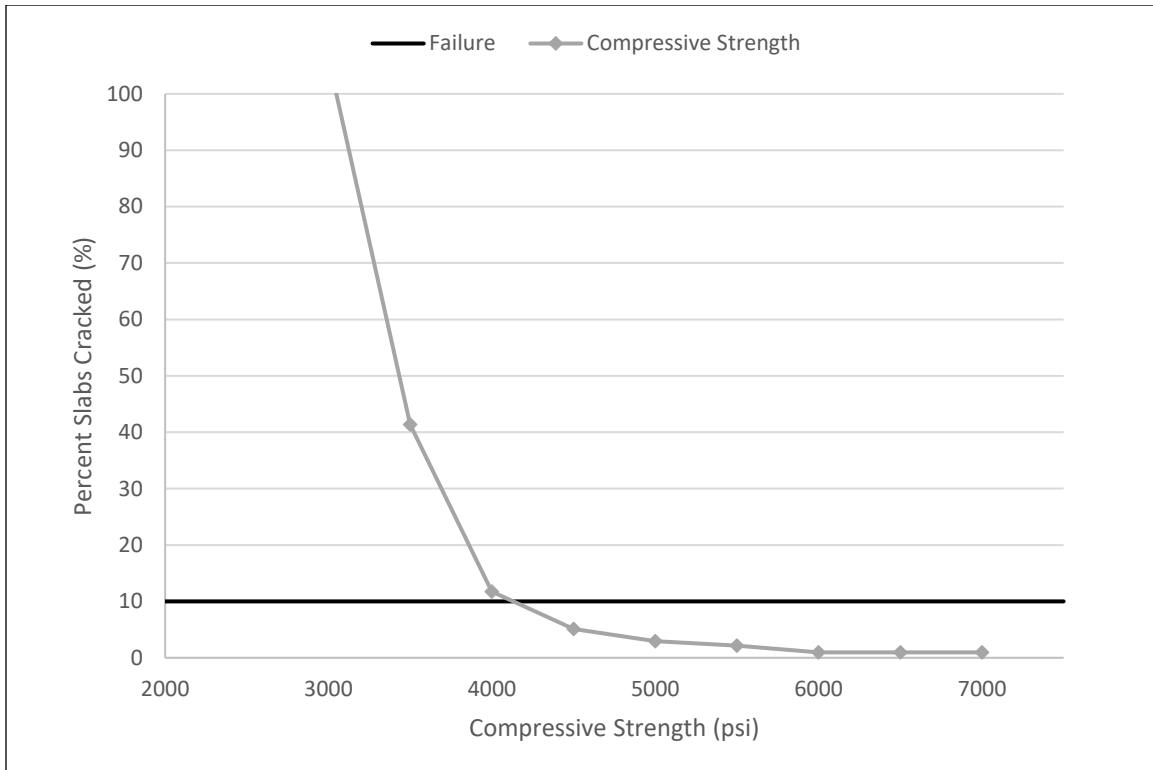


**Figure 65. Line graph. Compressive strength vs. percent slabs cracked, JPCP.**

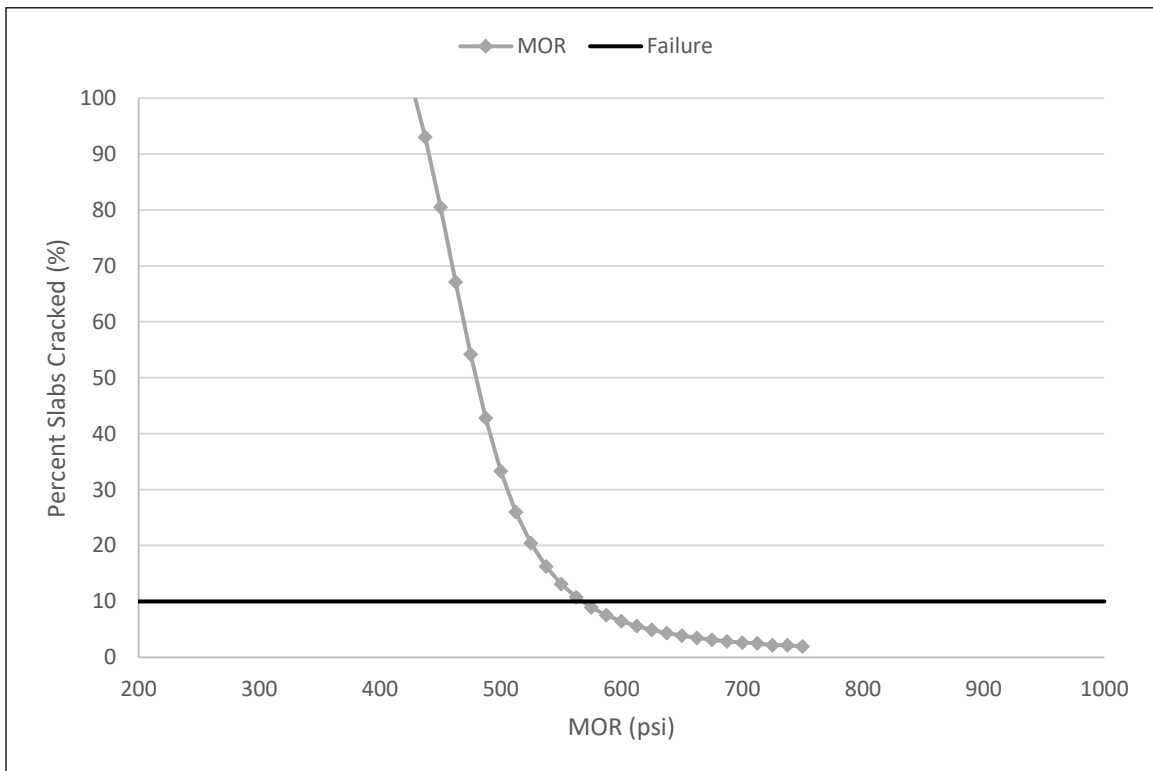


**Figure 66. Line graph. MOR vs. percent slabs cracked, JPCP.**

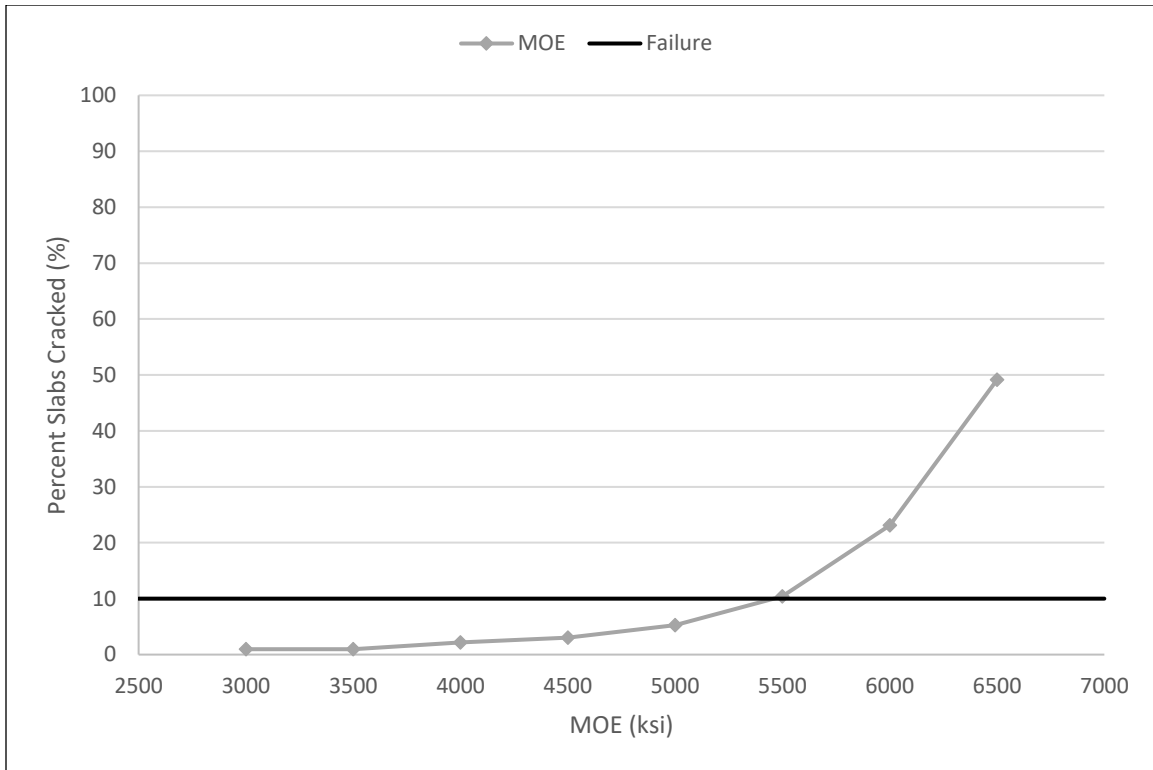


**Figure 67. Line graph. MOE vs. percent slabs cracked, JPCP.**

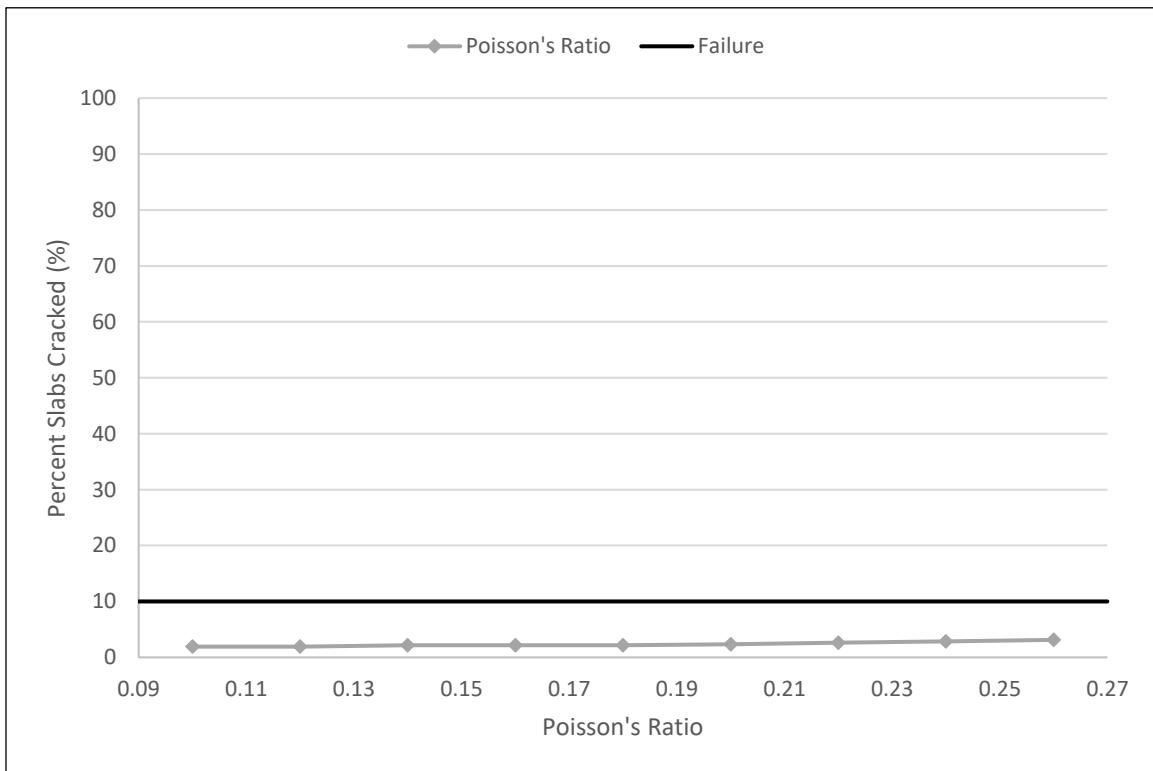


**Figure 68. Line graph. Poisson's ratio vs. percent slabs cracked, JPCP.**

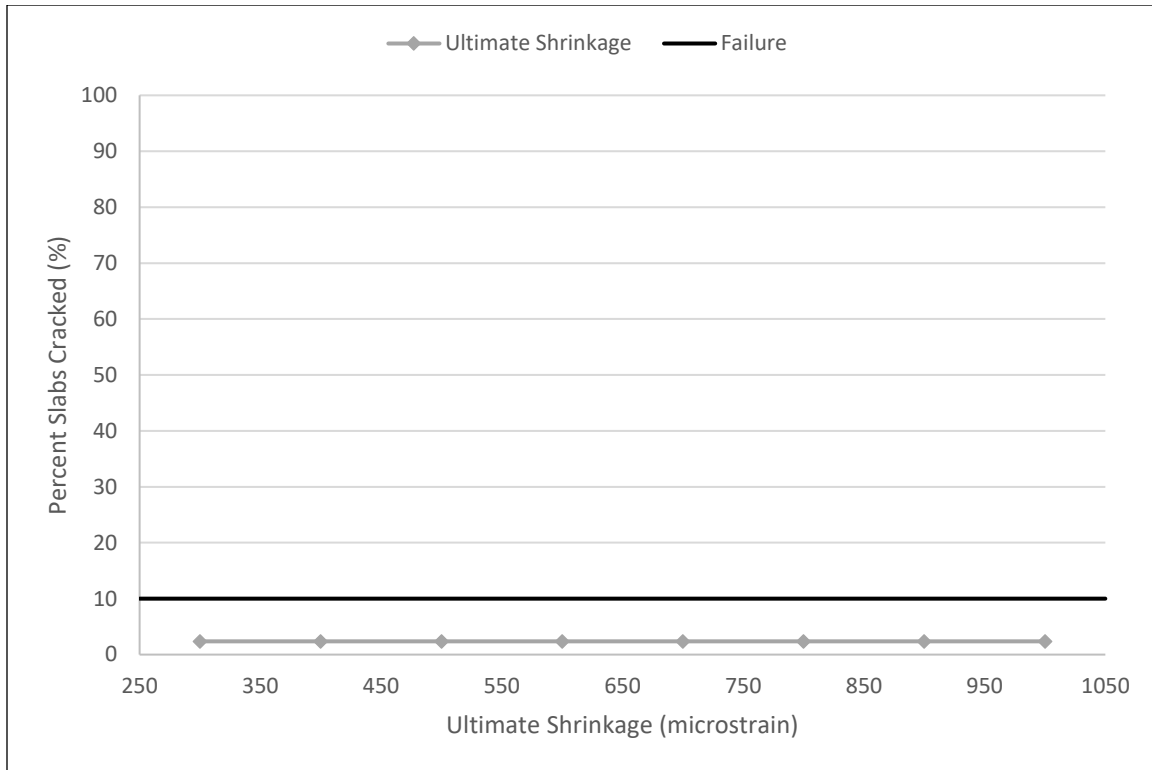


**Figure 69. Line graph. Ultimate shrinkage vs. percent slabs cracked, JPCP.**

From these figures, there are some clear threshold values that should be established for JPCP pavements. Based on figure 65, compressive strength should have a minimum DAR value of 4,500 psi (31.0 MPa) for JPCP. Only three of the mixtures batched for this study did not reach a compressive strength value of 4,500 psi (31.0 MPa) by 28 days. Figure 66 indicates that DAR of 600 psi (4.1 MPa) is an acceptable minimum for MOR for mixtures used in JPCP. All 12 mixtures achieved MOR values above this threshold.

In addition, the sensitivity of predicted distresses to unit weight was analyzed. It was found that mean joint faulting was extremely sensitive to this input value. If the unit weight of the mixture was below 149 pcf (2386.8 kg/m<sup>3</sup>), then mean joint faulting was predicted above the failure threshold of 0.125, as shown in figure 70. Similarly, the 28-day compressive strength, MOR, MOE, and unit weights were input at level 3 and analyzed. The resulting distresses all predicted



failure of mean joint faulting regardless of strength, since the measured unit weights were below 149 pcf (2386.8 kg/m<sup>3</sup>). This is believed to occur as a result of the increased curling deflection caused by lower unit weights (Ceylan et al. 2012). More research is needed to determine if unit weight has a significant impact on faulting, since faulting is traditionally believed to be a function of pavement foundation properties. Foundation properties that lead to curling of slab are ejection of materials from beneath the concrete slab, temperature variations, and moisture change. As the curling of slab is also influenced by unit weight of concrete, it is warranted to study the effect of unit weight of concrete on faulting.

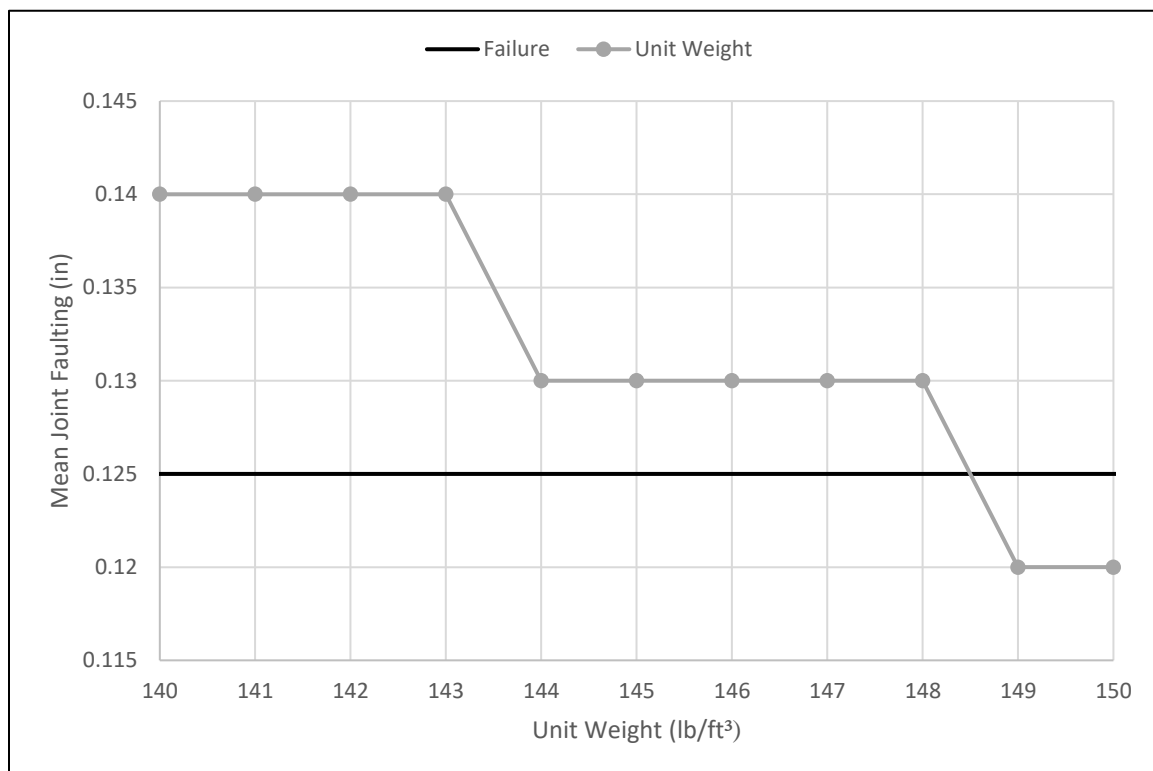


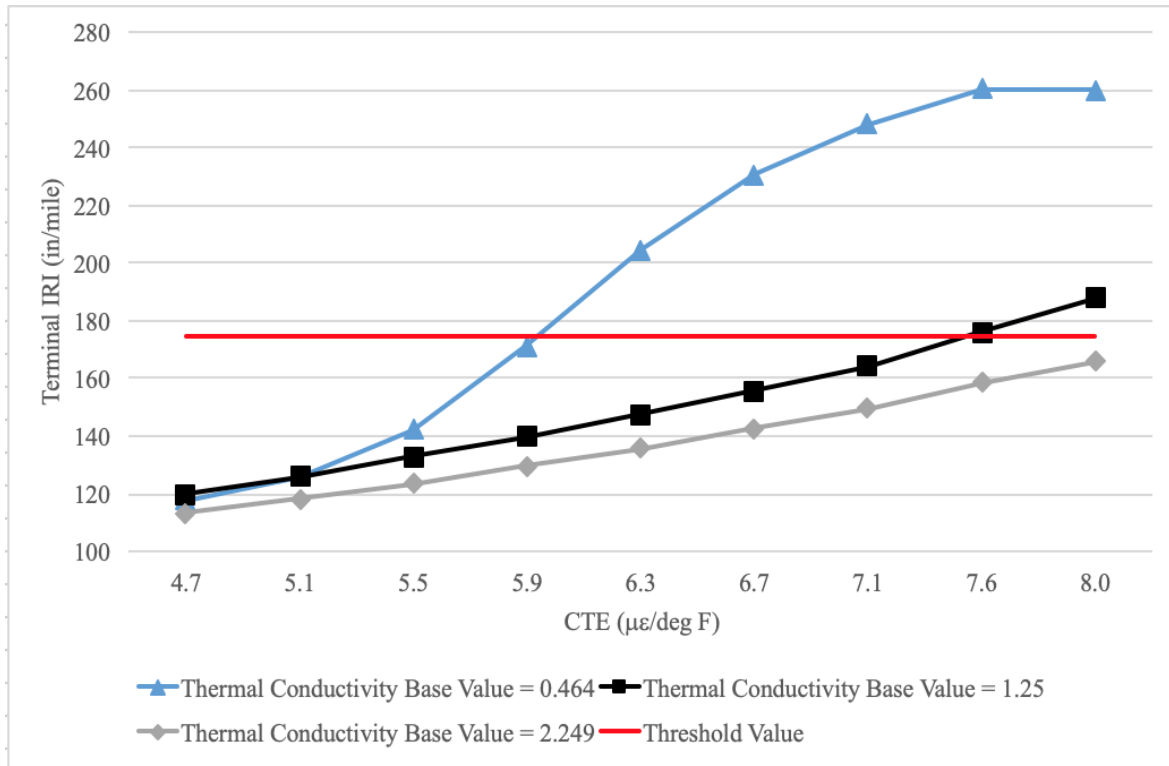
**Figure 70. Line graph. Unit weight vs. mean joint faulting, JPCP.**

## SENSITIVITY ANALYSES FOR THERMAL PROPERTIES

CTE has previously been proven to be the most impactful thermal property input. During these analyses, the base values of heat capacity and thermal conductivity were used as 0.28 BTU/lb-°F

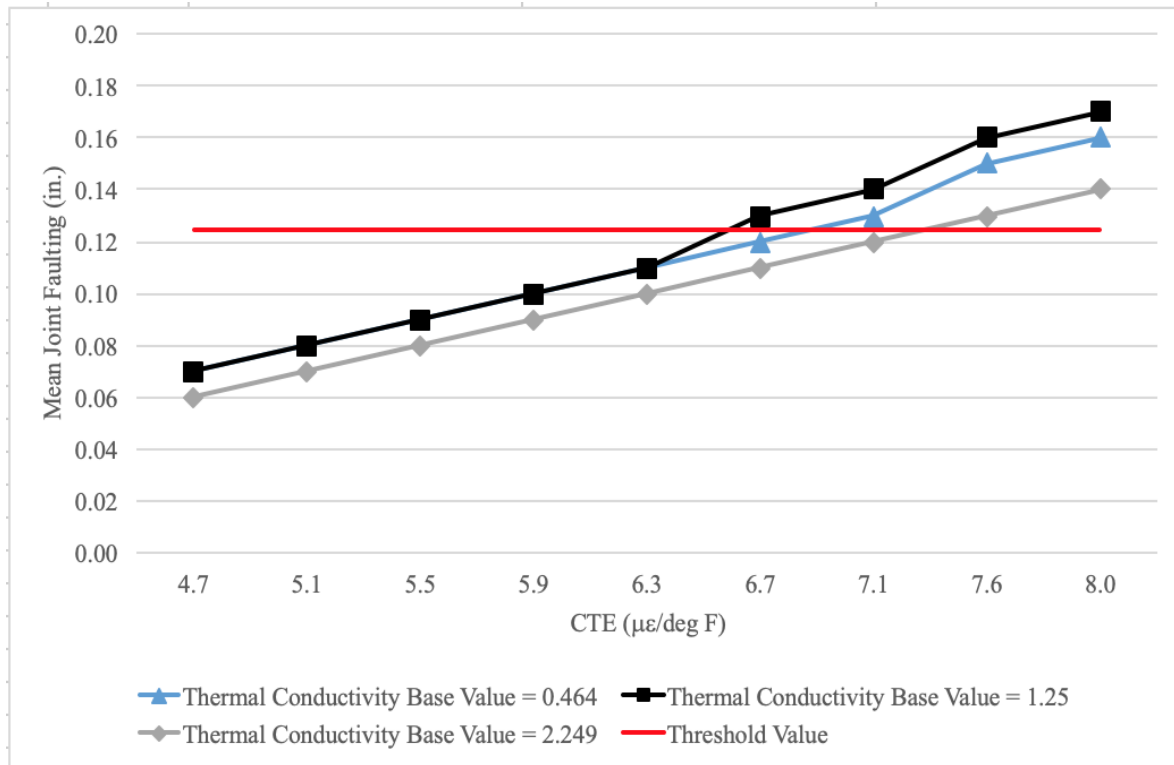
and 1.25 BTU/hr-ft-°F, respectively. Two additional analyses were performed using the extreme lab-tested thermal conductivity values of 0.464 and 2.249 BTU/hr-ft-°F as base values. The analyses used a 0.4  $\mu\epsilon/\text{°F}$  increment for CTE values ranging from 4.70 to 8.0  $\mu\epsilon/\text{°F}$ . The lower value was selected because it was close to the lowest lab-tested CTE value, and the higher value of 8.0  $\mu\epsilon/\text{°F}$  was selected to clearly demonstrate the trend between CTE and the performance indicator of concern.

Figure 71 illustrates an expected relationship between CTE and terminal IRI. A higher CTE value is typically correlated to an IRI increase due to the higher cracking and faulting. The analyses containing the extreme lab-tested thermal conductivity values showed a dramatic effect on pavement performance prediction. A higher thermal conductivity value is expected to provide less pavement distress due to its ability to insulate the PCC layer better. The test containing the higher thermal conductivity base value of 2.249 BTU/hr-ft-°F supported this expectation by resulting in a slightly lower terminal IRI prediction. The analysis containing the smaller thermal conductivity base value of 0.464 BTU/hr-ft-°F differed from the other trials and demonstrated a rapid increase in terminal IRI prediction after the CTE value of 5.5  $\mu\epsilon/\text{°F}$  was surpassed. These analyses proved that CTE and thermal conductivity play a crucial role in predicting pavement distresses in the MEPDG approach.



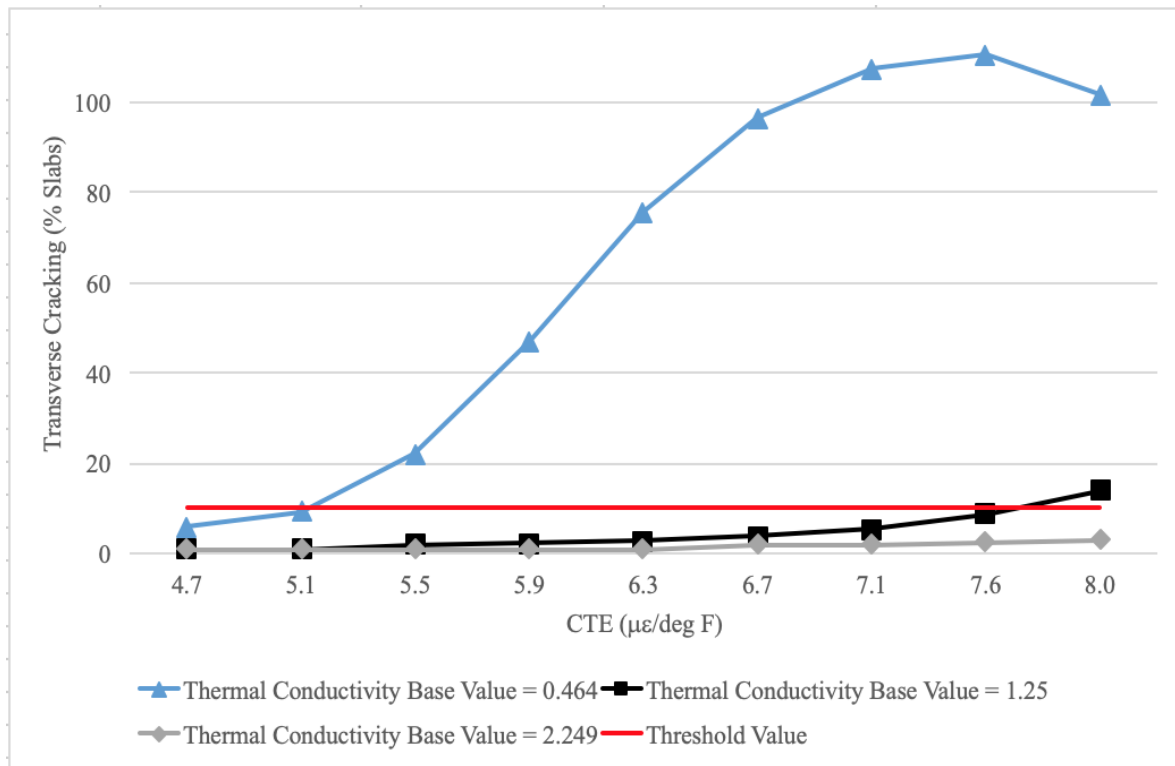
**Figure 71. Line graph. CTE's effect on terminal IRI.**

Figure 72 provides important insight into the impact CTE plays in the faulting of a pavement structure. A study performed by Mallela et al. (2005) highlighted the impact that CTE has on mean joint faulting. These analyses supported that higher CTE values are expected to result in an increased mean joint faulting. The increasing trend of mean joint faulting is accelerated when the lower thermal capacity is combined. Once again, the analysis using the high thermal conductivity base value displayed less predicted distress.



**Figure 72. Line graph. CTE's effect on mean joint faulting.**

Figure 73 proves that higher CTE values affected the transverse cracking of the pavement structure. Field studies have proven higher CTE values allow for an increase in transverse cracking primarily because of the PCC mixture's curling behavior. This curling occurs primarily due to temperature variation throughout the concrete layer, which increases along with an increase in CTE. It is important to note the behavior of the analysis using a low thermal conductivity base value. This analysis exhibited a dramatic increase in cracking prediction compared to the other analyses using higher thermal conductivity values. Figure 74 proves that both thermal conductivity and CTE played a critical role in transverse cracking prediction in the MEPDG.



**Figure 73. Line graph. CTE's effect on transverse cracking.**

### Sensitivity Analyses for Thermal Conductivity

The sensitivity analyses conducted for thermal conductivity ranged from 0.44 to 2.30 BTU/hr-ft-°F. These values were selected based on lab-tested values for the 12 GDOT-approved mixtures. For these analyses, the default values of 5.1 µε/°F and 0.28 BTU/lb-°F were used for CTE and heat capacity, respectively. Two additional analyses were performed for each pavement distress using the extreme lab-tested CTE values of 4.66 and 5.45 µε/°F as base values.

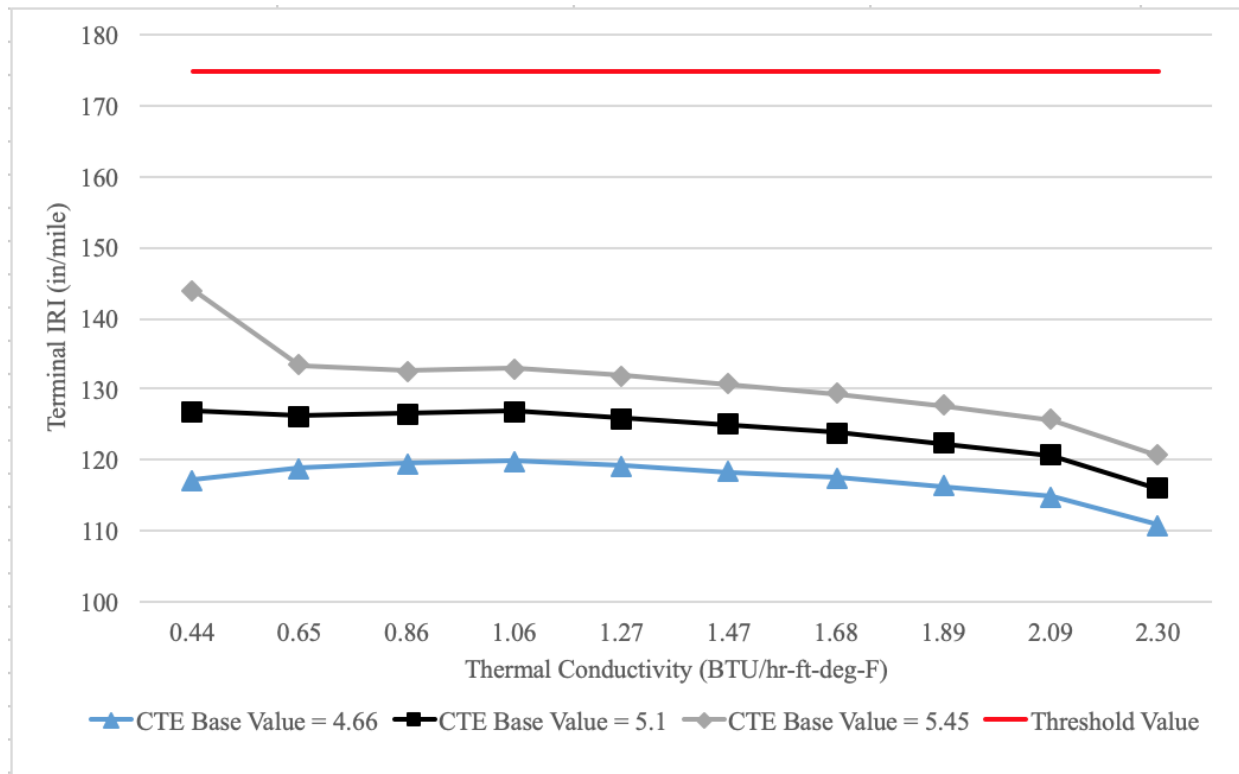


**Figure 74. Line graph. Thermal conductivity's effect on terminal IRI.**

Figure 75 and figure 76 demonstrated little interaction between the predicted distresses and change of thermal conductivity values. The lower thermal conductivity values resulted in higher predicted distresses; however, CTE exhibited a more impactful effect in the distress prediction process. Figure 76 illustrated that a lower thermal conductivity value created a higher predicted transverse cracking percentage. This supported that a decrease in thermal conductivity reduces the concrete's ability to insulate temperature changes and, in return, prevents the structure's ability to release heat flow efficiently. Due to this interaction between the heat and pavement, a lower thermal conductivity resulted in more distresses, specifically transverse cracking. While thermal conductivity in the PCC layer decreased, the thermal diffusivity also decreased the layer's effectiveness as a thermal buffer, resulting in higher predicted distresses.

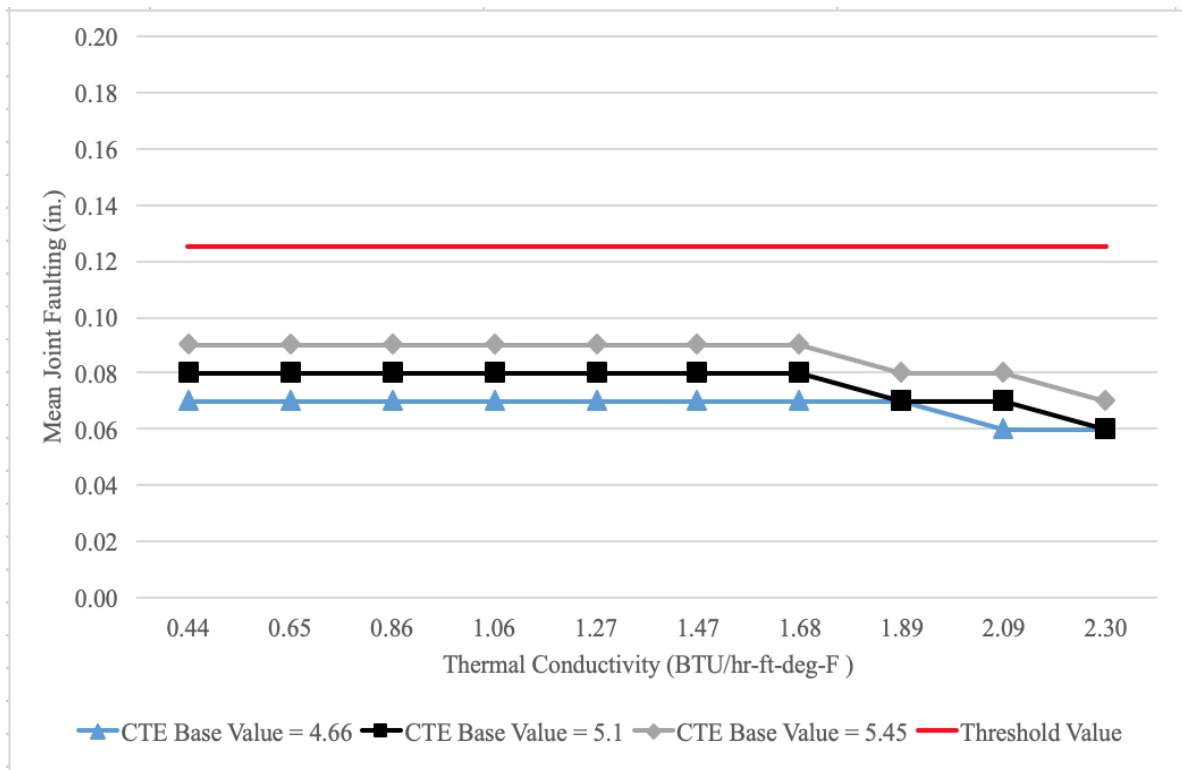


**Figure 75. Line graph. Thermal conductivity's effect on mean joint faulting.**

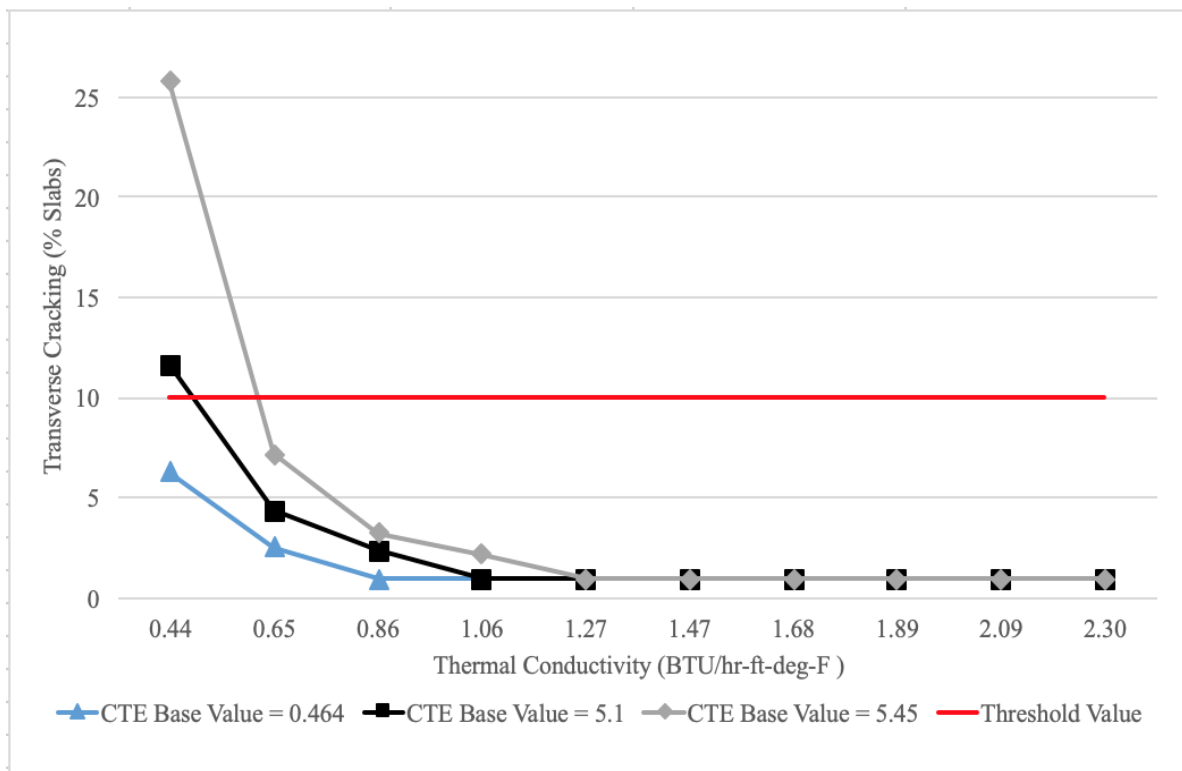


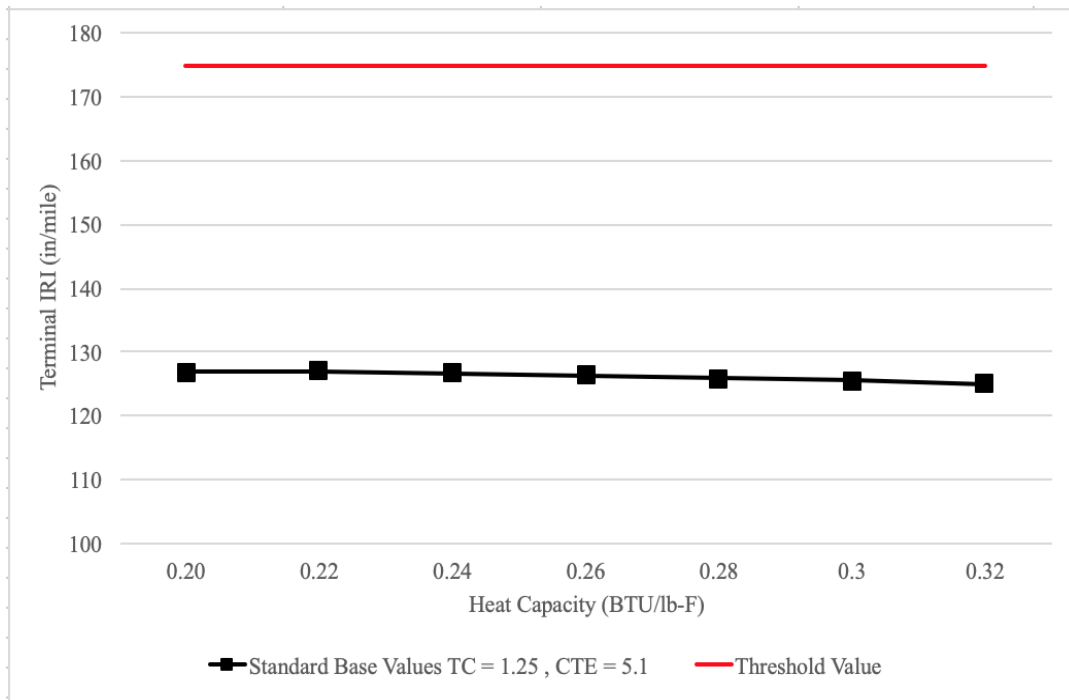
**Figure 76. Line graph. Thermal conductivity's effect on transverse cracking.**

## **Sensitivity Analyses for Heat Capacity**

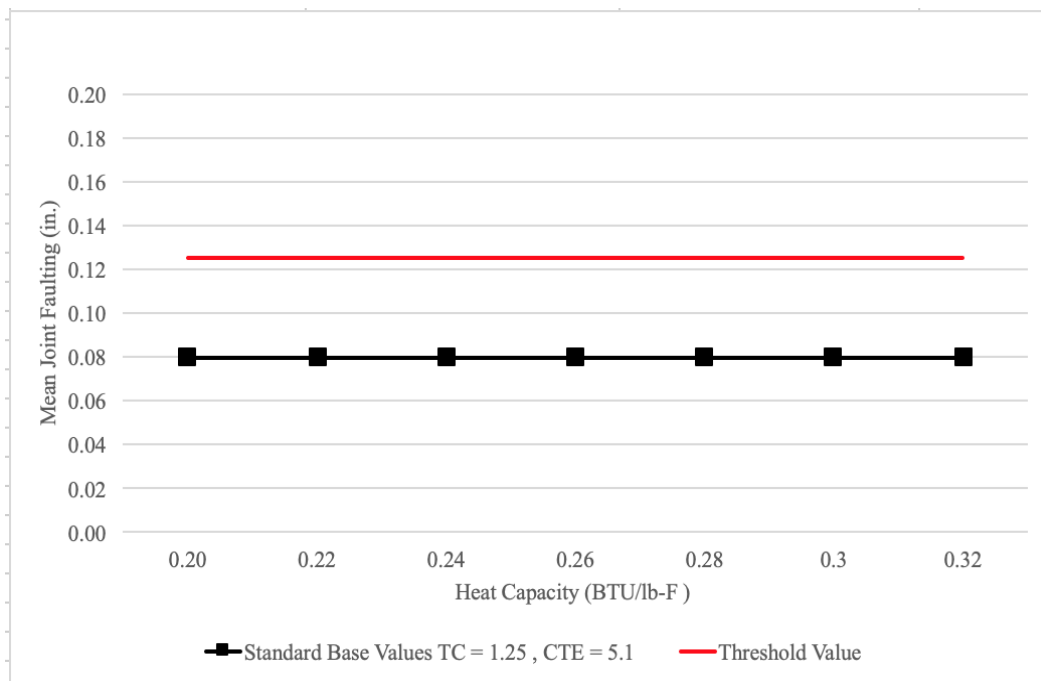
Heat capacity was a thermal property to undergo inspection with AASHTOWare Pavement ME Design's predicted distresses. The heat capacity values ranged from 0.20 to 0.32 BTU/lb-°F. These values were selected based on typical PCC heat capacity values, with the default value for heat capacity in the MEPDG. For these analyses, the default values of  $5.1 \mu\epsilon/\text{°F}$  and 1.25 BTU/hr-ft-°F were used for CTE and thermal conductivity, respectively. Extreme base values for CTE and thermal conductivity were investigated; however, AASHTOWare Pavement ME Design does not allow these analyses to be run due to a “stability failure” in the program.

Figure 77, figure 78, and figure 79 demonstrated little interaction between this heat capacity and the pavement performance predictions. Previous studies similarly determined this thermal property to have minimal impact on the distress predictions. Due to its limited role in the MEPDG prediction process, the recommended heat capacity value of 0.28 BTU/lb-°F should continue to be used as the default input for this thermal property.





**Figure 77. Line graph. Heat capacity's effect on terminal IRI.**



**Figure 78. Line graph. Heat capacity's effect on mean joint faulting.**

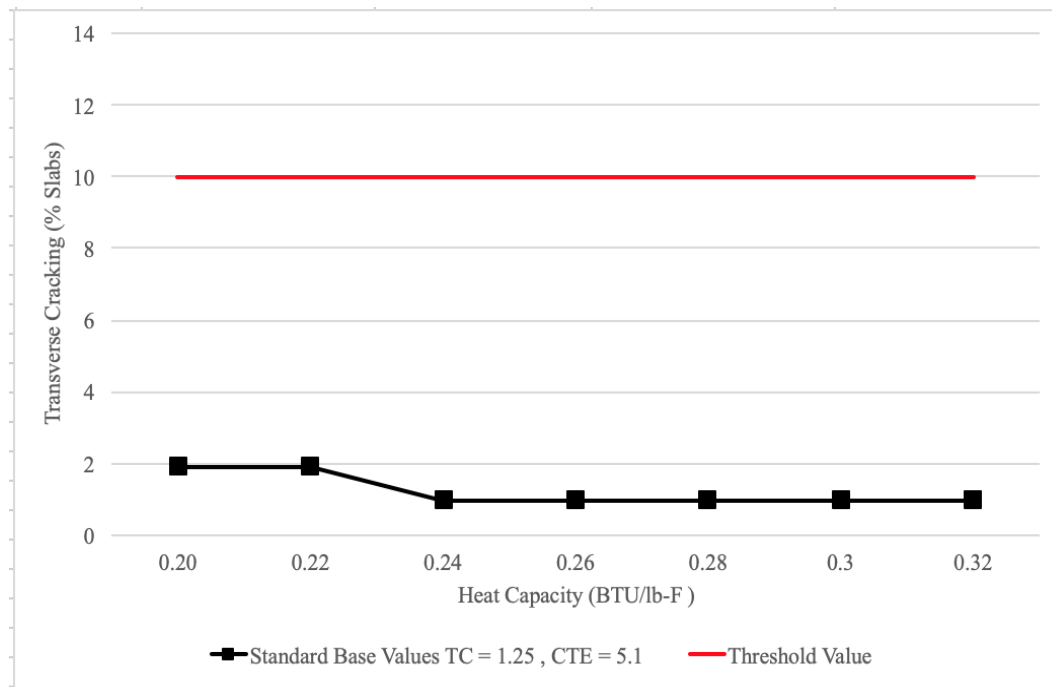


**Figure 79. Line graph. Heat capacity's effect on transverse cracking.**

## CRCP RESULTS

CRCP displayed sensitivity to only two of the mechanical properties for which it was analyzed—MOR and compressive strength. These sensitivities followed the same trend as JPCP; the stronger the mixture, the less distress was predicted. The mechanical properties were plotted against punchout, as this is the distress that typically reached failure first. For compressive strength, the failure threshold was never reached even at the minimum allowable input of 2,500 psi (17.2 MPa), as shown in Figure 80. Since failure was not incited, the DAR of 3,000 psi (20.7 MPa) is an acceptable design requirement for CRCP pavements. All 12 mixtures batched in this study exceeded this DAR, with a minimum tested 28-day compressive strength of 4,140 psi (28.5 MPa). For MOR, the section experienced rapid deterioration below 500 psi (3.4 MPa) with failure occurring around 450 psi (3.1 MPa), as shown in Figure 81. The current DAR of 600 psi (4.1 MPa) is acceptable for CRCP designs. All 12 mixtures exceeded this DAR with a minimum tested MOR

value of 620 psi (4.3 MPa). The other mechanical properties analyzed showed no sensitivity in the CRCP design. The results for each property (i.e., MOE, Poisson's ratio, shrinkage, and unit weight) are shown in figure 82, figure 83, figure 84, and figure 85, respectively.

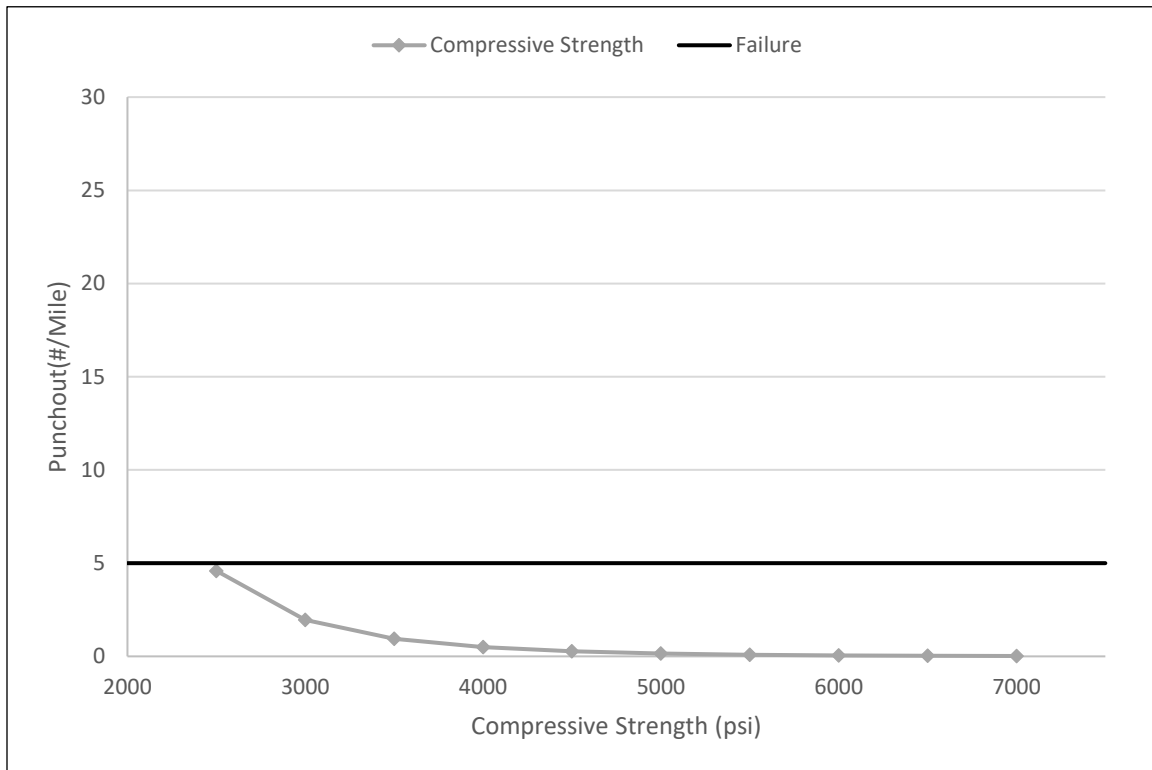


**Figure 80. Line graph. Compressive strength vs. punchout, CRCP.**

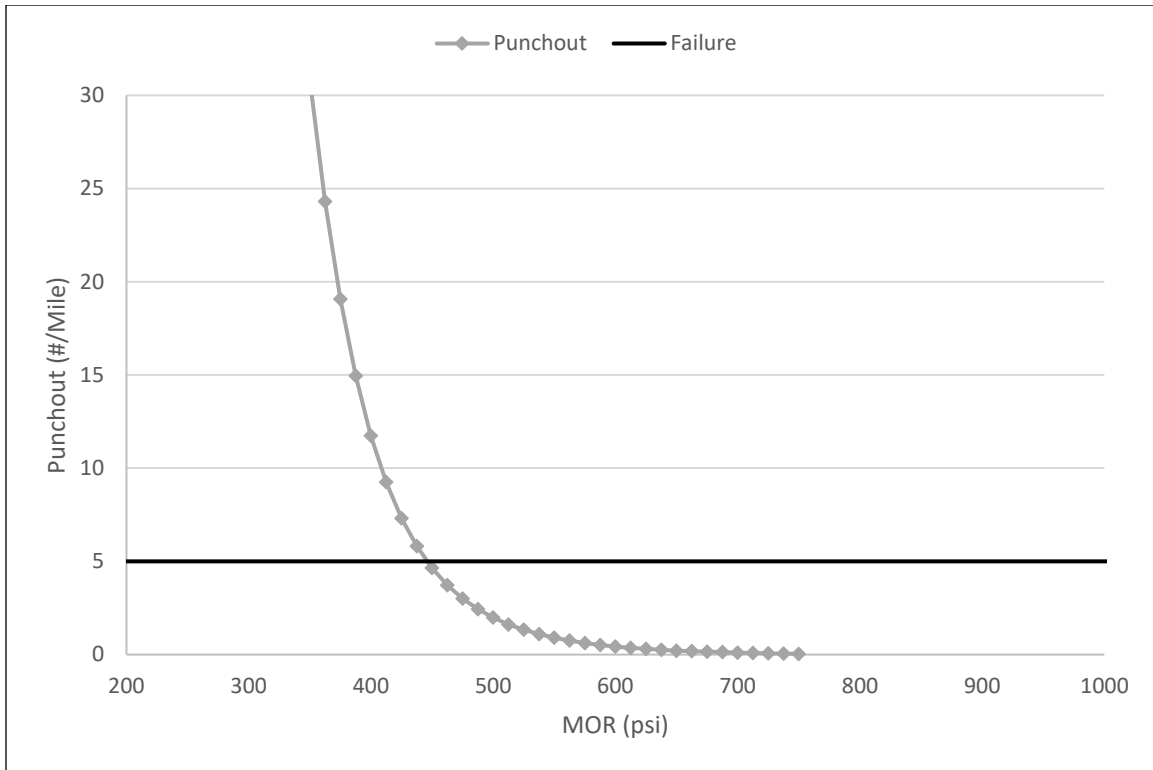


**Figure 81. Line graph. MOR vs. punchout, CRCP.**

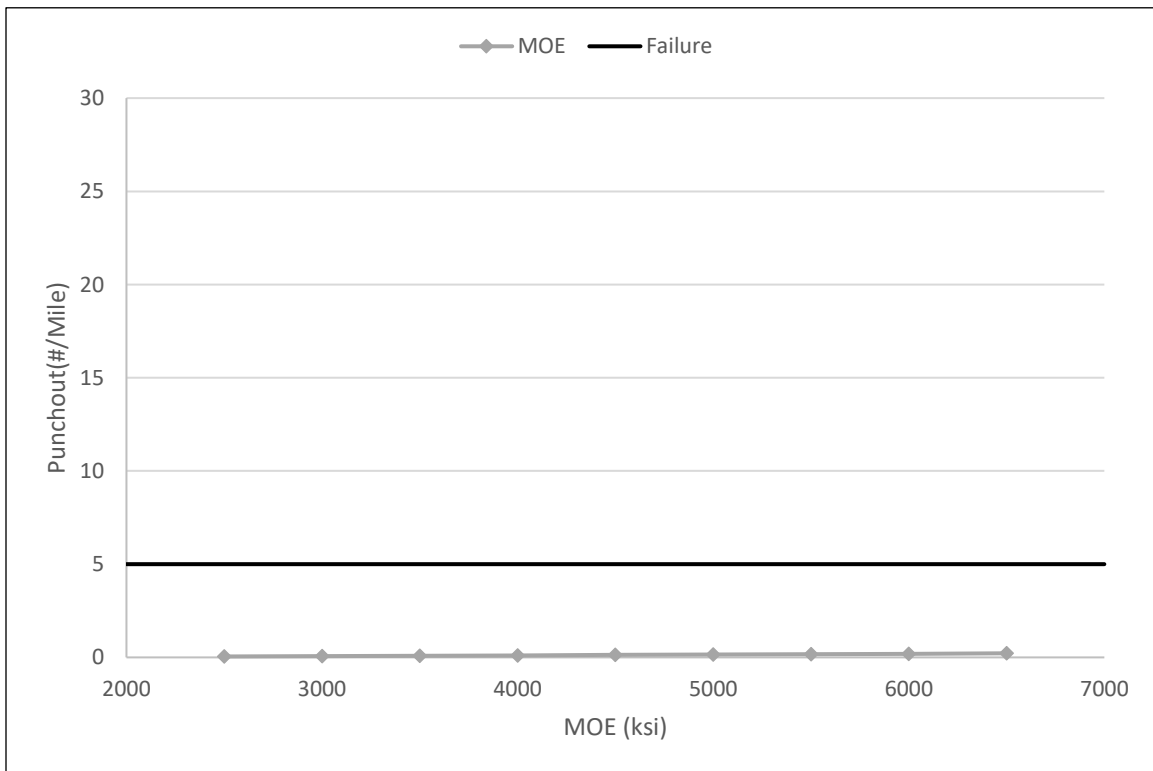


**Figure 82. Line graph. MOE vs. punchout, CRCP.**

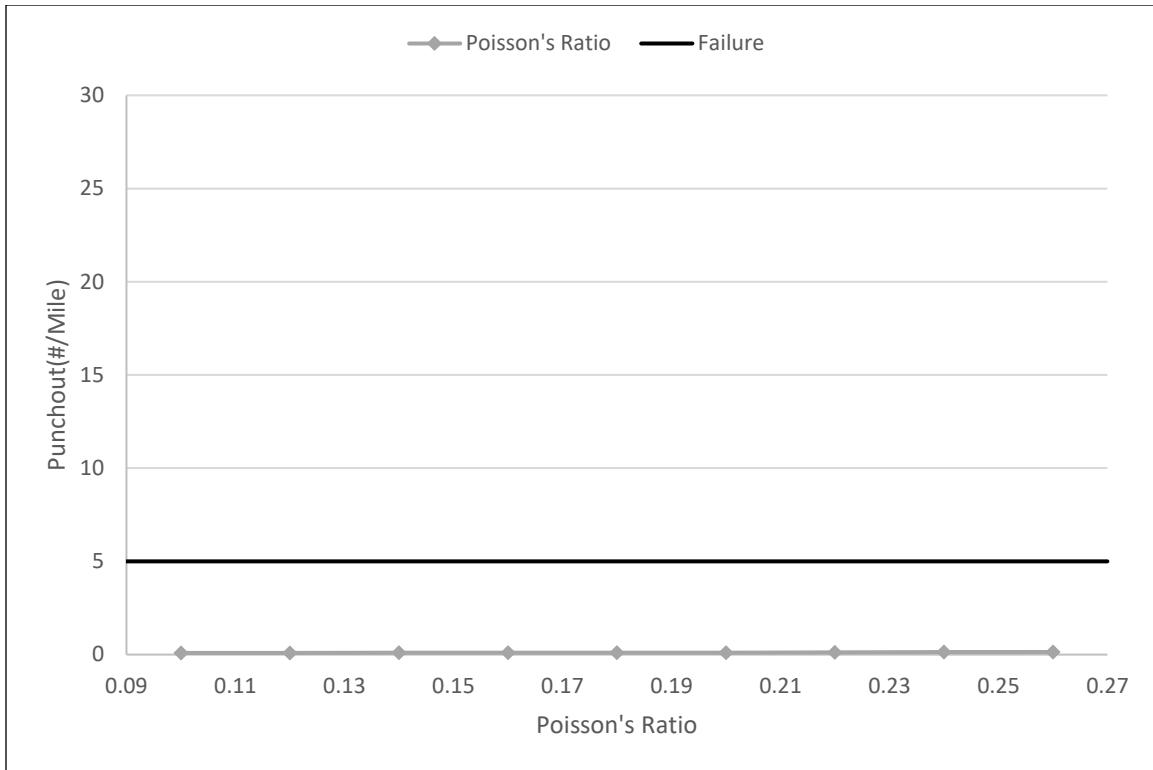


**Figure 83. Line graph. Poisson's ratio vs. punchout, CRCP.**

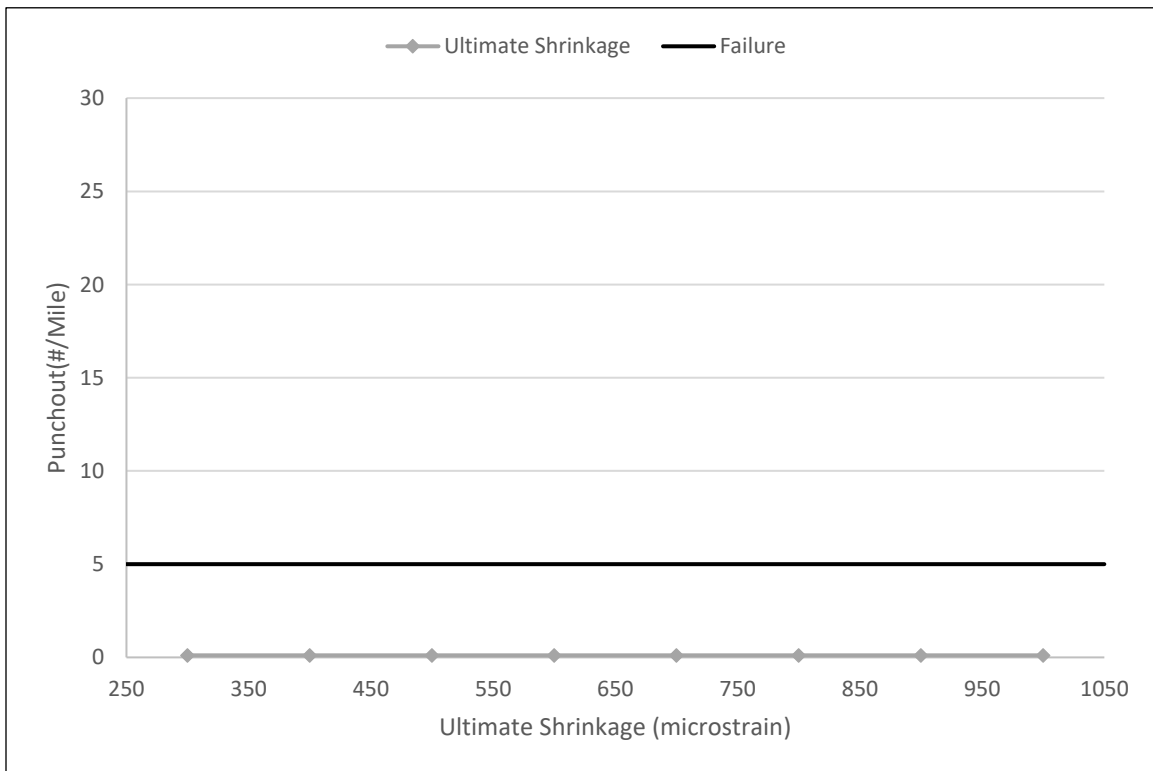


**Figure 84. Line graph. Ultimate shrinkage vs. punchout, CRCP.**

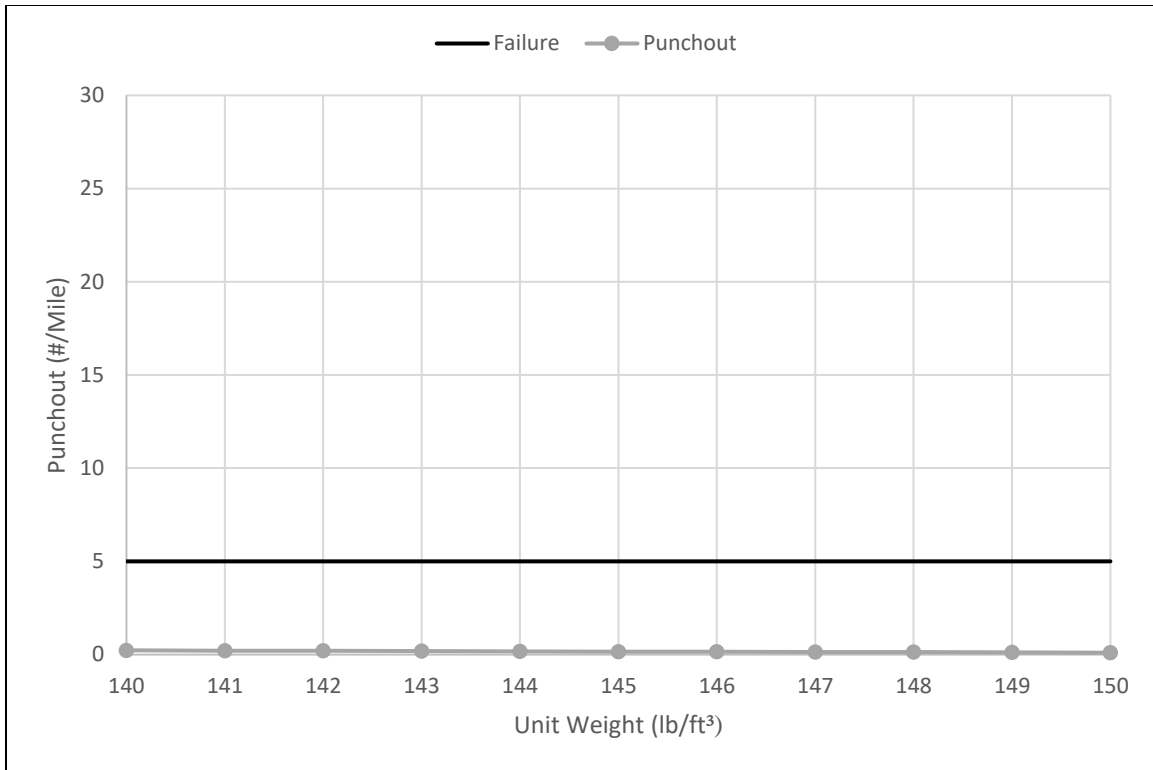


**Figure 85. Line graph. Unit weight vs. punchout, CRCP.**

## **SENSITIVITY TO INPUT LEVELS**

The laboratory-tested values were used to evaluate predicted performance at levels 1, 2, and 3 in AASHTOWare Pavement ME Design. Comparisons were made between design levels for each input to determine key differences in design levels. Recommendations are given based on the analysis for JPCP. These recommendations provide essential guidelines for which input level should be used in future designs. Additionally, guidelines on which mechanical inputs need to be tested up to 90 days for AASHTOWare Pavement ME Design are provided. These recommendations will aid designers in future designs, allowing for more cost-effective and accurate designs.

The sensitivity analyses were performed on the structure displayed in figure 86. All of the inputs used in this sensitivity analysis followed the recommended input values for a JPCP structure

by *The GDOT Pavement ME Design User Input Guide* (ARA 2015), excluding the thermal property being analyzed. The structure contained five separate layers that would most represent a typical GDOT design. The top layer was a 10-inch PCC layer using the recommended concrete property values. The second layer contained a 3-inch asphalt concrete interlayer using SuperPave 64-22. Underneath the interlayer, a 10-inch crushed gravel layer acted as the non-stabilized base. The structure then contained two subgrade A-7-6 sections at the bottom. A 12-inch compacted subgrade layer on the top was used to replicate typical GDOT practice, and the bottom subgrade portion acted as a semi-infinite layer.

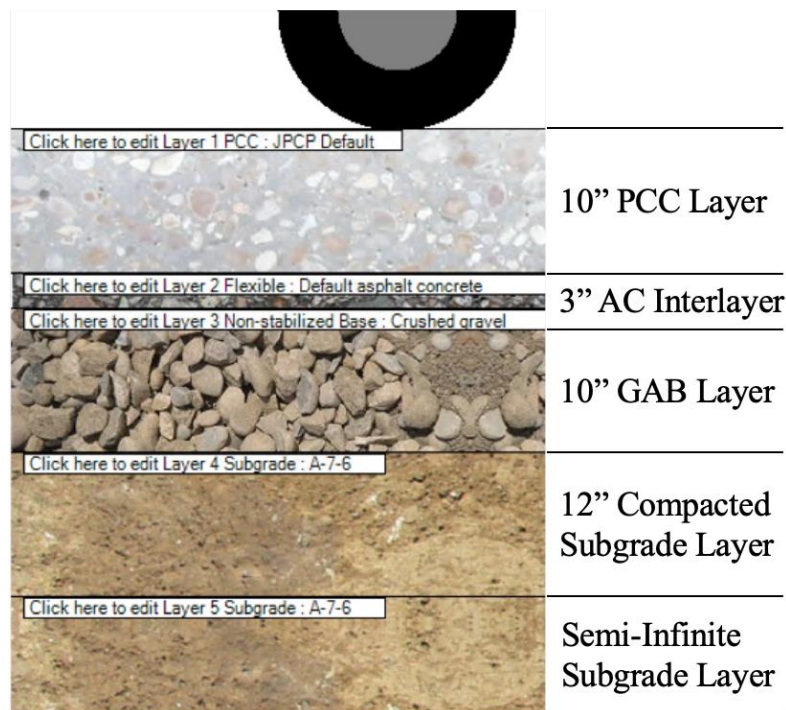


**Figure 86. Diagram. JPCP structure used in sensitivity analyses.**

The values from all 12 mixtures were used to complete level 1, 2, and 3 analyses and find predicted distresses and optimized thicknesses. To find optimized thicknesses, the concrete layer was varied by 0.25-inch (6.4-mm) intervals starting at 7-inch (177.8 mm) until the predicted distresses were below failure thresholds. Mean joint faulting was not considered in the thickness

analysis since all 12 mixtures experienced failure in this threshold due to low unit weight values. Predicted distresses and thicknesses were expected to decrease as the inputs transitioned from level 3 to level 1, since level 3 is the most conservative design level. In this study, more conservative refers to the design level that predicts the highest distress and has the largest optimized thickness. As seen in a previous study by Ping (2008), this expectation is not always met. Due to differences in inputs between levels, mainly between using compressive strength or MOR values, level 1 designs may actually be more conservative than level 2 designs. Comparisons between input levels and their associated distress are shown in figure 87. For clarity, the same figure is shown below the failure threshold in figure 88 to illustrate differences between levels for mixtures that did not experience predicted failure.

As shown in figure 88, half of the mixtures predicted more distress for level 1 designs compared to the level 2 designs; however, these differences are insignificant in most cases. For mixtures 8 and 10, the underprediction by the level 2 design results in a pavement that fails at every other input level, while passing at level 2. Similarly, when comparing optimized thicknesses in figure 89, mixtures 8 and 10 result in significantly thinner pavements sections. Based on this analysis, caution should be used when conducting level 2 designs for new JPCP. It is unclear if the predicted distress and thickness from level 2 provide an accurate representation of the field pavement distress or whether it is highly influenced by a material property input since field validation was not performed. However, it can be inferred that the key differences between levels that is likely causing these discrepancies is MOE inputs because levels 1 and 3 require MOE, while level 2 does not. For mixtures 8 and 10, the MOE values are larger than 5,500 ksi (39.7 GPa) to induce predicted failures. MOE was also shown in another study to be a very sensitive input in predicting slab cracking (Schwartz et al. 2011).



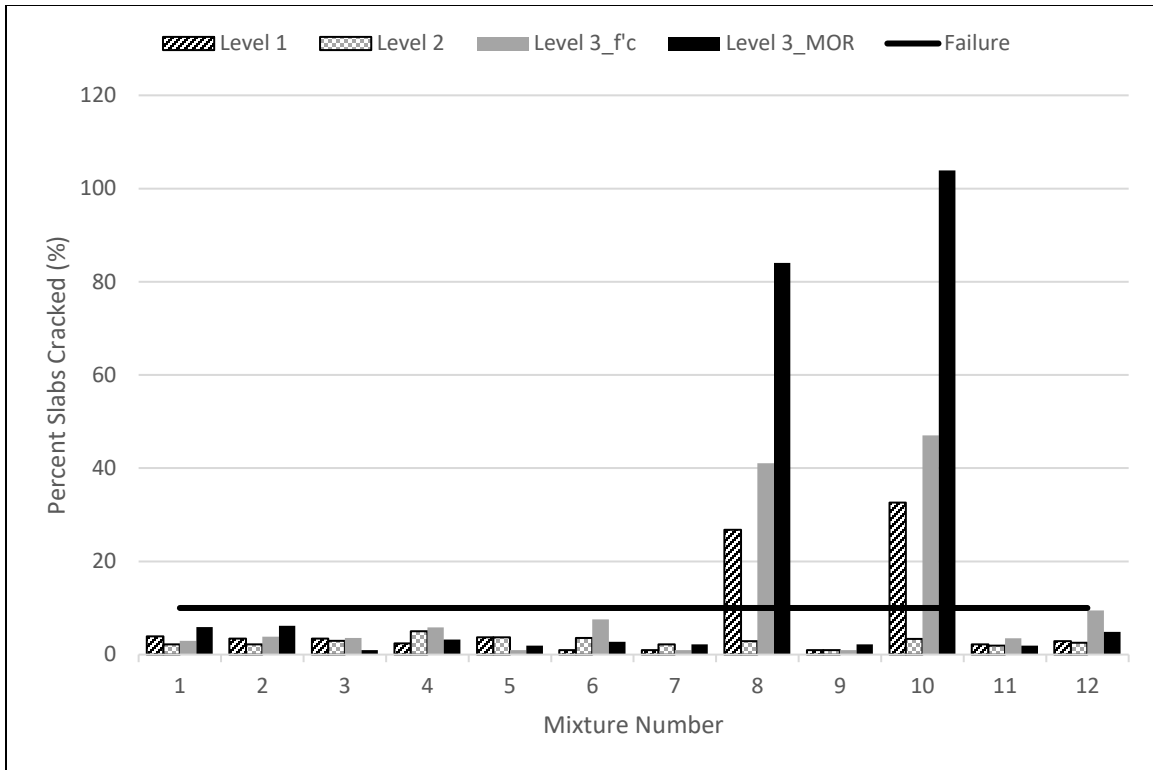


**Figure 87. Bar graph. Design levels compared for JPCP distresses.**

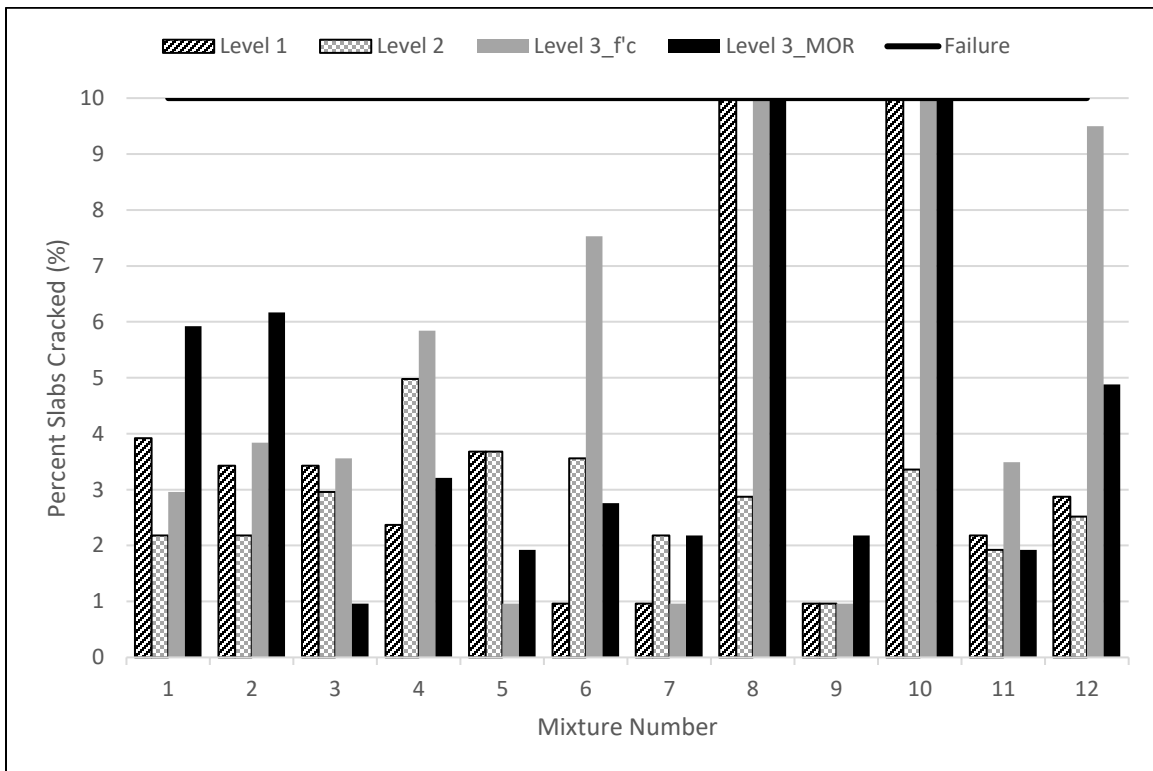


**Figure 88. Bar graph. Design levels compared for JPCP distresses below failure.**

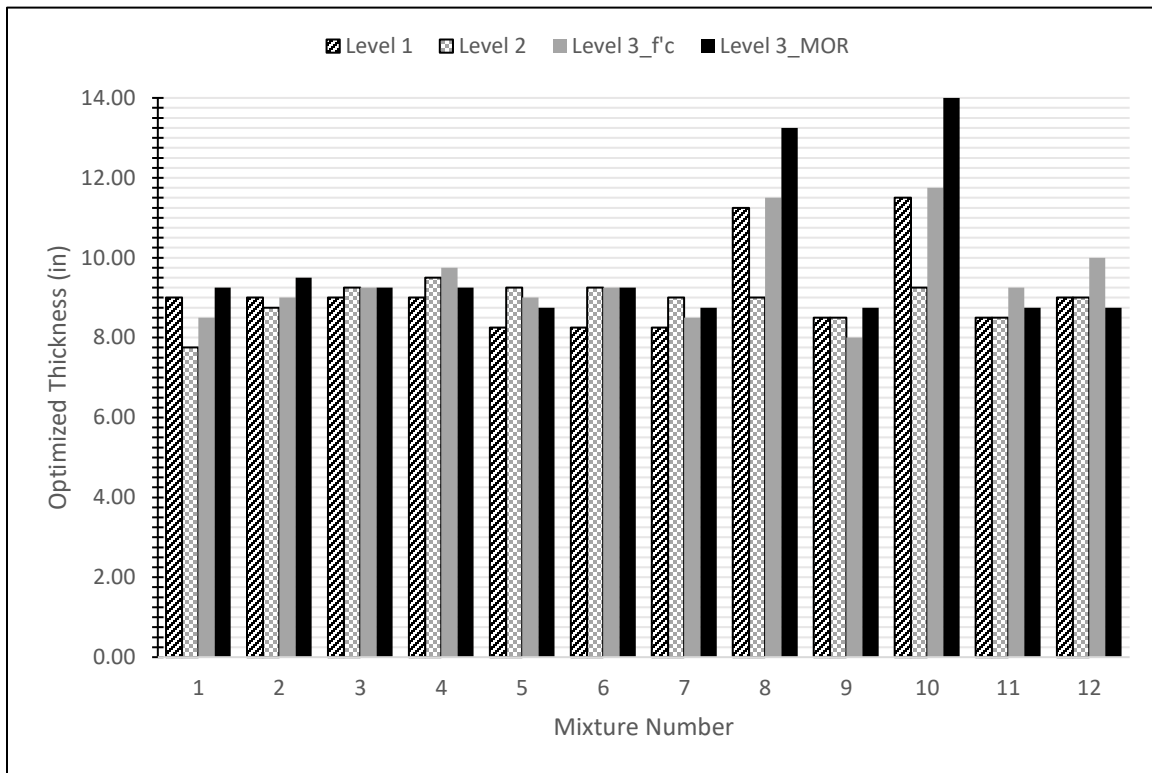


**Figure 89. Bar graph. Optimized thicknesses by level for JPCP.**

## STATISTICAL ANALYSIS

Using laboratory-tested values for all 12 mixtures, a statistical analysis was performed. The predicted distresses for each mixture were analyzed for their impact on predicted distresses. Using a least squares regression model, the effect of each design input was determined to be statistically significant or not. For JPCP, four inputs were found to have a significant impact on predicted distresses: MOR, compressive strength, unit weight, and Poisson's ratio. Specifically, for IRI and percent slabs crack, MOR and compressive strength were the only inputs that had a statistically significant impact on predicted distresses. Poisson's ratio and unit weight were the only two inputs that had a significant impact on mean joint faulting. These results are summarized in table 65. A p-value lower than 0.05 means that the input is statistically impactful on predicted distresses. The

conclusions from the preliminary sensitivity analysis were confirmed by the results of this effect test.

**Table 65. Input effect test, JPCP.**

Source	LogWorth	P-value
MOR	1.757	<b>0.01751</b>
Unit Weight	1.556	<b>0.02778</b>
Poisson's Ratio	1.359	<b>0.04378</b>
Cement Content	0.396	0.40173
W/cm	0.262	0.54660
MOE	0.242	0.57292

Bold = statistically significant

The same process was performed for CRCP. Only compressive strength and MOR impacted predicted distresses in a statistically significant manner. MOR and compressive strength were impactful on both IRI and punchout. The results of the least squares regression model for CRCP and each of the inputs' effects on the model are shown in table 66.

**Table 66. Input effect test, CRCP.**

Source	LogWorth	P-value
MOR	2.298	<b>0.00503</b>
MOE	0.468	0.34012
Unit Weight	0.434	0.36804
Poisson's Ratio	0.401	0.39751
W/cm	0.327	0.47138
Cement Content	0.027	0.93925

## CHAPTER 9. CONCLUSIONS AND RECOMMENDATIONS

This study aims to develop the aforementioned concrete materials database specific to Georgia's rigid pavements. Twelve (12) GDOT-approved concrete mixtures using Georgia-specific concrete materials were batched, tested, and analyzed for these properties. Through this study, the key inputs database for rigid pavement design in the MEPDG were developed. The materials library includes compressive strength ( $f'_c$ ), modulus of elasticity and modulus of rupture, coefficient of thermal expansion, portland cement concrete heat capacity, thermal conductivity, and ultimate shrinkage.

Based on the results from this study, there are three main recommendations: (1) the GDOT DAR for compressive strength of JPCP is suggested to be changed to 4,000 psi (27.6 MPa); (2) the GDOT DAR for MOR is acceptable for rigid pavements; and (3) static MOE testing should be used when performing laboratory tests for AASHTOWare Pavement ME Design inputs. Currently, GDOT's DAR for compressive strength is 3,000 psi (20.7 MPa) and 3,500 psi (24.1 MPa) for class 1 and 2 mixtures, respectively. Based on the sensitivity results presented in this study, JPCP will experience failure for compressive strengths below this threshold. Additionally, all 12 mixtures examined in this study exceeded a compressive strength of 4,000 psi (27.6 MPa) by 28 days, showing that most of the mixtures used in Georgia already exceed 4,000 psi (27.6 MPa). Therefore, the standard requirements should be changed to match field conditions. For MOR, 600 psi (4.1 MPa) and 700 psi (4.8 MPa) for class 1 and 2 mixtures, respectively, were found to be acceptable DAR. Static MOE testing is recommended to be used when performing laboratory tests for AASHTOWare Pavement ME Design inputs. The dynamic tests do not provide results that are easily converted to static values.

It should be noted that the design thickness of JPCP does not always increase as the input level goes from 1 to 3. Instead, properties such as  $f'_c$ , MOR, MOE, and CTE significantly affect the thickness design. Other design factors, such as joint spacing and dowel diameter, will also affect thickness. While levels 1 and 3 analyses require the measured MOE as input value, level 2 estimates the MOE from measured  $f'_c$ . Since MOE greater than 5,500 ksi (39.7 GPa) is prone to predict significant percent slab cracking, caution is necessary when level 2 input with over 5,500 ksi MOE value is utilized. Further, mixtures with higher MOE are expected to give higher CTE.


When the MEPDG faulting model is available, future work should investigate the impact of unit weight on faulting. Also, study of the impact of large MOE values on pavement performance is recommended. It was determined that unit weight was critical to the predicted faulting in AAASHTOWare Pavement ME Design. This was attributed to the prediction model in AASHTOWare Pavement ME Design incorporating curling deflections into its calculations. Further research is necessary to determine if unit weight is this impactful on faulting when the final MEPDG faulting model is available. If the current model is validated through further research, then recommendations should be made for GDOT to design future pavements with thicker sections or higher unit weights. MOE values over 5,500 ksi (39.7 GPa) are shown to cause large predictions in pavement distresses.

Based on the input level analysis, caution should be used when conducting level 2 designs for new JPCP. It is unclear if the predicted distress and thickness from level 2 provide an accurate representation of the field performance of rigid pavement. The research team recommends verification of the field performance with the Calibration Assessment Tool (CAT). With the GDOT local calibration setting in PMED V2.6 using CAT with transferred distress data format

from past decades, the field validation can be completed and the results will allow GDOT to select the final input level that reflects the field rigid pavement performance.

## APPENDICES

### APPENDIX A – MATERIAL SPECIFICATION SHEETS



Stockbridge  
3925 North Henry Blvd  
Stockbridge, GA 30281  
678-229-7885

05/06/2019

### 570-#57 (25290)

Procedure	Sieve/Test	Average	Unit	GADOT 57
	1 1/2" (37.5mm)	100.0	%	100.0-100.0
	1" (25mm)	98.3	%	95.0-100.0
	3/4" (19mm)	83.3	%	
	1/2" (12.5mm)	37.2	%	25.0-60.0
	3/8" (9.5mm)	16.5	%	
	#4 (4.75mm)	1.4	%	0.0-10.0
	#8 (2.36mm)	0.6	%	0.0-5.0
	#200 (75µm)	0.00	%	
	LA Abrasion (B,500)	46	%	0-50
	FM	6.96		
	SE	57	%	
	Absorption	0.6	%	
	Total Moisture	1.02	%	
	SPGR (Dry,Gsb)	2.609		
	SPGR (SSD)	2.625		
	SPGR (Apparent,Gsa)	2.652		
	Unit Wt (Loose)	90	lb/ft3	
	Unit Wt (Rodded)	97	lb/ft3	



Kennesaw  
1272 Duncan Road  
Kennesaw, GA 30144  
770-427-2401

05/08/2019

**570-#57 (25290)**

Procedure	Sieve/Test	Average	Unit	ASTM 57
	1 1/2" (37.5mm)	100.0	%	100.0-100.0
	1" (25mm)	97.1	%	95.0-100.0
	3/4" (19mm)	83.8	%	
	1/2" (12.5mm)	37.1	%	25.0-60.0
	3/8" (9.5mm)	16.7	%	
	#4 (4.75mm)	2.6	%	0.0-10.0
	#8 (2.36mm)	1.4	%	0.0-5.0
	#200 (75µm)	0.00	%	
	LA Abrasion (B,500)	41.8		
	Wash Loss (#200/75µm)	0.5	%	
	Absorption	0.65		
	Total Moisture	1.31	%	
	SPGR (Dry,Gsb)	2.745		
	SPGR (SSD)	2.763		
	SPGR (Apparent,Gsa)	2.795		
	Unit Wt (Loose)	100.3	lb/ft3	
	Unit Wt (Rodded)	108.7	lb/ft3	





Adairsville  
292 E Mitchell Road  
Adairsville, GA 30103  
770-773-3217

05/08/2019

**570-#57 (25291)**

Procedure	Sieve/Test	Average	Unit	GADOT 57
	2" (50mm)	100.0	%	
	1 1/2" (37.5mm)	100.0	%	100.0-100.0
	1" (25mm)	99.4	%	95.0-100.0
	3/4" (19mm)	84.5	%	
	1/2" (12.5mm)	41.5	%	25.0-60.0
	3/8" (9.5mm)	17.5	%	
	#4 (4.75mm)	1.5	%	0.0-10.0
	#8 (2.36mm)	0.6	%	0.0-5.0
	#200 (75µm)	0.00	%	0.00-1.50
	LA Abrasion (B,500)	18	%	0-60
	Flat/Elongated (5:1)	0.85	%	
	-#200 (75µm)	0.24	%	
	Absorption	0.08	%	
	Total Moisture	0.51	%	
	SPGR (Dry,Gsb)	2.846		
	SPGR (SSD)	2.847		
	SPGR (Apparent,Gsa)	2.851		
	Unit Wt (Loose)	96	lb/ft3	
	Unit Wt (Rodded)	104	lb/ft3	



## Basic Quality Statistical Summary Report

**Plant** 01209-Ruby Quarry  
**Product** 0570-GDOT #57 Stone  
**Specification** GADOT 57  
**Period** 01/01/2019 - 05/06/2019

Sieve/Test	Tests	Average	St Dev	Target	Specification
1 1/2" (37.5mm)	163	100.0	0.00	100-100	100-100
1" (25mm)	163	98.5	0.80	97-100	95-100
3/4" (19mm)	163	85.7	3.88		
1/2" (12.5mm)	163	42.5	4.37	32-48	25-60
3/8" (9.5mm)	163	20.4	3.28		
#4 (4.75mm)	163	1.1	0.55	0-5	0-10
#8 (2.36mm)	163	0.1	0.21	0-2	0-5
#200 (75µm)	1	0.10			
Pan	163	0.00	0.000		

**Query** Query Selections  
Date Created 05/06/2019  
Date Range 01/01/2019 - 05/06/2019  
Plant Ruby Quarry

## Detail Quality Statistical Summary Report

**Plant** 01-Burke Pit  
**Product** 2 B-Burke Concrete Sand  
**Specification** 2 B Burke Concrete Sand  
**Period** 05/06/2019 - 05/10/2019

Sieve/Test	Tests	Average	Min	Max	Range	St Dev	Target	Specification	PWS
3/8" (9.5mm)	5	100	100	100	0	0.0		100-100	100.0
#4 (4.75mm)	5	100	100	100	0	0.0		95-100	100.0
#8 (2.36mm)	5	99	98	99	1	0.4			
#16 (1.18mm)	5	90	87	91	4	1.5		45-95	100.0
#30 (0.6mm)	5	60	55	61	6	2.6			
#50 (0.3mm)	5	21	19	23	4	1.8		8-30	100.0
#100 (0.15mm)	5	2	1	4	3	1.3		0-10	100.0
Pan	5	0.0	0.0	0.0	0.0	0.00			
FM	5	2.297	2.262	2.385	0.123	0.0499			
SE	2	93.500	91.000	96.000	5.000	3.5355			
Wash Loss (#200/75um)	1	0.418	0.418	0.418	0.000				

**Query** Query Selections  
 Date Created 05/10/2019  
 Date Range 05/06/2019 - 05/10/2019  
 Plant Burke Pit  
 Sample Type Shipping



## Cement Mill Test Report

Month of Issue: April 2019

Plant: Calera, AL  
Product: Portland Cement Type I  
Silo: 17, 18J, 19, 20  
Manufactured: March 2019

### ASTM C150 and AASHTO M85 Standard Requirements

CHEMICAL ANALYSIS			PHYSICAL ANALYSIS		
Item	Spec limit	Test Result	Item	Spec limit	Test Result
Rapid Method, X-Ray (C114)			Air content of mortar (%) (C185)	12 max	7
SiO <sub>2</sub> (%)	---	19.8	Blaine Fineness (m <sup>2</sup> /kg) (C204)	260	396
Al <sub>2</sub> O <sub>3</sub> (%)	---	4.7	-325 (%) (C430)	---	97.2
Fe <sub>2</sub> O <sub>3</sub> (%)	---	3.2	Autoclave expansion (%) (C151)	0.80 max	0.06
CaO (%)	---	62.6	Compressive strength (MPa, [PSI]) (C109)		
MgO (%)	6.0 max	3.0	1 day		14.4 [2090]
SO <sub>3</sub> (%)	3.0 max *	3.0	3 days	12.0 [1740] min	27.0 [3910]
Loss on Ignition (%)**	3.5 max	2.7	7 days	19.0 [2760] min	33.7 [4890]
Insoluble residue (%)	1.5 max	0.51	28 days (Reflects previous month's data)	---	44.3 [6420]
CO <sub>2</sub> (%)	---	1.7	Time of setting (minutes)		
Limestone (%)	5.0 max	2.3	Vicat Initial (C191)	45 - 375	101
CaCO <sub>3</sub> in Limestone (%)	70 min	99	Heat of Hydration (kJ/kg) (C1702)		
Inorganic Process Addition (Baghouse Dust)	5.0 max	2.0	3 days (for information only)***	---	298
Adjusted Potential Phase Composition (C150)			Mortar Bar Expansion (%) (C1038)***	0.020 max	0.003
C3S (%)	---	54	Density (C188)		3.13
C2S (%)	---	15			
C3A (%)	---	7			
C4AF (%)	---	10			
ASTM C150 and AASHTO M85 Optional Chemical Requirements:					
NaEq (%)	0.60 max	0.36			

\* May exceed 3.0% SO<sub>3</sub> maximum based on our C1038 results of < 0.020% expansion at 14 days.

\*\* Loss on Ignition max of 3.5% when limestone is an ingredient.

\*\*\* Test result represents most recent value and is provided for information only.

We certify that the above described cement, at the time of shipment, meets the chemical and physical requirements of applicable FDOT Section 921, ALDOT, GDOT, TDOT, MDOT, INDOT, La DOTD, NCDOT, ODOT, PennDOT, VDOT, SCDOT, AHTD Specifications for TYPE I;

ASTM C150 & AASHTO M85 STANDARD SPECIFICATIONS FOR TYPE I CEMENT;

ASTM C150 & AASHTO M85 OPTIONAL CHEMICAL REQUIREMENTS FOR TYPE I LOW ALKALI CEMENT.

Certified By:

Nicholas T. Ewing - Quality Coordinator

Argos USA - Roberta  
8039 Highway 25, Calera, AL 35040  
Phone: 205.688.2721

Report created: 04/17/2019



Materials Testing & Research Facility  
2650 Old State Hwy 113  
Taylorsville, GA 30178  
770-684-0102

ASTM C618 / AASHTO M295 Testing of  
Bowen Fly Ash

Sample Date: 10/1 - 10/31/18

Report Date: 12/13/2018

Sample Type: Monthly

MTRF ID: 3146BN

Sample ID:

Chemical Analysis	Results	ASTM Limit Class F/C	AASHTO Limit Class F/C
Silicon Dioxide (SiO <sub>2</sub> )	<u>47.49</u> %		
Aluminum Oxide (Al <sub>2</sub> O <sub>3</sub> )	<u>21.30</u> %		
Iron Oxide (Fe <sub>2</sub> O <sub>3</sub> )	<u>18.08</u> %		
Sum (SiO <sub>2</sub> +Al <sub>2</sub> O <sub>3</sub> +Fe <sub>2</sub> O <sub>3</sub> )	<u>86.87</u> %	70.0/50.0 min	70.0/50.0 min
Sulfur Trioxide (SO <sub>3</sub> )	<u>2.07</u> %	5.0 max	5.0 max
Calcium Oxide (CaO)	<u>4.26</u> %		
Magnesium Oxide (MgO)	<u>1.19</u> %		
Sodium Oxide (Na <sub>2</sub> O)	<u>0.99</u> %		
Potassium Oxide (K <sub>2</sub> O)	<u>2.32</u> %		
Sodium Oxide Equivalent (Na <sub>2</sub> O+0.658K <sub>2</sub> O)	<u>2.52</u> %		
Moisture	<u>0.14</u> %	3.0 max	3.0 max
Loss on Ignition	<u>1.23</u> %	6.0 max	5.0 max
Available Alkalies, as Na <sub>2</sub> O <sub>e</sub>	<u>1.03</u> %	Not Required	1.5 max* <small>*when required by purchaser</small>
<b>Physical Analysis</b>			
Fineness, % retained on 45-µm sieve	<u>14.48</u> %	34 max	34 max
Strength Activity Index - 7 or 28 day requirement			
7 day, % of control	<u>82</u> %	75 min	75 min
28 day, % of control	<u>82</u> %	75 min	75 min
Water Requirement, % control	<u>98</u> %	105 max	105 max
Autoclave Soundness	<u>0.01</u> %	0.8 max	0.8 max
Density	<u>2.47</u>		

The test data listed herein was generated by applicable ASTM methods. The reported results pertain only to the sample(s) or lot(s) tested. This report cannot be reproduced without permission from Boral Resources.

  
Doug Rhodes, CET  
Facility Manager



## APPENDIX B – MIXTURE DESIGNS

Mixture 1 Batched 4/11/2019								
Mix Proportion (SSD)						Material Properties		
Material	Weight	Volume (cf)	Volume Check	Unit Cost (\$/ton)	Amount (\$)	Material	S.G.	A.C
Cement	541.00	2.75	0.102	120	32.46	Cement	3.15	-
Fly Ash	0	0.00	0.000	100	0.00	Fly Ash	2.30	-
BFS	0	0.00	0.000	100	0.00	BFS	2.89	-
Metakaolin	0	0.00	0.000	100	0.00	Metakaolin	2.60	-
RCA	0	0.00	0.000	18	0.00	RCA	2.46	2.82
Rock	1947.00	11.77	0.436	18	17.52	Rock	2.65	0.49
Sand	1266.10	7.66	0.284	18	11.39	Sand	2.65	1.53
Water	233.17	3.74	0.138	0.6	0.07			
Air	0.040	1.08	0.040	-	-			
		27.00	1.00	-	-			
				Total Cost =	61.45			
Mix Characteristics								
w/c		0.43						
Unit Weight (pcf)		147.7						
Cementitious material (lb)		541						
Suppl. Cementitious Mat.	Percent (%)	Weight (lb)						
Fly Ash replacement (%)	0	0						
BFS replacement (%)	0	0						
Metakaolin Replacement (%)	0	0						
RCA %	0	0						
Moisture Content								
sand mc (%)	11.08	mc-ssd	0.0955					
rock mc (%)	0.48	mc-ssd	-0.0001					
RCA mc (%)	1.65	mc-ssd	-0.0117					
Batch Weights (yd <sup>3</sup> )								
Cement	541	lb						
Fly Ash	0	lb						
BFS	0	lb						
Metakaolin	0	lb						
RCA	0	lb						
Rock	1947	lb						
Sand	1387	lb						
Water	112	lb						
AEA	0.3	fl oz./cwt						
AEA	48	ml						
HRWRA	6.0	fl oz./cwt						
HRWRA	0	ml						
Batch Weights (ft <sup>3</sup> )								
Batch size	3.75	cf						
Cement	75.1	lb						
Fly Ash	0.0	lb						
BFS	0.0	lb						
Metakaolin	0.0	lb						
RCA	0.0	lb						
Rock	270.4	lb						
Sand	192.6	lb						
Water	15.6	lb						
AEA	6.7	ml						
HRWRA	0.0							

**Mixture 2 Batched 4/16/2019**

### Mix Proportion (SSD)

Material	Weight	Volume (cf)	Volume Check	Unit Cost (\$/ton)	Amount (\$)
Cement	541.00	2.75	0.102	120	32.46
Fly Ash	0	0.00	0.000	100	0.00
BFS	0	0.00	0.000	100	0.00
Metakaolin	0	0.00	0.000	100	0.00
RCA	0	0.00	0.000	18	0.00
Rock	2084.00	12.60	0.467	18	18.76
Sand	995.77	6.02	0.223	18	8.96
Water	283.48	4.54	0.168	0.6	0.09
Air	0.040	1.08	0.040	-	-
		27.00	1.00	-	-
				Total Cost =	60.26

## Material Properties

Material	S.G.	A.C
Cement	3.15	-
Fly Ash	2.30	-
BFS	2.89	-
Metakaolin	2.60	-
RCA	2.46	2.82
Rock	2.65	0.49
Sand	2.65	1.53

### Mix Characteristics

w/c	0.52
Unit Weight (pcf)	144.6
Cementitious material (lb)	541

Suppl. Cementitious Mat.	Percent (%)	Weight (lb)
Fly Ash replacement (%)	0	0
BFS replacement (%)	0	0
Metakaolin Replacement (%)	0	0
RCA %	0	0

### Moisture Content

sand mc (%)	10.7	mc-ssd	0.0917
rock mc (%)	0.476	mc-ssd	-0.00014
RCA mc (%)	1.65	mc-ssd	-0.0117

Batch Weights (yd <sup>3</sup> )
1
2
3
4
5
6
7
8
9
10
11
12
13
14
15
16
17
18
19
20
21
22
23
24
25
26
27
28
29
30
31
32
33
34
35
36
37
38
39
40
41
42
43
44
45
46
47
48
49
50
51
52
53
54
55
56
57
58
59
60
61
62
63
64
65
66
67
68
69
70
71
72
73
74
75
76
77
78
79
80
81
82
83
84
85
86
87
88
89
90
91
92
93
94
95
96
97
98
99
100

Cement	541	lb
Fly Ash	0	lb
BFS	0	lb
Metakaolin	0	lb
RCA	0	lb
Rock	2084	lb
Sand	1087	lb
Water	192	lb
AEA	0.3	fl oz./cwt
AEA	48	ml
HRWRA	6.0	fl oz./cwt
HRWRA	0	ml

Batch Weights (ft<sup>3</sup>)

Batch size	3.75	cf
Cement	75.1	lb
Fly Ash	0.0	lb
BFS	0.0	lb
Metakaolin	0.0	lb
RCA	0.0	lb
Rock	289.4	lb
Sand	151.0	lb
Water	26.7	lb
AEA	6.7	ml
HRWRA	0.0	

**Mixture 3 Batched 4/3/2019**

Mix Proportion (SSD)					
Material	Weight	Volume (cf)	Volume Check	Unit Cost (\$/ton)	Amount (\$)
Cement	595.00	3.03	0.112	120	35.70
Fly Ash	0	0.00	0.000	100	0.00
BFS	0	0.00	0.000	100	0.00
Metakaolin	0	0.00	0.000	100	0.00
RCA	0	0.00	0.000	18	0.00
Rock	1863.00	11.27	0.417	18	16.77
Sand	1199.93	7.26	0.269	18	10.80
Water	255.85	4.10	0.152	0.6	0.08
Air	0.050	1.35	0.050	-	-
		27.00	1.00	-	-
				Total Cost =	63.34

Material Properties		
Material	S.G.	A.C
Cement	3.15	-
Fly Ash	2.30	-
BFS	2.89	-
Metakaolin	2.60	-
RCA	2.46	2.82
Rock	2.65	0.49
Sand	2.65	1.53

### Mix Characteristics

w/c	0.43
Unit Weight (pcf)	145.0
Cementitious material (lb)	595

Suppl. Cementitious Mat.	Percent (%)	Weight (lb)
Fly Ash replacement (%)	0	0
BFS replacement (%)	0	0
MetaKaolin Replacement (%)	0	0
RCA %	0	0

### Moisture Content

sand mc (%)	1.493	mc-ssd	-0.00037
rock mc (%)	0.239	mc-ssd	-0.00251
RCA mc (%)	1.65	mc-ssd	-0.0117

Batch Weights (yd <sup>3</sup> )
----------------------------------

Cement	595	lb
Fly Ash	0	lb
BFS	0	lb
Metakaolin	0	lb
RCA	0	lb
Rock	1858	lb
Sand	1199	lb
Water	261	lb
AEA	0.7	fl oz./cwt
AEA	114	ml
HRWRA	6.0	fl oz./cwt
HRWRA	0	ml

Batch Weights (ft<sup>3</sup>)

Batch size	3.75	cf
Cement	82.6	lb
Fly Ash	0.0	lb
BFS	0.0	lb
Metakaolin	0.0	lb
RCA	0.0	lb
Rock	258.1	lb
Sand	166.6	lb
Water	36.2	lb
AEA	15.9	ml
HRWRA	0.0	



**Mixture 4 Batched 4/09/2019**

### Mix Proportion (SSD)

Material	Weight	Volume (cf)	Volume Check	Unit Cost (\$/ton)	Amount (\$)
Cement	600.00	3.05	0.113	120	36.00
Fly Ash	0	0.00	0.000	100	0.00
BFS	0	0.00	0.000	100	0.00
Metakaolin	0	0.00	0.000	100	0.00
RCA	0	0.00	0.000	18	0.00
Rock	1900.00	11.49	0.426	18	17.10
Sand	1111.75	6.72	0.249	18	10.01
Water	282.00	4.52	0.167	0.6	0.08
Air	0.045	1.22	0.045	-	-
		27.00	1.00	-	-
				Total Cost =	63.19

## Material Properties

Material	S.G.	A.C
Cement	3.15	-
Fly Ash	2.30	-
BFS	2.89	-
Metakaolin	2.60	-
RCA	2.46	2.82
Rock	2.65	0.49
Sand	2.65	1.53

### Mix Characteristics

w/c	0.47
Unit Weight (pcf)	144.2
Cementitious material (lb)	600

Suppl. Cementitious Mat.	Percent (%)	Weight (lb)
Fly Ash replacement (%)	0	0
BFS replacement (%)	0	0
MetaKaolin Replacement (%)	0	0
RCA %	0	0

### Moisture Content

sand mc (%)	7	mc-ssd	0.0547
rock mc (%)	0.31	mc-ssd	-0.0018
RCA mc (%)	1.65	mc-ssd	-0.0117

[illegible]

Cement	600	lb
Fly Ash	0	lb
BFS	0	lb
Metakaolin	0	lb
RCA	0	lb
Rock	1897	lb
Sand	1173	lb
Water	225	lb
AEA	0.5	fl oz./cwt
AEA	89	ml
HRWRA	6.0	fl oz./cwt
HRWRA	0	ml

Batch Weights (ft<sup>3</sup>)

Batch size	3.75	cf
Cement	83.3	lb
Fly Ash	0.0	lb
BFS	0.0	lb
Metakaolin	0.0	lb
RCA	0.0	lb
Rock	263.4	lb
Sand	162.9	lb
Water	31.2	lb
AEA	12.3	ml
HRWRA	0.0	

**Mixture 5 Batched 3/11/2019**

Mix Proportion (SSD)					
Material	Weight	Volume (cf)	Volume Check	Unit Cost (\$/ton)	Amount (\$)
Cement	508.95	2.59	0.096	120	30.54
Fly Ash	71.05	0.50	0.018	100	3.55
BFS	0	0.00	0.000	100	0.00
Metakaolin	0	0.00	0.000	100	0.00
RCA	0	0.00	0.000	18	0.00
Rock	2050.00	12.40	0.459	18	18.45
Sand	923.72	5.59	0.207	18	8.31
Water	285.94	4.58	0.170	0.6	0.09
Air	0.050	1.35	0.050	-	-
		27.00	1.00	-	-
				Total Cost =	60.94

Material Properties		
Material	S.G.	A.C
Cement	3.15	-
Fly Ash	2.30	-
BFS	2.89	-
Metakaolin	2.60	-
RCA	2.46	2.82
Rock	2.65	0.49
Sand	2.65	1.53

### Mix Characteristics

w/c	0.49
Unit Weight (pcf)	142.2
Cementitious material (lb)	580

Suppl. Cementitious Mat.	Percent (%)	Weight (lb)
Fly Ash replacement (%)	12.25	71.05
BFS replacement (%)	0	0
Metakaolin Replacement (%)	0	0
RCA %	0	0

### Moisture Content

sand mc (%)	2.69	mc-ssd	0.0116
rock mc (%)	1.01	mc-ssd	0.0052
RCA mc (%)	1.65	mc-ssd	-0.0117

Batch Weights (yd <sup>3</sup> )
1
2
3
4
5
6
7
8
9
10
11
12
13
14
15
16
17
18
19
20
21
22
23
24
25
26
27
28
29
30
31
32
33
34
35
36
37
38
39
40
41
42
43
44
45
46
47
48
49
50
51
52
53
54
55
56
57
58
59
60
61
62
63
64
65
66
67
68
69
70
71
72
73
74
75
76
77
78
79
80
81
82
83
84
85
86
87
88
89
90
91
92
93
94
95
96
97
98
99
100

Cement	509	lb
Fly Ash	71	lb
BFS	0	lb
Metakaolin	0	lb
RCA	0	lb
Rock	2061	lb
Sand	934	lb
Water	265	lb
AEA	1.0	fl oz./cwt
AEA	172	ml
HRWRA	6.0	fl oz./cwt
HRWRA	0	ml

Batch Weights (ft<sup>3</sup>)

Batch size	3.75	cf
Cement	70.7	lb
Fly Ash	9.9	lb
BFS	0.0	lb
Metakaolin	0.0	lb
RCA	0.0	lb
Rock	286.2	lb
Sand	129.8	lb
Water	36.7	lb
AEA	23.8	ml
HRWRA	0.0	

## Mixture 6 Batched 3/12/2019

### Mix Proportion (SSD)

Material	Weight	Volume (cf)	Volume Check	Unit Cost (\$/ton)	Amount (\$)
Cement	465.74	2.37	0.088	120	27.94
Fly Ash	114.26	0.80	0.029	100	5.71
BFS	0	0.00	0.000	100	0.00
Metakaolin	0	0.00	0.000	100	0.00
RCA	0	0.00	0.000	18	0.00
Rock	1908.00	11.54	0.427	18	17.17
Sand	1124.52	6.80	0.252	18	10.12
Water	258.68	4.15	0.154	0.6	0.08
Air	0.050	1.35	0.050	-	-
		27.00	1.00	-	-
				Total Cost =	61.03

### Material Properties

Material	S.G.	A.C
Cement	3.15	-
Fly Ash	2.30	-
BFS	2.89	-
Metakaolin	2.60	-
RCA	2.46	2.82
Rock	2.65	0.49
Sand	2.65	1.53

### Mix Characteristics

w/c	0.45
Unit Weight (pcf)	143.4
Cementitious material (lb)	580

Suppl. Cementitious Mat.	Percent (%)	Weight (lb)
Fly Ash replacement (%)	19.7	114.26
BFS replacement (%)	0	0
Metakaolin Replacement (%)	0	0
RCA %	0	0

### Moisture Content

sand mc (%)	4.16	mc-ssd	0.0263
rock mc (%)	1.24	mc-ssd	0.0075
RCA mc (%)	1.65	mc-ssd	-0.0117

### Batch Weights (yd<sup>3</sup>)

Cement	466	lb
Fly Ash	114	lb
BFS	0	lb
Metakaolin	0	lb
RCA	0	lb
Rock	1922	lb
Sand	1154	lb
Water	215	lb
AEA	1.1	fl oz./cwt
AEA	189	ml
HRWRA	6.0	fl oz./cwt
HRWRA	0	ml

### Batch Weights (ft<sup>3</sup>)

Batch size	3.75	cf
Cement	64.7	lb
Fly Ash	15.9	lb
BFS	0.0	lb
Metakaolin	0.0	lb
RCA	0.0	lb
Rock	267.0	lb
Sand	160.3	lb
Water	29.8	lb
AEA	26.2	ml
HRWRA	0.0	

### Mixture 7 Batched 3/19/2019

#### Mix Proportion (SSD)

Material	Weight	Volume (cf)	Volume Check	Unit Cost (\$/ton)	Amount (\$)
Cement	459.97	2.34	0.087	120	27.60
Fly Ash	162.031	1.13	0.042	100	8.10
BFS	0	0.00	0.000	100	0.00
Metakaolin	0	0.00	0.000	100	0.00
RCA	0	0.00	0.000	18	0.00
Rock	1985.00	12.00	0.445	18	17.87
Sand	1009.58	6.11	0.226	18	9.09
Water	262.48	4.21	0.156	0.6	0.08
Air	0.045	1.22	0.045	-	-
		27.00	1.00	-	-
				Total Cost =	62.73

#### Material Properties

Material	S.G.	A.C
Cement	3.15	-
Fly Ash	2.30	-
BFS	2.89	-
Metakaolin	2.60	-
RCA	2.46	2.82
Rock	2.65	0.49
Sand	2.65	1.53

#### Mix Characteristics

w/c	0.42
Unit Weight (pcf)	143.7
Cementitious material (lb)	622

Suppl. Cementitious Mat.	Percent (%)	Weight (lb)
Fly Ash replacement (%)	26.05	162.031
BFS replacement (%)	0	0
Metakaolin Replacement (%)	0	0
RCA %	0	0

#### Moisture Content

sand mc (%)	2.69	mc-ssd	0.0116
rock mc (%)	0.33	mc-ssd	-0.0016
RCA mc (%)	1.65	mc-ssd	-0.0117

#### Batch Weights (yd<sup>3</sup>)

Cement	460	lb
Fly Ash	162	lb
BFS	0	lb
Metakaolin	0	lb
RCA	0	lb
Rock	1982	lb
Sand	1021	lb
Water	254	lb
AEA	1.0	fl oz./cwt
AEA	184	ml
HRWRA	6.0	fl oz./cwt
HRWRA	0	ml

#### Batch Weights (ft<sup>3</sup>)

Batch size	3.75	cf
Cement	63.9	lb
Fly Ash	22.5	lb
BFS	0.0	lb
Metakaolin	0.0	lb
RCA	0.0	lb
Rock	275.3	lb
Sand	141.8	lb
Water	35.3	lb
AEA	25.5	ml
HRWRA	0.0	

**Mixture 8 Batched 3/26/2019**

Mix Proportion (SSD)					
Material	Weight	Volume (cf)	Volume Check	Unit Cost (\$/ton)	Amount (\$)
Cement	479.77	2.44	0.090	120	28.79
Fly Ash	125.235	0.87	0.032	100	6.26
BFS	0	0.00	0.000	100	0.00
Metakaolin	0	0.00	0.000	100	0.00
RCA	0	0.00	0.000	18	0.00
Rock	1976.00	11.95	0.443	18	17.78
Sand	1028.18	6.22	0.230	18	9.25
Water	260.15	4.17	0.154	0.6	0.08
Air	0.050	1.35	0.050	-	-
		27.00	1.00	-	-
				Total Cost =	62.16

Material Properties		
Material	S.G.	A.C
Cement	3.15	-
Fly Ash	2.30	-
BFS	2.89	-
Metakaolin	2.60	-
RCA	2.46	2.82
Rock	2.65	0.49
Sand	2.65	1.53

### Mix Characteristics

w/c	0.43
Unit Weight (pcf)	143.3
Cementitious material (lb)	605

Suppl. Cementitious Mat.	Percent (%)	Weight (lb)
Fly Ash replacement (%)	20.7	125.235
BFS replacement (%)	0	0
Metakaolin Replacement (%)	0	0
RCA %	0	0

### Moisture Content

sand mc (%)	5.49	mc-ssd	0.0396
rock mc (%)	0.68	mc-ssd	0.0019
RCA mc (%)	1.65	mc-ssd	-0.0117

Batch Weights (yd <sup>3</sup> )
----------------------------------

Cement	480	lb
Fly Ash	125	lb
BFS	0	lb
Metakaolin	0	lb
RCA	0	lb
Rock	1980	lb
Sand	1069	lb
Water	216	lb
AEA	1.1	fl oz./cwt
AEA	197	ml
HRWRA	6.0	fl oz./cwt
HRWRA	0	ml

Batch Weights (ft<sup>3</sup>)

Batch size	3.75	cf
Cement	66.6	lb
Fly Ash	17.4	lb
BFS	0.0	lb
Metakaolin	0.0	lb
RCA	0.0	lb
Rock	275.0	lb
Sand	148.5	lb
Water	30.0	lb
AEA	27.3	ml
HRWRA	0.0	

**Mixture 9 Batched 3/21/2019**

### Mix Proportion (SSD)

Material	Weight	Volume (cf)	Volume Check	Unit Cost (\$/ton)	Amount (\$)
Cement	479.97	2.44	0.090	120	28.80
Fly Ash	110.035	0.77	0.028	100	5.50
BFS	0	0.00	0.000	100	0.00
Metakaolin	0	0.00	0.000	100	0.00
RCA	0	0.00	0.000	18	0.00
Rock	1777.00	10.75	0.398	18	15.99
Sand	1249.11	7.55	0.280	18	11.24
Water	258.42	4.14	0.153	0.6	0.08
Air	0.050	1.35	0.050	-	-
		27.00	1.00	-	-
				Total Cost =	61.61

## Material Properties

Material	S.G.	A.C
Cement	3.15	-
Fly Ash	2.30	-
BFS	2.89	-
Metakaolin	2.60	-
RCA	2.46	2.82
Rock	2.65	0.49
Sand	2.65	1.53

## Mix Characteristics

w/c	0.44
Unit Weight (pcf)	143.5
Cementitious material (lb)	590

Suppl. Cementitious Mat.	Percent (%)	Weight (lb)
Fly Ash replacement (%)	18.65	110.035
BFS replacement (%)	0	0
Metakaolin Replacement (%)	0	0
RCA %	0	0

### Moisture Content

sand mc (%)	3.59	mc-ssd	0.0206
rock mc (%)	0.51	mc-ssd	0.0002
RCA mc (%)	1.65	mc-ssd	-0.0117

Batch Weights (yd <sup>3</sup> )
1
2
3
4
5
6
7
8
9
10
11
12
13
14
15
16
17
18
19
20
21
22
23
24
25
26
27
28
29
30
31
32
33
34
35
36
37
38
39
40
41
42
43
44
45
46
47
48
49
50
51
52
53
54
55
56
57
58
59
60
61
62
63
64
65
66
67
68
69
70
71
72
73
74
75
76
77
78
79
80
81
82
83
84
85
86
87
88
89
90
91
92
93
94
95
96
97
98
99
100

Cement	480	lb
Fly Ash	110	lb
BFS	0	lb
Metakaolin	0	lb
RCA	0	lb
Rock	1777	lb
Sand	1275	lb
Water	232	lb
AEA	1.1	fl oz./cwt
AEA	192	ml
HRWRA	6.0	fl oz./cwt
HRWRA	0	ml

Batch Weights (ft<sup>3</sup>)

Batch size	3.75	cf
Cement	66.7	lb
Fly Ash	15.3	lb
BFS	0.0	lb
Metakaolin	0.0	lb
RCA	0.0	lb
Rock	246.9	lb
Sand	177.1	lb
Water	32.3	lb
AEA	26.7	ml
HRWRA	0.0	

**Mixture 10 Batched 3/28/2019**

Mix Proportion (SSD)					
Material	Weight	Volume (cf)	Volume Check	Unit Cost (\$/ton)	Amount (\$)
Cement	479.97	2.44	0.090	120	28.80
Fly Ash	110.035	0.77	0.028	100	5.50
BFS	0	0.00	0.000	100	0.00
Metakaolin	0	0.00	0.000	100	0.00
RCA	0	0.00	0.000	18	0.00
Rock	1777.00	10.75	0.398	18	15.99
Sand	1249.11	7.55	0.280	18	11.24
Water	258.42	4.14	0.153	0.6	0.08
Air	0.050	1.35	0.050	-	-
		27.00	1.00	-	-
				Total Cost =	61.61

Material Properties		
Material	S.G.	A.C
Cement	3.15	-
Fly Ash	2.30	-
BFS	2.89	-
Metakaolin	2.60	-
RCA	2.46	2.82
Rock	2.65	0.49
Sand	2.65	1.53

### Mix Characteristics

w/c	0.44
Unit Weight (pcf)	143.5
Cementitious material (lb)	590

Suppl. Cementitious Mat.	Percent (%)	Weight (lb)
Fly Ash replacement (%)	18.65	110.035
BFS replacement (%)	0	0
Metakaolin Replacement (%)	0	0
RCA %	0	0

### Moisture Content

sand mc (%)	7	mc-ssd	0.0547
rock mc (%)	0.31	mc-ssd	-0.0018
RCA mc (%)	1.65	mc-ssd	-0.0117

Batch Weights (yd <sup>3</sup> )
1
2
3
4
5
6
7
8
9
10
11
12
13
14
15
16
17
18
19
20
21
22
23
24
25
26
27
28
29
30
31
32
33
34
35
36
37
38
39
40
41
42
43
44
45
46
47
48
49
50
51
52
53
54
55
56
57
58
59
60
61
62
63
64
65
66
67
68
69
70
71
72
73
74
75
76
77
78
79
80
81
82
83
84
85
86
87
88
89
90
91
92
93
94
95
96
97
98
99
100

Cement	480	lb
Fly Ash	110	lb
BFS	0	lb
Metakaolin	0	lb
RCA	0	lb
Rock	1774	lb
Sand	1317	lb
Water	193	lb
AEA	1.1	fl oz./cwt
AEA	192	ml
HRWRA	6.0	fl oz./cwt
HRWRA	0	ml

Batch Weights (ft<sup>3</sup>)

Batch size	3.75	cf
Cement	66.7	lb
Fly Ash	15.3	lb
BFS	0.0	lb
Metakaolin	0.0	lb
RCA	0.0	lb
Rock	246.4	lb
Sand	183.0	lb
Water	26.8	lb
AEA	26.7	ml
HRWRA	0.0	

**Mixture 11 Batched 4/18/2019**

### Mix Proportion (SSD)

Material	Weight	Volume (cf)	Volume Check	Unit Cost (\$/ton)	Amount (\$)
Cement	478.80	2.44	0.090	120	28.73
Fly Ash	121.2	0.84	0.031	100	6.06
BFS	0	0.00	0.000	100	0.00
Metakaolin	0	0.00	0.000	100	0.00
RCA	0	0.00	0.000	18	0.00
Rock	1867.00	11.29	0.418	18	16.80
Sand	1129.39	6.83	0.253	18	10.16
Water	282.00	4.52	0.167	0.6	0.08
Air	0.040	1.08	0.040	-	-
		27.00	1.00	-	-
				Total Cost =	61.84

## Material Properties

Material	S.G.	A.C
Cement	3.15	-
Fly Ash	2.30	-
BFS	2.89	-
Metakaolin	2.60	-
RCA	2.46	2.82
Rock	2.65	0.49
Sand	2.65	1.53

### Mix Characteristics

w/c	0.47
Unit Weight (pcf)	143.6
Cementitious material (lb)	600

Suppl. Cementitious Mat.	Percent (%)	Weight (lb)
Fly Ash replacement (%)	20.2	121.2
BFS replacement (%)	0	0
Metakaolin Replacement (%)	0	0
RCA %	0	0

### Moisture Content

sand mc (%)	7.86	mc-ssd	0.0633
rock mc (%)	0.4	mc-ssd	-0.0009
RCA mc (%)	1.65	mc-ssd	-0.0117

Batch Weights (yd <sup>3</sup> )
----------------------------------

Cement	479	lb
Fly Ash	121	lb
BFS	0	lb
Metakaolin	0	lb
RCA	0	lb
Rock	1865	lb
Sand	1201	lb
Water	212	lb
AEA	0.8	fl oz./cwt
AEA	142	ml
HRWRA	6.0	fl oz./cwt
HRWRA	0	ml

Batch Weights (ft<sup>3</sup>)

Batch size	3.75	cf
Cement	66.5	lb
Fly Ash	16.8	lb
BFS	0.0	lb
Metakaolin	0.0	lb
RCA	0.0	lb
Rock	259.1	lb
Sand	166.8	lb
Water	29.5	lb
AEA	19.7	ml
HRWRA	0.0	



**Mixture 12 Batched 4/23/2019**

### Mix Proportion (SSD)

Material	Weight	Volume (cf)	Volume Check	Unit Cost (\$/ton)	Amount (\$)
Cement	478.80	2.44	0.090	120	28.73
Fly Ash	121.2	0.84	0.031	100	6.06
BFS	0	0.00	0.000	100	0.00
Metakaolin	0	0.00	0.000	100	0.00
RCA	0	0.00	0.000	18	0.00
Rock	1867.00	11.29	0.418	18	16.80
Sand	1084.74	6.56	0.243	18	9.76
Water	282.00	4.52	0.167	0.6	0.08
Air	0.050	1.35	0.050	-	-
		27.00	1.00	-	-
				Total Cost =	61.44

## Material Properties

Material	S.G.	A.C
Cement	3.15	-
Fly Ash	2.30	-
BFS	2.89	-
Metakaolin	2.60	-
RCA	2.46	2.82
Rock	2.65	0.49
Sand	2.65	1.53

### Mix Characteristics

w/c	0.47
Unit Weight (pcf)	142.0
Cementitious material (lb)	600

Suppl. Cementitious Mat.	Percent (%)	Weight (lb)
Fly Ash replacement (%)	20.2	121.2
BFS replacement (%)	0	0
Metaakolin Replacement (%)	0	0
RCA %	0	0

### Moisture Content

sand mc (%)	10.0884681	mc-ssd	0.085584681
rock mc (%)	0.30243353	mc-ssd	-0.001875665
RCA mc (%)	1.65	mc-ssd	-0.0117

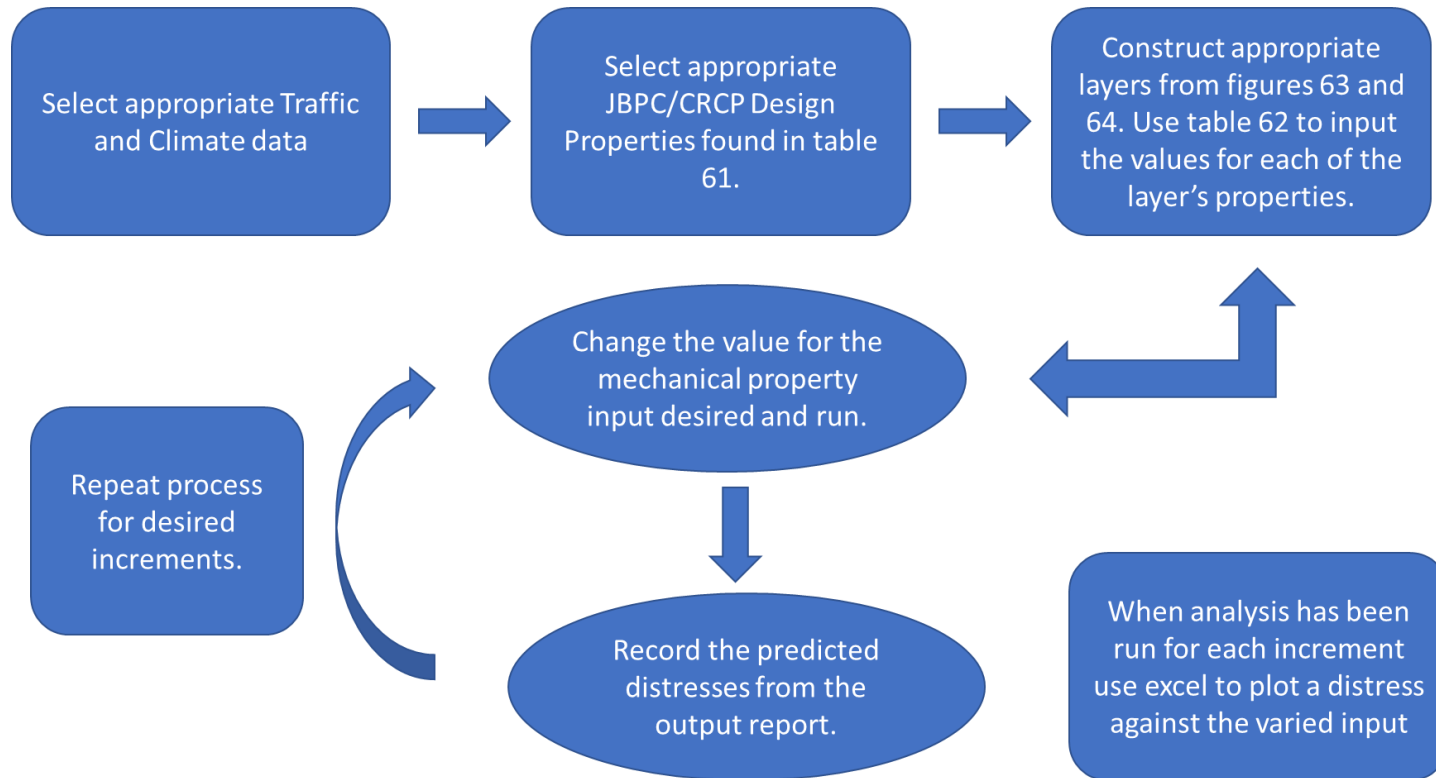
Batch Weights (yd <sup>3</sup> )
----------------------------------

Cement	479	lb
Fly Ash	121	lb
BFS	0	lb
Metakaolin	0	lb
RCA	0	lb
Rock	1863	lb
Sand	1178	lb
Water	193	lb
AEA	1.1	fl oz./cwt
AEA	195	ml
HRWRA	6.0	fl oz./cwt
HRWRA	0	ml

Batch Weights (ft<sup>3</sup>)

Batch size	3.75	cf
Cement	66.5	lb
Fly Ash	16.8	lb
BFS	0.0	lb
Metakaolin	0.0	lb
RCA	0.0	lb
Rock	258.8	lb
Sand	163.6	lb
Water	26.8	lb
AEA	27.1	ml
HRWRA	0.0	

## APPENDIX C – SENSITIVITY ANALYSIS PROCESS



## **APPENDIX D – PROPOSED STANDARD OPERATING PROCEDURES (SOPS)**

### **Georgia Department of Transportation Office of Materials and Testing**

#### **Proposed Standard Operating Procedure (SOP) – DRAFT**

Measurements of Compressive Strength, Modulus of Rupture, Young's Modulus, Ultimate Shrinkage, Thermal Conductivity, and Coefficient of Thermal Expansion (CTE)

---

#### **I. General**

The purpose of this Standard Operating Procedure is to outline the methodology for measuring Compressive Strength, Modulus of Rupture, Modulus of Elasticity, Shrinkage, Thermal Conductivity, and Coefficient of Thermal Expansion of concrete mixes. Compressive Strength and Modulus of Rupture are designed to be performed with a compressive testing machine in accordance with ASTM C39 (AASHTO T22) and ASTM C78 (AASHTO T23), respectively. Pine's Coefficient of Thermal Expansion System was used in testing the Concrete's CTE in accordance with AASHTO T336. Thermal Conductivity is designed to be performed with a needle probe through a line source test method in accordance with ASTM D5334-14. The measurement of mechanical and thermal concrete mixture properties is a very technical process requiring highly skilled testing personnel, precision testing equipment, and close adherence to design guidelines and test procedures to assure high-quality mix designs. It is a requirement for lab certification that the design equipment must meet all requirements and tolerances stated in the test procedures. Equipment calibration records shall be furnished to OMAT for review prior to initial certification and shall always be available for inspection. In case commercial laboratories that satisfy the requirements are not available, research universities in Georgia that have extensive experience in measuring concrete mechanical and thermal properties should conduct the tests.

#### **II. Specimen Fabrication**

This procedure governs the sampling procedure to fabricate concrete mixtures to measure its mechanical and thermal properties.

##### **A. Sampling**

The sampling, testing, and inspection duties are to be performed by a GDOT engineer:

References: GDOT Specifications

- Section 500 (Concrete Structures)
- Section 800 (Coarse Aggregate)
- Section 801 (Fine Aggregate)
- Section 830 (Portland Cement)
- Section 832 (Curing Agents)

- Section 880 (Water)
- GDT 35
- QPL 10 (Approved Ready-Mix Concrete Plants)
- QPL 13 (Air-Entraining Admixtures)
- QPL 14 (Chemical Admixtures for Concrete)
- QPL 16 (Membrane Curing Compounds)

In case ready-mix concrete is used, the frequency at which materials are sampled and tested should be as established in the Sampling, Testing, and Inspection Manual. Detailed information can be found in SOP 10.

## B. Standard Procedure for Specimen Fabrication

### 1. Preparing Specimen Molds

- All Molds should conform to standard ASTM standards C192-19 for given aggregate size and testing function, as well as testing devices utilized. The various specimen dimensions and types for each test are located in table 67.
- The number of specimens and number of test batches should be in accordance with each test method and procedure unless otherwise noted. At Least 3 specimens per test age and condition shall be formed.
- Cylindrical Specimens
  - The same cylindrical mold dimensions should be used as control specimen dimensions.
  - All Cylindrical specimens other than creep shall be molded and cured along the cylinder axis as the vertical axis.
- Prismatic Specimens
  - Beams for flexural and shrinkage shall be formed along the long axis as the horizontal.

**Table 67. Specimen dimensions.**

Property of Concern	Specimen Type	Specimen Dimensions
Compressive Strength	Cylinder	4 x 8 or 6 x 12 (See GDT 35)
Modulus of Rupture	Beam	3 x 4 x 16 or 6 x 6 x 22
Youngs Modulus	Cylinder	4 x 8
Ultimate Shrinkage	Beam	4 x 4 x 10
Thermal Conductivity	Cylinder	4 x 8
Coefficient of Thermal Expansion	Cylinder	4 x 8

2. Mixing

- a. Before mixing concrete materials, bring all material to room temperature of 68–86°F (20–30°C) unless stipulated.
- b. Aggregate weights and moisture content should be calculated following *ASTM C566: Standard Test Method for Total Evaporable Moisture Content of Aggregate by Drying*.
- c. Mixing procedure should follow *ASTM C192: Standard Practice for Making and Curing Concrete Test Specimens in the Laboratory*.

3. Batch Testing

- a. After batching concrete, immediately begin fresh concrete property testing for quality assurance and to confirm the desired properties/behavior of the mixture. The fresh concrete property standards are listed in table 68.

**Table 68. Fresh concrete property standards.**

<b>Fresh Concrete Property</b>	<b>Test Standard ID</b>
Temperature	AASHTO T309/ASTM C1064
Slump	AASHTO T119/ASTM C143
Unit Weight	AASHTO T121/ASTM C138
Pressure Meter Air Content	AASHTO T152/ASTM C231

4. Molding

a. Placement

- i. When placing concrete within molds, maintain parameters listed in table 69 and ensure proper consolidation method is utilized.

**Table 69. Concrete placement guide.**

<b>Specimen Type and Size</b>	<b>Mode of Consolidation</b>	<b>Number of Layers of Approximate Equal Depth</b>
Cylinders: Diameter, inch (mm)		
3 or 4 (75–100)	Rodding	2
6 (150)	Rodding	3
9 (225)	Rodding	4
Up to 9 (225)	Vibration	2
Prisms and Horizontal Creep Cylinders: Depth, inch (mm)		
Up to 8 (200)	Rodding	2
Over 8 (200)	Rodding	3 or More
Up to 8 (200)	Vibration	1
Over 8 (200)	Vibration	2 or More

b. Consolidation

- i. Consolidate according to vibratory or tamping rod based off specimen size listed in table 70.

**Table 70. Consolidation recommendations.**

<b>Cylinders</b>		
<b>Diameter of Cylinder, in. (mm)</b>	<b>Diameter of Rod, in. (mm)</b>	<b>Number of Strokes/Layer</b>
3 (75) to < 6 (150)	3/8±1/16 (10±2)	25
6 (150)	5/8±1/16 (16±2)	25
8 (200)	5/8±1/16 (16±2)	50
10 (250)	5/8±1/16 (16±2)	75
<b>Beams and Prisms</b>		
<b>Top Surface Area of Specimen, in<sup>2</sup> (cm<sup>2</sup>)</b>	<b>Diameter of Rod, in. (mm)</b>	<b>Number of Roddings/Layer</b>
25 (160) or less	3/8±1/16 (10±2)	25
26–49 (165–310)	3/8±1/16 (10±2)	One for each 1 in. <sup>2</sup> (7 cm <sup>2</sup> ) of surface
50 (320) or more	5/8±1/16 (16±2)	One for each 2 in. <sup>2</sup> (14 cm <sup>2</sup> ) of surface
<b>Horizontal Creep Cylinders</b>		
<b>Diameter of Cylinder, in. (mm)</b>	<b>Diameter of Rod, in. (mm)</b>	<b>Number of Roddings/Layer</b>
6 (150)	5/8±1/16 (16±2)	50 total, 25 along both sides of axis

5. Curing

a. Initial Curing

- i. Upon the completion of placement, cover specimens with impervious material to prevent water evaporating from concrete specimens.

b. Mold Removal

- i. Remove the specimens from the molds 24±8 hours after casting. For concrete with prolonged setting time, molds shall not be removed until 20±4 hours after final set. If needed, determine the setting times in accordance with Test Method C403/403M.

c. Final Cure

- i. After mold removal, cure specimens at temperature of 70–77°F (21–25°C) until the time of testing.
- ii. First 48 hours of final cure should be in a vibration-free environment.
- iii. For moist curing condition, the entire free surface of the specimen should be subjected to water, maintained through submerge tank or moisture room in accordance with *ASTM C511-13: Standard Specification for Mixing Rooms, Moist*

### **III. Test Procedures**

#### **A. Standard Practice Test Method for Compressive Strength of Cylindrical Concrete Specimens (AASHTO T22 / ASTM C39)**

1. Place Concrete Specimen upon lower bearing block in accordance with utilized testing device on the load deck.
2. Place upper bearing block on top of specimen and fit within the loading deck area.
3. Seat the loading block onto the upper bearing block and ensure the loading stress is zeroed to begin the test.
4. Loading
  - a. Loading Speed:  $35 \pm 7$  psi and maintained through the latter half of the testing procedure.
  - b. Continually apply load until the indicator displays a continually lowered stress or automatic stop has been issued.
  - c. Note and record the break type and fracture pattern and its accordance with Typical Fracture type diagram.

#### **B. Standard Test Method for Flexural Strength of Concrete (Using Simple Beam with Third-Point Loading) (AASHTO T23 / ASTM C78)**

1. Manipulate the specimen such that the top casted side is facing upward toward the loading block.
2. Center the specimen along both support sides and ensure consistent contact is made across the specimen.
3. Bring the loading block to the surface of the specimen and zero the loading device.
4. Load the specimen with a rate of 125–175 psi/min until rupture or a rapid decrease in applied load to the specimen, or until automatic stop is applied.
5. Inspect the specimen to ensure a clean break through several aggregate pieces and not through the cement line (see figure 90).
6. Compare the specimen break to the specimen break guide to ensure a proper break to confirm proper compressive strength test has been conducted.



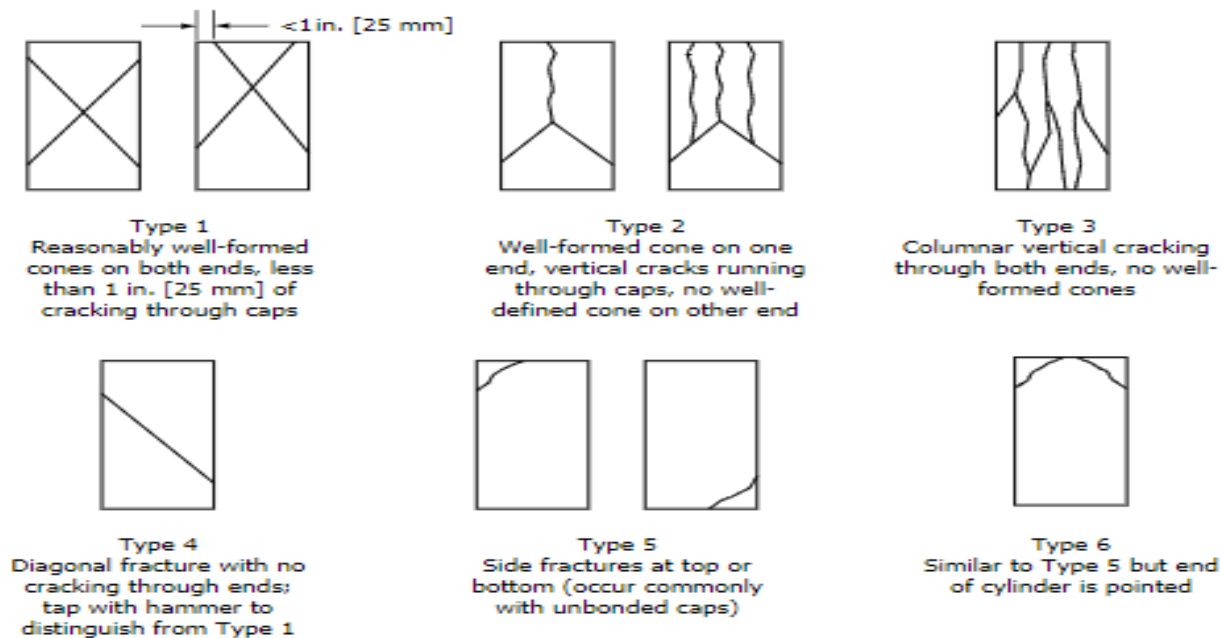


**Figure 90. Diagrams. Concrete compressive strength fracture types (ASTM C78).**

### **C. Standard Test Method for Fundamental Transverse Resonant Frequencies of Concrete Specimens (ASTM C215)**

#### **1. Testing procedure:**

Note: This test only applies to the longitudinal dynamic modulus of rigidity that was used in RP 18-03.

- a. Place Specimen horizontally along two supports that allows the free vibration from impact of the testing specimen.
- b. Dry the surface of the specimen to ensure proper contact between the accelerometer and the specimen, whereas a wax or glue material can also be used.
- c. Prepare the waveform analyzer for testing procedures within given operational guides.
- d. After the waveform analyzer is prepped, begin recording the accelerometer and strike the specimen along the long axis specimens' axis.
- e. Repeat the impact test at least three times per iteration to obtain a representative sample of the specimen.

### **D. Standard Test Method for Length Change of Hardened Hydraulic-Cement Mortar and Concrete (AASHTO T160 / ASTM C157)**

#### **1. Storage**

- a. After the concrete specimen is removed from curing mold, obtain the overall length or difference of length from a given value.

- b. After initial reading, store specimen in either submerged tank, air dry room, or in environmental chamber to ensure most consistent humidity and moisture transfer.

2. Testing

- a. Rerecord the length or difference of length measurement for each specimen according to the listed schedule and return to storage condition.
  - i. Testing days after initial length test: 3, 7 days after initial, then every week for 3 months to determine near-ultimate shrinkage value

**E. Standard Test Method for Determination of Thermal Conductivity (ASTM D5334-14)**

1. Preparation

- a. After the 28-day final curing phase, obtain specimens from each batch and have three different moisture conditions (oven dry, saturated, and air dried) per batch.
  - i. Oven Dry – Obtained by placing the concrete specimens in an oven at a temperature of  $100\pm5^{\circ}\text{F}$  ( $38\pm3^{\circ}\text{C}$ ) for  $24\pm1$  hour.
  - ii. Air Dry – Obtained by placing two cylinders into a controlled environmental chamber maintaining a temperature of  $73\pm3^{\circ}\text{F}$  ( $23\pm2^{\circ}\text{C}$ ) and a relative humidity of  $50\pm4$  percent. The specimens remain in this chamber for a 24-hour period to ensure homogeneous temperature and moisture throughout the specimen.
  - iii. Saturated – After 28 days, move the concrete specimens from the moisture curing tank to a water tank inside the environmental chamber for a 24-hour period.
- b. To prepare the concrete specimen, obtain the mass to 0.01 g, and the length of the specimen to 0.01 mm.
- c. Drill a hole along the central long axis of the specimen to the depth of the probe device utilized.

2. Testing

- a. After placing the probe inside the hole, ensure the probe is fully embedded with the specimen.
- b. Connect the heating probe to the reading device and annotate the test.
- c. Conduct several tests (more than five) for each specimen condition with sufficient time spacing between the heating phases to ensure the specimen has reached an equilibrium state
- d. Rerun the test with the specimens of each condition to obtain the thermal conductivity values per moisture condition. During the test, a temperature of  $73\pm3^{\circ}\text{F}$  ( $23\pm2^{\circ}\text{C}$ ) and a relative humidity of  $50\pm4$  percent should be maintained.

## **F. Standard Method of Test for Coefficient of Thermal Expansion of Hydraulic Cement Concrete (AASHTO T 336)**

1. Preparation
  - a. To prepare specimen mold, cut off equal parts on polar ends of cylindrical concrete specimen to obtain a length of  $117.8 \pm 2.54$  mm ( $7.0 \pm 0.1$  inch)
  - b. Condition specimens to limewater mix tank of  $23 \pm 2^\circ\text{C}$  ( $73 \pm 4^\circ\text{F}$ ) and ensure within a 24-hour period the specimen has an increase of mass by 0.5 percent.
2. Testing
  - a. After preparing the specimens, perform CTE testing on concrete cylinders that were subjected to a uniform increase from  $50\text{--}122^\circ\text{F}$  ( $10\text{--}50^\circ\text{C}$ ) and a decrease of  $50\text{--}122^\circ\text{F}$  ( $10\text{--}50^\circ\text{C}$ ) in temperature.
  - b. Measure the change in length of the specimen in millimeters as the heating and cooling cycles occur; the average change in length of the concrete specimen per unit change in temperature is the resulting CTE.

## **IV. Maintenance**

This list should serve as a guideline for when the mechanical and thermal properties of concrete mixtures should be re-evaluated:

1. Field cores taken for performance evaluation and remaining design life prediction.
2. Concrete mixtures with new admixtures.
3. Concrete mixtures with any recycled materials.
4. Concrete mixtures that use limestone as an aggregate source.
5. Concrete mixtures in pavements that failed to reach the design life.

If the measured properties don't meet the following criteria, the mixtures should be re-tested until the GDOT engineer approves the lab results:

1. Compressive strength  $\geq 4000$  psi
2. Modulus of elasticity  $\leq 5,500$  ksi
3. Modulus of rupture  $\geq 600$  psi for Class 1 and  $\geq 700$  psi for Class 2 mixtures, respectively.
4. Coefficient of Thermal Expansion  $\leq 5.5$  microstrain/ $^\circ\text{F}$
5. Thermal conductivity  $\geq 1.0$  BTU/hr-ft- $^\circ\text{F}$

## **ACKNOWLEDGMENTS**

The University of Georgia acknowledges the financial support for this work provided by the Georgia Department of Transportation (GDOT). The authors thank the technical manager, Mr. Ian Rish, and his Office of Materials and Testing (OMAT) team members, Mr. Phillip Snider and Jason Waters, for research support and partnership. Special thanks also to the project manager, Mr. Sunil Thapa, who advised the research team in successfully performing the study and assisted in the coordination of project meetings with GDOT. Finally, the team expresses thanks for the continuous support from Supriya Kamatkar and her leadership in the Performance-based Management and Research Office.

## REFERENCES

- Advanced Concrete Pavement Technology. (2012). *Continuously Reinforced Concrete Pavement Performance and Best Practices*. TechBrief.
- Alexander, M.G. and Milne, T.I. (1995). “Influence of Cement Blend and Aggregate Type on Stress–Strain Behaviour and Elastic Modulus of Concrete 92-M24.” *ACI Materials Journal*, 92(3), pp. 227–235.
- Applied Research Associates (ARA). (2015). *Implementation of the Mechanistic–Empirical Pavement Design Guide in Georgia*. Research Project FHWA-GA-14-11-17.
- Bentz, D.P., Peltz, M.A., Duran-Herrera, A., Valdez, P., and Juarez, C.A. (2011). “Thermal Properties of High-volume Fly Ash Mortars and Concretes.” *Journal of Building Physics*, 34(3), pp. 263–275.
- Caltrans. (2015). “Concrete Pavement Guide.” In D. o. M. P. Program (Ed.), *Concrete Pavement Guide*, Sacramento, CA, pp. 210.211–210.210.
- Ceylan, H., Kim, S., Schwartz, C.W., Li, R., and Gopalakrishnan, K. (2012). “Effect of PCC Material Properties on MEPDG Jointed Plain Concrete Pavement (JPCP) Performance Prediction.” *Proceedings of 10<sup>th</sup> International Conference on Concrete Pavements*, Quebec City, Quebec, Canada, July 8–12, pp. 236–251. [https://lib.dr.iastate.edu/ccee\\_conf/5](https://lib.dr.iastate.edu/ccee_conf/5).
- Chen, H. and Texas Department of Transportation (Producer). (2013). *Concrete Paving Selections*. [Powerpoint Presentation], September 4, 2018.
- Chintakunta, S. (2007). *Sensitivity of Thermal Properties of Pavement Materials Using Mechanistic–Empirical Pavement Design Guide*. Master’s thesis. Iowa State University, Ames, Iowa.
- Dos Santos, W.N. (2003). “Effect of Moisture and Porosity on the Thermal Properties of a Conventional Refractory Concrete.” *Journal of the European Ceramic Society*, 23(5), pp. 745–755. [https://doi.org/10.1016/S0955-2219\(02\)00158-9](https://doi.org/10.1016/S0955-2219(02)00158-9).
- Durham, S.A., Chorzepa, M.G., Kim, S.-H., and Citir, N. (2018). *Evaluating the Performance of Georgia’s CRCPs Using Ground Penetrating Radar (GPR)*. Report FHWA-GA-1639, University of Georgia, Athens, GA. [http://g92018.eos-intl.net/eLibSQL14\\_G92018\\_Documents/16-39.pdf](http://g92018.eos-intl.net/eLibSQL14_G92018_Documents/16-39.pdf).
- Georgia Department of Transportation (GDOT). (2013). “Section 430–Portland Cement Concrete Pavement.” *Standard Specifications: Construction of Transportation Systems*, 2013 edition, Atlanta, GA, pp. 362–379. <http://www.dot.ga.gov/PartnerSmart/Business/Source/specs/DOT2013.pdf>.
- Google (Cartographer). (2019). Quarry Location. Retrieved from <https://www.google.com/maps/@33.5033078,-84.7093232,9z/data=!3m1!4b1!4m2!6m1!1s1dvAA-HlpaC3mN8Vp0hRMu4WYJFGy-As6>.

- Highway Research Board. (1962). *The AASHTO Road Test*. Washington, DC. <http://onlinepubs.trb.org/Onlinepubs/sr/sr61g/61g.pdf>.
- Kim, S.-H. (2012). *Determination of Coefficient of Thermal Expansion for Portland Cement (10-04)*. Final Report, RP 10-04, Georgia Department of Transportation, Marietta, GA.
- Kim, S.-H., Yang, J., Nam, B.H., and Jeong, J.-H. (2015). “Effect of Materials and Age on the Coefficient of Thermal Expansion of Concrete Paving Mixture.” *Road Materials and Pavement Design*, 16(2), pp. 445–458.
- Kim, S., Worthey, H., Brink, W., Von Quintus, H., Durham, S., and Chorzepa, M. (2020). *Development of Innovative & Effective Training Modules and Methods for Pavement Designers for Rapid Deployment and Continuous Operation of MEPDG*. Final Report, RP 17-18, Georgia Department of Transportation.
- Kodide, U. (2010). *Thermal Conductivity and its Effects on the Performance of PCC Pavements in MEPDG*. Master’s thesis in Civil Engineering, Louisiana State University, Baton Rouge, LA.
- Kosmatka, S.H., Kirkoff, B., and Panarese, W.C. (2002). *Design and Control of Concrete Mixtures*. 14th edition, Portland Cement Association, Skokie, IL.
- Kosmatka, S.H. and Wilson, M.L. (2016). *Design and Control of Concrete Mixtures*. 16th ed., Vol. EB001, Portland Cement Association, Skokie, IL.
- Mallela, J., Abbas, A., Harman, T., Rao, C.T., Liu, R.F., Darter, M.I., and Trb. (2005). “Measurement and Significance of the Coefficient of Thermal Expansion of Concrete in Rigid Pavement Design.” *Rigid and Flexible Pavement Design 2005*, Transportation Research Board National Research Council, Washington, DC, pp. 38–46.
- Meddah, M.S., Ztouni, S., and Belaabes, S. (2010). “Effect of Content and Particle Size Distribution of Coarse Aggregate on the Compressive Strength of Concrete.” *Construction and Building Materials*, 24, pp. 505–512.
- Merine, M. (2018). *VDOT Mechanistic–Empirical Pavement Design (MEPDG) Implementation*. Virginia Department of Transportation, presented at the Virginia Concrete Conference, Richmond, VA, March 2.
- Miller, J.S. and Bellinger, W.Y. (2014). *Distress Identification Manual for The Long-Term Pavement Performance Program*. Publication No. FHWA-HRT-13-092, Federal Highway Administration, Office of Infrastructure Research and Development, McLean, VA. <https://www.fhwa.dot.gov/publications/research/infrastructure/pavements/ltp/13092/13092.pdf>.
- NCHRP. (2004). *Guide for Mechanistic–Empirical Design of New and Rehabilitated Pavement Structures*. ARA, Inc., ERES Division, Champaign, IL.
- Pavement Interactive. (n.d.). “Punchout.” <https://www.pavementinteractive.org/reference-desk/pavement-management/pavement-distresses/punchout/>.
- Pavement Interactive. (2001). “Roughness.” <https://www.pavementinteractive.org/reference-desk/pavement-management/pavement-evaluation/roughness/>.

- Peck, R. and Devore, J.L. (1986). *Statistics: The Exploration and Analysis of Data*. 7th edition, Brooks/Cole, Cengage Learning, Boston, MA.
- Ping, W.V. (2008). *Engineering Properties of Florida Concrete Mixes for Implementing the AASHTO Recommended Mechanistic–Empirical Rigid Pavement Design Guide*. Project No. OMNI 018598, Florida State University, Tallahassee, FL.
- Quintus, H.V.L., Darter, M.I., Bhattacharya, B.B., and Titus-Glover, L. (2015). *Implementation and Calibration of the MEPDG in Georgia Task Order 3*. Final Report, FHWA/GA-014-11-17.
- Rao, C. (2014). *Guidelines for PCC Inputs to AASHTOWare Pavement ME*. FHWA/MS-DOT-RD-14-260, Champaign, IL.
- Rashid, M.A., Mansur, M.A., and Paramasivam, P. (2002). “Correlations Between Mechanical Properties of High-Strength Concrete.” *Journal of Material in Civil Engineering*, 14(3), pp. 230–238.
- Roesler, J.R., Hiller, J.E., and Brand, A.S. (2016). *Continuously Reinforced Concrete Pavement Manual: Guidelines for Design, Construction, Maintenance, and Rehabilitation*. FHWA-HIF-16-026, Federal Highway Administration, McLean, VA. Retrieved from <https://www.fhwa.dot.gov/pavement/concrete/pubs/hif16026.pdf>.
- Sabih, G. and Tarefder, R.A. (2016). “Impact of Variability of Mechanical and Thermal Properties of Concrete on Predicted Performance of Jointed Plain Concrete Pavements.” *International Journal of Pavement Research and Technology*, 9, pp. 436–444.
- Salman, M.M. and Al-Amawee, A.H. (2006). “The Ratio between Static and Dynamic Modulus of Elasticity in Normal and High Strength Concrete.” *Journal of Engineering and Development*, 10(2), 1813-7822, pp. 163–174.
- Schuring, D.J. (1977). *A New Look at the Definition of Tire Rolling Loss*. Presented at the Tire Rolling Losses and Fuel Economy – An R&D Planning Workshop, Troy, MI, October 18–20.
- Schwartz, C.W., Li, R., Kim, S., Ceylan, H., and Gopalakrishnan, K. (2011). *Sensitivity Evaluation of MEPDG Performance Prediction*. Final Report, NCHRP Project 1-47, Transportation Research Board of the National Academies, Washington, DC.
- Shin, A.H.C. and Kodide, U. (2012). “Thermal Conductivity of Ternary Mixtures for Concrete Pavements.” *Cement & Concrete Composites*, 34(4), pp. 575–582. doi:10.1016/j.cemconcomp.2011.11.009.
- Tanesi, J., Ardani, A.A., and Leavitt, J.C. (2013). “Reducing the Specimen Size of the AASHTO T 97 Concrete Flexural Strength Test for Safety and Ease of Handling.” *Transportation Research Record*, 2342, pp. 99–105.
- Taylor, P.C., Yurdakul, E., and Ceylan, H. (2014). “Performance Engineered Mixtures for Concrete Pavements in the US.” *Civil, Construction and Environmental Engineering Conference Presentations and Proceedings*, 24. [http://lib.dr.iastate.edu/ccee\\_conf/24](http://lib.dr.iastate.edu/ccee_conf/24).

- Tsai, Y.J. and Wang, Z. (2014). *Critical Assessment of I-85 CRCP Crack Spacing Patterns and Their Implications for Long-term Performance*. Report No. FHWA-GA-14-1239, Federal Highway Administration, Washington, DC.
- Weingroff, R.F. (2014). “Celebrating A Century of Cooperation.” *Public Roads*, 78(2). <https://www.fhwa.dot.gov/publications/publicroads/14sepoct/03.cfm>.
- Willis, J.R., Robbins, M.M., and Thompson, M. (2015). *Effects of Pavement Properties on Vehicular Rolling Resistance: A Literature Review*. Technical Report, National Center for Asphalt Technology (NCAT), Auburn University, Auburn, AL.